



CELLULAR REGULATORS OF MYOBLAST
MIGRATION AND MYOGENESIS

GEORGI ALEKSANDROV DIMCHEV

A thesis submitted in partial fulfilment of the requirements of
the Manchester Metropolitan University for the degree of
Doctor of Philosophy

Institute for Biomedical Research into Human Movement and
Health (IRM), Faculty of Science and Engineering,
Manchester Metropolitan University

2012

ABSTRACT

Migration of myogenic cells is an important step in myogenesis and skeletal muscle repair. Migration is required for the cells to reach the site of damage, for their alignment and subsequent fusion. Limited migration is also one of the limitations of proposed therapies of diseases, such as Duchenne Muscular Dystrophy (DMD). Therefore, revealing the regulators of myogenic cell migration is important for improving our knowledge of myogenesis, but could also be applied in therapies for conditions, associated with loss of muscle mass and muscle weakness.

In this thesis, extracellular and intracellular regulation of C2C12 myoblast migration was investigated. It was demonstrated that medium conditioned by myotube cultures *in vitro*, is capable of inducing the migration and chemotaxis of myoblasts. A model of serially passaged myoblasts was used to reveal potential changes in the migratory behaviour of these cells, in the context of skeletal muscle ageing. PI3K/AKT and MAPK/ERK pathways were investigated and their requirement for the process of myoblast migration was revealed. Further activation of these pathways with phospho-tyrosine phosphatase and PTEN inhibitor Bpv(Hopic) was associated with larger increases in myoblast migration. Silencing of either PI3K/AKT or MAPK/ERK signalling pathways, in a situation where the other pathway remained activated, resulted in a significant inhibition of myoblast migration. Similarly, inhibition of FAK signalling, using the PF-228 inhibitor did not significantly affect PI3K/AKT and MAPK/ERK pathways, but resulted in reduced myoblast migration, suggesting the indispensability of individual signalling pathways for myoblast migration in response to myotube CM, regardless of the activity of other signalling pathways. Finally, considering the link between myoblast fusion and migration and in an attempt to propose genetic targets for future research, an investigation was made on the expression of Spire and Formin genes, involved in actin polymerisation and intracellular trafficking, in myoblasts undergoing differentiation and fusion. The expression of these genes was revealed in C2C12 myoblasts and it was demonstrated that the expression levels of two of these genes (Spire1 and Formin1) are altered following inhibition of myoblast differentiation/fusion by both 10 μ M Bpv(Hopic) and serial passaging, suggesting their potential association with these processes. Further investigations to reveal the function of Spire and Formin genes and their protein products in skeletal muscle are proposed.

ACKNOWLEDGMENTS

I would like to thank my director of studies Professor Claire Stewart for her continued guidance, for giving me the freedom and support to perform independently my PhD research and for her dedication to making me a better researcher.

I would like to thank my supervisor Doctor Nasser Al-Shanti for his continued support and guidance.

Their invaluable contribution to the completion of this thesis is most appreciated.

I wish to thank the Institute for Biomedical Research in Human Movement and Health (IRM) where this work was carried out. Many thanks to Manchester Metropolitan University and the IRM for providing the vital financial support allowing me to complete this PhD Thesis.

AUTHORS DECLARATION

I declare that the work in this thesis was carried out in accordance with the regulations of Manchester Metropolitan University. Apart from the help and advice acknowledged, the work within was solely completed and carried out by the author.

Any views expressed in this thesis are those of the author and in no way represent those of Manchester Metropolitan University and the Institute for Biomedical Research in Human Movement and Health.

This thesis has not been presented to any other University for examination either in the United Kingdom or overseas. No portion of the work referred to in this Research Project has been submitted in support of an application for another degree or qualification of this or any other university or institute of learning.

Copyright in text of this Research Project rests with the author. The ownership of any intellectual property rights which may be described in this Research Project is vested in Manchester Metropolitan University and may not be made available for use to any third parties without the written permission of the University.

SIGNED:

DATE:

DEDICATION

To my mum and dad, Kristina and Alexander, who have always believed in me and supported me in everything throughout my life.

To my girlfriend Alba. Your love and your smile was all I needed to overcome all the hard and frustrating moments, endless hours and long weekends spent in the lab and in front of the monitor. I am so lucky to have you next to me!

TABLE OF CONTENTS

ABSTRACT	ii
ACKNOWLEDGEMENTS	iii
AUTHORS DECLARATION	iv
DEDICATION	v
TABLE OF CONTENTS.....	vi
LIST OF FIGURES	xii
ABBREVIATIONS	xv
1. INTRODUCTION	2
1.1. OVERVIEW	2
1.2. SKELETAL MUSCLE DEVELOPMENT.....	2
1.3. MOLECULAR REGULATORS OF MUSCLE DEVELOPMENT	4
1.4. POSTNATAL SKELETAL MUSCLE REGENERATION AND PLASTICITY.....	6
1.5. SATELLITE CELLS ARE OF MAJOR IMPORTANCE OF MUSCLE REPAIR	7
1.6. MUSCLE REGENERATION PHASES.....	8
1.7. MARKERS OF SATELLITE CELLS.....	11
1.8. SELF-RENEWAL OF SATELLITE CELLS	12
1.9. COMMON EXTRACELLULAR FACTORS REGULATING MUSCLE REGENERATION.....	13
1.10. SKELETAL MUSCLE AND AGEING	17
1.11. PROPOSED THERAPIES FOR MUSCULAR DYSTROPHIES OR TRAUMAS	20
1.12. CELL MIGRATION.....	23
1.13. “STEPS” OF CELL MIGRATION	24
1.14. RHO GTPases.....	28
1.15. PTEN/PI3K PATHWAY INVOLVEMENT IN CELL MIGRATION	30
1.16. MAPKs IN CELL MIGRATION	34
1.17. MATRIX METALLOPROTEINASES	35
1.18. MIGRATION OF MYOGENIC PRECURSORS.....	36
1.19. AIMS, OBJECTIVES AND HYPOTHESIS	37
2. MATERIALS AND METHODS.....	40
2.1. MATERIALS, GENERAL EQUIPMENT AND SPECIALIZED SOFTWARE.....	40
2.1.1. CHEMICALS, SOLVENTS AND REAGENTS	40
2.1.2. CELL CULTURE	40
2.1.3. CELL CULTURE REAGENTS	40
2.1.4. PLASTICWARE	41
2.1.5. LIVE IMAGING.....	41
2.1.6. BIOCHEMICAL ASSAYS	42
2.1.7. REAL-TIME PCR	42
2.1.8. SDS-PAGE AND WESTERN LIGAND BLOTTING.....	42
2.1.9. FLOW CYTOMETRY	43
2.2. METHODS AND PROTOCOLS	43
2.2.1. CELL CULTURE.....	43
2.2.1.1. INDUCING PROLIFERATION AND DIFFERENTIATION OF C2C12 MYOBLASTS	43
2.2.1.2. PASSAGING OF CELLS.....	44

2.2.1.3. CELL CRYOPRESERVATION AND RESURRECTION	44
2.2.2. WOUND HEALING ASSAY WITH LIVE IMAGING EXAMINATION	45
2.2.2.1. WOUND HEALING METHOD	45
2.2.3. LIVE IMAGING MIGRATION ANALYSIS	46
2.2.4. CELL DEATH ANALYSIS BY LIVE IMAGING	46
2.2.5. TRANSWELL INSERTS MIGRATION ASSAY	47
2.2.5.1. PRINCIPLE	47
2.2.5.2. METHOD	47
2.2.6. PHALLOIDIN-FITC STAINING	48
2.2.7. BIOCHEMICAL ASSAYS	49
2.2.7.1. PROTEIN ASSAY	49
2.2.7.2. CREATINE KINASE (CK) ASSAY	50
2.2.8. WESTERN BLOTS	50
2.2.8.1. SAMPLE PREPARATION	51
2.2.8.2. GEL ELECTROPHORESIS	51
2.2.8.3. ELECTROPHORETIC TRANSFER.....	53
2.2.8.4. BLOCKING.....	54
2.2.8.5. DETECTION	55
2.2.8.6. NITROCELLULOSE MEMBRANE STRIPPING	56
2.2.9. RNA EXTRACTION	56
2.2.10. REAL-TIME PCR	58
2.2.10.1. PRINCIPLE	58
2.2.10.2. METHOD	61
2.2.10.2.1. SYBR® GREEN.....	61
2.2.10.2.2. TAQMAN®.....	63
2.2.10.3. ANALYSIS.....	64
2.2.11. FLOW CYTOMETRY	64
2.2.11.1. PRINCIPLE	64
2.2.11.2. PROPIDIUM IODIDE AND CELL CYCLE EXAMINATION.....	65
2.2.11.3. METHOD	65
2.2.11.4. ANALYSIS.....	66
2.2.12. STATISTICAL ANALYSES	66
3. MYOTUBE CONDITIONED MEDIA ENHANCES C2C12 MYOBLAST MIGRATION	68
3.1. INTRODUCTION	68
3.2. AIMS, OBJECTIVES AND HYPOTHESIS	70
3.3. MATERIALS AND METHODS.....	71
3.3.1. CELL CULTURE	71
3.3.2. CONDITIONED MEDIA GENERATION	71
3.3.3. CELL TREATMENTS AND RECONSTITUTION OF INHIBITORS	72
3.3.4. WOUND HEALING ASSAY AND LIVE IMAGING	72
3.3.5. LIVE IMAGING MIGRATION ANALYSIS	72
3.3.6. CELL DEATH QUANTIFICATIONS BY LIVE IMAGING.....	73
3.3.7. PHALLOIDIN STAINING	73
3.3.8. TRANSWELL INSERTS	73
3.3.9. WESTERN BLOTS	73
3.3.10. RNA ISOLATIONS AND REAL-TIME PCR.....	74
3.3.11. STATISTICAL ANALYSES	74

3.4. METHOD DEVELOPMENT	74
3.4.1. WOUND HEALING ASSAY METHOD SET-UP	74
3.4.2. WOUND HEALING LIVE IMAGING MIGRATION ANALYSIS	77
3.5. RESULTS	82
3.5.1. CELL CULTURE MEDIA, CONDITIONED IN VITRO BY C2C12 MYOTUBES IS CAPABLE OF INDUCING WOUND CLOSURE OF C2C12 MYOBLASTS	82
3.5.2. OPTIMIZATION OF MYOBLAST MIGRATION: COMPARISONS OF CONDITIONED MEDIA, SERUM FREE-MEDIA, GROWTH MEDIA AND DIFFERENTIATION MEDIA	83
3.5.3. IMPACT OF CULTURE CONDITIONS ON CHEMOTAXIS.....	86
3.5.4. MEDIA CONDITIONED BY VIABLE OR SERUM STARVED/ATROPHYING MYOTUBES IS MORE POTENT AT INDUCING MIGRATION AND WOUND HEALING COMPARED TO MEDIA CONDITIONED BY INJURED/CRUSHED MYOTUBES	89
3.5.5. PI3K AND ERK1/2 PATHWAYS ARE ACTIVATED BY CM, GM AND DM, BUT NOT BY SF	93
3.5.6. REDUCTION OF MYOGENIN EXPRESSION WITH CM VS DM.	96
3.5.7. MYOBLAST MIGRATION, INDUCED BY CONDITIONED MEDIA, IS REDUCED BY INHIBITION OF PI3K/AKT AND MAPK/ERK PATHWAYS WITH LY294002 AND UO126.....	97
3.6. DISCUSSION.....	104
3.6.1. MEDIA CONDITIONED BY MATURE MYOTUBES IS ABLE TO INDUCE WOUND HEALING AND MIGRATION OF MYOBLASTS.....	104
3.6.2. MEDIA CONDITIONED BY LIVING MYOTUBES IS MORE POTENT AT INDUCING MIGRATION AND WOUND HEALING, AS COMPARED TO MEDIA CONDITIONED BY FACTORS RELEASED FROM DAMAGED MYOTUBES	105
3.6.3. PI3K/AKT AND MAPK/ERK SIGNALLING PATHWAYS ARE INDUCED IN RESPONSE TO CM AND THEIR INHIBITION LEADS TO REDUCED MYOBLAST MIGRATION	106
3.6.4. CONCLUSIONS AND THESIS DIRECTIONS.....	108
4. SERIALY PASSAGED C2C12 CELLS DEMONSTRATE ALTERED MIGRATION BEHAVIOUR	110
4.1. INTRODUCTION	110
4.2. AIMS, OBJECTIVES AND HYPOTHESIS	111
4.3. METHODS	112
4.3.1. CELL CULTURE	112
4.3.2. CONDITIONED MEDIA GENERATION	112
4.3.3. WOUND HEALING ASSAY AND LIVE IMAGEING	112
4.3.4. ANALYSIS OF CELL MIGRATION.....	113
4.3.5. CELL DEATH QUANTIFICATIONS BY LIVE IMAGEING	113
4.3.6. WESTERN BLOTS	113
4.3.7. RNA ISOLATIONS AND REAL-TIME PCR.....	113
4.3.8. CREATINE KINASE (CK) ASSAY	114
4.3.9. SERIAL PASSAGING	114
4.3.10. STATISTICAL ANALYSES	114
4.4 RESULTS	115
4.4.1. SERIALY PASSAGED C2C12 MYOBLASTS (P50) DEMONSTRATED AN IMPAIRED CAPACITY TO DIFFERENTIATE COMPARED TO LOW PASSAGE (P5) CELLS	115
4.4.2. SIGNIFICANTLY HIGHER LEVELS OF P-ERK1/2 AND ELEVATED LEVELS OF P-AKT WITH P50 MYOBLASTS VS P5 MYOBLASTS IN RESPONSE TO CM117	

4.4.3. SERIALY PASSAGED (P50) C2C12 MYOBLASTS DEMONSTRATED HIGHER MIGRATION CAPACITY, AS COMPARED TO LOW PASSAGE (P5) MYOBLASTS, IN RESPONSE TO MEDIA CONDITIONED BY P5 MYOTUBES..	120
4.4.4. MEDIA CONDITIONED BY P50 CELLS are LESS POTENT IN INDUCING MIGRATION IN WOUND HEALING ASSAY THAN MEDIA CONDITIONED BY P5 CELLS	122
4.5. DISCUSSION.....	127
4.5.1. SERIALY PASSAGED C2C12 MYOBLASTS (P50) DEMONSTRATED IMPAIRED CAPACITY TO DIFFERENTIATE COMPARED TO LOW PASSAGE C2C12 MYOBLASTS (P5).....	127
4.5.2. SERIALY PASSAGED (P50) C2C12 MYOBLASTS DEMONSTRATED ELEVATED LEVELS OF P-AKT AND P-ERK1/2 IN RESPONSE TO CM, AS COMPARED TO LOW PASSAGE (P5) OF MYOBLASTS, WHICH WAS ASSOCIATED WITH HIGHER MIGRATION CAPABILITY OF P50 VS P5 MYOBLASTS	127
4.5.3. MEDIA CONDITIONED BY P50 CELLS ARE LESS POTENT IN WOUND HEALING ASSAYS THAN MEDIA CONDITIONED BY P5 CELLS.....	128
4.5.4. CONCLUSIONS	129
4.5.5. THESIS DIRECTIONS	129
5. MAPK/ERK AND PI3K/AKT PATHWAYS ARE REQUIRED FOR BPV(HOPIC)-INDUCED C2C12 MYOBLAST MIGRATION. REQUIREMENT OF FAK PATHWAY FOR MYOBLAST MIGRATION.....	132
5.1. INTRODUCTION	132
5.2. AIMS, OBJECTIVES AND HYPOTHESIS	134
5.3. METHODS	135
5.3.1. CELL CULTURE	135
5.3.2. CONDITIONED MEDIA GENERATION	135
5.3.3. CELL TREATMENTS AND RECONSTITUTION OF INHIBITORS	135
5.3.4. WOUND HEALING ASSAY AND LIVE IMAGEING	135
5.3.5. ANALYSIS OF CELL MIGRATION.....	136
5.3.6. CELL DEATH QUANTIFICATIONS BY LIVE IMAGEING	136
5.3.7. WESTERN BLOTS	136
5.3.8. RNA ISOLATIONS AND REAL-TIME PCR.....	136
5.3.9. CREATINE KINASE (CK) ASSAY.....	137
5.3.10. FLOW CYTOMETRY	137
5.3.11. STATISTICAL ANALYSES	137
5.4 RESULTS	138
5.4.1. DIFFERENTIATION OF C2C12 MYOBLASTS IS SIGNIFICANTLY AFFECTED BY 10 μ M, BUT NOT BY 1 μ M BPV(HOPIC).....	138
5.4.2. INCREASED PERCENTAGE OF C2C12 MYOBLASTS IN S/G2-PHASE OF THE CELL CYCLE AFTER TREATMENT WITH 10 μ M BPV(HOPIC)	141
5.4.3. THE PHOSPHO-TYROSINE PHOSPHATASE INHIBITOR BPV(HOPIC) IS ABLE TO FURTHER ACTIVATE PI3K/AKT AND MAPK/ERK SIGNALLING PATHWAYS AND TO INCREASE MYOBLAST MIGRATION IN RESPONSE TO CM	142
5.4.4. THE ACTION OF BPV(HOPIC) ON CELL MIGRATION IS REDUCED BY INHIBITING THE PI3K/AKT PATHWAY WITH LY294002	152
5.4.5. THE ACTION OF BPV(HOPIC) ON CELL MIGRATION IS REDUCED BY INHIBITING THE MAPK/ERK PATHWAY WITH UO126.....	160

5.4.6. THE ACTION OF BPV(HOPIC) ON CELL MIGRATION IS REDUCED BY INHIBITING THE FAK PATHWAY WITH PF-228, DESPITE ONGOING PI3K/AKT AND MAPK/ERK ACTIVATION.....	167
5.5. DISCUSSION.....	178
5.5.1. MYOBLAST DIFFERENTIATION IS REDUCED BY 10µM, BUT NOT BY 1µM BPV(HOPIC).....	178
5.5.2. BPV(HOPIC) INCREASED C2C12 MYOBLAST MIGRATION AND ENHANCED ACTIVATION OF MAPK/ERK AND PI3K/AKT PATHWAYS.....	178
5.5.3. INHIBITION OF EITHER MAPK/ERK OR PI3K/AKT PATHWAYS RESULTED IN INHIBITION OF MYOBLAST MIGRATION TO BASAL CONTROL LEVELS	179
5.5.4. FAK IS NOT AFFECTED BY BPV(HOPIC) AT CONCENTRATIONS BELOW 2µM, BUT ITS INHIBITION REDUCES MYOBLAST MIGRATION WITH OR WITHOUT BPV(HOPIC)	180
5.5.5. CONCLUSION.....	183
6. SPIRE AND FORMIN GENES ARE EXPRESSED IN C2C12 MYOBLASTS.....	185
6.1. THESIS DIRECTIONS	185
6.2. BACKGROUND	185
6.3. AIMS, OBJECTIVES AND HYPOTHESIS	186
6.4. METHODS	188
6.4.1. CELL CULTURE.....	188
6.4.2. RNA ISOLATIONS AND REAL-TIME PCR.....	188
6.4.3. CREATINE KINASE (CK) ASSAY.....	188
6.4.4. FLOW CYTOMETRY	188
6.4.5. SERIAL PASSAGING	189
6.4.6. CELL TREATMENTS AND RECONSTITUTION OF INHIBITORS	189
6.4.7. STATISTICAL ANALYSES	189
6.5. RESULTS.....	191
6.5.1. SERIALLY PASSAGED C2C12 MYOBLASTS (P50) DEMONSTRATED IMPAIRED CAPACITY TO DIFFERENTIATE COMPARED TO LOW PASSAGE CELLS (P5), WHICH WAS FURTHER REDUCED BY TREATMENT WITH 10µM BPV(HOPIC).....	191
6.5.2. CELL CYCLE PROGRESSION: IMPACT OF PASSAGING AND BPV (HOPIC).....	194
6.5.3. DIFFERENTIAL EXPRESSION OF MYOGENIC REGULATORY FACTORS IN RESPONSE TO BPV(HOPIC) AND SERIAL PASSAGING.....	196
6.5.4. DIFFERENTIAL EXPRESSION OF SPIRE AND FORMIN GENES IN RESPONSE TO BPV(HOPIC) AND SERIAL PASSAGING.....	204
6.6. DISCUSSION.....	217
6.6.1. SERIALLY PASSAGED C2C12 MYOBLASTS (P50) DEMONSTRATE IMPAIRED CAPACITY TO DIFFERENTIATE COMPARED TO LOW PASSAGE CELLS (P5), WHICH IS FURTHER REDUCED BY TREATMENT WITH 10µM BPV(HOPIC).....	217
6.6.2. DIFFERENTIAL EXPRESSION OF SPIRE AND FORMIN GENES IN RESPONSE TO BPV(HOPIC) AND SERIAL PASSAGING.....	218
6.6.3. CONCLUSIONS	220
7. DISCUSSION AND FUTURE DIRECTIONS	222
7.1. AIMS OF THESIS.....	222
7.2. CONDITIONED MEDIA AND THE IMPORTANCE OF SECRETED FACTORS FOR MYOBLAST MIGRATION.....	223

7.3. THE IMPACT OF SERIAL PASSAGING ON MYOBLAST MIGRATION AND SECRETOME - IMPLICATIONS FOR AGEING?	225
7.4. SIGNALLING PATHWAYS REGULATING MYOBLAST MIGRATION - CONTRIBUTION OF PI3K/AKT, MAPK/ERK AND FAK PATHWAYS	227
7.5. CHANGES IN SIGNALLING PATHWAYS MIGHT EXERT EFFECTS NOT ONLY ON MYOGENIC MIGRATION, BUT ALSO ON PROCESSES SUCH AS CELL DEATH, PROLIFERATION OR DIFFERENTIATION	230
7.6. POTENTIAL THERAPEUTIC APPLICATIONS FOR BISPEROXOVANADIUM COMPOUNDS IN MUSCLE REGENERATION	232
7.7. SPIRE AND FORMIN GENES ARE EXPRESSED IN MYOBLASTS - POSSIBLE IMPLICATIONS FOR MYOBLAST FUSION AND MIGRATION.....	235
7.8. NOVELTY OF THE FINDINGS	237
7.9. SUMMARY AND FUTURE DIRECTIONS	238
8. REFERENCES	245
APPENDICES	280
Appendix 1. Wound healing assay with JNK inhibitor SP600125.....	280
Appendix 2. Abstract of conference proceedings	281

LIST OF FIGURES

Figure 1.1. A schematic representation of a somite.	3
Figure 1.2. The stages of adult skeletal muscle regeneration.	10
Figure 1.3. Soluble factors in myogenesis.	14
Figure 1.4. A model of the steps required for cell migration to occur.	27
Figure 1.5. Regulation of actin polymerization by Rac and Cdc42.	29
Figure 1.6. Regulation of actin cytoskeleton structures by Rho.	30
Figure 1.7. Opposing actions of PI3K and PTEN on phospholipids.	31
Figure 1.8. PTEN exerts effects on FAK and MAPK signalling to regulate cell migration	33
Figure 2.1. Myoblasts are capable of fusing with each other to form multinucleated myotubes.	44
Figure 2.2. Transwell inserts representation.	47
Figure 2.3. SDS polyacrylamide gel preparation.	52
Figure 2.4. A representation of the semi-dry protein transfer method.	53
Figure 2.5. Ponceau S staining.	54
Figure 2.6. Detection and quantification of target proteins.	55
Figure 2.7. Trizol lysate phase separation.	57
Figure 2.8. Comparison of PCR products in Real-time PCR between SYBR® Green and TaqMan® chemistries.	59
Figure 2.9. Real-time PCR Ct value.	60
Figure 2.10. Melting curve in Real-time PCR.	62
Figure 2.11. A schematic representation of the mechanisms of Flow cytometry.	65
Figure 3.1. Optimization of wound healing assay.	76
Figure 3.2. Effect of Mitomycin-C on myoblast migration.	77
Figure 3.3. Demonstration of the demarcations established in a wound healing assay. ...	79
Figure 3.4. An example of cell count analysis.	80
Figure 3.5. Illustrative photomicrographic quantification of cell migration using tracking of the migration distance.	81
Figure 3.6. Photomicrographic representation of wound healing assay (20h post wound).	82
Figure 3.7. Subconfluent cultures of C2C12 myoblasts incubated for 48h in CM or SF.	83
Figure 3.8. Wound healing assay with cell count analysis (CM, DM, GM, SF).	84
Figure 3.9. Cell tracking and cell death analysis (CM, DM, GM, SF).	86
Figure 3.10. Examination of chemotaxis by transwell inserts (CM, DM, GM, SF).	87
Figure 3.11. Transwell inserts cell quantifications (CM, DM, GM, SF).	88
Figure 3.12. Transwell inserts cell quantifications between GM 10% and GM 2%.	89
Figure 3.13. Changes in morphology of myotube cultures during conditioning with SF media for 3 days.	90
Figure 3.14. Wound healing assay with cell count analysis (CM vs CM-crushed).	91
Figure 3.15. Cell tracking and cell death analysis (CM vs CM-crushed).	92
Figure 3.16. Examination of cell chemotaxis by transwell inserts comparing CM vs CM- crushed.	93
Figure 3.17. Western blots (GM, DM, SF, CM).	94
Figure 3.18. pAKT quantification (GM, DM, SF, CM).	95
Figure 3.19. pERK 1/2 quantification (GM, DM, SF, CM).	96
Figure 3.20. Myogenin and MyoD expression (DM, GM, CM).	97

Figure 3.21. Western blots (CM with 10µM LY294002 and 5µM UO126).....	98
Figure 3.22. Quantification of pAKT (CM with 10µM LY294002 and 5µM UO126). ...	99
Figure 3.23. Quantification of pERK1/2 (CM with 10µM LY294002 and 5µM UO126).	100
Figure 3.24. Wound healing assay with cell count analysis (CM with 10µM LY294002 and 5µM UO126).....	101
Figure 3.25. Cell tracking and cell death analysis (CM with 10µM LY294002 and 5µM UO126).	102
Figure 4.1. Phase-contrast microscopy investigating the effects of DM on p5 or p50 myoblasts.	115
Figure 4.2. CK assay, measuring CK activity between p5 and p50 myoblasts incubated for 3 days with DM.....	116
Figure 4.3. Examining the gene expression of MyoD and Myogenin between p5 and p50 myoblasts at d1 following treatment with DM.	117
Figure 4.4. Western blots (p5 vs p50 myoblasts in CM).	118
Figure 4.5. Quantification of pAKT levels (p5 vs p50 myoblasts in CM).....	119
Figure 4.6. Quantification of pERK1/2 levels (p5 vs p50 myoblasts in CM).....	120
Figure 4.7. Wound healing assay with cell count analysis (p5 vs p50 myoblasts in CM).	121
Figure 4.8. Cell tracking and cell death analysis (p5 vs p50 myoblasts in CM).....	122
Figure 4.9. Wound healing assay with cell count analysis (p5 myoblasts with p5 CM or p50 CM).....	124
Figure 4.10. Cell tracking and cell death analysis (p5 myoblasts with p5 CM or p50 CM).	125
Figure 5.1. Effects of different concentrations of BpV(Hopic) on myotube formation.	139
Figure 5.2. CK assay (DM with different concentrations of BpV(Hopic)).....	140
Figure 5.3. RT-PCR analyses of MyoD and Myogenin mRNA expression levels following different concentrations of Bpv(Hopic).	141
Figure 5.4. Flow cytometric analysis (DM vs DM+10µM BpV(Hopic)).....	142
Figure 5.5. Anti-phospho-tyrosine Western blot analyses (py20 antibody) tested the specificity of different concentrations of Bpv(Hopic).	143
Figure 5.6. Western blot analysis (CM with different concentrations of Bpv(Hopic)). .	144
Figure 5.7. Quantification of pAKT levels (CM, CM+1µM Bpv(Hopic) and CM+2µM Bpv(Hopic)).....	145
Figure 5.8. Quantification of pERK1/2 levels (CM, CM+1µM Bpv(Hopic) and CM+2µM Bpv(Hopic)).....	147
Figure 5.9. Preliminary experiments examining the migration potential between CM and 1µM, 2µM and 10µM concentrations of Bpv(Hopic).	148
Figure 5.10. Cell adhesion assay examines the time required for cells to adhere to the substratum (0.2% gelatin).	149
Figure 5.11. Wound healing assay with cell count analysis (CM vs CM+1µM Bpv(Hopic)).....	151
Figure 5.12. Cell tracking and cell death analysis (CM vs CM+1µM Bpv(Hopic)).....	152
Figure 5.13. Western blots (CM, CM+1µM Bpv(Hopic) and CM+1µM Bpv(Hopic)+10µM LY294002).....	153
Figure 5.14. Quantification of pAKT levels (CM, CM+1µM Bpv(Hopic) and CM+1µM Bpv(Hopic)+10µM LY294002).....	154
Figure 5.15. Quantification of pERK1/2 levels (CM, CM+1µM Bpv(Hopic) and CM+1µM Bpv(Hopic)+10µM LY294002).	156
Figure 5.16. Wound healing assay with cell count analyses (CM, CM+1µM Bpv(Hopic) and CM+1µM Bpv(Hopic)+10µM LY294002).....	158

Figure 5.17. Cell tracking and cell death analysis (CM, CM+1 μ M Bpv(Hopic) and CM+1 μ M Bpv(Hopic)+10 μ M LY294002).	159
Figure 5.18. Western blots (CM, CM+1 μ M Bpv(Hopic) and CM+1 μ M Bpv(Hopic)+5 μ M UO126).	160
Figure 5.19. Quantification of pAKT levels (CM, CM+1 μ M Bpv(Hopic) and CM+1 μ M Bpv(Hopic)+5 μ M UO126).	161
Figure 5.20. Quantification of pERK1/2 levels (CM, CM+1 μ M Bpv(Hopic) and CM+1 μ M Bpv(Hopic)+5 μ M UO126).	163
Figure 5.21. Wound healing assay with cell count analysis (CM, CM+1 μ M Bpv(Hopic) and CM+1 μ M Bpv(Hopic)+5 μ M UO126).	165
Figure 5.22. Cell tracking and cell death analyses (CM, CM+1 μ M Bpv(Hopic) and CM+1 μ M Bpv(Hopic)+5 μ M UO126).	166
Figure 5.23. Western blots investigating the effect of 1 μ M, 2 μ M and 10 μ M concentrations of Bpv(Hopic) on p-FAK(Tyr397) activation.	167
Figure 5.24. Western blots (CM, CM+2 μ M PF-228, CM+2 μ M Bpv(Hopic), CM+2 μ M Bpv(Hopic)+2 μ M PF-228).	168
Figure 5.25. Quantification of pFAK levels (CM, CM+2 μ M PF-228, CM+2 μ M Bpv(Hopic), CM+2 μ M Bpv(Hopic)+2 μ M PF-228).	170
Figure 5.26. Quantification of pAKT levels (CM, CM+2 μ M PF-228, CM+2 μ M Bpv(Hopic), CM+2 μ M Bpv(Hopic)+2 μ M PF-228).	171
Figure 5.27. Quantification of pERK1/2 levels (CM, CM+2 μ M PF-228, CM+2 μ M Bpv(Hopic), CM+2 μ M Bpv(Hopic)+2 μ M PF-228).	172
Figure 5.28. Wound healing assay with cell count analysis (CM, CM+2 μ M PF-228, CM+2 μ M Bpv(Hopic), CM+2 μ M Bpv(Hopic)+2 μ M PF-228).	174
Figure 5.29. Cell tracking and cell death analysis (CM, CM+2 μ M PF-228, CM+2 μ M Bpv(Hopic), CM+2 μ M Bpv(Hopic)+2 μ M PF-228).	176
Figure 6.1. Effects of Bpv(Hopic) and serial passaging on myotube formation.....	192
Figure 6.2. CK assay, measuring CK activity between p5 and p50 myoblasts incubated for 3 days in DM with and without 10 μ M Bpv(Hopic).	193
Figure 6.3. Flow cytometric analysis (p5 and p50 myoblasts incubated in DM with and without 10 μ M Bpv(Hopic)).	195
Figure 6.4. Analysis of the percentage of p5 and p50 cells in S/G2-phases of the cell cycle after treatment with DM or DM+10 μ M Bpv for 20h.	196
Figure 6.5. MyoD gene expression levels in p5 and p50 myoblasts incubated for 3 days in DM with and without 10 μ M Bpv(Hopic).	199
Figure 6.6. Myogenin gene expression levels in p5 and p50 myoblasts incubated for 3 days in DM with and without 10 μ M Bpv(Hopic).	203
Figure 6.7. Spire1 gene expression levels in p5 and p50 myoblasts incubated for 3 days in DM with and without 10 μ M Bpv(Hopic).	207
Figure 6.8. Spire2 gene expression levels in p5 and p50 myoblasts incubated for 3 days in DM with and without 10 μ M Bpv(Hopic).	210
Figure 6.9. Formin1 gene expression levels in p5 and p50 myoblasts incubated for 3 days in DM with and without 10 μ M Bpv(Hopic).	213
Figure 6.10. Formin2 gene expression levels in p5 and p50 myoblasts incubated for 3 days in DM with and without 10 μ M Bpv(Hopic).	215

ABBREVIATIONS

ARP2/3 = actin-related protein 2/3
BMPs = Bone morphogenic proteins
BpV = Bisperoxovanadium
CDC42 = Cell division control protein 42 homolog
CK = Creatine Kinase
CM = Conditioned media
DM = Differentiation media
DMD = Duchenne muscular dystrophy
DMEM = Dulbecco's modified Eagles medium
ECM = Extracellular matrix
ERK = Extracellular signal-regulated kinases
FAK = Focal adhesion kinase
FGF = Fibroblast growth factors
GM = Growth media
HGF = Hepatocyte growth factor/scatter factor
IGFs = Insulin growth factors
IL-6 = Interleukin-6
JNK = c-Jun N-terminal kinases
LIF = Leukemia inhibitory factor
MAPK = Mitogen-activated protein kinase
MBS = Myosin binding subunit
MHC = Myosin heavy chain
MLC = Myosin light-chain
MLCK = Myosin light-chain kinase
MMPs = Matrix metalloproteinases
MRFs = Myogenic regulatory factors
NO = Nitric oxide
N-WASP = neuronal Wiskott-Aldrich Syndrome protein
P160-ROCK = p160-Rho-associated protein kinase
PDGF = Platelet-derived growth factor
PI3K = Phosphoinositide 3-kinase
PIP2 = Phosphatidylinositol 4,5 bisphosphate
PIP3 = Phosphatidylinositol 3,4,5 trisphosphate
PTEN = Phosphatase and tensin homologue deleted on chromosome 10
RAC = Ras-related C3 botulinum toxin substrate
RHO = Ras homolog gene family
SCAR = Suppressor of cAMP receptor
SF = Serum-free
SHH = Sonic hedgehog homolog
TGF- = Transforming growth factor beta
TNF- = Tumor necrosis factor-alpha
WASP = Wiskott-Aldrich syndrome protein
WAVE = WASP-family verpolin homologous

CHAPTER 1

1. INTRODUCTION

1.1. OVERVIEW

Skeletal muscle is a remarkable tissue, which is able to adapt to a variety of stimuli and physiological demands. However, it also responds to different pathological conditions, associated with loss of muscle mass or muscle wasting, leading to weakness, loss of functional independence or even death. These maladaptations can occur as a consequence of ageing, traumatic injuries, muscular dystrophies, cancer cachexia and other diseases. Finding muscle-specific treatments for these conditions will help improve the health and lifestyle of millions of people worldwide and will reduce the increasing health and socio-economic burden associated with symptoms of muscle loss. Significant research efforts have been focused on developing treatments for devastating diseases, such as Duchenne muscular dystrophy (DMD), and clinical trials have been performed, but with limited success. Further work is needed in all areas of muscle research. Improving our understanding of the mechanisms and the molecular regulators that control processes, such as muscle development and regeneration, may provide us with important tools in our struggle to improve the symptoms associated with various conditions or diseases affecting skeletal muscle.

1.2. SKELETAL MUSCLE DEVELOPMENT

All skeletal muscles, excluding those of the head, originate from the somites and are formed in a highly complicated yet coordinated process involving different classes of progenitor cells (including embryonic myoblasts, foetal myoblasts and satellite cells) and a variety of internal and external cues. For detailed reviews on the origin of muscle and muscle progenitor cells and the regulators involved, see: (Bailey *et al.*, 2001, Buckingham *et al.*, 2003, Cossu and Biressi, 2005, Hawke and Garry, 2001, Messina and Cossu, 2009).

Somites are masses of mesoderm in the developing vertebrate embryo, distributed along the two sides of the neural tube, adjacent to the notochord (Figure 1.1). Somites develop into distinct cellular compartments that later become the dermis (dermatome), vertebrae (sclerotome) and skeletal muscle (myotome). A somite is divided into the epaxial (which gives rise to the back musculature) and hypaxial (giving rise to limb, abdominal and intercostal

musculature) domains (Buckingham *et al.*, 2003, Christ and Ordahl, 1995, Kablar *et al.*, 1997).

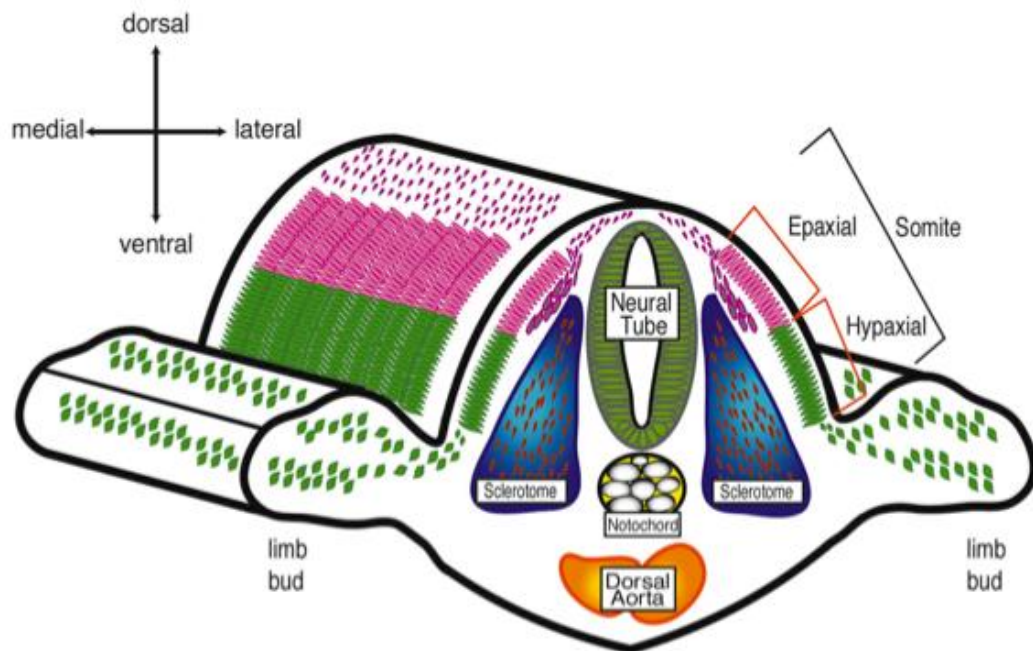


Figure 1.1. A schematic representation of a somite. Somite is separated into epaxial and hypaxial regions, with its surrounding structures, including the notochord, neural tube and dorsal aorta, which can provide signals regulating the fate and movement of precursor cells. Precursor cells originating from the epaxial region of a somite contribute to the back musculature, while precursor cells from the hypaxial region migrate to the newly formed limb buds. Figure is adapted from (Hawke and Garry, 2001).

Progenitor cells, originating in the hypaxial domain of the somite, delaminate and migrate into the limb bud, where they proliferate and express myogenic determination factors. It is thought that local factors from neighboring tissues provide the instructions for the muscle progenitor cells to migrate, proliferate and initiate the myogenic differentiation program (Buckingham *et al.*, 2003, Hawke and Garry, 2001). The first muscle fibres, known as primary fibres, form around embryonic days 11-14 in mouse limbs. Around embryonic days 14-16, initially smaller in size, secondary fibres form parallel to the primary fibres and innervation begins (Cossu and Biressi, 2005, Messina and Cossu, 2009, Ontell and Kozeka, 1984). It is thought that two distinct cell types contribute to primary (embryonic myoblasts) and secondary fibres (foetal myoblasts). Biressi *et al.* show that purified embryonic and foetal myoblasts express different genes,

revealing that they are intrinsically different cell populations (Biressi *et al.*, 2007), which is also supported by an observation that they also behave differently in cell culture (Cossu and Molinaro, 1987).

After secondary fibre formation, basal lamina develops around each fibre and at this stage satellite cells, playing a central role in postnatal myogenesis and muscle regeneration, can be morphologically identified, lying between the basal lamina and the fibre. During peri- and post-natal periods, satellite cells divide at a slow rate and part of their progeny fuse with adjacent fibres to contribute new nuclei and thus increase the size of the fibres (Cossu and Biressi, 2005, Messina and Cossu, 2009). At the end of postnatal growth, satellite cells enter in a quiescent state, but can later be activated to contribute to muscle regeneration, if muscle damage occurs (reviewed in (Charge and Rudnicki, 2004)).

The exact origin of satellite cells of the trunk and limbs remains debatable. Different concepts proposed origins of the satellite cells from the somites, from preexisting lineages, such as embryonic, foetal myoblasts, or endothelial cell precursors, or from both somitic and nonsomitic sources (Hawke and Garry, 2001, De Angelis *et al.*, 1999, Zammit *et al.*, 2006). However, the prevalent concept to date is that all muscle progenitors, including satellite cells, derive from the somites (Schienda *et al.*, 2006, Schultz and McCormick, 1994, Gros *et al.*, 2005).

1.3. MOLECULAR REGULATORS OF MUSCLE DEVELOPMENT

The coordination of the events required for morphological development of the skeletal musculature, is extremely complex, involving a variety of intrinsic and extrinsic factors. Most of the knowledge of the embryology of myogenesis comes from experimental manipulations of chick embryos and chick/quail chimeras and gene knockout studies in mice, which have revealed a great amount of information on the external and internal cues guiding this process. These studies have provided a relatively good understanding of the main molecular regulators driving the development of muscle and are described below.

In the newly formed somites, progenitors respond to signals, such as Wnt proteins, Sonic hedgehog homolog (SHH) and Bone morphogenic proteins (BMPs), which are derived from anatomically adjacent structures, such as the neural tube, notochord, the overlying ectoderm and the aorta (Cossu *et al.*, 1996, Hawke and Garry, 2001, Maroto *et al.*, 1997, Miller *et al.*, 1999, Munsterberg and

Lassar, 1995). Pax-3 gene is important during limb development for the activation of myogenic regulatory factors (MRFs), such as Myf5 and MyoD (Maroto *et al.*, 1997, Tajbakhsh *et al.*, 1997). MyoD and myf5 expression is important for muscle precursor cell determination to a myogenic fate, as shown in double Myf5/MyoD mutants, where no skeletal muscle forms, as cells in the somite do not locate correctly to sites of myogenesis and therefore adopt non-myogenic fates (Rudnicki *et al.*, 1993, Tajbakhsh *et al.*, 1996). It is generally considered that MyoD and Myf5 play central roles in myogenic fate determination, while Myogenin, MRF4 and Mef2 are involved in the process of terminal differentiation of the committed precursor cells into muscle fibres. It is known that cells that migrate from the somite have not yet activated the myogenic determination genes of the MyoD family, and they only start expressing these when they reach their final location, triggered by signalling molecules from the local environment, such as Wnt and SHH (Buckingham *et al.*, 2003, Cossu and Borello, 1999, Tajbakhsh *et al.*, 1998, Tajbakhsh and Buckingham, 1994). Before muscle progenitors upregulate the expression of MyoD and Myf5, in order to form skeletal muscle, they need to proliferate locally. Fibroblast growth factors (FGF) signalling is thought to be important for myoblast proliferation (Edom-Vovard *et al.*, 2001, Prykhodzij and Neumann, 2008) and also migration in the limb (Webb *et al.*, 1997).

In addition to Pax3, other genes, such as c-Met, msx1 and Lbx, are important for myogenic precursor cells during development (Bendall *et al.*, 1999, Brohmann *et al.*, 2000, Gross *et al.*, 2000, Wang and Sassoon, 1995, Yang *et al.*, 1996). c-Met, a tyrosine kinase receptor for HGF, produced by non-somatic mesodermal cells is important for both delamination and migration of the precursor cells from the somites (Dietrich *et al.*, 1999). In mutant mouse embryos, which lack functional c-Met or HGF, skeletal muscle is absent from the limbs (Bladt *et al.*, 1995, Schmidt *et al.*, 1995). Lbx1 is a transcription factor, which is also implicated in the migration of the cells from the somite (Schafer and Braun, 1999). Along with other factors important for embryonic myogenesis, gene expression of both Lbx1 and c-Met are also shown to be dependent on Pax3 (Epstein *et al.*, 1996, Mennerich *et al.*, 1998).

As muscle is able to regenerate after damage, it is thought that this process shares many similarities with embryonic myogenesis on a molecular level, but differences are also proposed. Zhao and Hoffman have used samples of

regenerating muscle to demonstrate that embryonic positional signals, such as Wnt, SHH, and BMP, are not induced in postnatal muscle regeneration (Zhao and Hoffman, 2004). Others have later shown that Wnt is important for myogenic progenitor proliferation and differentiation during post-natal myogenesis and regeneration and that SHH also plays roles in post-natal muscle regeneration (Brack *et al.*, 2008, Le Grand *et al.*, 2009, Straface *et al.*, 2009). Embryonic myogenesis and regeneration indeed share similarities in the requirement of factors involved in muscle proliferation and differentiation, such as FGFR4, MyoD, Myf5 and Myogenin (Cornelison and Wold, 1997, Grounds *et al.*, 1992, Zhao and Hoffman, 2004). Fusion and migration mechanisms are also similar: c-Met and HGF signalling, for example, remain of major importance for satellite cells activation and migration during adult muscle regeneration (Bischoff, 1997, Tatsumi *et al.*, 1998, Zhao and Hoffman, 2004). Thus, muscle regeneration and muscle development share similarities on a molecular level, but further research will reveal in greater detail the regulators driving both processes. In the following chapters, the regenerative capacity of satellite cells and their progeny will be reviewed, along with their potential involvement in proposed therapies for muscle degenerative diseases, such as DMD.

1.4. POSTNATAL SKELETAL MUSCLE REGENERATION AND PLASTICITY

Postnatally, adult mammalian skeletal muscle is a relatively stable tissue with little turnover of nuclei - no more than 1-2% of myonuclei are replaced every week (Schmalbruch and Lewis, 2000). The constitutive cell type and the contractile unit of skeletal muscle, the multinucleated myofibre, is terminally differentiated and incapable of mitotic activity. Nevertheless, skeletal muscle has a remarkable ability to adapt to various stimuli and physiological demands, such as exercise, disuse, denervation, hypoxia, nutritional intervention, genetic disorders and others (Charge and Rudnicki, 2004, Fluck and Hoppeler, 2003, Hawke and Garry, 2001). It has the ability of rapid regeneration following injury (e.g. extensive physical activity, such as resistance training) and is able to increase (hypertrophy) or decrease (atrophy) in mass. This is possible due to the activity of a small population of cells resident in adult skeletal muscle, known as satellite cells, which make possible its regenerative ability, even after repetitive injury.

This is of major importance, because if skeletal muscle is left unrepaired, it can lead to loss of muscle mass, locomotive deficiency and ultimately even death.

1.5. SATELLITE CELLS ARE OF MAJOR IMPORTANCE OF MUSCLE REPAIR

Satellite cells, first described by Mauro in 1961 (Mauro, 1961), and thus considered as providing the oldest known stem cell niche, are small mononuclear cells sandwiched between the basement membrane/basal lamina and the plasmalemma of mature muscle fibres. They are present in all skeletal muscles, although differently distributed (Gibson and Schultz, 1982). Under normal physiological conditions, satellite cells are quiescent. They are characterised by small nucleus with increased amounts of heterochromatin, compared to myofibre nuclei, reduced nuclear to cytoplasmic ratio and reduced organelle numbers, which suggests lower transcription activity and supports the notion that they are normally in a quiescent state (Schultz *et al.*, 1978, Snow, 1983). However, upon injury, satellite cells are activated and are able to proliferate, self-renew and differentiate. Their progeny are able to fuse with each other or with preexisting myofibres, thus promoting regeneration of damaged muscles by contributing new myonuclei to muscle fibres undergoing repair (reviews: (Kuang *et al.*, 2008, Zammit, 2008)). Indeed, resistance training studies have demonstrated increased satellite cell activity and addition of myonuclei to muscles that undergo hypertrophy (Adams, 2006, Kadi *et al.*, 1999), underpinning their importance not only to repair processes, but also for hypertrophy. Further evidence for this has been provided by selective irradiation experiments, causing death or preventing proliferation of satellite cells, which resulted in reduced muscle regeneration and hypertrophy (Adams *et al.*, 2002, Alameddine *et al.*, 1989, Li *et al.*, 2006, Quinlan *et al.*, 1995, Rosenblatt and Parry, 1992). Thus, it is commonly accepted that satellite cells and their fusion competent progeny of myoblasts, by supplying myonuclei to growing or regenerating myofibres, are responsible for skeletal muscle plasticity and ability to repair and grow in mass after e.g. traumas or exercise (reviews: (Adams, 2006, Charge and Rudnicki, 2004, Hawke and Garry, 2001).

1.6. MUSCLE REGENERATION PHASES

Muscle regeneration following injury, is known to involve two phases - degenerative and regenerative phases (Carosio *et al.*, 2011, Charge and Rudnicki, 2004, Crisco *et al.*, 1994). The degenerative phase, following muscle injury, involves the events leading to necrosis of the muscle fibres: disruption of the myofibre sarcolemma, increased myofibre permeability leading to calcium influx, activation of calpain proteases that induce the cleavage of myofibrillar and cytoskeletal proteins, which subsequently leads to proteolysis of the myofibres (Belcastro *et al.*, 1998, Bodensteiner and Engel, 1978, Charge and Rudnicki, 2004, Kwak *et al.*, 1993, Oberc and Engel, 1977). The disruption of the myofibre sarcolemma results in increased serum levels of CK, which is normally restricted to the myofibre cytosol. This increase in serum CK levels is an event usually observed after mechanical stress or in muscle degenerative diseases (Coulton *et al.*, 1988, Nicholson *et al.*, 1979, Percy *et al.*, 1979). The damaged tissues are thought to release factors, which attract circulating inflammatory cells to the injured site, in order to clear the debris, and the last can also activate the satellite cells and thus trigger the muscle repair process/regeneration phase (Bischoff, 1986, Fielding *et al.*, 1993, Lescaudron *et al.*, 1999, Tidball, 1995, Tidball, 2005). Neutrophils are the first inflammatory cells to infiltrate the site of muscle injury, followed by macrophages (Belcastro *et al.*, 1996, Fielding *et al.*, 1993, Tidball, 1995). Inflammatory cells contribute not only to cell debris removal, but also to facilitating the regenerating phase of damaged muscle (Arnold *et al.*, 2007, Lescaudron *et al.*, 1999, Merly *et al.*, 1999, Robertson *et al.*, 1993, St Pierre and Tidball, 1994). Macrophages are shown to secrete growth factors and cytokines that can activate satellite cells and induce proliferation of myoblasts (Cantini and Carraro, 1995, Cantini *et al.*, 1994, Massimino *et al.*, 1997, Merly *et al.*, 1999). It is demonstrated that neutrophils play a prominent role in muscle regeneration, possibly due to their ability to clear debris by phagocytosis and to recruit other inflammatory cells (Teixeira *et al.*, 2003). It has also been demonstrated that reduction of the inflammatory response by pharmacological depletion of monocytes/macrophages leads to moderately impaired repair of the injured muscle (Summan *et al.*, 2006). These studies support the notion that inflammatory cells act as an integral part of muscle regeneration processes by clearing cellular

debris and also by providing mediators necessary for the complete regeneration of injured muscle.

The regenerative phase of post-injured skeletal muscle is mediated through the activity of the satellite cells residing within the muscle tissue (Figure 1.2). The expansion of myogenic cells provides a source of new myonuclei for regenerating myofibres and, as previously discussed, numerous experiments have demonstrated the importance of proliferating myogenic precursors for this process. Under normal physiological conditions, satellite cells are quiescent, but in response to secreted factors released in the damaged environment (after injury, exercise or in pathological conditions and degenerative diseases), they are activated. They migrate to the site of damage, proliferate to generate a progeny of myoblasts, which are capable of fusing with damaged myofibres and of differentiating in order to promote muscle repair (reviewed in (Charge and Rudnicki, 2004, Hawke and Garry, 2001, Turner and Badylak, 2011)). Satellite cell activation is not restricted to the damaged site; damage to fibre triggers activation and migration of satellite cells along the entire length of the fibre, and in rare conditions satellite cells from adjacent muscles are able to be recruited (Schultz *et al.*, 1985, Schultz *et al.*, 1986).

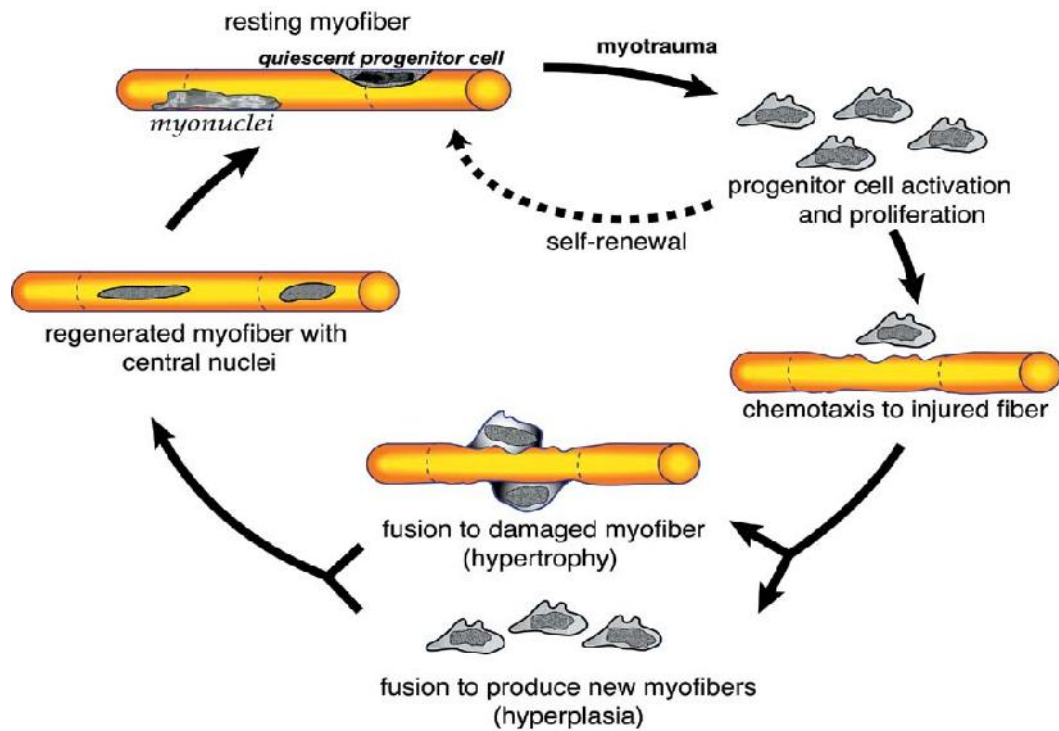


Figure 1.2. The stages of adult skeletal muscle regeneration.

After myofibre damage, resident satellite cells are activated, migrate to the damaged area and proliferate to generate a progeny of fusion competent myoblasts. Some of the satellite cells will self-renew and return to quiescent stage to contribute to future regeneration events. The generated progeny of myoblasts will fuse with each other or add new myonuclei to the damaged myofibre, thus promoting its repair. Figure is adapted from (Hawke and Garry, 2001).

It has been suggested that other non-muscle stem cell populations can also participate in the muscle regeneration process or in maintaining the satellite cell pool (reviewed in (Otto *et al.*, 2009)), including: neural stem cells (Galli *et al.*, 2000), bone marrow (Ferrari *et al.*, 1998), mesenchymal stem cells (Young *et al.*, 2001), adipose tissue stem cells (Di Rocco *et al.*, 2006). However, the level of their contribution remains elusive and more research is needed in this area. The contribution of non-muscle stem cell populations and their potential involvement in muscle regeneration is beyond the scope of this review.

It is thought that quiescent satellite cells do not express genes belonging to the MRF family (MyoD, Myogenin, MRF4), with the exception of Myf5 (Beauchamp *et al.*, 2000, Zammit *et al.*, 2004a). Once activated, satellite cells enter the cell cycle, proliferate as myoblasts and upregulate the expression of MyoD and Myf5 genes, providing the myogenic fate determination required for further differentiation and muscle repair (Charge and Rudnicki, 2004, Cooper *et al.*,

1999, Cornelison *et al.*, 2000, Cornelison and Wold, 1997, Creuzet *et al.*, 1998, Smith *et al.*, 1994, Yablonka-Reuveni and Rivera, 1994, Zammit, 2008). Following the proliferation phase, myogenin and MRF4 upregulation will trigger the differentiation of the myoblasts, followed by permanent exit from the cell cycle.

It is considered that the temporal balance between pathways, such as Notch and Wnt, is of major importance in regulating the proliferation and differentiation of satellite cells. Notch appears to be important for satellite cell proliferation, blocking differentiation until there are sufficient numbers of progenitor cells for repair (Conboy and Rando, 2002, Kuang *et al.*, 2007). Wnt is an important regulator of differentiation, while GSK3b is reported to mediate the cross-talk between Notch and Wnt pathways to precisely coordinate the events of proliferation and differentiation (Brack *et al.*, 2008).

Activation of muscle-specific proteins, such as Myosin heavy chain (MHC), characterise the differentiation phase, which is followed by the fusion of the cells with the damaged muscle fibre in order to promote its repair (Charge and Rudnicki, 2004). Myoblasts can also fuse with each other, forming myotubes to initiate de novo formation of myofibres within the basal lamina of cells that have been destroyed (Doherty *et al.*, 2005). Fusion alone, is a complex process involving variety of cytoskeletal and transmembrane proteins and signalling mechanisms. Cadherins and calpains are some of the proteins shown to have important functions in the process of myoblast fusion (Dourdin *et al.*, 1999, Kaufmann *et al.*, 1999). The regeneration process is finalised after the remodelling of connective tissue and blood vessels and the functional recovery of skeletal muscle.

1.7. MARKERS OF SATELLITE CELLS

Since their discovery, the identification of specific satellite cell markers has facilitated the research in the area of muscle regeneration. These markers include Pax7, M-cadherin, Myf5, c-Met, CD34, Calveolin-1, Syndecans -3 and -4 (Allen *et al.*, 1995, Beauchamp *et al.*, 2000, Cornelison *et al.*, 2001, Cornelison and Wold, 1997, Irintchev *et al.*, 1994, Seale *et al.*, 2000, Volonte *et al.*, 2005). All satellite cells express Pax7 (an orthologue of Pax3), which is present in both quiescent and activated states, and its expression is downregulated upon myogenic

differentiation (Halevy *et al.*, 2004, Seale *et al.*, 2000). Pax3 is expressed only in quiescent satellite cells in a few muscle groups (Relaix *et al.*, 2006, Tedesco *et al.*, 2010). Pax 7 is shown to be required for satellite cells survival and maintenance, demonstrated by the fact that Pax7-null animals show defects in regenerative myogenesis (Oustanina *et al.*, 2004). Pax7 ^{-/-} mice, whose muscles have satellite cells absence, fail to grow postnatally, show a 50% decrease in body weight and die within 2 weeks after birth (Mansouri *et al.*, 1996, Seale *et al.*, 2000). However, Lepper *et al.*, applying Cre/loxP lineage tracing and conditional gene inactivation, have suggested that Pax7, along with Pax3, may not be required during adult limb muscle regeneration, even after repetitive injury, which is in obvious contrast with the essential roles of these genes during embryonic myogenesis (Lepper *et al.*, 2009). It seems, therefore, that Pax7 may be required up to the juvenile period when progenitor cells transition into quiescence.

1.8. SELF-RENEWAL OF SATELLITE CELLS

Satellite cells are a heterogeneous population, consisting of stem cells and committed myogenic progenitors and that not all of them possess stem cell properties (Kuang *et al.*, 2008, Kuang *et al.*, 2007, Schultz, 1996, Zammit, 2008). It is suggested that approximately 80% of the satellite cells divide rapidly and contribute to muscle regeneration, while the other 20% serve as “reserve cells” to replenish the satellite cell pool. This supports the notion that satellite cells are able to self-renew - an important characteristic of a stem cell, allowing the maintenance of the number of cells for future regeneration events (Kuang *et al.*, 2007, Sacco *et al.*, 2008). As described by Otto *et al.*, in order for the satellite cell pool to be maintained, a proportion of the satellite cell progeny must either stop itself from progressing down the myogenic lineage and revert back to quiescent state, or they must alternatively divide asymmetrically to form both differentiated and non-differentiated progeny (Otto *et al.*, 2009). There is evidence that both scenarios may occur *in vivo*, which means that they are not mutually exclusive (Kuang *et al.*, 2007, Zammit *et al.*, 2004b). Signalling pathways, such as Notch and Wnt seem to differentially regulate symmetric and asymmetric division of satellite cells (Conboy and Rando, 2002, Le Grand *et al.*, 2009).

1.9. COMMON EXTRACELLULAR FACTORS REGULATING MUSCLE REGENERATION

After muscle injury, myogenic progenitors and subsequent muscle regeneration can be regulated by different stimuli from various sources, such as signals released from injured fibres or from invading inflammatory cells (Bischoff, 1986, Chen and Quinn, 1992, Merly *et al.*, 1999, Tidball, 2005). Such factors, involved in the regulation of satellite cell activation, include HGF (Tatsumi *et al.*, 1998), nitric oxide (NO) (Anderson, 2000, Wozniak and Anderson, 2007) and possibly FGF (Floss *et al.*, 1997). These and other factors have been shown to exert effects on muscle regeneration not only by directly influencing myogenic cells, but also indirectly by influencing other important components/processes, such as inflammatory cells, angiogenesis, neuron formation and extracellular matrix secretion. A schematic representation of the complexity of growth factors influencing satellite cells is presented on Figure 1.3.

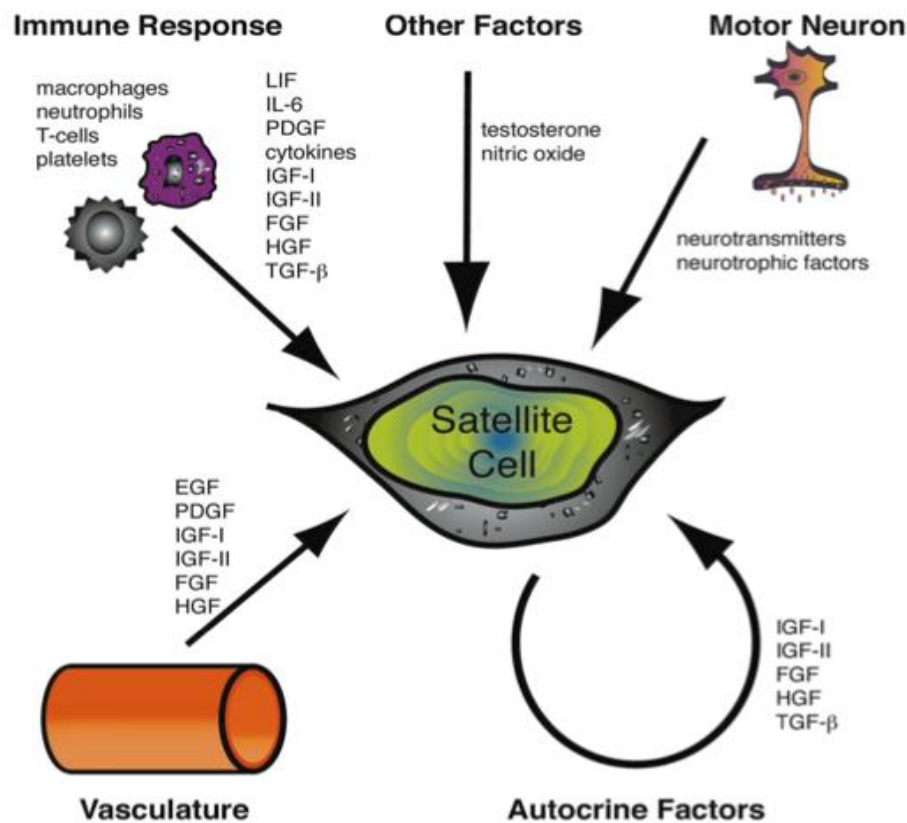


Figure 1.3. Soluble factors in myogenesis.

Many soluble factors may be released from different tissues or cells that can modulate the activity of satellite cells and control processes, such as proliferation, migration or differentiation of both myogenic and non-myogenic cells. The balance of these soluble factors can ultimately determine the state of the muscle tissue or the regeneration process. Figure adapted from (Hawke and Garry, 2001).

Below, the effects of some of the most well-studied growth factors on satellite cells and skeletal muscle adaptation are summarised. A detailed review of the involvement of different soluble factors during muscle regeneration would be beyond the scope of this thesis. More detailed information is provided in the following reviews (Charge and Rudnicki, 2004, Hawke and Garry, 2001, Husmann *et al.*, 1996, Karalaki *et al.*, 2009).

Members of the FGF family, despite a wide variety of functions, are mostly known for their mitogenic effects. FGF6 is of particular interest in skeletal muscle repair, as its expression is muscle specific and is upregulated during muscle regeneration (Floss *et al.*, 1997, Kastner *et al.*, 2000). Sources of FGF include the infiltrating macrophages (Tidball, 1995) or the damaged muscle itself, depending on the degree of injury (Clarke *et al.*, 1993). Four receptors for FGFs have been identified (FGFR 1-4), all are transmembrane tyrosine kinases, of which FGFR-1

and FGFR-4 are most prominent in satellite cells. In addition to their proposed role in regulating satellite cell activation, FGFs have mostly been implicated in mediating myogenic proliferation and inhibiting differentiation (Allen and Boxhorn, 1989, Charge and Rudnicki, 2004, Doumit *et al.*, 1993, McFarland *et al.*, 1993, Rosenthal *et al.*, 1991, Sheehan and Allen, 1999, Yablonka-Reuveni *et al.*, 1999, Kastner *et al.*, 2000). MAP kinase signalling pathway is important for the FGF-mediated effect on proliferation (Jones *et al.*, 2001).

Transforming growth factor beta (TGF- β) belongs to a family of growth factors, consisting of TGF β 1, 2 and 3, transducing their signals through the SMAD family of proteins (Whitman, 1998). Myostatin is also known as a member of this family. TGF- β is released by platelets and also secreted by muscle cells and is known to inhibit both proliferation and differentiation of satellite cells, although the actions of TGF- β often vary depending on which other growth factors are present (Allen and Boxhorn, 1987, Assoian and Sporn, 1986, Lafyatis *et al.*, 1991, Lefaucheur and Sebille, 1995, Husmann *et al.*, 1996, McLennan and Koishi, 2002). Like FGF, it is able to stimulate angiogenesis (Roberts *et al.*, 1986) and the synthesis of extracellular matrix (ECM) proteins (Ignotz and Massague, 1986). TGF- β exerts indirect functions on muscle regeneration by modulating the immune response - it is known to be chemotactic and to activate monocytes, which also induce angiogenesis and secrete growth factors (Husmann *et al.*, 1996). Other roles of TGFs during muscle regeneration, reviewed in (McLennan and Koishi, 2002), include motor neuron survival and reduced myoblast fusion.

Insulin growth factors (IGFs) are well known for their proliferation and differentiation effects, influencing muscle metabolism and stimulating protein synthesis. IGFs are upregulated in regenerating muscle (Edwall *et al.*, 1989, Krishan and Dhoot, 1996, Levinovitz *et al.*, 1992) and are well known promoters of cell survival (mediated by Phosphoinositide 3-kinase (PI3K) pathway), proliferation and differentiation, influencing myogenic regulatory factors, which lead to muscle hypertrophy (Adams and McCue, 1998, Allen and Boxhorn, 1989, Coleman *et al.*, 1995, Florini *et al.*, 1991, Vandeburgh *et al.*, 1991, Stewart and Rotwein, 1996). Increasing the levels of IGF-I within muscle cells by various *in vivo* and *in vitro* methods leads to increases in muscle mass and sustained or enhanced hypertrophy (Adams and McCue, 1998, Barton-Davis *et al.*, 1998, Chakravarthy *et al.*, 2000, Musaro *et al.*, 2001). The effects of IGF-I on muscle hypertrophy are due to both activation of satellite cell proliferation, allowing more

myonuclei to fuse to existing myofibres, and to increasing the protein synthesis in existing myofibres (Bark *et al.*, 1998, Barton-Davis *et al.*, 1998, Musaro *et al.*, 1999, Musaro and Rosenthal, 1999, Semsarian *et al.*, 1999). IGFs may also be implicated in promoting muscle reinnervation during muscle repair (Vergani *et al.*, 1998).

Leukaemia inhibitory factor (LIF) and interleukin-6 (IL-6) are members of the IL-6 family of cytokines, sharing common receptor component and mediating their actions through shared signalling pathways (Hibi *et al.*, 1996, Pennica *et al.*, 1995). LIF acts as proliferating factor (Bower *et al.*, 1995, Spangenburg and Booth, 2002) and can be produced by regenerating muscle to increase the rate and extent of muscle regeneration (Barnard *et al.*, 1994, Kurek *et al.*, 1996b, White *et al.*, 2001). It is thought that LIF stimulates myoblast proliferation by JAK2-STAT3 signalling pathways (Spangenburg and Booth, 2002). LIF and IL-6 expression in healthy muscle is low, with their expression increased in injured muscle, suggesting trauma factor roles (Kurek *et al.*, 1996b). The role of LIF during muscle regeneration is supported by studies demonstrating that skeletal muscle regeneration is attenuated after injury in mice with targeted mutation of LIF, while exogenous administration of LIF improved the regenerative process (Kurek *et al.*, 1997). In addition, *in vivo* administration of LIF to the site of injury in mdx mice results in increased rate of muscle regeneration (Austin *et al.*, 2000, Kurek *et al.*, 1996a), supporting its beneficial function for muscle repair. IL-6 has a role in regulating the inflammation process after muscle injury and is implicated in muscle repair (Gadient and Patterson, 1999, Toumi *et al.*, 2006), in glucose metabolism and glycogen sparing (Glund *et al.*, 2007, Keller *et al.*, 2003a, Keller *et al.*, 2003b).

Hepatocyte growth factor (HGF), or scatter factor, is a key factor involved in the activation of satellite cells after injury, stimulating their proliferation and inhibiting their differentiation (Allen *et al.*, 1995, Gal-Levi *et al.*, 1998, Miller *et al.*, 2000, Tatsumi *et al.*, 1998). HGF is able to transduce its downstream signals via its tyrosine kinase receptor, c-Met, which is broadly expressed in quiescent satellite cells (Anastasi *et al.*, 1997). HGF transcripts and protein levels are increased during regeneration and it has been shown to be present in crushed muscle extract, known for its activating effect on satellite cells (Jennische *et al.*, 1993, Suzuki *et al.*, 2002, Tatsumi *et al.*, 1998, Tatsumi *et al.*, 2001). HGF is able to activate quiescent satellite cells by activating the p38-MAPK and PI3K

signalling pathways (Shi and Garry, 2006) or, alternatively, by down regulating caveolin-1 expression, leading to up-regulation of the ERK pathway (Volonte *et al.*, 2005).

An important consideration of all cytokines and growth factors in muscle repair, is that the functions exerted by these soluble factors, depend on the concentrations in which they are present and on their interaction with other factors. For example, HGF and TGF- β both act as chemoattractants for satellite cells at lower concentrations, but not at high concentrations (Bischoff, 1997). Similarly, Platelet-derived growth factor (PDGF) at low doses was shown to induce migration of fibroblasts, while high doses induced proliferation (De Donatis *et al.*, 2008). In this way, cells are able to respond differently to an increasing gradient of stimulus. Interaction of different secreted factors with each other must also be considered. For example, low doses of IGF-I, co-incubated with non-apoptotic doses of Tumor necrosis factor-alpha (TNF- α), lead to myoblast cell death not exerted by the respective concentrations of these two factors on their own (Saini *et al.*, 2008). Therefore, although we have a good idea of how different soluble factors can influence myogenic precursors in isolation and at specific doses, a better understanding is required on how these factors may interact with each other and what intracellular pathways and regulators would be differentially affected.

1.10. SKELETAL MUSCLE AND AGEING

Aged skeletal muscle is characterised with a decline in functional properties, including power, strength and endurance, partly due to the overall reduction in size of the muscles and to the switch in fibre type with age fibres (reviewed in (Brack and Rando, 2008)). The progressive and generalised loss of skeletal muscle mass and strength is known as sarcopenia, a term commonly used to describe age-related changes that occur within skeletal muscle (Cruz-Jentoft *et al.*, 2010, Doherty, 2003). Both intrinsic and extrinsic factors have been investigated and shown to be altered in aged muscle and a decrease in the number of satellite cells has also been reported. In mouse models, at birth satellite cells contribute to approx. 30% (neonatal) of the sublamellar muscle nuclei, but decrease to ~ 2-4% in adult animals (Charge and Rudnicki, 2004, Hawke and Garry, 2001, Snow, 1977). The reduction of satellite cell number has long been considered as one of the reasons for the age related muscle decline in its capacity to regenerate (Gibson

and Schultz, 1983). However, studies have been divergent, showing either a significant decline in the number of satellite cells in aged muscle, or little change or even increased numbers in aged compared to young muscles (which could also be explained by the differences in species, ages, muscle types compared and experimental procedures used for counting) (Brack and Rando, 2008). Brack and Rando suggested that although the reduced number of satellite cells in very old individuals can indeed contribute to the decline in regenerative potential, this decline with age is more severe than can be accounted for on the basis of even the largest estimates of decline in satellite cells number. Therefore, the functionality, not only the number, of muscle progenitors with age may be impaired.

Previous research has suggested that the proliferative potential of isolated satellite cells is reduced with age when they are passaged in culture conditions, coinciding with telomere shortening, and thus replicative senescence of satellite cells with ageing (Decary *et al.*, 1997, Schultz and Lipton, 1982, Webster and Blau, 1990). However, it has also been suggested that telomerase activity is retained in old muscle and it is only the myoblast progeny, when induced to differentiate that show deterioration of telomerase activity (O'Connor *et al.*, 2009). Other intrinsic factors have been proposed to play a role in ageing of skeletal muscle. Reports have revealed that expression levels of regulators of muscle differentiation, such as S100B and RAGE, are altered in old vs. young human satellite cells (Beccafico *et al.*, 2010). Using a C2C12 *in vitro* model of multiple population doublings, which retains telomerase activity, Sharples *et al.*, in our laboratories, reported that myoblasts subjected to multiple divisions displayed intrinsic differences in their growth and differentiation potential, as compared to low passage of cells, including altered IGF-I, myogenin, IGFBP-5 and IGFBP-2 expression and changes in the levels of Akt and c-Jun N-terminal kinases (JNK)1/2 phosphorylation (Sharples *et al.*, 2011). Importantly, reduced expression of myogenic regulatory factors, such as myoD and myogenin, coincide with reduced differentiation of senescent myoblasts (Bigot *et al.*, 2008). These data strongly suggest that intrinsic changes may play a major role in skeletal muscle ageing and sarcopenia.

Changes in the systemic environment are also associated with sarcopenia. It is known that old muscle is able to regenerate when transplanted in young animal, while regeneration of young muscle transplanted in old animal is impaired (Carlson and Faulkner, 1989), suggesting that the host environment is also of

major importance in muscle functionality and regenerative potential (Brack and Rando, 2007). Furthermore, parabiotic experiments, which unite the circulatory system of two animals, demonstrated rejuvenation of aged progenitor cells (both *in vivo* and *in vitro*) by exposure to a young systemic environment and vice versa – with a decline in functionality of young satellite cells exposed to an older systemic environment (Conboy *et al.*, 2005).

How can the extrinsic environment be altered with age, so that it affects the muscle regeneration capacity? It is known that the inflammatory response is very important for muscle regeneration (Tidball, 2005). Possible explanation for the effect of the old systemic environment to muscle regeneration is the reduced rates of phagocytic removal of muscle debris in old animals, coinciding with slow muscle regeneration (Grounds, 1987, Zacks and Sheff, 1982). Higher levels of pro-inflammatory cytokines, such as IL-6 and TNF- α , are also associated with lower muscle mass and strength in older men and women (Visser *et al.*, 2002). A decline in the Notch signalling pathway with age is another explanation (Conboy *et al.*, 2005). Notch is a major pathway regulating the activation and expansion of satellite cells during embryogenesis (Vasyutina *et al.*, 2007) and in the adult (Conboy and Rando, 2002); furthermore, forced activation of Notch signalling in injured muscle of aged mice restores regenerative potential to this tissue (Conboy *et al.*, 2003). On the other hand, Wnt signalling has been shown to be increased in aged muscle and in myogenic progenitors exposed to aged serum, potentially the cause of the increase in tissue fibrosis in aged muscle (Brack *et al.*, 2007). IGF signalling is also altered in old systemic environment. As previously discussed, IGF-I is important for muscle regeneration (Musaro and Rosenthal, 2006, Scicchitano *et al.*, 2009). It stimulates myogenic differentiation and proliferation and muscle hypertrophy (Engert *et al.*, 1996, Musaro *et al.*, 2001, Musaro *et al.*, 1999, Musaro and Rosenthal, 1999, Musaro and Rosenthal, 2006, Rosenthal and Cheng, 1995). It is reported that IGF-I declines during postnatal life (Velasco *et al.*, 1998), which is possibly linked to muscle atrophy with age and a decline in regeneration capacity. Supporting the important role of IGF signalling in ageing muscles, studies in which transgenic mice overexpressing the local form of IGF-I demonstrated sustained muscle mass and efficient regenerative mechanisms in senescent muscles, compared with wildtype animals (Musaro *et al.*, 2001). Therefore, changes in both the systemic environment and in the muscle progenitor

cells themselves are possibly responsible for the decline in muscle mass and strength with age and warrant further investigation.

1.11. PROPOSED THERAPIES FOR MUSCULAR DYSTROPHIES OR TRAUMAS

Muscular dystrophies are hereditary muscle diseases, characterised by chronic skeletal muscle weakness and degeneration. The most severe case, Duchenne Muscular Dystrophy, is a genetic X-linked recessive disease that affects approximately one in 3,500 male births. It is caused by mutations in the dystrophin gene, including insertions or deletions, causing frameshift errors, which lead to the dystrophin protein being completely or partially lost (Hoffman *et al.*, 1988, Hoffman and Dressman, 2001, Muntoni *et al.*, 2003). Dystrophin is the largest gene in the human genome (2.4Mb of length with 79 exons), it encodes a cytoplasmic protein, which participates in connecting the cytoskeleton of a muscle cell to the surrounding ECM through the cell membrane. It is important for keeping the integrity of a muscle cell, as it protects muscle fibres from injury when they contract and relax (Blake *et al.*, 2002, Petrof, 2002). When dystrophin is missing, as in DMD patients, this leads to vulnerability and damage of muscle fibres during contraction, resulting in constant damage-repair cycles. As a consequence, muscle damage prevails and patient mobility is highly affected, resulting in wheelchair dependency by the age of 10-12 years and in most cases death due to respiratory failure between the age of 17 and 30 (reviews: (Cossu and Sampaolesi, 2007, Emery, 2002, Nowak and Davies, 2004, Quattrocelli *et al.*, 2010)).

Depletion of the satellite cell pool is observed in muscular dystrophy patients due to continuous activation and repair of damaged fibres (Jejurikar and Kuzon, 2003, Webster and Blau, 1990). Satellite cells, triggering the muscle regeneration process, are unable to comply with the rate of damage and cannot ultimately compensate for the devastating degeneration that is constantly taking place in the muscle tissue. Furthermore, due to the continuous damage-repair cycles, it has been shown that satellite cells undergo telomere erosion, or senescence, which may further contribute to reducing the regeneration response after muscle damage and worsening the condition of the patients (Lund *et al.*, 2007). Fibrosis, or scar tissue formation, is a common feature in the muscles of DMD patients, which causes muscle dysfunction and contributes to the severity of the DMD phenotype

(Zhou and Lu, 2010). To date, the only clinical treatments for muscular dystrophy are steroid administration and assisted ventilation to facilitate breathing when ventilator muscles are affected. They result in amelioration of the symptoms, but either show side effects or are only able to provide slightly longer life without providing a cure to the disease (Cossu and Sampaolesi, 2004, Daftary *et al.*, 2007). Currently, there is no cure for DMD. There is, however, extensive research focused on finding a therapy to alleviate the symptoms associated with this devastating disease. Different approaches have been tested in animal models, as described below, some of culminating in promising results, but human clinical trials have failed to produce satisfactory improvement in the mobility and muscle strength of the patients (reviewed in: (Aartsma-Rus *et al.*, 2010, Otto *et al.*, 2009, Palmieri and Tremblay, 2010, Palmieri *et al.*, 2010, Quattrocelli *et al.*, 2010, Smythe *et al.*, 2000, Smythe *et al.*, 2001, Sugita and Takeda, 2010)).

The two main approaches proposed for treatment of DMD are endogenous activation and exogenous delivery of muscle cells. The first strategy aims at activating, or reinforcing, the endogenous pool of cells by different molecules, including IGF-I, in order to induce muscle hypertrophy to override the loss in muscle mass (Abmayr *et al.*, 2005, Cassano *et al.*, 2008, Pelosi *et al.*, 2007). The second, more promising approach relies on delivering exogenous factors (gene or cell therapies) to the patient, to improve muscle regeneration.

The gene therapies, including the exon skipping approach or forced read-through of premature stop codons, target the dystrophin gene product (Benchouir *et al.*, 2007, Lu *et al.*, 2003). Approximately 15% of DMD patients carry a mutation within the dystrophin gene, which encodes a premature stop codon, thus causing production of an incomplete dystrophin protein (Aartsma-Rus *et al.*, 2006, Aartsma-Rus *et al.*, 2010). A forced read-through therapy, through the introduction of specific drugs, aims at forcing cells to ignore the preferentially mutated stop codon. Alternatively, and due to mutations of the dystrophin gene, the open reading frame may be disrupted, leading to prematurely truncated, nonfunctional dystrophin protein (Monaco *et al.*, 1988). The exon skipping approach would permit, by introducing antisense oligonucleotides, the splicing of an mRNA molecule, so that an exon is skipped and the open reading frame is restored, ultimately enabling the improved expression of dystrophin. This method would still lead to the production of an incomplete dystrophin protein, however it would be partially functional, which would therefore decrease the severity of the

disease (Aartsma-Rus *et al.*, 2010, Spitali *et al.*, 2009, van Deutekom *et al.*, 2001). The gene therapies, however, are not a solution for patients in advanced stage of the disease, where muscle tissue is already largely infiltrated by fibrotic tissue. Additional disadvantages, requiring solution or additional research, are the need for periodic redelivery, potential side effects, host immune responses and the need for optimising efficiencies (Aartsma-Rus *et al.*, 2010, Adams *et al.*, 2007, Fletcher *et al.*, 2007). Adeno-associated virus (AAV) is emerging as a vector choice for muscle gene therapy applications (Athanasopoulos *et al.*, 2004, Sugita and Takeda, 2010, Yang *et al.*, 2011), but further research and clinical trials are needed to understand whether effective clinical treatments may be applied.

Given the ongoing complexities of the gene therapies, cell therapy is being investigated as a promising alternative approach to treat muscular dystrophies, which has attracted a lot of attention. Cell therapy relies on the delivery of exogenous cells (by systemic or local injections), which would fuse with damaged dystrophic muscles, repair them and by contributing their myonuclei, containing the normal variant of the gene, at least partially restore the normal musculature and reduce the futile repair cycles culminating in muscle loss. Different types of cells with myogenic potential are considered as potential candidates for transplantation, including embryonic stem cells, induced pluripotent stem cells (iPSs), bone marrow derived stem cells (BMSCs), circulating progenitors and myogenic cells (Satellite cells and myoblasts) (Bhagavati and Xu, 2005, Gussoni *et al.*, 2002, Nakagawa *et al.*, 2008, Peault *et al.*, 2007). Extensive research is still ongoing to verify which would be the most appropriate cell type to use for cell therapy.

A large proportion of the research focused on DMD has been based on using transgenic animals, such as the mdx mouse, carrying the X-linked mutation of the dystrophin gene, which mimics the DMD genotype in humans. Transplantation of healthy myoblasts to this model was first reported as early as in 1989, as an attempt to restore dystrophin expression in immunodeficient mdx mice (Partridge *et al.*, 1989). In mdx mice, myoblast transfer therapy shows beneficial effects - protecting muscles from damage by exercise (Brussee *et al.*, 1998). Myoblast transfer therapy is also promising, because some of the transplanted myoblasts survive as muscle precursor cells in the tissue and are subsequently able to repair damaged muscle fibres (Morgan *et al.*, 1993, Yao and Kurachi, 1993). Although significant improvement of muscle regeneration and functionality was achieved

after cell therapy in mdx mice, clinical trials in humans were far less successful. Clinical trials in the early 90s produced limited positive results (Mendell *et al.*, 1995, Tremblay *et al.*, 1993). Three main problems were associated with the low survival of transplanted cells, limited spreading and migration of transplanted cells and immune rejection (Fan *et al.*, 1996, Gussoni *et al.*, 1997, Moens *et al.*, 1996, Skuk *et al.*, 2004, Smythe *et al.*, 2001).

It is known that after severe traumatic injury, the natural repair mechanisms are not sufficient to return the muscle in its pre-damaged state, which leads to formation of scar tissue and diminished functionality (Menetrey *et al.*, 1999, Turner and Badylak, 2011). Therapeutic strategies to improve the regenerative capacity of skeletal muscle tissue following traumas are required. Tissue engineering and *in vitro* tissue synthesis are potential therapies, however, this technology is still not sufficiently advanced and other problems, such as biocompatibility and issues of functional integration of this tissue in the human body remain to be resolved (Koning *et al.*, 2009, Turner and Badylak, 2011). Cell therapies, such as myoblast transplantation, are not only proposed for muscular dystrophies, but can also potentially be applied in treating loss of muscle tissue after traumas (review: (Turner and Badylak, 2011)). Therefore, an ability to enhance the process of muscle regeneration would highly depend on improving our understanding of the factors and regulators that control it.

1.12. CELL MIGRATION

As suggested above, part of the problem associated with cell therapy for DMD may be enabling the cells to migrate to and home in the DMD muscle. Similarly, cell migration is an essential process in the development and maintenance of multicellular organisms. Important events, such as tissue development, immune responses and wound healing all depend on the migration capacity of various cell types. Cell migration is a highly complicated process, still not completely understood, which can depend on various extracellular cues and requires the synchronous activity of many intracellular factors (Lauffenburger and Horwitz, 1996, Raftopoulou and Hall, 2004, Ridley, 2001, Welf and Haugh, 2011). Cell migration can be affected by soluble extracellular factors, acting across extensive distances, or by the extracellular matrix. These extracellular factors elicit different intracellular responses in a cell, which can include the activation or inhibition of

signal transduction pathways and target molecules, gene transcription, reorganization of the cytoskeleton, changes in the distribution or trafficking of cell surface receptors. Each of these intracellular processes is highly complicated, involving many molecules, and it is both fascinating and extremely challenging to comprehend and assemble the entire picture of how all of these events are coordinated and synchronized in order to drive cell migration. Many of the studies investigating these processes and their regulators have been conducted in *Dyctiostelium*, fibroblasts or neutrophils and although the main intracellular mechanisms driving cell migration are thought to be conserved and shared among eukaryotes, it needs to be considered that the process of cell migration has not been investigated in detail in muscle progenitor cells and that some differences may exist between different cell types.

As discussed above, muscle regeneration requires satellite cells to migrate to the site of injury in order to participate in the process of muscle repair. In order to fuse into multinucleated myotubes, myoblasts must align with each other and migration is a requirement for this process to occur. Limited cell spreading and migration is one of the reported problems related to proposed cell therapies of DMD, although recent articles question this concept (Lafreniere *et al.*, 2009, Skuk *et al.*, 2011). Therefore, more research is needed to elucidate the mechanism of muscle precursor cells migration, both *in vitro* and *in vivo*. By revealing which extra- and intracellular factors are regulating the migration of muscle progenitor cells, we may better understand the processes of myogenesis, regeneration and ultimately apply this knowledge for therapies of hereditary muscle diseases, improving muscle regeneration and muscle function.

1.13. “STEPS” OF CELL MIGRATION

In order to migrate, the cell must establish stable adhesions with the substratum, preferentially formed at the leading edge. Contractile forces must then be generated for the cell to propel forward, while the adhesion complexes remain fixed on the substratum and eventually reach the rear of the cell (Ananthakrishnan and Ehrlicher, 2007, Lauffenburger and Horwitz, 1996, Schwartz and Horwitz, 2006). The process of cell migration may be separated in the following steps: polarisation of the cell membrane, formation of cell protrusions at the leading edge and stable contacts between the cell and the extracellular substrate,

contraction of the cytoskeleton leading to translocation of the cell and release of the cell-substrate contacts at the rear of the cell (Lauffenburger and Horwitz, 1996). These events must be highly coordinated and are regulated by a variety of intracellular signalling molecules, including mitogen-activated protein kinase (MAPK) cascades, lipid kinases, small GTPases, phospholipases, Serine/Threonine and Tyrosine kinases, cytoskeleton modifying proteins and scaffold proteins (Raftopoulou and Hall, 2004).

Polarisation of the cell, or establishing a front and rear end, is an important requirement for persistent migration. It is coupled with the extension of membrane processes at the cell front, including lamellipodia and filopodia (Nobes and Hall, 1999). Lamellipodia are broad, flat, sheet-like structures, serving as a site for newly formed adhesive contacts, thus enabling the cell to propel forward and move. Filopodia are thin, needle-like projections, considered to have cell substrate exploratory functions and involved in determining the direction of movement (Mejillano *et al.*, 2004, Parsons *et al.*, 2010). Upon activation by migratory stimuli, both structures are coupled with local actin polymerization and both contain actin and actin-associated proteins.

Formation of attachment sites, or focal adhesions, is an important step for the movement of adherent cell types. Focal adhesions establish the link of the cell to the ECM via adhesion receptors, such as integrins. Upon ligand binding, integrins cluster and recruit actin filaments and signalling proteins to their cytoplasmic domain, thus forming focal adhesions. Integrins, in addition to being cell surface receptors that interact with the ECM, are also able to mediate various intracellular signals (Brakebusch and Fassler, 2003, Hynes, 2002). Ligated integrins can serve to mediate signals to PI3K and Ras homolog gene family (Rho) of small GTPases, which can regulate cytoskeletal dynamics and myosin-dependent contraction (Berrier and Yamada, 2007). Thus, integrins are important for processes, such as cell adhesion, migration and maintenance of cell polarity. Formation of adhesive complexes is coupled by the phosphorylation of a group of cytoskeletal associated proteins upon cell adhesion to a substratum, including focal adhesion kinase (FAK), paxillin and tensin (Lo *et al.*, 1994, Schaller and Parsons, 1994, Turner, 1994). Stress fibres also play a role in cell adhesion. They are contractile cytoskeletal structures, which are anchored at focal adhesions, linking the cell to the extracellular matrix and are considered as major mediators of cell contraction (Kaunas *et al.*, 2005, Pellegrin and Mellor, 2007).

Cell body contraction, as discussed in Ridley (2001), is dependent on actinomyosin contractility and can be regulated by Rho (Ridley, 2001). Stress fibres and their associated focal adhesions are driving forces for cell contraction and the importance of their regulation by Rho may differ according to the cell type and whether the cells are adherent or not. Contractility is also important for the disassembly of focal adhesions (Lauffenburger and Horwitz, 1996, Schwartz and Horwitz, 2006), suggesting that cell migration requires synchronization between finely coordinated events, rather than just a sequence of independent steps.

Rear release, or “tail” detachment, is an important factor for a cell to move forward and it can often be a limiting step of cell migration (Cox and Huttenlocher, 1998, Palecek *et al.*, 1998, Ridley, 2001). During rear release, a large proportion of the integrins are left on the substratum as the cell detaches and moves forward (Regen and Horwitz, 1992). However, integrins remaining on the cell surface are also able to be transported to the cell anterior to serve for new adhesion formation. In slowly moving cells, such as myoblasts, “tail” detachment appears to depend on the action of the protease calpain, which degrades focal adhesion components at the rear of cells (Glading *et al.*, 2000, Ridley, 2001). Integrin recycling may also be a key regulator of cell adhesions, integrin turnover and thus cell migration (Caswell and Norman, 2006, Jones *et al.*, 2006, Pellinen and Ivaska, 2006). A schematic representation of the steps of cell migration is presented in Figure 1.4.

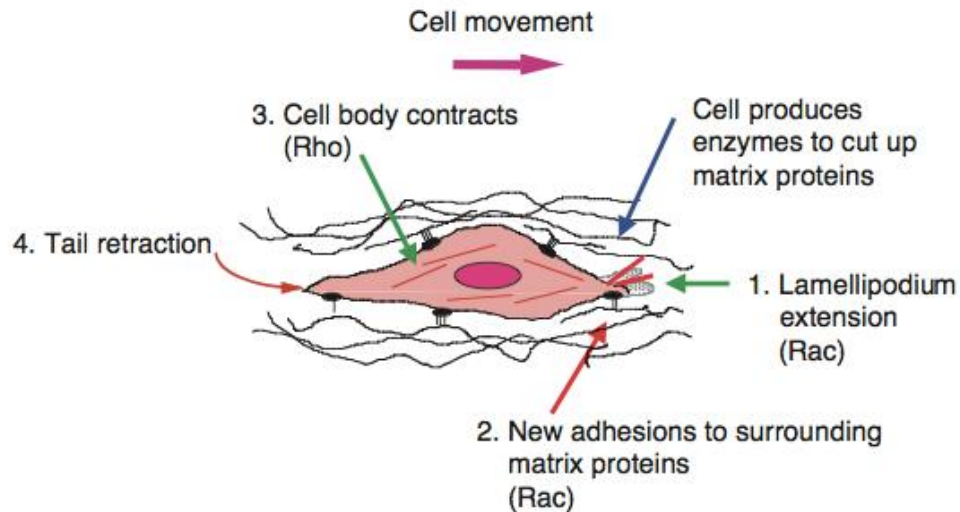


Figure 1.4. A model of the steps required for cell migration to occur.

In order to migrate, a cell needs to extend membrane protrusions, such as filopodia (not shown) or lamellipodia, allowing the cell to pull forward. The cell then needs to contract, in order to propel forward, and at the same time release its “tail”. All these steps are mediated by members of the Rho family of small GTPases. Model proposed by (Ridley, 2001).

In recent years there has been increasing attention on the importance of the endo/exocytic cycle of integrins as an important regulator of cell motility (Caswell and Norman, 2006, Jones *et al.*, 2006, Pellinen and Ivaska, 2006). Different kinases, modulators of the actin cytoskeleton and members of the Rab small GTPases and Arf GTPase families have been implicated as regulators of this process. In particular, the Rabip4 protein, an effector of Rab4, might be an interesting candidate for further investigation in skeletal muscle myoblasts (Fouraux *et al.*, 2004, Vukmirica *et al.*, 2006). Studies in NIH-3T3 fibroblasts have demonstrated that overexpression of Rabip4, involved in regulation of α -integrins traffic, leads to an increased motility of cells, while Rabip4 knock-down resulted in reduced cell motility (Vukmirica *et al.*, 2006). To our knowledge, studies of integrin recycling and how it affects migration of myogenic precursor cells are still lacking. Altering the rates of integrin recycling, therefore, might be an approach to modify the motility of myogenic precursor cells and possibly improve the spreading of donor myoblasts in dystrophic muscles.

1.14. RHO GTPASES

The Rho family of GTPases, and in particular Rho, Cell division control protein 42 homolog (*cdc42*) and Ras-related C3 botulinum toxin substrate (*Rac*), seem to play a pivotal role in regulating signal transduction pathways that link cell surface receptors to a variety of intracellular responses important for cell migration (for detailed reviews: (Raftopoulou and Hall, 2004, Ridley, 2001). They are best known as regulators of the actin cytoskeleton, but also cell polarity, gene expression, microtubule dynamics and vesicular trafficking. The Rho family of GTPases act as molecular switches, cycling between active GTP-bound and inactive GDP-bound states (Moon and Zheng, 2003, Schmidt and Hall, 2002, Zheng, 2001). When activated, they can interact with downstream cellular target proteins (effectors), in order to elicit different intracellular responses (Bishop and Hall, 2000).

Rac and Cdc42 regulate the polymerization of actin to form lamellipodial and filopodial protrusions, involved in propelling the cell forward and defining the direction of movement. Cdc42 and Rac are required at the front of migrating cells (Nobes and Hall, 1995, Raftopoulou and Hall, 2004). Rac is important for regulation of actin polymerization and formation of membrane protrusions, such as lamellipodia. In migrating fibroblasts, Rac is concentrated at the leading edge of the cell (Kraynov *et al.*, 2000). Cdc42 is required for filopodia formation, involved in determining the direction of cell migration and cell polarity, but doesn't seem to be important for the ability of a cell to move (Ridley, 2001, Sepp and Auld, 2003). Rac and Cdc42 regulation of protrusion formation is established via the activation of the Ser/Thr kinase PAK. PAKs can act on different substrates implicated in actin cytoskeleton rearrangement (Szczepanowska, 2009). PAKs can activate LIM kinase (LIMK), which inhibits cofilin, a protein involved in actin filament disassembly, and thus allows the accumulation of polymerized actin at the leading edge of cells (Arber *et al.*, 1998, Cau and Hall, 2005, Edwards *et al.*, 1999, Obermeier *et al.*, 1998, Stanyon and Bernard, 1999, Szczepanowska, 2009). Members of the WASp/SCAR/WAVE family of scaffold proteins (Wiskott-Aldrich syndrome protein = WASp; Suppressor of cAMP receptor = SCAR; WASP-family verpolin homologous = WAVE) are also key regulators of actin polymerization through stimulation of the actin-related protein 2/3 (Arp2/3) complex, which is able to initiate the actin polymerization process (Takenawa and

Miki, 2001, Weaver *et al.*, 2003). Cdc42 can activate WASp and neuronal Wiskott-Aldrich Syndrome protein (N-WASp), while Rac interacts with the Scar/WAVE family (Eden *et al.*, 2002, Rohatgi *et al.*, 1999, Rohatgi *et al.*, 2000, Rohatgi *et al.*, 2001). A schematic representation of these events is presented on Figure 1.5.

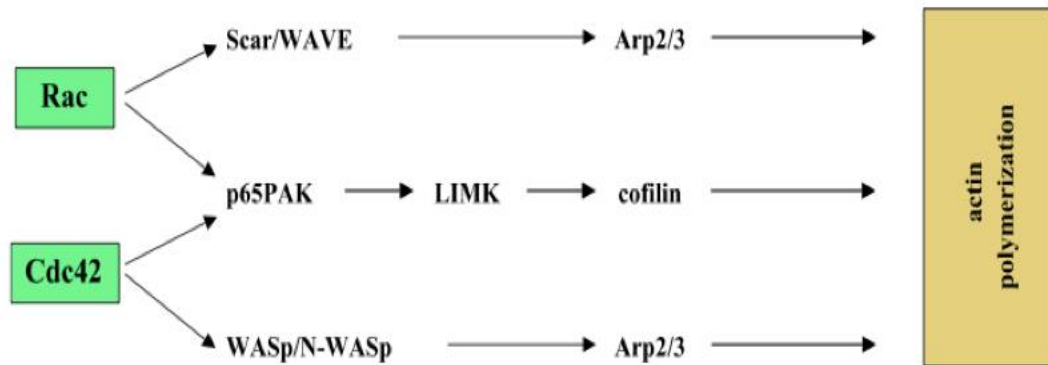


Figure 1.5. Regulation of actin polymerization by Rac and Cdc42. Figure adapted from (Raftopoulou and Hall, 2004).

Rho, along with other signals, such as Src tyrosine kinase, FAK and PAK, is thought to be important for focal adhesion disassembly (Ridley, 2001). It is also involved in the assembly of actin:myosin filaments, which allows the contraction of the cell and propelling of its cell body forward. A target of Rho is the Ser/Thr kinase p160-Rho-associated protein kinase (p160ROCK) and together they are also important in rear cell detachment in leukocytes and macrophages (Alblas *et al.*, 2001, Nobes and Hall, 1999, Worthylake and Burridge, 2003). Similar to PAK, in its active state p160ROCK activates LIMK, which inactivates cofilin, leading to stabilization of actin filaments within actin:myosin filament bundles (Maekawa *et al.*, 1999, Sumi *et al.*, 2001). p160ROCK, via phosphorylation of the myosin binding subunit (MBS) of myosin light chain phosphatase, leads to increase myosin2 activity, which cross-links actin filaments to generate contractile forces (Amano *et al.*, 2000, Hall, 2005, Kawano *et al.*, 1999, Totsukawa *et al.*, 2000). The Rho-mammalian diaphanous (mDia) pathway is also linked to regulating focal adhesion turnover and actin stress fibres (Satoh and Tominaga, 2001, Yamana *et al.*, 2006), both important respectively for tail retraction and for cell contraction. A schematic representation of these events is presented on Figure 1.6. Together these studies illustrate the complexities of cell

migration and exemplify that malfunctions in any one of these processes could impact on the migratory capacity of cells.

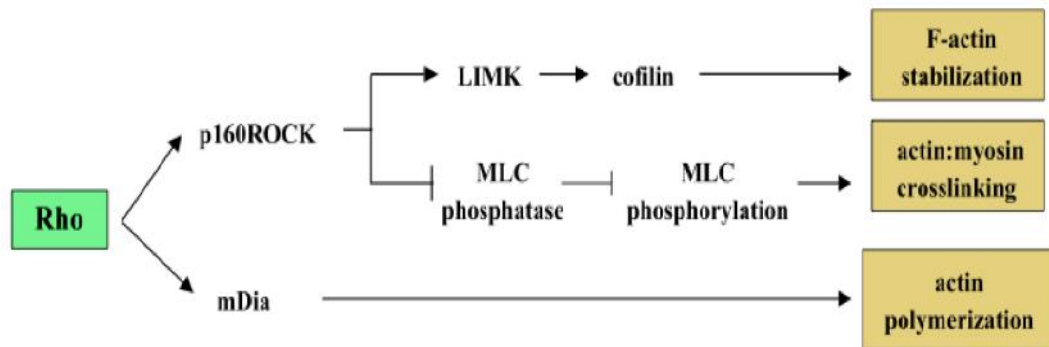


Figure 1.6. Regulation of actin cytoskeleton structures by Rho. Figure adapted from (Raftopoulou and Hall, 2004).

1.15. PTEN/PI3K PATHWAY INVOLVEMENT IN CELL MIGRATION

The PTEN/PI3K/AKT pathway is an important pathway regulating the signalling of multiple biological processes, such as cell survival, proliferation and migration (Blanco-Aparicio *et al.*, 2007, Dahia, 2000, Leslie *et al.*, 2005). PI3Ks are able to phosphorylate the inositol ring of phosphatidylinositol 4,5 bisphosphate (PIP₂) converting it into phosphatidylinositol 3,4,5 trisphosphate (PIP₃), which binds Akt kinase/PKB, leading to its translocation to the plasma membrane where it is activated by PDK1 (Figure 1.7) (Blanco-Aparicio *et al.*, 2007, Engelman *et al.*, 2006, Kandel and Hay, 1999). Akt activation is important for processes, such as glucose metabolism, cell proliferation, survival, transcription and cell migration (Zhao, 2007). Phosphatase and tensin homologue deleted on chromosome 10 (PTEN), a dual protein/lipid phosphatase, antagonizes PI3K via the dephosphorylation of PIP₃, converting it back to PIP₂, leading to negative regulation of Akt and other downstream targets (Cully *et al.*, 2006, Yamada and Araki, 2001). On the contrary, loss of PTEN function results in accumulation of PIP₃ and activation of Akt, thus perpetuating the effect of PI3K activation (Figure 1.7).

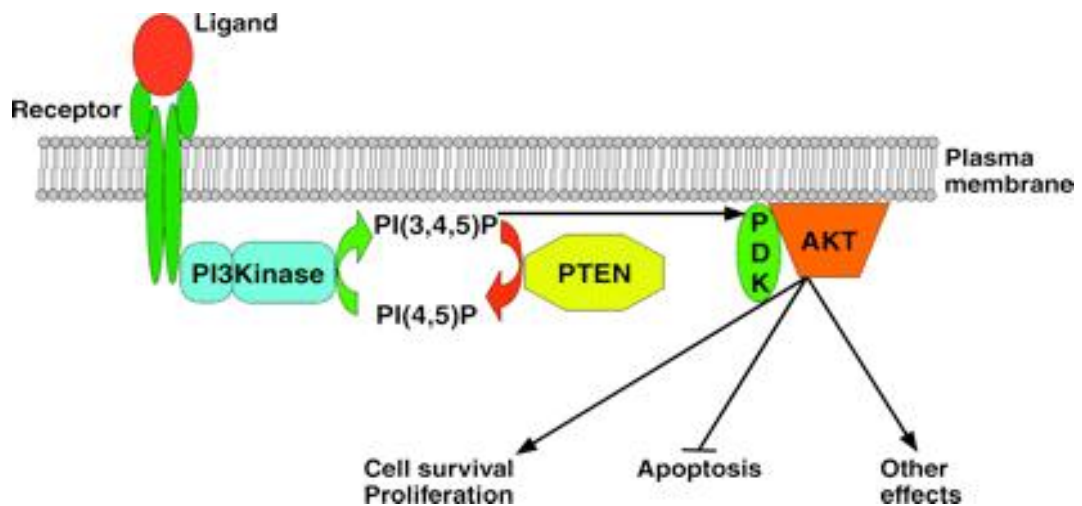


Figure 1.7. Opposing actions of PI3K and PTEN on phospholipids. Once activated by the binding of a ligand to a membrane receptor, PI3K phosphorylates PIP2 to PIP3, leading to PDK1 translocation to the plasma membrane, which then is able to phosphorylate and activate Akt. PI3K/Akt pathway is involved in many processes, such as cell survival, proliferation, migration. PTEN acts as a negative regulator of PI3K and Akt by dephosphorylating PIP3 to PIP2. Figure adapted from (Planchon *et al.*, 2008).

Adding to the migration story above, PI 3-kinases and PIP3 are known as regulators of cell polarity and migration (Stephens *et al.*, 2002). PI3K and PIP3 co localise at the centres of actin polymerization at the leading edge of migrating cells (Funamoto *et al.*, 2002, Merlot and Firtel, 2003). Localisation of PI3-kinase at the front of migrating cells, has been shown to be coupled with a decreased distribution of its antagonist PTEN at the front, but increased abundance at the rear (Funamoto *et al.*, 2002, Iijima and Devreotes, 2002). Spatially regulated PI3K/PTEN signalling is thus believed to underlie cell polarisation and directional cell migration (Comer and Parent, 2007, Iijima and Devreotes, 2002). Rac activation is also dependent on PI3K activity, and inhibitors of PI3K are shown to block Rac activation (Royal *et al.*, 2000, Sander *et al.*, 1998). The production of PIP3 leads to an increase in active Rac in many cell types and overexpression of constitutively activated PI 3-kinase in fibroblasts generates extensive lamellipodia and membrane ruffling through Rac activation (Reif *et al.*, 1996). PI3K and Rac are able to directly interact with each other and Rac activation also stimulates PI3K, leading to the production of PIP3, thus a positive feedback loop exists, which has the potential to influence migration (Benard *et al.*, 1999, Bokoch *et al.*, 1996, Genot *et al.*, 2000, Hawkins *et al.*, 1995, Servant *et al.*, 2000).

As described by Zhao (2007), PTEN has two functional domains - the C2 domain and a phosphatase domain (Zhao, 2007). The C2 domain binds membrane lipids, while the phosphatase domain carries the enzymatic function of the protein by catalysing the dephosphorylation of PIP3 to PIP2. Manipulation of cell migration by PTEN can be regulated not only by its effect on PIPs, but also via its protein phosphatase activity (Dey *et al.*, 2008, Leslie *et al.*, 2007, Maier *et al.*, 1999) and independently through its C2 domain (Okumura *et al.*, 2005, Raftopoulou *et al.*, 2004). However, the protein phosphatase function of PTEN is important for its function. Dey *et al.* demonstrated that in glioma cells PTEN is able to control integrin-directed migration in a lipid phosphatase, PI3K/AKT independent manner (Dey *et al.*, 2008). PTEN has been shown to dephosphorylate FAK and to inhibit the integrin-mediated cell spreading and migration on fibronectin (Gu *et al.*, 1998, Gu *et al.*, 1999). It is also able to inhibit ERK/MAPK pathway, after both integrin and growth factor activation, at the the level of Shc, reducing its phosphorylation and interaction with downstream targets, such as Grb2. PTEN seems to control two migratory pathways: 1) directionally persistent migration induced by FAK/p130-Cas, characterised by extensive organization of actin microfilaments and focal adhesions and 2) ShC/MEK1 - random type of motility with less actin cytoskeletal and focal adhesion organization (Figure 1.8).

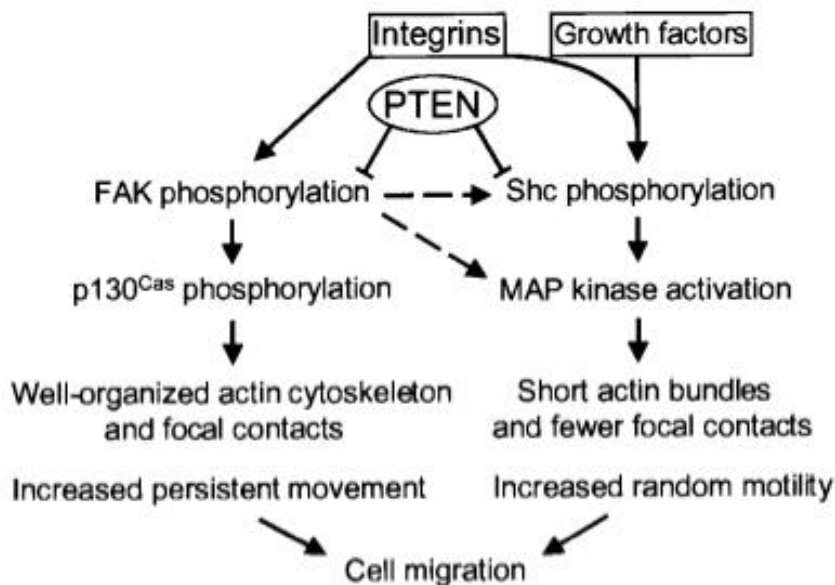


Figure 1.8. PTEN exerts effects on FAK and MAPK signalling to regulate cell migration. As described by Gu *et al.* (Gu *et al.*, 1998, Gu *et al.*, 1999), integrins (via FAK and Shc/MAPK/ERK) and Growth factors (via Shc/MAPK/ERK) are both involved in regulation of cell movement. PTEN can dephosphorylate, and thus inhibit, both FAK and Shc and in this way regulate two distinct pathways involved in either persistent or random cell movement.

In mammalian cells genetically lacking PTEN, migration is increased compared to cells normally expressing the phosphatase (Liliental *et al.*, 2000, Suzuki *et al.*, 2003). Liliental *et al.* demonstrated that PTEN deficiency resulted in increased fibroblast motility by Rac1 and Cdc42 dependent mechanisms (Liliental *et al.*, 2000). PTEN inhibition by pharmacological agents, such as bisperoxovanadium (BpV) compounds, has been shown to result in enhancement of epithelial cell migration, as shown by a wound healing model (Lai *et al.*, 2007). Inhibition of PTEN by BpV compounds has been shown to culminate in increased levels of phospho-Akt (Lai *et al.*, 2007, Schmid *et al.*, 2004). Indeed Castaldi *et al.* have demonstrated that high concentrations (10 μ M) of BpV are able to block myoblast differentiation and to induce myogenic cells to acquire gene expression profile of circulating progenitors, while maintaining their myogenic potential (Castaldi *et al.*, 2007). BpV treated C2C12 cells, delivered by intra-arterial injection in dystrophic mice, were able to reach muscle tissue and contribute to muscle repair with higher efficiency compared to untreated cells. However, the effect of PTEN inhibition or BpV compounds on myoblast migration itself was not studied.

1.16. MAPKS IN CELL MIGRATION

In addition to the pathways described above, Mitogen-activated protein (MAP) kinases, which are serine/threonine specific protein kinases that respond to a variety of extracellular stimuli, also regulate many cellular processes (Pearson *et al.*, 2001). MAP kinases form the MAPK cascade, consisting of three enzyme - MAP kinase (MAPK), MAPK kinase kinase (MAPKK) and MAPK kinase kinase kinase (MAPKKK). MAPKs, including JNK, p38 and ERK, control a vast array of physiological processes (Johnson and Lapadat, 2002), including cell migration (reviewed in (Huang *et al.*, 2004b)).

JNK has been shown to be involved in regulating cell migration, with its inhibition leading to reduced cell migration. It has been shown to regulate said migration through modulating the phosphorylation of paxillin and the subsequent formation of focal adhesions (Huang *et al.*, 2008, Kimura *et al.*, 2008, Wei *et al.*, 2010). JNK has also been implicated in regulating cytoskeleton reorganization by influencing regulators, such as profilin and cortactin, which are upregulated by active JNK and downregulated by dominant negative JNK mutant (Jasper *et al.*, 2001). As described by Huang *et al.*, many JNK substrates have been identified, of which paxillin, spir, DCX, MAP1B and MAP2 are all candidates, all are also directly involved in cell migration (Huang *et al.*, 2004b).

p38 is less well characterised in terms of its involvement in cell migration, although it is known that its pharmacological inhibition can reduce migration (Saika *et al.*, 2004, Sharma *et al.*, 2003). It is believed that the involvement of p38 in cell migration may be accomplished via its effects on MAPKAP 2/3 and cytoskeletal regulators, such as paxillin (Huang *et al.*, 2004a, Huang *et al.*, 2004b) and caldesmon (Goncharova *et al.*, 2002b).

ERKs 1/2 are also known as regulators of cell migration, being stimulated by variety of extracellular cues, which are able to activate the Ras-Raf-MEK1/2-ERK1/2 signalling pathway (Johnson and Lapadat, 2002, Seger and Krebs, 1995). Pharmacological inhibition of the ERK pathway by PD98059 and UO126 has been demonstrated to reduce cell migration in various cell types, including myoblasts (Al-Shanti *et al.*, 2011, Huang *et al.*, 2004b, Lind *et al.*, 2006, Teranishi *et al.*, 2009, Webb *et al.*, 2000). Furthermore, dominant negative ERK and MEK1 inhibit cell migration, while active MEK1 can promote migration (Jo

et al., 2002, Lai *et al.*, 2001, Webb *et al.*, 2000). Various downstream targets of ERK1/2 may exert effects on cell migration. As described by Huang *et al.* (Huang *et al.*, 2004b), ERK may regulate cell migration by exerting effects on integrin activation, Myosin light-chain kinase (MLCK), FAK, calpain, paxilin and thus regulating the actin cytoskeleton, membrane protrusion and focal adhesion turnover (Chou *et al.*, 2003, Glading *et al.*, 2004, Leloup *et al.*, 2007, Nguyen *et al.*, 1999, Teranishi *et al.*, 2009, Webb *et al.*, 2004).

1.17. MATRIX METALLOPROTEINASES

Having investigated the complex intracellular signalling pathways, involved in manipulating cell migration, it is important to remember they do not function in isolation. For the satellite cells to migrate to the injured site and to participate in myofibre repair, the surrounding ECM needs to be degraded or remodeled. Matrix metalloproteinases (MMPs) are integral to this process. They degrade ECM constituents, thereby facilitating migration and tissue remodeling (Nagase and Woessner, 1999). Myoblasts have been shown to migrate through the basement membrane and through connective tissue barriers, such as the endomysium and perimysium (Hughes and Blau, 1990, Phillips *et al.*, 1990, Watt *et al.*, 1994). MMPs are expressed in skeletal muscle *in vitro* and their inhibition leads to a decrease in the migration speed of myoblasts (Nishimura *et al.*, 2008). Overexpression of MMP-1 or MMP-2 on the other hand, increased the migration of myoblasts *in vitro* (Allen *et al.*, 2003). MMP9 overexpression has been demonstrated to improve myoblast migration and engraftment (Morgan *et al.*, 2010). Thus, matrix metalloproteinases are key to successful migration of myogenic precursors and to muscle regeneration. PI3K and MAPK pathways have been implicated in regulating MMP9 production in the HT1080 metastatic cell line and brain astrocytes (Kim *et al.*, 2001, Arai *et al.*, 2003), however, little is known about what regulates the expression of MMPs in myogenic precursors and, therefore, further research is needed in this area.

1.18. MIGRATION OF MYOGENIC PRECURSORS

Although many regulators of cell migration have been elucidated in different cell types, relatively little research has focused on the field of myogenic progenitor cell migration. Due to the limited dispersion of transplanted/injected cells in proposed DMD therapies, this therapeutic strategy may be more successful if myoblast migration were improved. Therefore, research has mostly focused on the effects that certain mitogenic factors or proteolytic enzymes exert on myoblast or satellite cell chemotaxis or movement. A few soluble factors have been reported to act as chemoattractants for satellite cells or myoblasts - among them HGF, IL-4, TGF β , TNF α , RANTES (a.k.a. CCL5), PDGF-A, PDGF-B, FGF, IGF-I and platelet lysate (Amano *et al.*, 2002, Bischoff, 1997, Corti *et al.*, 2001, Lafreniere *et al.*, 2004, Lafreniere *et al.*, 2006, Ranzato *et al.*, 2009, Torrente *et al.*, 2003). As previously discussed, it is important to note that the action of certain soluble factors may be altered by their concentration. It is thus obligatory, not only to know which soluble factors act as chemoattractants, but also to understand how they can interact with each other and what intracellular events are responsible for the effects they exert on the cell. Critically, few myogenic migration inhibitors have been investigated. Sphingosine-1 phosphate is one of the proposed inhibitors of myoblast migration acting via Rho-dependent mechanisms (Becciolini *et al.*, 2006). Prostacyclin GI₂ (PGI₂) is another inhibitor acting as a brake for migration, which also enhances cell fusion (i.e. facilitates cell-cell contact) (Bondesen *et al.*, 2007). Interestingly, it has previously been demonstrated that myoblasts lacking MyoD migrate longer distances into host muscle, although it remained unclear whether this occurred due to increased proliferation or enhanced migration capacity (Smythe and Grounds, 2001). It seems logical that migration and fusion are two linked processes. It will be interesting to further investigate whether migration is indeed dependent on differentiation/fusion and how blocking/inhibiting one will influence the other.

Regulators of cell adhesion and ECM degradation have been studied in relation with myoblast migration. Calpains are also shown to regulate myoblast migration by influencing the formation of stress fibres and focal adhesions (Dedieu *et al.*, 2004, Leloup *et al.*, 2006), while MMPs are suggested to facilitate the migration of myoblasts by participating in the remodeling of the ECM (Allen *et al.*, 2003, Chen and Li, 2009, El Fahime *et al.*, 2000, Nishimura *et al.*, 2008, Wang *et al.*,

2009). The urokinase-type plasminogen Activator (uPA) serine protease, implicated in ECM degradation, is also known to regulate myoblast migration. It was reported that expression of uPA was elevated by treatment with growth factors, increasing myoblasts migration, and that its inhibition by serine protease inhibitor (aprotinin) or specific uPA inhibitor (amiloride), resulted in reduced myoblast migration *in vivo* (El Fahime *et al.*, 2002).

Signalling pathways, including MAPK and PI3K pathways, have been implicated as regulators of myoblast migration, although results have been divergent (Al-Shanti *et al.*, 2011, Leloup *et al.*, 2007, Kawamura *et al.*, 2004, Kim *et al.*, 2011, Ranzato *et al.*, 2009, Suzuki *et al.*, 2000). Both N-WASP and WAVE2, which are activated downstream of PI3K, are required for the migration of myoblasts via lamellipodia formation induced by HGF (Kawamura *et al.*, 2004). Ras and Ral pathways are also shown to be involved in myoblast migration (Suzuki *et al.*, 2000). Akirin1 has been elucidated as a possible regulator of chemotaxis of both macrophages and myoblasts via reorganisation of their actin cytoskeletons, leading to more efficient lamellipodia formation via a PI3K dependent pathway (Salerno *et al.*, 2009). Recent work in our laboratory has implicated the necessity of MAPK and PI3K pathways for migration of C2 cells, demonstrating that pharmacological inhibition of both pathways leads to a decrease in their migration in response to foetal bovine serum (Al-Shanti *et al.*, 2011). However, considering the lack of general agreement and insufficient research on the role of signalling pathways in myoblast migration, it was hypothesised that further research is needed in this field.

1.19. AIMS, OBJECTIVES AND HYPOTHESIS

The aim of this thesis is to elucidate the cellular and molecular regulators of skeletal muscle regeneration, in the context of myoblast migration. The initial objectives were to explore the contribution of factors released from myogenic cells on the migration of myoblasts, thus exploring the extracellular factors regulating the process. The regulation of myoblast migration was also investigated in the context of ageing, using a model of serially passaged C2C12 myoblasts. Subsequent objectives were to link the migration of myogenic cells, in response to these secreted factors, to signalling pathways, thus exploring the extracellular-mediated, intracellular regulation of myoblast migration. It would also be

revealed what effect the modulation of signalling pathways would exert on myoblast migration, potentially suggesting targets to enhance their migratory capacity. Finally, in an attempt to propose new genetic targets for investigation in skeletal muscle, potentially linked with fusion and migration, the expression of 4 genes (Spire1, Spire2, Formin1 and Formin2) involved in actin polymerization were assessed. It was hypothesised that myogenic cells would release factors capable of increasing migration of C2C12 myoblasts and that signalling pathways, such as PI3K/AKT and MAPK/ERK, would be required for this increase. It was hypothesised that serial passaging of myoblasts would lead to changes in the migratory behaviour of these cells. Finally, it was hypothesised that genes involved in actin polymerization (such as Spire1, Spire2, Formin1 and Formin2) would be expressed in C2C12 myoblasts and that their expression would be altered with differentiation/fusion.

The C2C12 cell line in this thesis was chosen due to the capability of these cells to differentiate and form large multinucleated myotubes. It is also a very popular model of investigation of skeletal muscle myogenesis and considered as a useful tool for exploring the regulation of myogenesis at both genetic and protein level.

CHAPTER 2

2. MATERIALS AND METHODS

2.1. MATERIALS, GENERAL EQUIPMENT AND SPECIALIZED SOFTWARE

2.1.1. CHEMICALS, SOLVENTS AND REAGENTS

All general chemicals and solvents (analytical (AnalaR) or molecular biology/tissue culture grade) were purchased from Sigma (Poole, UK) and BDH (Poole, UK), unless otherwise specified. All inhibitors were purchased from Merck-Calbiochem (Darmstadt, Germany), unless otherwise specified.

2.1.2. CELL CULTURE

All cell culture experiments were performed under a Class II microbiological safety cabinet (Labcaire SC-R Recirculating Class II, North Somerset, UK). All cell incubations were performed in Triple Red Laboratory Technology Nuaire DH Autoflow CO₂ Air Jacketed Incubator (Buckinghamshire, UK). Liquid, media and supernatants were discarded using an IBS Integra Biosciences Vacusafe Comfort (Chur, Switzerland). All solutions used for cell culture were prepared with distilled water from Elgastat option 4 water purifier (Elga Ltd., High Wycombe, UK). Cell microscopy and photography were performed using Leica Microsystems (Wetzlar, Germany) CMS GmbH light microscope (Leica DMI6000B) with digital photography, recording capabilities (Leica CTR 6000), using Leica Application Suite software (Wetzlar, Germany). For fluorescent microscopy, images were taken using Leica DMI 6000B imaging system with FITC-fluorescence L5 filter cube (excitation wavelength=480/40nm).

2.1.3. CELL CULTURE REAGENTS

Sterile Lonza BioWhittaker Dulbecco's Modified Eagle's Medium (DMEM) w/ 4.5g Glucose per Liter, w/ L-Glutamine (584mg/L) was purchased from BioWhittaker (Wokingham, UK). Heat-inactivated (hi) foetal bovine serum (FBS) was purchased from Gibco (Paisley, UK) and hi horse serum (HS) - from Southern Group Laboratory (Corby, UK). Sterile penicillin-streptomycin solution and 10x trypsin solution were purchased from BioWhittaker (Wokingham, UK). Non-sterile L-glutamine was purchased from BDH (Poole, UK) and non-sterile

Gelatin type A from porcine skin was purchased from Sigma-Aldrich Chemie (Steinheim, Germany). Phosphate buffered saline (PBS) tablets were from Oxoid Ltd. (Basingstoke, UK). All solutions were prepared non-sterile in distilled water and were sterilized by autoclaving at 121°C in a bench top autoclave from Prestige Medical (Birmingham, UK) before usage in cell culture.

2.1.4. PLASTICWARE

Tissue culture flasks (T75 and T175), 12 and 6 well Nunclon™ surface multi-well dishes were purchased from Nunc Life Sciences, Thermo Fisher Scientific (Rockslide, Denmark). 96 well plates for protein assays were also purchased from Nunc Life Sciences, Thermo Fisher Scientific (Roskilde, Denmark). 24 well plate Corning® Costar® cell culture plates, used for transwell insert assays, were purchased from Sigma-Aldrich (Dorset, England). MicroAmp® Optical 96-Well Reaction Plates for Applied Biosystems StepOnePlus Real-time PCR system were purchased from Applied Biosystems (Warrington, UK). 96 well plates for Bio-Rad Chromo4™ real-time PCR detector were purchased from Bio-Rad (Hercules, CA, USA). BD Falcon 96 well clear UV plates for use with Creatine Kinase assay were purchased from BD Biosciences (San Jose, CA, USA). Cryogenic vials, 15ml and 50ml sterile centrifuge tubes, cell scrapers and pipette tips for tissue culture, biochemistry and flow cytometry were purchased from Fisher Scientific (Loughborough, UK). Aerosol resistant tips (ART™), used for RNA work, were from Molecular BioProducts Inc. (San Diego, CA, USA) and 0.25, 0.5, 1.5 ml RNase Free Microfuge tubes for RNA work were purchased from Applied Biosystems (Ambion-The RNA Company, Cheshire, UK). 0.5, 1.5 and 2 ml tubes were also purchased from Eppendorf (Hamburg, Germany) Syringes were from Terumo (Leuven, Belgium) and syringe filters (0.22 µm) from Corning, (Lowell, MA, USA). 6.5mm permeable polycarbonate transwell® membrane supports (8.0µm pore size), packaged in 24 well plates, were from Corning® Costar® and purchased from Sigma-Aldrich (Dorset, England).

2.1.5. LIVE IMAGING

Live imaging microscopy was performed using Leica DMI6000B microscope equipped with an autoflow incubator, CO₂ controller, heating unit and temperature controller, thus allowing maintenance of 5% CO₂, 37°C atmosphere.

Videos were generated and exported using the Leica Application Suite software (Wetzlar, Germany).

2.1.6. BIOCHEMICAL ASSAYS

All values from protein and CK assays were obtained using a Bio-Tek ELISA plate reader (Winooski, VT, USA). BCA protein assay reagents for protein assay were purchased from Pierce (Division of Thermo Fisher Scientific, Roskilde, Denmark) and for CK assay - from Catachem, Inc. (Connecticut, NE, USA).

2.1.7. REAL-TIME PCR

RNA concentrations and purity were assessed using a Biotech Photometer (WPA UV1101, Biochrom, Cambridge, UK). Two Real-time PCR systems were used: a Bio-Rad Chromo4™ real-time PCR detector (Hercules, CA, USA) and Applied Biosystems StepOnePlus Real-time PCR system. Results were analyzed by Opticon Monitor version 3.1.32 (MJ Geneworks Inc., Bio-Rad Laboratories, Inc., Hercules, CA, USA) and StepOne Software v2.2.2 (Applied Biosystems, Life Technologies). Reagents for real time PCR were from Applied Biosystems (Carlsbad, CA, USA).

2.1.8. SDS-PAGE AND WESTERN LIGAND BLOTTING

Proteins were loaded on polyacrylamide gels and were electrophoresed on a Jencons TV200 Twin Plate Wide Mini-gel electrophoresis unit (Jencons, a VWR division, East Grinstead, West Sussex, UK), purchased from Sci-plas (Cambridge, UK), using Hoefer mighty slim 5X20 Power supply (Holliston, MA, USA). Pre-made running buffer (10x TGS) was from Bio-Rad (Bio-Rad Laboratories Ltd., Hertfordshire, UK). Semi-dry protein transfer on nitrocellulose membranes was performed by Semi Dry Unit-V20-SDB (Witec AG, Littau, Germany) with Hoefer DC Power Supply PS3000 (Holliston, MA, USA). Hybond ECL Nitrocellulose membranes were purchased from GE Healthcare Life Sciences, (Buckinghamshire, UK). HRP substrate used was West Dura or West Femto Supersignal kits (Pierce, Rockford, IL, USA). Chemiluminescence was detected on Biorad Imaging System (Hercules, CA, USA) with Quantity One Software 4.6.2 (Bio-Rad, Hercules, CA, USA).

2.1.9. FLOW CYTOMETRY

Flow Cytometry was performed on BD FACSCalibur™ (Becton Dickinson, Franklin Lakes, NJ, USA) with Cell Quest Pro Software (Becton Dickinson, Franklin Lakes, NJ, USA). Cell cycle analysis was performed using Modfit™ software (Verity Software House, Topsham, ME, USA). Reagents for Flow cytometry were purchased from BD (BD Biosciences, San Jose, CA, USA).

2.2. METHODS AND PROTOCOLS

2.2.1. CELL CULTURE

All cell culture experiments were performed with the C2C12 cell line, which was purchased from the American Tissue Culture Collection (ATCC; Rockville, MD, USA).

2.2.1.1. INDUCING PROLIFERATION AND DIFFERENTIATION OF C2C12 MYOBLASTS

Cells were induced to proliferate and expanded in 10% foetal bovine serum (FBS) DMEM media, containing 1% Pen-strep (10000 U/ml) and 200mM L-glutamine (known as Growth media=GM). C2C12 myoblasts are able to differentiate and fuse into myotubes upon serum withdrawal (Blau *et al.*, 1985, Tollefsen *et al.*, 1989). Myoblasts were induced to differentiate and to fuse into myotubes, once confluency was achieved, upon withdrawal of GM and addition of 2% horse serum (HS) DMEM media, containing 1% Pen-strep (10000 U/ml) and 200mM L-glutamine (DM). Figure 2.1 demonstrates the differences between proliferating myoblasts kept in GM and myoblasts, which have undergone differentiation and fusion into multinucleated myotubes following transfer to and culture in DM. For all experiments, cells were seeded on flasks or multi-well dishes, pre-coated for 15min at room temperature with 0.2% Gelatin.

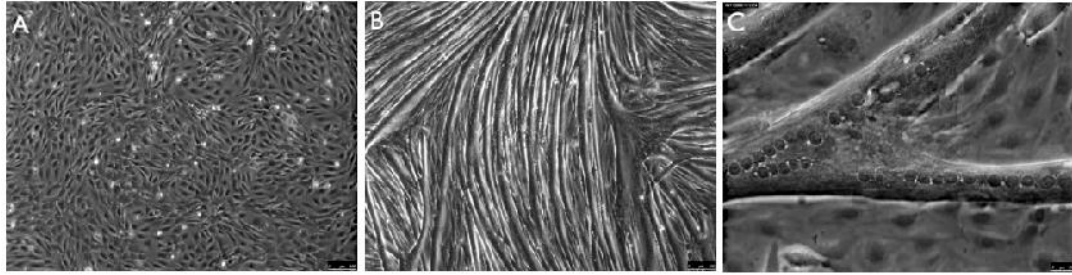


Figure 2.1. Myoblasts are capable of fusing with each other to form multinucleated myotubes. Myoblasts supplemented with 10% FBS DMEM (GM) are induced to proliferate and do not differentiate and fuse into myotubes until highly confluent (A). Differentiation is induced, following washing, once GM is replaced with 2% HS DMEM (DM). Extensive myotube formation is evident following 5 days in 2% HS DMEM (DM) 10x objective; (B). Multinucleated myotubes are formed following fusion of mononucleated myoblasts 20x objective, 1.6x magnification (C).

2.2.1.2. PASSAGING OF CELLS

Passaging of cells was performed by aspirating culture media, washing cells with PBS to remove any remaining serum, trypsinizing with 0.05% Trypsin/0.02% Ethylenediaminetetraacetic acid (EDTA) for 3-5 minutes at 37°C to detach cells adhered to the substrate and resuspending the cells in pre-warmed GM (in at least 1:6 ratio of trypsin:GM) to deactivate the action of the trypsin. For cell counting, cell suspension was prepared in a 1:1 dilution in trypan blue stain (Bio Whittaker, Wokingham, UK) and cells were counted with a Neubauer haemocytometer (Assistent, Sondheim, Germany). Viable cells exclude the trypan blue dye and only the dead cells, where membrane integrity is disrupted, are positively stained. After cells were counted and the numbers adjusted for dilution and stock volumes, cells were seeded with GM in a flask or a multi-well dish, pre-coated with 0.2% Gelatin. Working volumes were normally 15ml of media for T75 flask, 2ml of media/well for a 6-well multidish and 1ml of media/well for a 12-well plate.

2.2.1.3. CELL CRYOPRESERVATION AND RESURRECTION

For preparation of cell stocks, confluent cell monolayers were trypsinized and cells counted with a Neubauer haemocytometer, as described in section 2.2.1.2. Cell numbers were diluted in GM to 1×10^6 cells.ml⁻¹. 10% dimethyl sulphoxide (DMSO; BDH, Poole, UK) was added to the cell suspension in a dropwise

manner and cells were transferred to 1ml cryovials. Cryovials were placed into freezing chambers purchased from Nalgene (Rochester, NY, USA) containing isopropyl alcohol and the chamber was transferred for overnight storage at -80°C. This procedure allows gradual freezing of the cells at a rate of $-1^{\circ}\text{C}\cdot\text{min}^{-1}$, which allows the reduction in metabolism of the cells and allows enhanced survival upon resuscitation. Following overnight incubation at -80°C, cryovials were transferred to liquid nitrogen for long term storage. The growth of ice crystals is reduced in liquid nitrogen, thus enhancing cell survival during long term storage.

For restoring cell stocks from liquid nitrogen, cryovials were placed at room temperature in a cell culture safety cabinet until thawed and cell suspension quickly transferred to a 0.2% Gelatin pre-coated flask, containing warm GM.

2.2.2. WOUND HEALING ASSAY WITH LIVE IMAGING EXAMINATION

In order to investigate the migration potential of C2C12 cells in response to specific factors, a wound healing assay was established. In the wound healing assay, a scratch/wound was created in a monolayer of confluent cells, usually using a pipette tip, and the progress of wound closure by the cells was observed over time. The advantages of this method is that it is easy to perform and relatively cheap, while at the same time, if combined with Live imaging microscopy and appropriate analyses, it can provide useful information not only on the migration of cells, but also on their behavior, morphology, proliferation and cell death.

2.2.2.1. WOUND HEALING METHOD

Cells were seeded in pre-gelatinised 12 well plates at a confluency of 80,000 cells/well in GM. Once 80-90% confluency was reached (generally, on the next day after seeding), GM was removed, cell monolayers were washed with PBS and 0.1% FBS DMEM media, containing 1% Pen-Strep (10000 U/ml) and 200mM L-glutamine, was added (known as quiescent media). Cells were incubated for 20 hours in quiescent media before a wound was made, using a sterilized pipette tip, and live imaging examination of the wound closure was initiated. Live imaging for wound healing/cell migration studies was performed using Leica DMI6000B microscope equipped with an autoflow incubator, maintaining 5% CO₂

atmosphere at 37°C. CO₂ controller, temperature controller and heating unit were turned on the day before the experiment was initiated for the atmosphere conditions inside the incubator to be stabilised. Multi-well dishes containing the wounded cell monolayers were placed on a movable stage inside the incubator, X and Y coordinates were set in 4 random locations along the length of each wound and images were acquired every 15min at 10x magnification. To study migration in the absence of conflicting proliferation, cell monolayers were pre-incubated for 3hrs in 10µg/ml of Mitomycin-C, (purchased from Sigma-Aldrich (Dorset, England)) before live imaging was initiated.

2.2.3. LIVE IMAGING MIGRATION ANALYSIS

Migration analyses were performed using Keynote'09 software version 5.1.1. (Apple Inc.), which was employed to draw lines, separated by equal distances, into images of the wound healing videos, enabling the creation of cell movement trajectories frame by frame into exported .AVI videos of migrating cells. ImageJ v1.45i software was used to count cells in different zones of the wounds and to track and calculate the distance of migration trajectories of cells.

2.2.4. CELL DEATH ANALYSIS BY LIVE IMAGING

To ensure consistency of data collection, cell death analyses during wound healing assays were performed using the same live imaging movies generated and analysed for cell migration. Each live imaging clip was separated into 6 equal areas using Keynote'09 software version 5.1.1. (Apple Inc.). The number of dying cells were manually counted frame by frame in each area for the duration of the movie. Dying cells were clearly obvious as floating cell bodies in the supernatant. The numbers of dying cells from the 6 random fields were summed and represented as the number of dying cells in each movie field over the total number of cells (alive+dead) in the same fields. At least 3 replicate movies were analysed per experiment.

2.2.5. TRANSWELL INSERTS MIGRATION ASSAY

2.2.5.1. PRINCIPLE

Transwell inserts allow the examination of chemotaxis. As shown on Figure 2.2, each transwell insert has an anchored microporous membrane, which is placed in a multi-well dish, thus providing upper and lower compartments. The upper compartment is inoculated with the cell suspension, while the lower compartment contains the chemoattractants or media to be tested. Usually, media composition in the upper and lower compartments differ, with cells suspended in serum-free (SF) media in the upper chamber, so that a chemoattractant gradient is established across the microporous membrane. This allows the cells in the upper compartment to migrate through the pores towards the lower compartment containing chemoattractants. Once cells have migrated through the pores, they adhere on the under-side of the membrane. Non-migrating cells on the upper side of the microporous membrane can be removed by gentle swabbing (thus not damaging the membrane or dislodging cells on the lower side), enabling the fixing, staining and counting of the migrated cells.

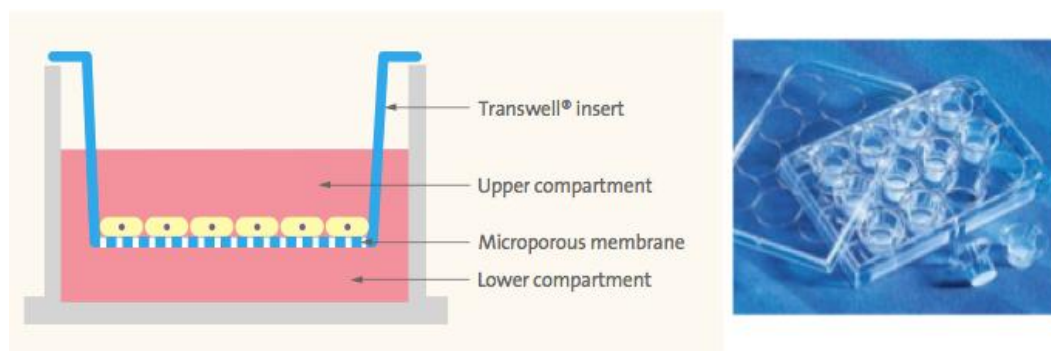


Figure 2.2. Transwell inserts representation. On the left, a schematic representation of a transwell insert. Cells, placed in the upper compartment, can cross the microporous membrane toward chemoattractants present in the lower compartment. On the right, a photograph of transwell inserts placed in a 12 well plate. Pictures were taken from Corning Transwell Permeable Supports Selection and User Guide (Corning Incorporated, CLS-CC-007W REV3, printed in USA, 2006).

2.2.5.2. METHOD

Trypsinized cells (see section 2.2.1.2) were centrifuged for 10min at 500g. Supernatant containing GM was discarded and cells were washed with PBS,

followed by another centrifugation for 10min at 500g. Cell pellets were resuspended in SF media, cells were counted and myoblast numbers were adjusted to 120,000 cells/ml.

Corning® Costar® 6.5mm permeable polycarbonate transwell membrane supports (8.0µm pore size) were placed in 24 well dishes, with each well (e.g. lower compartment) containing 600µL of test media. 200µL of the cell suspension (120,000 cells/ml) was added in a dropwise manner to the upper compartment of the transwell insert. Having initially optimised the timing of the experiments, it was determined that after 4h the experiment should be terminated. Each insert was washed by transfer to 600µL PBS, followed by fixation with 2.5% gluteraldehyde for 15min (Fisher Scientific, Fair Lawn, NJ, USA). Adherent cells were permeabilized for 3min in 0.5% Triton X-100 (BDH Labs, Poole, England), before staining for at least 20min at RT in Gill's no.1 haematoxylin (Thermo electron corp., Runcorn, UK), followed by a wash in 0.04% NH₄OH (Acros Organics, Geel, Belgium). Moist cotton buds were used to gently remove the cells on the upper membrane of the insert, ensuring only migrated cells remained on the membrane. Migrated cells were visualized on Leica DMI6000B inverted microscope and 3 random fields per insert were photographed. Cell counting was performed using Cell Counter plugin of ImageJ v1.45i.

2.2.6. PHALLOIDIN-FITC STAINING

Phalloidin is a toxin, which binds specifically to F-actin. When labelled with fluorescein molecules, such as FITC, phalloidin enables the visualization of the actin cytoskeleton within cells. Phalloidin staining was a useful tool to clearly visualize the morphology of well developed myotubes.

Phalloidin staining was performed directly in the multi-well dishes, in which the cell monolayers were grown. Cell monolayers were washed in PBS and fixed for 20min in freshly prepared 3.7% formaldehyde solution (H₂O) (Fischer Scientific, Loughborough, UK). Cell monolayers were incubated for 3min in 0.5% Triton X-100 followed by 30min at RT with 15µg/ml phalloidin-FITC (Sigma, St. Lois, MO, USA). Images were obtained using Leica DMI 6000B imaging system and a FITC-fluorescence L5 filter cube (excitation wavelength = 480/40nm).

2.2.7. BIOCHEMICAL ASSAYS

Protein assays were performed to measure the quantity of proteins in cell lysates prior to e.g. electrophoresis and Western blotting examination, in order to normalize loading. Protein determination was also employed in conjunction with CK assays to normalize enzyme activity to protein content.

2.2.7.1. PROTEIN ASSAY

Samples for protein assay were prepared by adding 200 μ L per well (for 6 well plate) lysis buffer (composed of: 10 mM TrisCl, 5mM EDTA, 50 mM sodium chloride, 30 mM sodium pyrophosphate, 50 mM sodium fluoride, 100 μ M sodium orthovanadate, 1 mM PMSF and 1% Triton X-100) for SDS PAGE analyses or 150 μ L per well (for 6 well plate) of Tris Mes Triton (TMT buffer; composed of: 0.05M Tris/Mes and 1% Triton-X100) for CK analyses. Following removal of cells from the substrata, using a scraper, lysed cells were collected and centrifuged for 2min at 8,000g to pellet and discard insoluble debris; samples were stored at -20°C until further analysis.

For the protein determination, BSA protein standards were prepared in either lysis (for western blot) or TMT (for CK assay) buffers at concentrations of 4, 2, 1, 0.5, 0.25, 0.125, 0.0625 and 0 mg.ml⁻¹. Standards were prepared by diluting 200mg BSA (in 0.9% sodium chloride and sodium azide a preservative; Pierce, Rockford, IL, USA) in 4.8ml buffer to obtain a 40mg.ml⁻¹ stock solution; 200 μ L were diluted in 1.8ml buffer (lysis or TMT) to obtain the first standard of 4mg.ml⁻¹. The remaining protein standards were prepared by serial dilutions of the 4mg.ml⁻¹ sample.

Protein assay was performed using BCA Protein Assay purchased from Pierce (Rockford, IL, USA). BCA reagents A & B were mixed in ratio 1:50. 200 μ L of the mixed solution was added in a 96 well plate with 10 μ L of the protein samples or standards. The 96 well plate was incubated at 37°C and absorbance was recorded after 45 or 60 minutes at 630 nM using a Bio-Tek ELISA plate reader (Winooski, VT, USA). Standard curves were automatically generated by plotting the average blank-corrected 630nM measurement of the loaded BSA standards against pre-programmed known concentrations in mg.ml⁻¹ and sample concentrations were calculated from the standard curve.

2.2.7.2. CREATINE KINASE (CK) ASSAY

CK assay was used to measure the *in vitro* differentiation of C2C12 mononucleated myoblasts into multinucleated myotubes. Samples were prepared as described above. A commercially available CK assay kit was employed (Catachem Inc., Connecticut, NE, USA). Reagents of the kit were mixed according to manufacturer's instructions and following addition of 6-10 μ L of each sample to the wells, 200 μ L of the mix was added to the wells of the 96 well UV plate (BD Biosciences, San Jose, CA, USA) using a multichannel pipette. The plate was incubated for 3min on a shaker at RT before being read on a Bio-Tek ELISA plate reader at 340nm absorbance. Readings were taken every minute for up to 10min. First and last readings were usually used to calculate the CK activity, according to the following equation:

$$\text{CK (U.l}^{-1}\text{)} = (A.\text{min}^{-1} \times \text{TV} \times 1000) \div (6.22 \times \text{SV})$$

$$A.\text{min}^{-1} = (\text{Final Absorbance} - \text{Initial Absorbance}) \div (\text{Final Reading Time} - \text{Initial Reading time (mins)})$$

Where:

- A.min⁻¹ = Change in absorbance per minute at 340 nM
- TV = Total volume (ml)
- 1000 = Conversion of units per ml to units per liter.
- 6.22 = Millimolar absorptivity of NADH at 340nM
- SV = Sample volume (ml)

Therefore, using 8 μ l of sample and 200 μ l of reagent the following equation applies:

$$\text{CK (U.l}^{-1}\text{)} = (A.\text{min}^{-1} \times 0.208 \times 1000) \div (6.22 \times 0.008)$$

2.2.8. WESTERN BLOTS

Western blots were performed to detect and quantify specific proteins in cell extracts isolated from C2C12 myoblasts subject to different treatments. Briefly, the method is based on isolating proteins from cell lysates and subjecting them to electrophoretic separation using SDS polyacrylamide gel electrophoresis (SDS-

PAGE). Separated proteins are transferred to a nitrocellulose membranes and primary antibodies specific to the proteins of interest are applied. Secondary antibodies, specific to the primary antibodies, are labelled with horseradish peroxidase (HRP) enzyme, which is able to produce a luminescent signal upon incubation with appropriate substrate. This enables, using appropriate capture systems, the detection and quantification of the proteins of interest.

2.2.8.1. SAMPLE PREPARATION

Cells were subjected to specific treatments for pre-determined periods of time before being lysed, as detailed above. Following protein extraction and determination of concentration, samples were loaded according to protein (30 μ g per sample in a maximum 90 μ L total volume used). 10 μ L of Color Burst Electrophoresis markers (Sigma, Poole, UK), diluted in lysis buffer, were prepared alongside the samples, as a reference for the molecular weight of migrating proteins (in kDA). 1/5 of the total sample volume of 5x Laemmli Sample buffer (6.8ml dH₂O, 2ml 0.5M Tris pH 6.8, 3.2ml Glycerol, 3.2ml 10% SDS, 0.8ml 2-mercaptoethanol, 1.6ml 1% bromophenol blue) was added to each sample. Samples and standards were boiled at 100°C for 5min, in order to reduce disulphide bonds and facilitate protein denaturation, followed by immediate transfer to ice.

2.2.8.2. GEL ELECTROPHORESIS

Samples, prepared in section 2.2.8.1. were subjected to SDS polyacrylamide gel electrophoresis (SDS-PAGE). Acrylamide, mixed with bisacrylamide, is able to form a polymer network/mesh when mixed with ammonium persulfate (APS) and N,N,N,N'-tetramethylethylenediamine (TEMED), which catalyzes the polymerization of the reaction. Proteins are able to migrate through the polyacrylamide mesh of the gel and are thus separated by size. Treating the samples with reducing agents, such as 2-mercaptoethanol, and adding sodium dodecyl sulfate (SDS) to the gels, helps to denature secondary or tertiary structures, disulfide bonds, and to maintain the proteins in a denatured state. SDS also negatively charges proteins and allows them to migrate to the positively charged electrode through the polyacrylamide gel. This allows the separation of proteins by molecular weight (with no influence of charge), as smaller proteins migrate through the pores of the gel faster than

larger ones. The higher the percentage of acrylamide, the slower the migration of proteins through the gel. According to the percentage of acrylamide, gels are composed of a stacking gel (usually 5% acrylamide; 3.75ml 30% Acrylamide 1% BIS, 1.12ml of 1.1M Tris HCL ph 6.8, 0.225ml 10% SDS, 17.4ml H₂O, 22.5µL of Tetramethylethylenediamine (TEMED), 337.5µL of APS), allowing fast migration of proteins and their aligning for separation, and a resolving gel (usually 6-12% acrylamide; 8.65% acrylamide: 11.35ml of 30% Acrylamide 1% BIS, 8.4ml 1.5M Tris Base pH 8.9, 1.35ml 10% SDS, 18ml dH₂O, 13.12µL TEMED, 306.25µL ammonium per-sulphate (APS)), which enables protein separation by size. A schematic representation of how the gels are structured is presented on Figure 2.3.

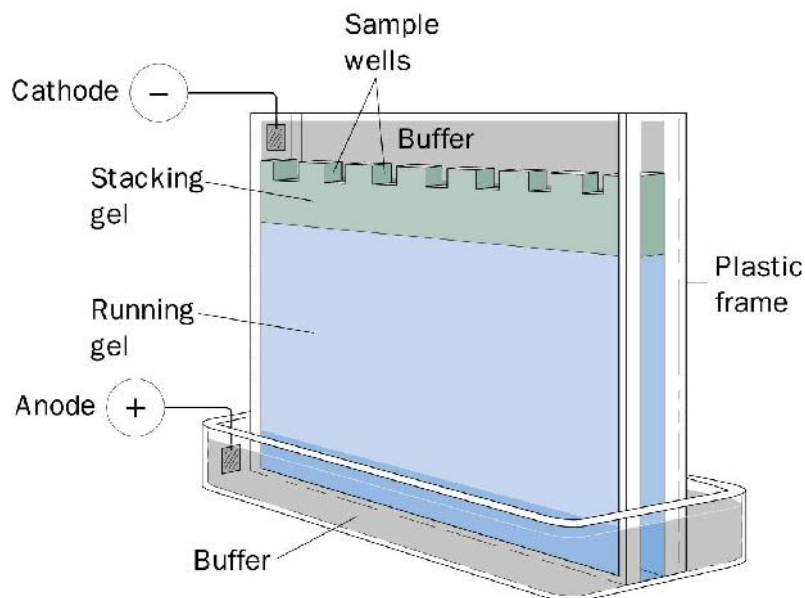


Figure 2.3. SDS polyacrylamide gel preparation. Gels are prepared as a stacking gel (usually containing 5% Acrylamide) poured on top of a resolving gel (usually containing 6-12% acrylamide). Samples are loaded into wells, formed by inserting a plastic comb into the stacking gel before it has polymerized. Once current is applied, negatively charged proteins migrate to the positive electrode. This allows the separation of proteins by size, as larger molecular weight proteins migrate more slowly through the pores of the gels, while smaller proteins are able to migrate more quickly. Source of image: www.siumed.edu (date accessed: 1st March 2012)

Gels were assembled using a Jencons TV200 Twin Plate Wide Mini-Gel Electrophoresis Unit, which was placed in a tank with 1x Running TGS buffer (25 mM Tris, pH 8.3, 192 mM glycine, 0.1% SDS in dH₂O) (Bio-Rad Laboratories

Ltd., Hertfordshire, UK). Following preparation of the resolving gel and the stacking gel, protein samples were loaded and voltage (175V) was applied until the bromophenol blue dye, included in the sample buffer, reached the interface between the stacking and the resolving gels. Voltage was subsequently decreased to 125V until the bromophenol blue dye reached the end of the resolving gel.

2.2.8.3. ELECTROPHORETIC TRANSFER

Following gel electrophoresis, proteins were transferred to nitrocellulose membrane to enable immune-detection. Semi-dry transfer was performed using the Witec AG, Semi Dry Unit-V20-SDB. Gel and nitrocellulose membrane were washed in transfer buffer (114 nM glycine, 19 mM Tris base, 33% methanol; pH 8.3) and sandwiched between 4 sheets of Whatman filter paper (Schleicher & Schuell, GmbH, Dassel, Germany), pre-immersed in transfer buffer. The proteins were electro-transferred from the gel to the nitrocellulose membrane at 20V for 90 min. using a Hoefer power supply. A schematic representation of the method is shown in Figure 2.4.

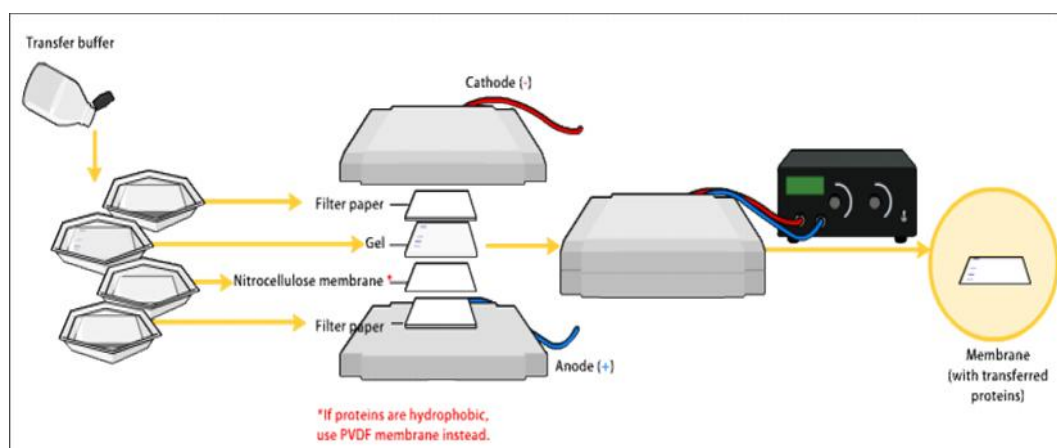


Figure 2.4. A representation of the semi-dry protein transfer method. Proteins are pulled from the gel to a nitrocellulose membrane using electric current, while retaining the same position they had on the gel. Source of picture: www.Wikipedia.org (date accessed: 1st March 2012)

The effectiveness and uniformity of the transfer were confirmed, following washing of the nitrocellulose membrane, in 0.1% Ponceau S in 5% acetic acid (Sigma, Poole, U.K). Ponceau S staining of proteins is reversible and can be completely removed by washing the membrane in dH₂O, followed by 1x TBST

buffer (1.21gr Trizma-Base, 8.78gr NaCl, 1ml Tween 20, dH2O to 1L, pH 7.4). A representative picture of nitrocellulose membrane following transfer of proteins and staining with Ponceau S is shown in Figure 2.5; uniformity of protein loading is illustrated.

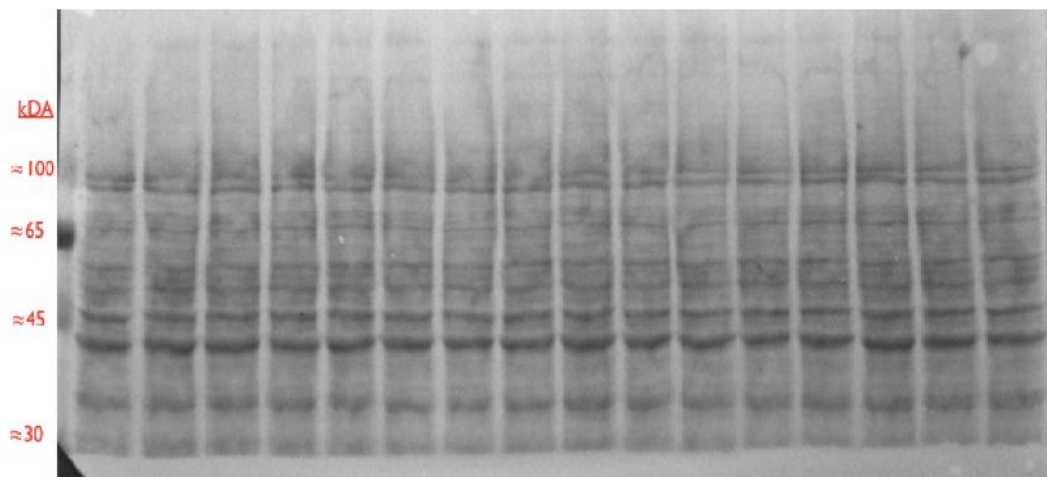


Figure 2.5. Ponceau S staining. Effectiveness and uniformity of protein transfer from the gel to the nitrocellulose membrane was verified with Ponceau S staining. Ineffective transfer, or incorrect protein loading would be evident with Ponceau S staining, therefore this acts as a secondary loading and primary transfer control. Red labels on the left indicate the molecular weight (in kDA), identified by the inclusion of a lane with Color Burst Electrophoresis markers.

2.2.8.4. BLOCKING

In order to detect specific proteins of interest following transfer, antibodies targeted against these proteins need to be incubated with the membrane. However, the nitrocellulose membrane has the strong ability to non-specifically bind proteins and therefore the possibility exists that the antibodies, which are proteins themselves, can bind to many sites of the nitrocellulose membrane and thus cause noise, difficulties in interpreting results or even false positive results. This can be avoided by blocking unbound sites of the membrane in solutions containing generic proteins, normally non-fat dry milk, gelatin or BSA, which bind to all free sites of the nitrocellulose membrane, thus reducing non-specificity and high background. Depending on the secondary antibodies used, nitrocellulose membranes were blocked for 1h at RT in either tris-buffered saline – 0.1% tween 20 plus 5% non-fat dry milk (TBST-M) or in 1% BSA (TBST-BSA).

2.2.8.5. DETECTION

Following blocking, membranes were incubated with primary antibody overnight at RT, followed by incubation with horseradish peroxidase (HRP)-conjugated secondary antibody diluted in blocking solution for 1h at RT. Steps were separated by washing the membranes with dH₂O, followed by 3 washes in 1x TBST for 15min each. All secondary antibodies were labelled with horseradish peroxidase (HRP). HRP is an enzyme, which participates in a chemical reaction when incubated with substrate which is oxidized by HRP, using hydrogen peroxide as the oxidizing agent, resulting in the production of a luminescent signal. This allows the detection and quantification of target proteins. The whole process is summarized on Figure 2.6.

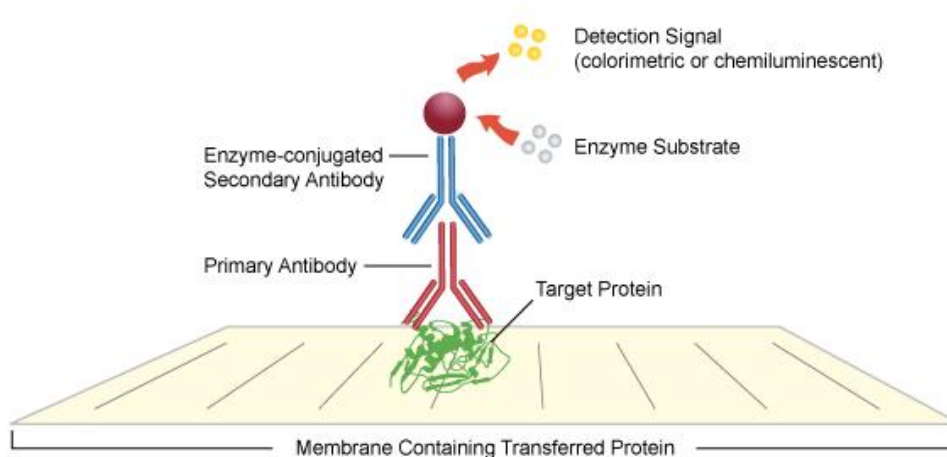


Figure 2.6. Detection and quantification of target proteins. Target proteins, transferred to nitrocellulose membranes, are bound by primary antibodies, which are recognized by enzyme-conjugated secondary antibodies. The enzyme, such as HRP, participates in a chemical reaction when a specific substrate is added, resulting in the emission of a detectable signal. The light signal can be detected by a camera, enabling the semi-quantification of the target proteins present on the nitrocellulose membrane. Source of picture: www.leinco.com (date accessed: 1st March 2012)

Enhanced chemiluminescence (ECL) HRP substrate, West Dura Supersignal (Pierce, Rockford, IL, USA), was applied to induce enzymatic reaction with the HRP tag of the secondary antibodies and chemiluminescence, proportionate to the amount of protein, was captured using the Biorad Imaging System (Hercules, CA, USA). Densitometry was further applied for quantifying the proteins. Where

appropriate, all phosphorylated forms of proteins investigated were normalized either to their respective total protein levels or to beta-actin. Antibodies were purchased from New England Biolabs (Hertfordshire, UK) or Promega (Southampton, UK), unless otherwise specified.

2.2.8.6. NITROCELLULOSE MEMBRANE STRIPPING

Nitrocellulose membranes, requiring antibodies to be stripped to enable re-probing, were incubated for 45min at 60°C with stripping buffer (10ml 10% SDS, 6.25ml 0.5M Tris, 0.4ml 2-mercaptoethanol, 33.5ml H₂O). Nitrocellulose membranes were washed for 1hr with dH₂O, followed by 3 washes for 15min in TBST. The incubation with 2-mercaptoethanol containing stripping buffer was performed in a biosafety cabinet.

2.2.9. RNA EXTRACTION

RNA was isolated from cells using Guanidinium thiocyanate-phenol-chloroform extraction, with Trizol® reagent (Invitrogen, Life Technologies, Paisley, UK). Trizol contains phenol and Guanidinium thiocyanate, which have cell lysing and protein denaturing actions, thus also preventing the activity of RNase and DNase enzymes. Following cell treatments, 330µL of Trizol® per well of a 6 well plate was added to the cell monolayers and plates were incubated for 5min at RT. Cell lysates were collected following scraping with a cell scraper to disrupt the cells, and stored at -20°C until further analysis. For RNA isolation, chloroform: Trizol® in 1:5 ratio was added to the lysate, solution was mixed, incubated for 10min., RT and centrifuged for 16min at 12,000xg. Chloroform, along with the phenol contained in the Trizol® reagent, causes the proteins to denature and precipitate and separates the RNA into an aqueous supernatant. Following addition of chloroform and centrifugation, a visible separation of the solution into three phases is visible (aqueous phase, interphase and organic phase), as shown in Figure 2.7. The majority of the RNA is present in the aqueous phase, while DNA and proteins are in the interphase and organic phases respectively. Following separation of the solution into three phases, the aqueous phase was transferred to a new tube and equal volume of ice-cold isopropanol was added. Isopropanol precipitates and recovers the RNA from the aqueous phase, which becomes visible as a pellet after 10min of centrifugation at 12,000xg. The RNA pellet was

washed with 75% EtOH, centrifuged at 8,000xg for 10min and air dried. Tris-EDTA (TE) buffer (Applied Biosystems, Ambion, Cheshire, UK) was added to reconstitute the RNA.

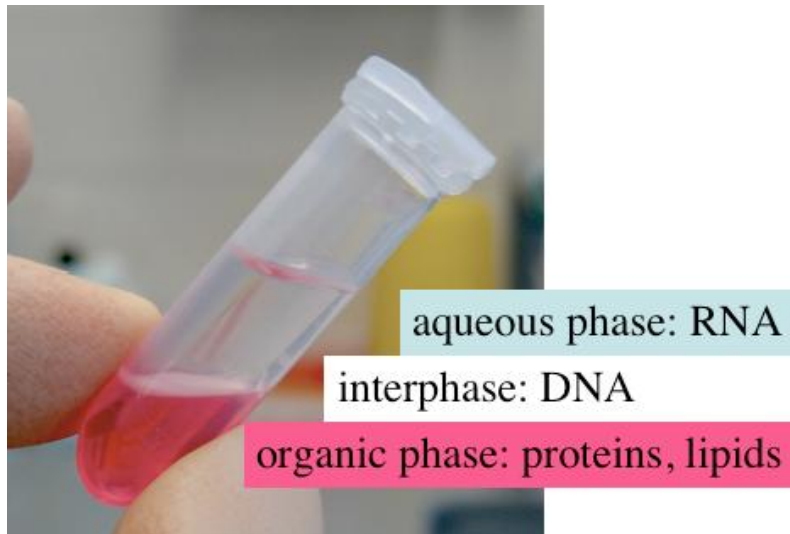


Figure 2.7. Trizol lysate phase separation. Following addition of chloroform to the Trizol® lysate and centrifugation, the solution is separated into 3 phases. RNA is isolated from the aqueous phase. Source of picture: www.openwetware.org (date accessed: 1st March 2012)

After reconstitution in TE buffer, RNA concentration and purity were assessed by UV spectroscopy, using a Biotech Photometer (WPA UV1101, Biochrom, Cambridge, UK). The absorbance of the diluted RNA sample was measured at 260 and 280 nm. Absorbance at 260nm was used to determine the RNA concentration, as it is known that A₂₆₀ reading of 1.0 is equivalent of 40µg/ml of RNA. A 260/280 ratio was used to assess the purity of RNA - it is known that a 260/280 ratio of 1.8-2.1 indicates a good purity of RNA solution, which can be used for Real-time PCR.

2.2.10. REAL-TIME PCR

2.2.10.1. PRINCIPLE

Gene expression can be altered in response to various conditions or different stages of cell development and is a key step in how many cellular processes, including differentiation, are accomplished. A commonly used method for investigating gene expression is Real-time PCR (RT-PCR), which quantifies the amount of mRNA molecules produced by a specific gene after it is transcribed. The method relies on converting the previously isolated mRNA (section 2.2.9) into complementary DNA (cDNA) by reverse transcription and amplifying the cDNA, while detecting in real time the amount of amplified DNA molecules (hence, the method is named Real-time PCR). The detection of amplified product is performed by labeling the DNA with molecules emitting fluorescence, which is proportionally increased with the amplification of the cDNA molecules with each cycle of the reaction. Two commonly used fluorescent tags in Real-time PCR are SYBR® Green dye and TaqMan® probes. SYBR® Green dye is the cheaper alternative - it binds to all double stranded DNA and is able to detect all amplified double-stranded DNA molecules. However, it may also detect non-specific reaction products. TaqMan® probes are more expensive, but can be synthesized for each unique target sequence and are therefore emitting fluorescence only when the specific PCR product is amplified. Comparison of both chemistries is presented on Figure 2.8.

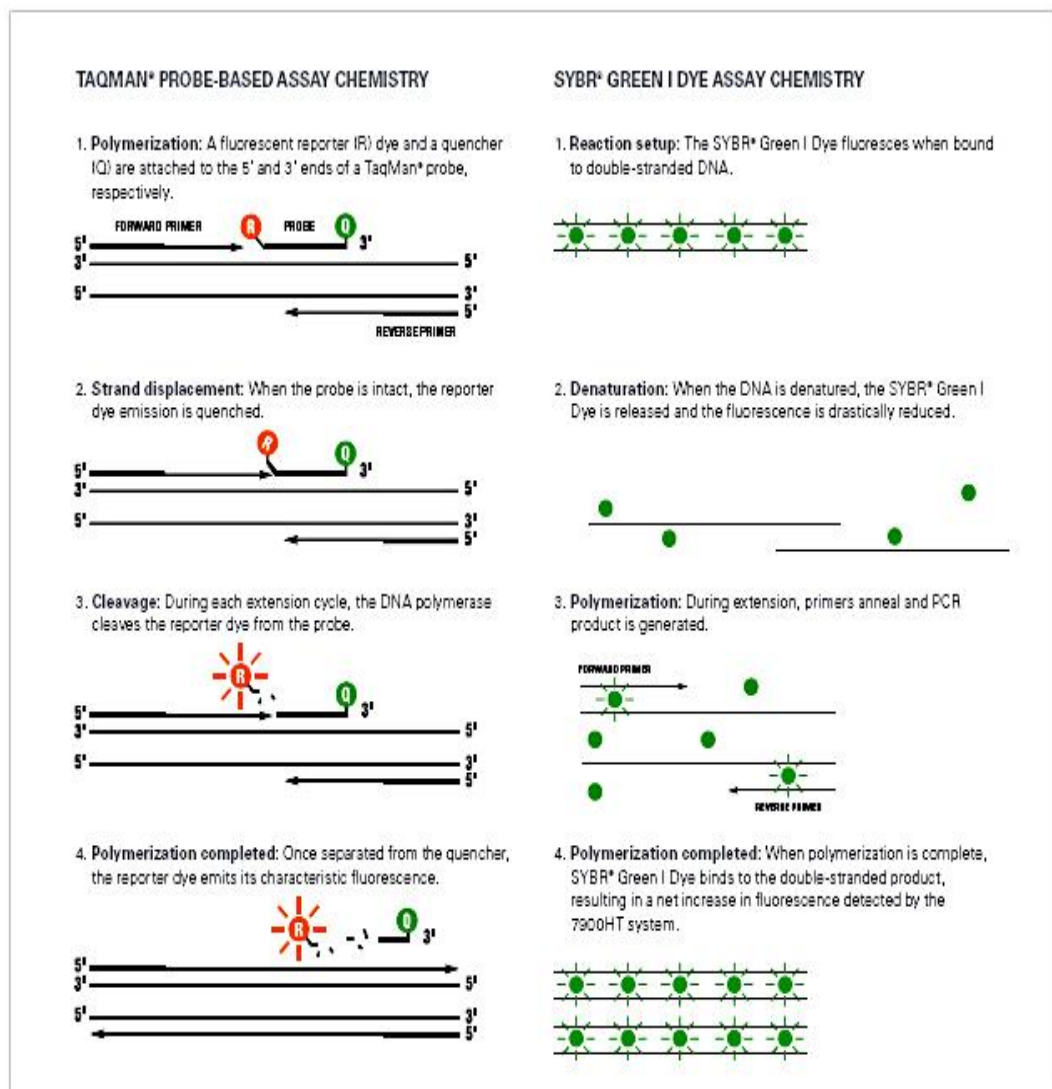


Figure 2.8. Comparison of PCR products in Real-time PCR between SYBR® Green and TaqMan® chemistries. TaqMan® detection is more specific, as it uses a specially designed probe for each target sequence, which emits fluorescence only when the target sequence has been replicated. SYBR® Green dye is less specific, as it binds to any double stranded DNA present in the reaction. Source of figure: www.appliedbiosystems.com (date accessed: 1st March 2012)

The increase in fluorescence with each cycle is detected enabling estimation of the rate of amplification and the abundance of the cDNA molecules generated. The higher the gene expression, i.e. the starting concentration of cDNA, the fewer number of amplification cycles it will take for the levels of fluorescence to reach a certain threshold (represented as Ct value). Thus, the lower the Ct value, the higher the gene expression level. Comparison of Ct values between different samples is therefore indicative of how gene expression between these samples

differ. Figure 2.9 shows an example of 3 samples with different gene expression levels and how this is represented by their Ct values.

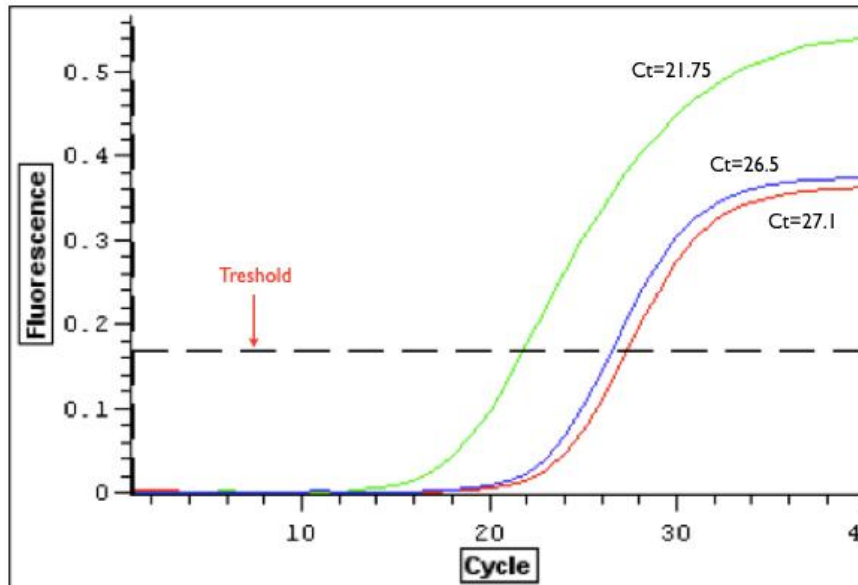


Figure 2.9. Real-time PCR Ct value. Real-time PCR analysis demonstrates the number of cycles required for 3 different samples to reach a specific fluorescence threshold (represented by their Ct value). The lower the Ct value, or the number of cycles required to reach the fluorescence threshold, the higher the expression of the gene. Thus, the sample represented by the green curve is the one with highest gene expression (Ct=21.75), followed by the blue one (Ct=26.5) and the red sample is the one with the lowest gene expression (Ct=27.1).

For the DNA amplification to take place in PCR, target DNA needs to be mixed with several other reaction components: 1) Pair of primers - short DNA fragments that serve as the starting point for DNA synthesis and defining the sequence to be amplified; 2) DNA polymerase - the enzyme that catalyzes the reaction (Taq polymerase is commonly used for PCR); 3) dNTPs - deoxynucleotidetriphosphates, the building blocks for DNA synthesis; 4) Cations, such as Mg^{2+} , acting as co-factors of DNA-polymerase enzyme and 5) buffer maintaining the correct pH required for the reaction to occur.

Optimum temperature conditions are required for DNA amplification. PCR reaction mix is subject to cycles of repeated heating and cooling, which allows the denaturation/melting of the complementary DNA strands and their separation into single strands, the annealing of the primers and the extension of the newly synthesized DNA strands by the DNA polymerase. The denaturation/melting of

the double stranded DNA molecules is accomplished by breaking the hydrogen bonds at 94-98°C. The temperature then needs to be decreased to 50-65°C for the primers to anneal. Taq DNA polymerase has an optimum activity temperature of 75-80°C, although a temperature of 72°C is commonly used. AmpliTaq Gold® DNA Polymerase, used in this thesis, consolidates the annealing and extension steps into one, at 60°C.

2.2.10.2. METHOD

Both SYBR® Green- and TaqMan®-based detection approaches were used in this thesis.

2.2.10.2.1. SYBR® GREEN

For SYBR® Green detection, Power SYBR® Green RNA-to-CT 1 step kit was used (Applied Biosystems, San Jose, CA, USA). The kit contained both AmpliTaq Gold® DNA Polymerase, required for DNA amplification and ArrayScript™ UP Reverse Transcriptase, the enzyme required for the reverse transcription of mRNA into cDNA. Final reaction volumes were 15µL per reaction, composed of 6µL RNA (10ng/µL), 7.5µL master Mix containing the Taq polymerase enzyme, 1.5µL primer mix and 0.12µL RT enzyme. The PCR reactions were performed on Bio-Rad Chromo4™ real-time PCR detector (Hercules, CA, USA) with Opticon Monitor version 3.1.32 (MJ Geneworks Inc., Bio-Rad Laboratories, Inc., Hercules, CA, USA) and also on Applied Biosystems StepOnePlus Real-time PCR system with StepOne™ Software v2.2.2 (Applied Biosystems Life technologies). The following program was used:

Stage	Step	Temperature	Time
Holding	Reverse transcription	48°C	30 min
Holding	Activation of TAQ polymerase	95°C	10 min
Cycling (40 cycles)	Denaturation	95°C	15 sec
	Annealing/Extension	60°C	1 min
Melt Curve generation	Denaturation	95°C	15 sec
	Annealing	60°C	15 sec
	Denaturation	95°C	15 sec

As SYBR® Green is able to detect any double stranded DNA, including primer dimers, contaminating DNA or non-specific products, it is important to perform melting curve analyses to confirm the specificity of the amplification. Melting curve analyses measure the temperature-dependent dissociation of the two DNA strands. As temperature is gradually increased, a sharp increase in fluorescence is observed when the product is amplified and a sharp decrease - at melting temperature (Figure 2.10). The temperature at which this peak appears is specific for each amplicon, depending on its size. Thus, a specific product is characterised with a sharp peak, while multiple peaks indicate non-specific amplification.

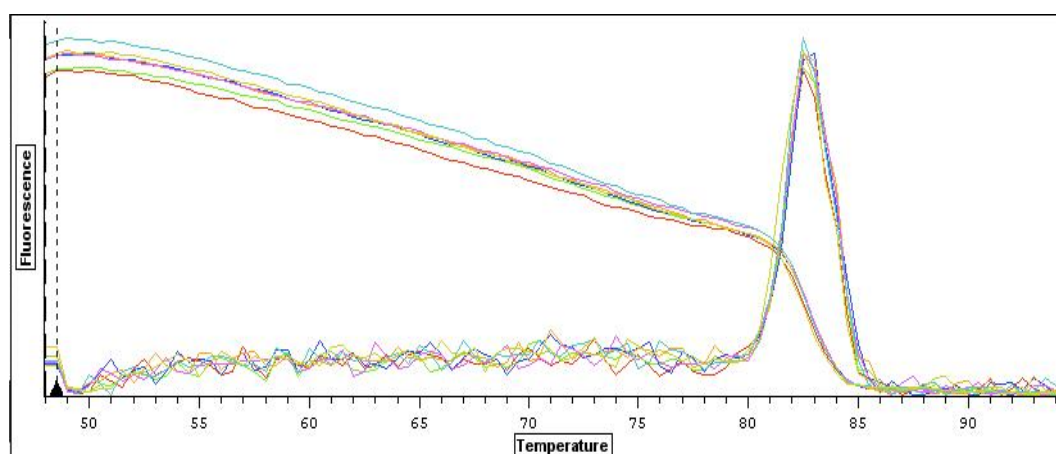


Figure 2.10. Melting curve in Real-time PCR. Generation of melting curve is important to verify the specificity of the amplification when SYBR® Green dye is used. A sharp peak, as shown on the figure, is indicative of specific amplification, while the presence of additional peaks would indicate non-specific amplification, primer dimers or contamination.

The following predesigned primer sets were ordered from Quiagen and were used with the SYBR-Green detection method: Polr2b (QT00154602), MyoD (QT00101983) and Myogenin (QT00112378).

2.2.10.2.2. TAQMAN®

For TaqMan® detection, TaqMan® RNA-to-CT™ 1-Step Kit was used (Applied Biosystems, San Jose, CA, USA). The kit contained both AmpliTaq Gold® DNA Polymerase, required for DNA amplification and ArrayScript™ UP Reverse Transcriptase, the enzyme required for the reverse transcription of mRNA into cDNA. Final reaction volume was 20µL per reaction, composed of 8.5µL of RNA (10ng/µL), 10µL master Mix containing the DNA polymerase enzyme, 1µL of primers mix and 0.5µL RT enzyme. Applied Biosystems StepOnePlus Real-time PCR system with StepOne Software v2.2.2 (Applied Biosystems, Life Technologies) was used. The following program cycles were used:

Stage	Step	Temperature	Time
Holding	Reverse Transcription	48°C	15 min
Holding	Activation of TAQ polymerase	95°C	10 min
Cycling (40 cycles)	Denaturation	95°C	15 sec
	Annealing/Extension	60°C	1min

The following predesigned primer sets were ordered from Applied Biosystems and were used with the TaqMan® detection method: Polr2b (Mm00464214_m1), MyoD (mm00440387_m1), Myogenin (mm00446194_m1), Spire1 (mm01258168_m1), Spire2 (mm00552235_m1), Formin1 (mm00439021_m1) and Formin2 (mm00444598_m1).

2.2.10.3. ANALYSIS

Relative quantification of gene expression was determined automatically by Opticon Monitor version 3.1.32 (MJ Geneworks Inc., Bio-Rad Laboratories, Inc., Hercules, CA, USA) and StepOne Software v2.2 (Applied Biosystems, Life Technologies). The relative quantification is based on analyzing changes in gene expression relative to a reference sample (control). One sample from the experiments was set as a calibrator/control and fold change to this calibrator was determined for all samples of the experiment. All samples were normalized to a housekeeping gene (Polr2b), which expression is known to remain consistent in C2C12 cells, regardless of the treatment.

2.2.11. FLOW CYTOMETRY

2.2.11.1. PRINCIPLE

Flow cytometry is a technique, which can be used for counting and examining the properties of particles or cells passing through a stream of liquid. A laser beam is directed to the stream of liquid and detectors are aimed at the point where the stream passes through the light beam. Detectors are oriented in line with the beam (Forward Scatter = FSC) or perpendicular to it (Side scatter = SSC). When a cell passes through the laser beam, it causes the light to be scattered and caught by the detectors, which provides information on the volume of the cell (FSC) or the inner complexity of the cell (SSC). Fluorescent detectors may also give information on fluorescent chemicals found in cells (Figure 2.11).

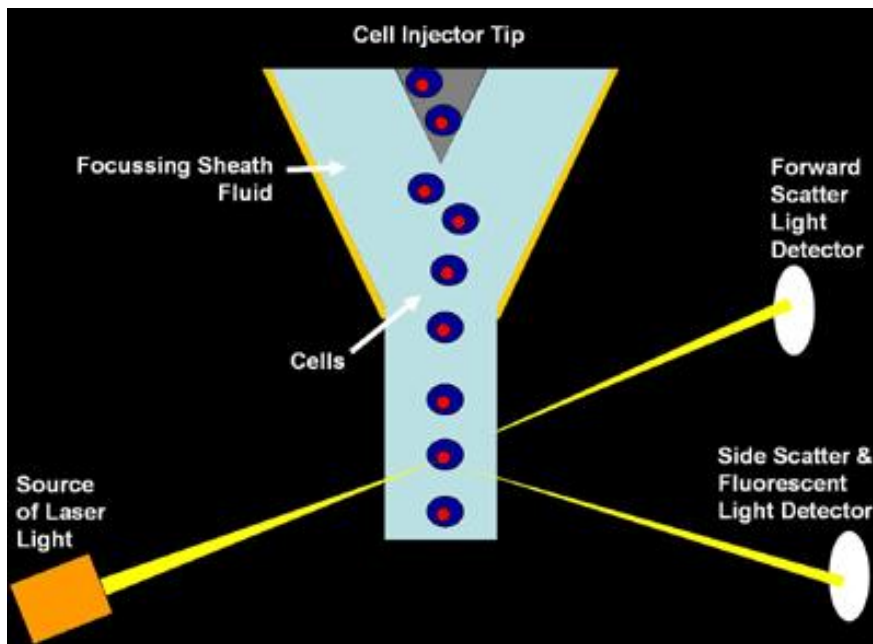


Figure 2.11. A schematic representation of the mechanisms of Flow cytometry. Picture source: www.gene-quantification.de (date accessed: 1st March 2012)

2.2.11.2. PROPIDIUM IODIDE AND CELL CYCLE EXAMINATION

One of the applications of Flow cytometry is the examination of the cells in different phases of the cell cycle. To achieve this, propidium iodide (PI) is used. PI is an intercalating agent - binding DNA between the bases. It is also a fluorescent molecule. Once PI binds to nucleic acids, its fluorescence is enhanced. Thus, when cells are permeabilized and treated with PI, their DNA content can be examined by Flow cytometry. Cells in the G₂-phase of the cell cycle have duplicated their DNA content and would therefore emit double the fluorescence of the cells in the G₁ phase. Cells can be sorted into three groups: cells in G₁-phase (“gap” phase, before cells undergo cellular division), cells in S-phase (DNA replication phase) and cells in G₂/M-phase (mitosis phase, twice the DNA of the G₁ phase).

2.2.11.3. METHOD

20hrs after cell treatment, monolayers were washed with PBS and cells were detached with trypsin (as described in 2.2.1.2.), harvested in a 15ml centrifuge tube and pelleted by centrifugation for 10min at 500g. The supernatant was removed, cells were washed with PBS and centrifuged. After centrifugation, the

PBS supernatant was removed and cells were fixed with 5ml of 75% EtOH, which was added in a dropwise manner to the cell pellet while vortexing. Samples were stored at -20°C overnight before centrifugation and removal of the EtOH supernatant. Cells were washed twice with PBS and 0.5ml PBS was retained with the cell pellet to enable resuspension. Cells were mixed and transferred to 3 ml BD Falcon flow cytometry tubes (BD Biosciences, San Jose, CA, USA). 50 µl of ribonuclease A (RNase) (50 µg.ml⁻¹) and 10µL of PI (50 µg.ml⁻¹) were added to the cell solution. RNase treatment was necessary as PI is also able to bind to RNA molecules. After 30min incubation at room temperature, samples were stored at 4°C for flow cytometric analysis 24 h later.

2.2.11.4. ANALYSIS

Flow cytometric analysis was performed on Cell Quest Pro software. Cell cycle was analyzed using Modfit™ software (Verity Software House, Topsham, ME, USA), which allows analysis of cells in G1/S/G2/M phases of the cell cycle.

2.2.12. STATISTICAL ANALYSES

Statistical analyses and significance of data were determined using GraphPad Prism version 5.00 for Mac OS X, GraphPad Software, San Diego California USA, www.graphpad.com. Statistical significance for interactions between two paired groups was determined with a Paired t-test, while unpaired t-test was used for unpaired groups. Statistical significance for interactions between more than two groups was determined with a one-way ANOVA, or with a one-way repeated measures ANOVA, when matched observations were investigated. When more than one factor was present, two-way ANOVA was performed to investigate for significances of factors or interactions, or two-way repeated measures (mixed model) ANOVA, when matched observations were investigated. When significances of factors were indicated by two-way ANOVA, this was followed up by examining the statistical significance for interactions between more than two groups within the factor with a One-way ANOVA with Bonferroni post-hoc analysis, or with a t-test for examination between two groups. All results are presented as mean +/- standard error of the mean (SEM). All values below p<0.05 were considered as significant.

CHAPTER 3

3. MYOTUBE CONDITIONED MEDIA ENHANCES C2C12 MYOBLAST MIGRATION

3.1. INTRODUCTION

Skeletal muscle regeneration requires the recruitment of muscle progenitor cells, known as satellite cells, to the site of injury. They are normally quiescent cells, but in response to muscle damage, they become activated, migrate to the site of injury and proliferate to generate a progeny of myoblasts, which are capable of fusing with damaged myofibres to promote muscle repair and restore normal tissue architecture (reviewed in (Charge and Rudnicki, 2004, Hawke and Garry, 2001, Turner and Badylak, 2011). The process of migration is important for myoblast alignment and their subsequent fusion into multinucleated myotubes (Louis *et al.*, 2008, Rochlin *et al.*, 2010). Furthermore, insufficient cell spreading and migration has long been considered as one of the limiting steps in proposed cell therapies of Duchenne Muscular Dystrophy, although recent articles question this concept (Lafreniere *et al.*, 2009, Skuk *et al.*, 2011). Revealing in more details the regulators of myoblast migration may contribute to our understanding of the process of muscle regeneration, as well as open new avenues for better treatments of muscular dystrophies or improvement of skeletal muscle regeneration.

Following muscle injury, various factors are secreted from both the damaged muscle tissue or infiltrating inflammatory cells (Bischoff, 1986, Chen and Quinn, 1992, Merly *et al.*, 1999, Tidball, 2005). The effect of soluble factors on myogenic progenitors migration was investigated *in vitro* and some have been reported to act as chemoattractants for satellite cells or myoblasts - among them HGF, IL-4, TGF , TNF , PDGF-A, PDGF-B, FGF, IGF-I and platelet lysate (Amano *et al.*, 2002, Bischoff, 1997, Corti *et al.*, 2001, Lafreniere *et al.*, 2004, Lafreniere *et al.*, 2006, Ranzato *et al.*, 2009, Torrente *et al.*, 2003). It is important to note that the action of growth factors may be altered by their concentration. For example, higher concentrations of HGF are suggested to inhibit, rather than induce migration of myoblasts (Bischoff, 1997). Similarly, PDGF at low doses was shown to induce migration, while high doses induced proliferation (De Donatis *et al.*, 2008). This underlies the importance of investigating in more detail not only the independent action of soluble factors on myogenic cells, but reveal the complexity of the microenvironment and the exact composition of the biochemical milieu, which influences the behavior of cells contributing to

muscle regeneration under different physiological conditions. To accomplish this immense task, it is important to begin with improving our understanding of how factors released from different cell types and niches affect processes, such as cell migration, contributing to muscle regeneration, in both healthy or pathological states. It has long been known, for example, that crushed muscle extract contains factors, such as HGF, which are able to induce activation and migration of satellite cells (Bischoff, 1997, Tatsumi *et al.*, 1998). Recent studies have begun to investigate the expression pattern and secretome of skeletal muscle cells and the expression of chemokines during myogenesis *in vitro* (Chan *et al.*, 2011, Cui *et al.*, 2009, Griffin *et al.*, 2010, Henningsen *et al.*, 2010, Henningsen *et al.*, 2011). Griffin *et al.* demonstrated that approximately 80 chemokines were expressed by primary myoblasts *in vitro*, with most mRNAs being detected at the time of differentiation and fusion, with their abundance dramatically dropping after that time point (Griffin *et al.*, 2010). Furthermore, media conditioned by differentiating myoblasts at the time of fusion, was able to induce myocyte migration. It is possible that chemokines expressed during myogenesis regulate myoblast proliferation and survival and might be key for positioning myoblasts for fusion. These observations, however, also suggest that fusing myoblasts may secrete factors to induce migration of myogenic cells and thus recruit more myonuclei to contribute to the myotube formation and muscle growth. To our knowledge, no other studies have focused on how the milieu of secreted factors at different stages of myogenesis affects myoblast migration. In particular, no studies have been performed to investigate whether mature growing myotubes or myotubes in a state of starvation or atrophy would secrete factors inducing myoblast migration. In this situation, recruitment of mononuclear cells may also be needed to reduce the impact of degenerating myotubes. Furthermore, it would also be important to reveal which signalling pathways are central to the migration of myoblasts in response to secreted factors. Based on previous studies, some of the potential candidates would include MAPK and PI3K pathways, which have previously been implicated as regulators of myoblast migration (Al-Shanti *et al.*, 2011, Leloup *et al.*, 2007, Kawamura *et al.*, 2004, Kim *et al.*, 2011, Ranzato *et al.*, 2009, Suzuki *et al.*, 2000). However, how modulation of different signalling pathways affect the migration of myoblasts, remains a relatively unexplored field.

3.2. AIMS, OBJECTIVES AND HYPOTHESIS

The main aim was to reveal the impact of secreted factors by muscle cells on myoblast migration and the role of underlying signalling pathways in this process. It was hypothesised that mature myotubes or atrophying or injured myotubes would secrete factors, able to induce myoblast migration and that PI3K/AKT and MAPK/ERK pathways would be involved in the regulation of this process. Therefore, the objectives were to investigate whether myotubes, grown in SF media, would secrete factors into this medium, which would be able to induce subsequent mononuclear myoblast migration. It was also tested whether myotubes injured by mechanical damage would release factors inducing comparable or enhanced migration. Migration would be assessed by wound healing assay and chemotactic responses using transwell inserts. Western blots would assess how MAPK/ERK and PI3K/AKT pathways are regulated in myoblasts treated with the conditioned media (CM) and how selective inhibition of these pathways with inhibitors, such as LY204002 (for PI3K) and UO126 (for MAP/ERK), would affect the migration of myoblasts.

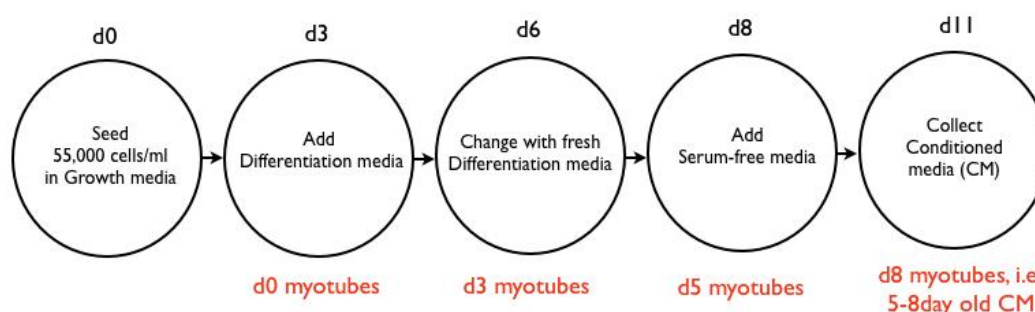
3.3. MATERIALS AND METHODS

3.3.1. CELL CULTURE

C2C12 myoblasts were cultured in a humidified 5% CO₂ atmosphere at 37°C. Cells were grown in 10% foetal bovine serum (FBS) DMEM media, containing 1% Pen-strep (10000 U/ml) and 200mM L-glutamine (Growth media, GM), in T75 flasks until confluent and split into multidish plates for experiments. In order to initiate differentiation, C2C12 cells were grown in 6 well plates until confluency was achieved, monolayers were washed with PBS and incubated in 2% horse serum (HS) DMEM media, containing 1% Pen-strep (10000 U/ml) and 200mM L-glutamine (Differentiation media, DM). For differentiation experiments lasting for more than 3 days, DM was refreshed on the third day.

3.3.2. CONDITIONED MEDIA GENERATION

C2C12 myoblasts in 6 well plates were triggered to differentiate into myotubes, in the presence of DM. To generate CM, cell monolayers were washed 2 times with PBS, SF DMEM, w/ 1% Pen-Strep (10000 U/ml), w/ 1% L-glut 200mM (SF) was added and plates were incubated for 3 hours in a humidified 5% CO₂ atmosphere at 37°C, in order to reduce the possibility of any residual serum components left in the wells. Cell monolayers were washed twice with PBS and SF media was added for conditioning by the cells. CM, incubated with 5 day old myotubes for 3 days, was designated as 5-8do (do=day old) CM. A schematic representation of conditioned media generation:



Following aspiration, CM was filtered through a sterile 0.22µm syringe filter, in order to remove cell debris, and stored for several days at 4°C until used. Preliminary experiments tested generation of conditioned media at different stages

of myotube development. The 5-8 day old time point was chosen due to the greater size of myotubes at this time and due to obtaining most consistent results at this time point.

For generation of media conditioned by crushed or wounded cells, the same procedure as described above was performed, however, after SF media addition, monolayers were damaged with a cell scraper until completely detached from the plate. Media and damaged cells were then incubated in a humidified 5% CO₂ atmosphere at 37°C for 3 days, together with control plates, where monolayers were not crushed. 3 days later, media was filtered through a sterile 0.22µm syringe filter, in order to clean all cell debris, and stored for several days at 4°C until used.

3.3.3. CELL TREATMENTS AND RECONSTITUTION OF INHIBITORS

Inhibitors were purchased from Merck-Calbiochem (Darmstadt, Germany). Inhibitors were diluted, according to manufacturer's instructions, in DMSO and stored at -20°C. All inhibitors were kept in mM concentration stocks and parts of the stocks were diluted to working concentrations in appropriate DMEM media before cell treatments. For cell treatments, equivalent concentrations of DMSO were added to control wells.

3.3.4. WOUND HEALING ASSAY AND LIVE IMAGING

Cells were grown in pre-gelatinised 12 well plates in GM until ~80-90% confluent. Cell monolayers were washed 3 times with PBS and DMEM 0.1% FBS media (quiescent media = QM) was added and incubated for 20h with the cells. In the last 3 hours of incubation with QM, 10µg/ml Mitomycin-C (Sigma-Aldrich) was added, in order to block proliferation, and monolayers were wounded with a sterile pipette tip, generating a wound of approximately 600µm in size. Wound healing with live imaging microscopy is described in section 2.2.2.1.

3.3.5. LIVE IMAGING MIGRATION ANALYSIS

Migration analysis was performed by Keynote'09 software version 5.1.1. (Apple Inc.), which was used to place lines into wound healing videos, which were separated by equal distance of each other, and to create cell movement

trajectories frame by frame into exported .AVI videos of migrating cells. ImageJ v1.45i software was used to count cells in different zones of the wounds and to track and calculate the distance of migration trajectories of cells.

3.3.6. CELL DEATH QUANTIFICATIONS BY LIVE IMAGING

The numbers of dying cells were counted frame by frame in each area for the duration of the movie, as described in section 2.2.4.

3.3.7. PHALLOIDIN STAINING

Phalloidin staining was performed directly in the multidishes wells, as described in section 2.2.6.

3.3.8. TRANSWELL INSERTS

C2C12 cells were grown in T75 flasks in the presence of GM, washed 3 times with PBS and detached from the flask by trypsinizing with 0.05% Trypsin/0.02% Ethylenediaminetetraacetic acid (EDTA) for 3-5 minutes at 37°C. Cells were resuspended in GM and were centrifuged for 10min at 500g. Supernatant containing GM was discarded and cells were washed with PBS, followed by another centrifugation for 10min at 500g. Cell pellets were resuspended in SF media, cells were counted and myoblast numbers were adjusted to 120,000 cells/ml. These cells were used with transwell inserts, method is described in section 2.2.5.2.

3.3.9. WESTERN BLOTS

Sample collection and preparation for SDS-PAGE was performed as described in section 2.2.8.1. Gel electrophoresis, membrane transfer, blocking and detection steps were performed, as described in sections 2.2.8.2-2.2.8.5. Primary AKTpan, pAKT, b-actin and ERKpan rabbit IgG antibodies were purchased from New England Biolabs (Hertfordshire, UK) and were incubated with membranes overnight at RT in 1:1000 concentration, diluted in 5% BSA/TBST. Primary pERK1/2 rabbit antibodies were purchased from Promega and were incubated with membranes overnight at RT in 1:5000 concentration, diluted in 0.1%

BSA/TBST. Secondary Goat Anti-rabbit HRP-conjugated antibodies were purchased from MP Biomedicals (United Kingdom) and were incubated with membranes for 1h at RT 1:5000 concentration, diluted in blocking solution. Membranes were blocked for 1h at RT in 5% non-fat dry milk/TBST (for antibodies purchased from New England Biolabs) or in 1% BSA/TBST for pERK1/2.

3.3.10. RNA ISOLATIONS AND REAL-TIME PCR

RNA extraction and TaqMan® Real-time PCR methods were performed as described in sections 2.2.9 and 2.2.10, respectively. The following predesigned primer sets were ordered from Applied Biosystems and were used with the TaqMan® detection method: Polr2b (Mm00464214_m1), MyoD (mm00440387_m1), Myogenin (mm00446194_m1).

3.3.11. STATISTICAL ANALYSES

Statistical analyses and significance of data were determined using GraphPad Prism version 5.00 for Mac OS X, GraphPad Software, San Diego California USA, www.graphpad.com. Statistical significance for interactions between two paired groups was determined with a Paired t-test, while unpaired t-test was used for unpaired groups. Statistical significance for interactions between more than two groups was determined with a one-way ANOVA, or with a one-way repeated measures ANOVA, when matched observations were investigated. All results are presented as mean +/- standard error of the mean (SEM). All values below $p < 0.05$ were considered as significant.

3.4. METHOD DEVELOPMENT

3.4.1. WOUND HEALING ASSAY METHOD SET-UP

In order to investigate the migration potential of C2C12 cells in response to specific factors, a wound healing assay was established. Wound healing assay is a widely used model to investigate the migration of adherent cell types on extracellular matrices, which provides with the possibility to quantify migration and observe the morphology and behaviour of migration cells. It is an easy and

inexpensive method to set up, which, combined with Live imaging microscopy, also provides sufficient information on various cell processes, such as migration, proliferation, cell death, cell morphology. Considering the high number of experiments planned in this thesis, the wound healing assay was considered as the most appropriate tool to quantify myoblast migration. In the wound healing assay, a scratch/wound is created in a monolayer of confluent cells, usually using a pipette tip, and the progress of wound closure by the cells is observed over time.

Different stages of the wound healing experiment preparations are illustrated in Figure 3.1. Wound size was approximately 600 μ m in length, although slight variations between experiments were impossible to avoid. Wound sizes between different wells were compared before each live imaging experiment was initiated, so that different treatments would be applied to wells with comparable wound sizes. Following wounding, cell monolayers were washed twice with PBS, in order to remove cell debris, and media with different composition or treatments were added to each well. After the X and Y coordinates on the microscope were set, live imaging movies were initiated, lasting for 20hrs, with frames being captured every 15min. Preliminary optimization experiments were tested at different time periods for performing the wound healing assay. 20 hours was chosen as the most appropriate period, considering the wound size and the speed of closure of the wound with different conditions tested.

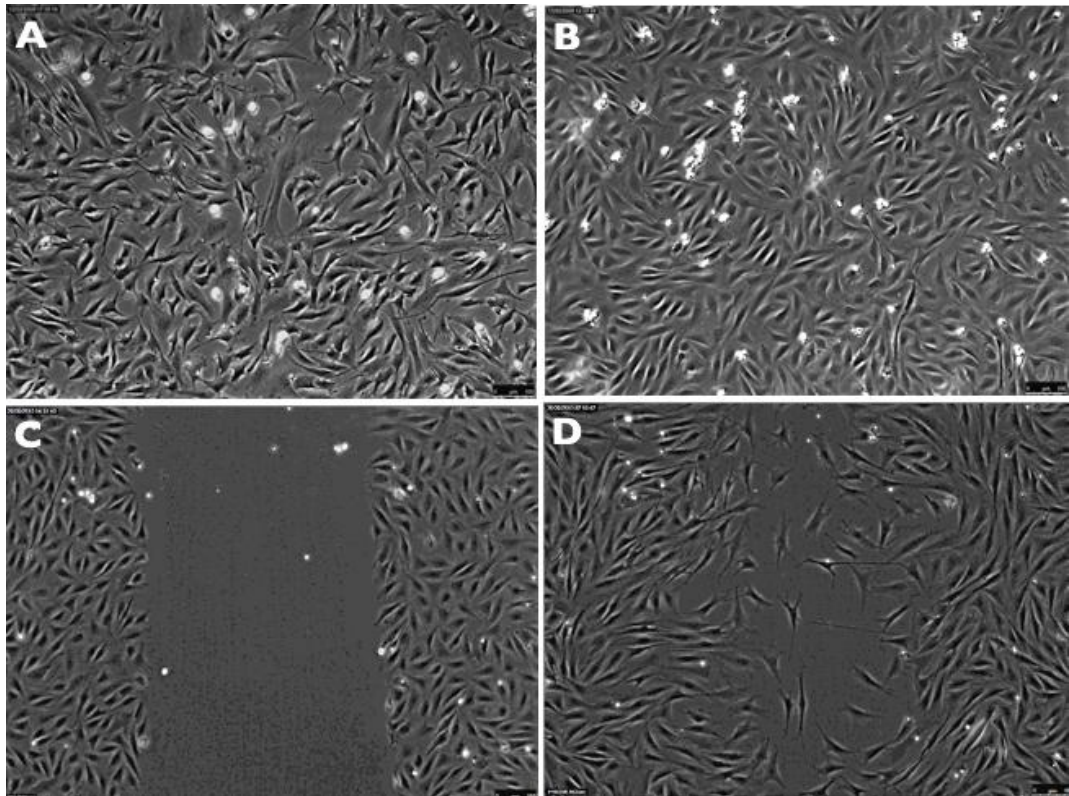


Figure 3.1. Optimization of wound healing assay. Cell monolayers were grown in 10% FBS media (GM) until approx. 80-90% confluent (A). GM was replaced with 0,1% FBS (Quiescent media) and cells were incubated for a further 20h (B). The cell monolayer was damaged (C) and wound closure/migration was captured with live imaging microscopy, usually for 20hrs (D).

To study migration in the absence of conflicting proliferation, cell monolayers were pre-incubated for 3hrs in 10 μ g/ml of Mitomycin-C, (purchased from Sigma-Aldrich (Dorset, England)) before live imaging was initiated. Preliminary experiments observing the velocity of wound closure between cells treated with 10 μ g/ml of Mitomycin-C and control media in the absence of Mitomycin-C, demonstrated that while proliferation was blocked with Mitomycin-C, the rate of wound closure and cell migration were not visually affected between treatments (Figure 3.2), with only a few proliferation events observed in the first 18hours of wound closure. Thus, the very low proportion of proliferation events, occurring without Mitomycin-C treatment, did not exert any visually detectable effects on the overall extent of migration. Never the less, although proliferation did not apparently influence the migratory capacity of cells during wound healing, in order to focus solely on the migration of cells and facilitate the migration analysis, it was decided to perform the live imaging wound closure experiments in the presence of 10 μ g/ml of Mitomycin-C. In order to verify the block of cell

proliferation following Mitomycin-C stimulation, observation was performed of multiple videos, which confirmed no visible proliferation events during the period of wound closure observed. Further proliferation assays were not performed, as satisfactory results were obtained from visual observations, indicating no proliferating cells during the migration/wound closure of cells. Furthermore, even if Mitomycin-C does not completely block proliferation of myoblasts in all experiments analysed, the number of proliferation events during wound closure in the presence of Mitomycin-C would be low enough to presume that wound closure is accomplished by migration and not by cell division.

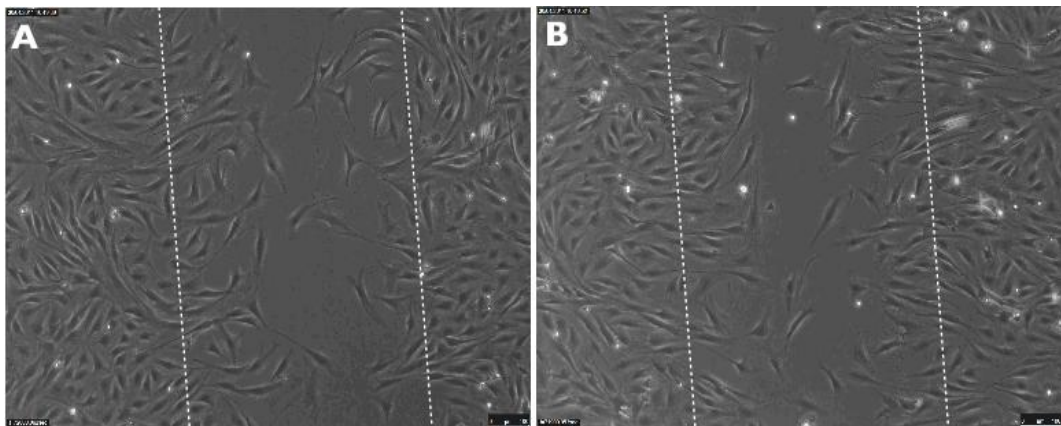


Figure 3.2. Effect of Mitomycin-C on myoblast migration. No visible difference in cell migration was observed between cells incubated with (A) and without (B) 10µg/ml of Mitomycin-C in the first 20h of wound closure.

3.4.2. WOUND HEALING LIVE IMAGING MIGRATION ANALYSIS

Cell migration in wound healing assays is normally analysed and quantified using several approaches - most commonly, by analyzing the percentage of wound area closed by cells, by counting the total number of cells infiltrating the wound, or by tracking individual cells from both sides of the wound and estimating the distance travelled by these cells. Usually, one of these approaches is selected. However, it must be noted that different cell types might migrate differently. Preliminary observations of the manner in which C2C12 myoblasts migrated during wound healing assays, demonstrated that many of the myoblasts exhibited random movement, migrating individually and the wound was not closed by a collective migration of the myoblasts in a sheet-like manner. Thus, analysis solely of the total number of cells infiltrating the wound, which examines collective cell migration, might not be the most appropriate analysis for all wound

healing experiments involving myoblasts. Therefore, different approaches of analyzing myoblast migration during wound healing were tested and assessed, with the idea that combination of two or more analyses would provide a better indication of how myoblast migration is affected by different treatments.

A method of analysis for counting the number of cells infiltrating the wound was therefore established. Given the independent migration of these cells, the wound area was divided into 3 areas of equal size and not only were the total number of cells in the wound area calculated, but also the number of cells infiltrating the central most area of the wound. The division of the wound into 3 distinct areas was accomplished by drawing (using relevant software) 4 lines along the length of the wound, with equal spacing between the marker lines, essentially dividing the wound into tertiles. Equal spacing between the lines was verified using Keynote'09 software version 5.1.1. (Apple Inc.). As shown in Figure 3.3, the first and last lines (marked with red arrows) indicate the edges of the wound, before the cells started to migrate. The lines marked with green arrows encompass the central area of the wound. On the same figure, counts were performed using ImageJ v1.45i to indicate how many cells in total had infiltrated the wound for a given time period and what percentage of them were situated in the central area of the wound. This methodology not only provided information relating to the number of cells migrating but also their capacity for linear migration. In this example, 63 cells in total infiltrating the wound were counted in (A), with 8% in the middle of the wound area, vs 99 cells in total infiltrating the wound in (B), with 25% in the middle of the wound. This indicates significantly more migration in condition B. The percentage of cells in the middle of the wound also provides a good indication of the rate of cell migration e.g. cells reaching the centre/h which was apparently enhanced in (B) vs (A).

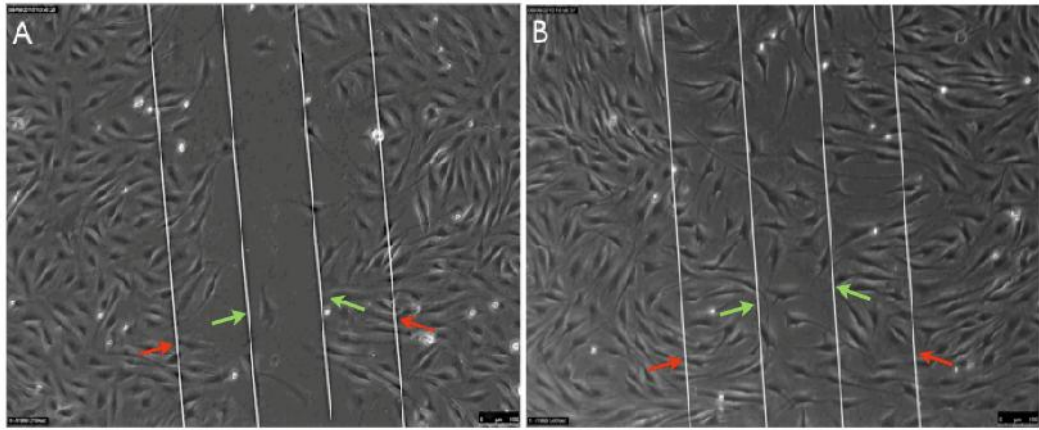


Figure 3.3. Demonstration of the demarcations established in a wound healing assay. To ascertain migration potential, the total number of cells infiltrating the wound was established. These photomicrographs reveal an example of how the cell count analysis was verified between two different types of wound closure. A condition inducing visually less wound closure, indicated fewer number of cells ($n = 63$) infiltrating the wound following cell count analysis (A), as compared to a condition inducing visually greater wound closure (B), resulting in higher number of cells following cell count analysis ($n = 99$ cells). Quantification of the percentage of cells in the middle of the wound also confirms these observations: 8% in the centre (A) vs 25% (B). Red arrows depict the lines marking the wound edge and green arrows the lines marking the central 1/3 of the wound site.

Another example of the cell counting method is provided in Figure 3.4. Counts indicated equivalent numbers of total cells infiltrating the wound between (A) and (B), however double the proportion of cells in the middle of the wound in (B) vs (A), suggesting enhanced cell spreading in (B) vs (A). This suggests that analysis of the total cell numbers infiltrating the wound may not always be indicative of the degree and nature of cell migration. A combination of different analyses might help obtaining better information on cell migration than using only one approach.

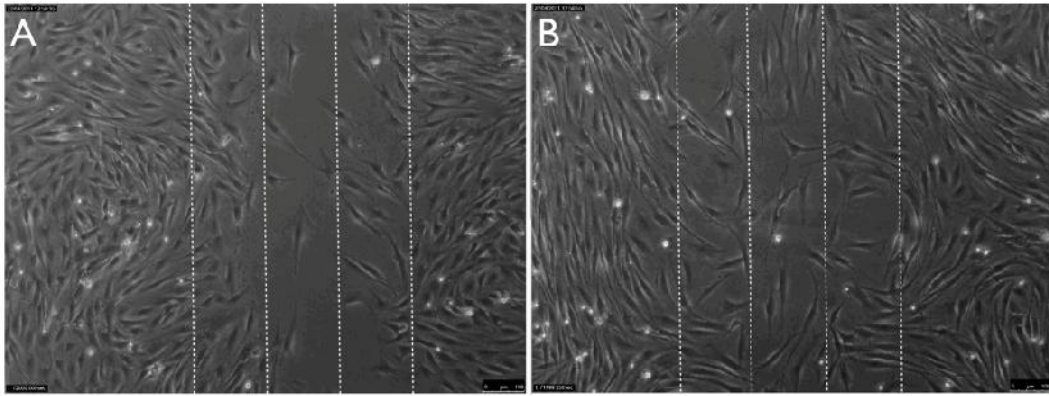


Figure 3.4. An example of cell count analysis. These photomicrographs reveal an example of how the cell count analysis was verified, by examining two different types of wound closure. Cell count analysis demonstrates equivalent total number of cells infiltrating the wound between type/condition A and type/condition B, but double the percentage of cells infiltrating the middle part of the wound in B vs A, suggestive of more cell migration and spreading of cells in the wound in condition B.

In addition to the method above, and in an attempt to look at directional migration, another cell migration assessment method was established to assess how the average migration distance of myoblasts is affected by different treatments. Cell tracking analysis was performed by selecting 8 cells from both sides of the wound, and the trajectories of these cells were created by tracking frame by frame their movement. The trajectories, drawn as lines, were exported as “.jpeg” files and their length was measured using ImageJ v1.45i. The average length of all 16 trajectories per movie was established. At least 3 movies per experimental group were analysed for every experimental protocol. The final results were calibrated to a size marker, included in the live imaging movies, and converted to μm units (Figure 3.5). Derived data for experimental studies illustrated that cell tracking analyses confirmed the results from the cell counting analyses.

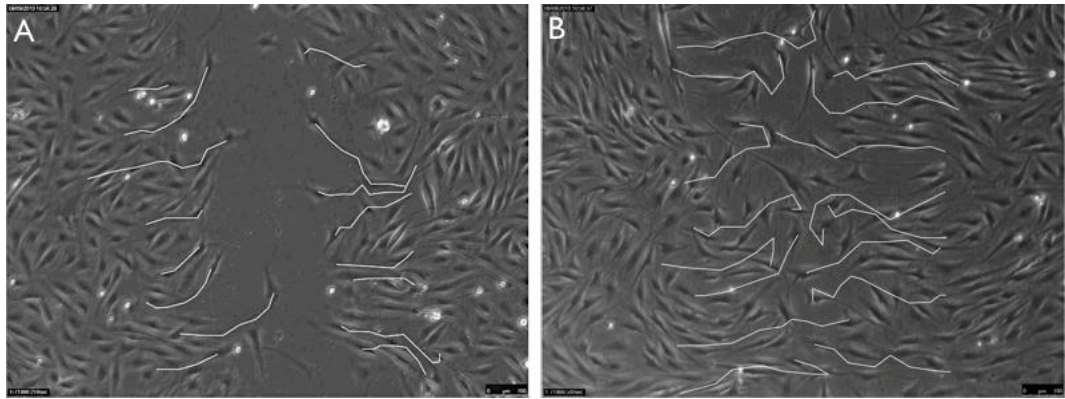


Figure 3.5. Illustrative photomicrographic quantification of cell migration using tracking of the migration distance. These photomicrographs reveal an example of how the migration distance analysis was verified, by examining two different types of wound closure. Visually reduced wound closure in condition A resulted in lower average migration distance (222um), as compared to condition B (average migration distance of 400um), which also demonstrated visually enhanced wound closure.

3.5. RESULTS

3.5.1. CELL CULTURE MEDIA, CONDITIONED IN VITRO BY C2C12 MYOTUBES IS CAPABLE OF INDUCING WOUND CLOSURE OF C2C12 MYOBLASTS

Having established these novel methods, for the purpose of our experiments, the hypothesis that myogenic cells are capable of secreting factors, which induce wound healing and migration was examined. SF DMEM media was incubated with well developed myotube cultures for 3 days, thus obtaining CM (as described in methods section 3.3.2). Preliminary wound healing assays were performed to visually compare the effect of the CM vs non-conditioned control SF media on wound closure. Consistent wound closure results were obtained using media conditioned for 3 days with 5do myotube cultures (i.e. 5-8do CM), or with 8-11do CM. Photomicrographic representation illustrates the accelerated wound closure observed with CM, compared to slower and incomplete closure with control SF (Figure 3.6). Furthermore, the numbers of floating, dead cells appears to be reduced in CM vs SF conditions.

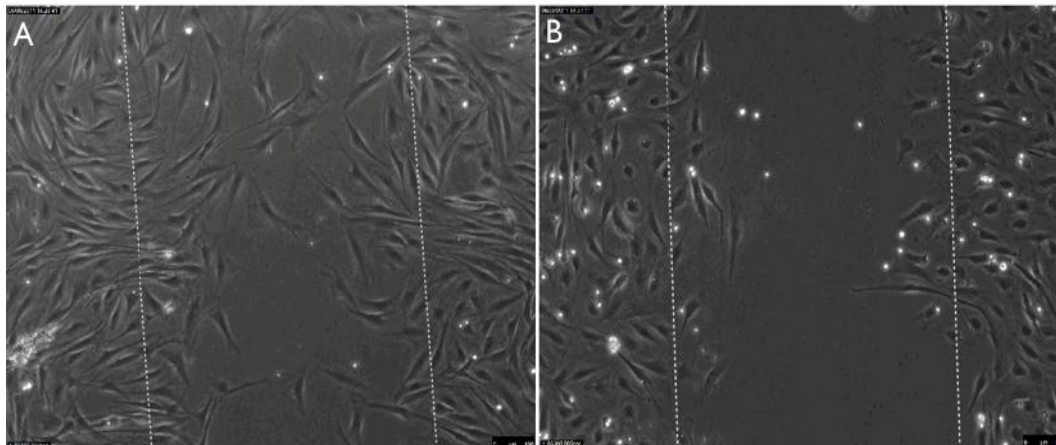


Figure 3.6. Photomicrographic representation of wound healing assay (20h post wound). Enhanced induction in wound closure at 24h is observed with CM incubated for 3 days with 5do myotubes (5-8do CM) (A) vs control SF media (B). (10x magnification). Images are representative of at least 4 experiments performed in duplicate.

A change in morphology between the cells incubated with CM vs SF was also observed and was most evident when cells were incubated for 48h (Figure 3.7). Cells in CM demonstrated a more elongated morphology, with filopodial

protrusions visible, while the cells incubated in SF demonstrated morphology more characteristic of senescent cells – being round in shape, and displaying easily visible perinuclear zones and centrally located nuclei.

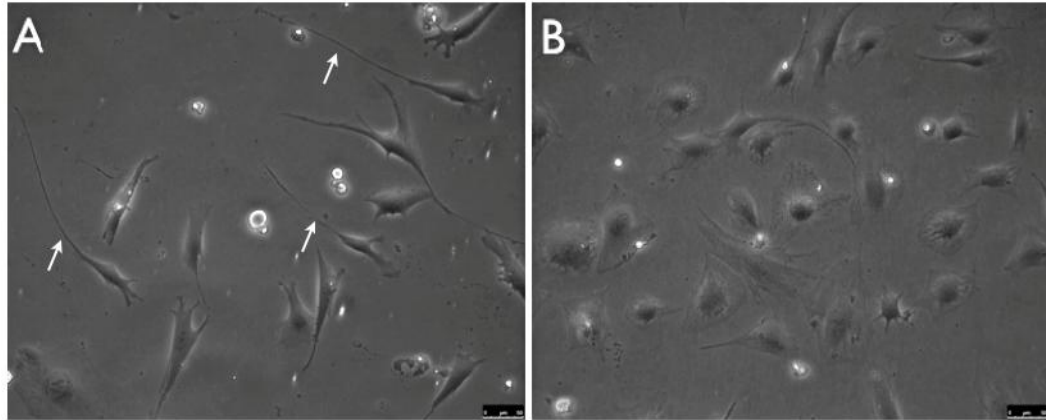


Figure 3.7. Subconfluent cultures of C2C12 myoblasts incubated for 48h in CM or SF. Morphological differences between the cell culture conditions were observed, with myoblasts in CM (A) having a more compact, elongated shape, with visible protrusions, such as filopodia (white arrows), while the myoblasts incubated in SF (B) possessed more rounded morphology, with easily visible centrally located nuclei. (20x magnification). Images are representative of 2 experiments performed in duplicate.

3.5.2. OPTIMIZATION OF MYOBLAST MIGRATION: COMPARISONS OF CONDITIONED MEDIA, SERUM FREE-MEDIA, GROWTH MEDIA AND DIFFERENTIATION MEDIA

Initial studies observed accelerated wound closure with CM vs. SF. To determine the specificity of these observations and to optimize conditions, the effects of CM on wound closure were compared with the effects of GM and DM. The migration was initially assessed morphologically and subsequently quantified by cell counting and tracking. As shown on Figure 3.8(A), CM, DM and GM, are capable of inducing wound healing to a greater extent than SF; with GM appearing most potent.

Total counts of the number of cells infiltrating the wound after 20h of culture (Figure 3.8B) demonstrated an increase in infiltrating numbers with GM vs CM (158 +/-13 vs 84 +/- 6, $p < 0.01$, equivalent to 188% increase), GM vs DM (158 +/- 13 vs 77 +/-6, $p < 0.001$, equivalent to 205% increase) and GM vs SF (158 +/- 13 vs 36 +/- 0, $p < 0.0001$, equivalent to 438% increase). Significantly more cells were also present within the wound site with CM vs SF (84 +/- 6 vs 36 +/-0, $p < 0.05$, equivalent to 233% increase) and also with DM vs SF (77 +/-5 vs 36 +/-0, $p < 0.05$,

equivalent to 213% increase). No significant difference, with regard to migration into the wound site, was found between CM and DM.

Analysis on the percentage of cells in the middle of the wound (Figure 3.8C) demonstrated significant increase with GM vs CM (22.3 +/- 2.4% vs 12 +/- 2%, $p < 0.01$), GM vs DM (22.3 +/- 2.4% vs 8 +/- 3.2%, $p < 0.001$) and GM vs SF (22.3 +/- 2.4% vs 3 +/- 2.1% $p < 0.0001$). Significant increases were also observed with CM vs SF (12 +/- 2% vs 3 +/- 2.1%, $p < 0.01$), but not between DM vs SF or CM vs DM.

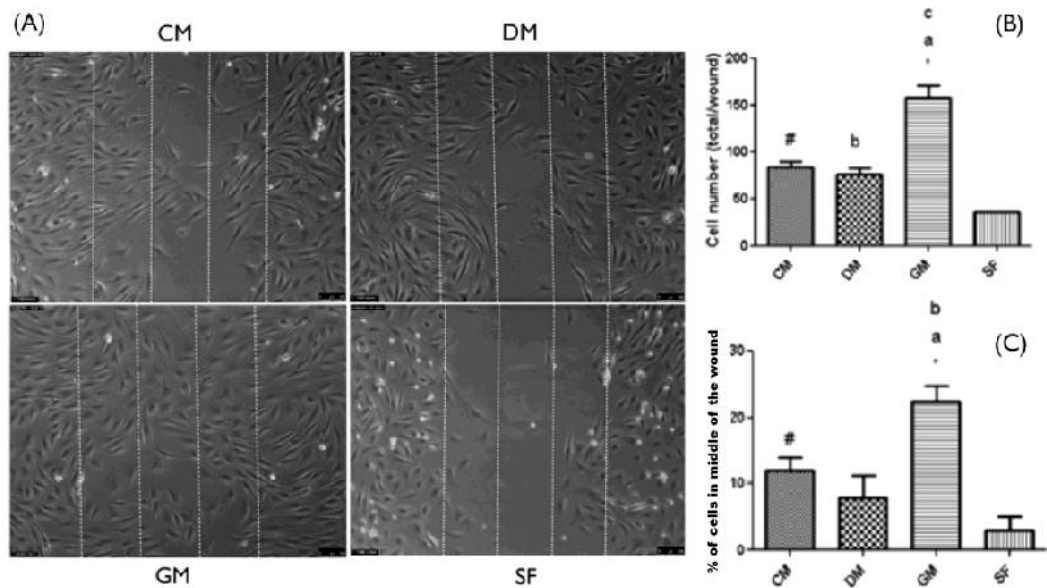


Figure 3.8. Wound healing assay with cell count analysis (CM, DM, GM, SF).

Wound healing assay (20h) comparing the effects of CM, DM, GM and SF indicated accelerated wound closure with CM, DM and GM, compared to SF, with GM appearing most potent (A). (10x magnification). Quantification of the total number of cells infiltrating the wound after 20h (B): impact of culture conditions was investigated on migration; significant increases were observed with GM vs CM ($p < 0.01$, represented by *), GM vs DM ($p < 0.001$, represented by a) and GM vs SF ($p < 0.0001$, represented by c); significant increases were observed with CM vs SF ($p < 0.05$, represented by #); and with DM vs SF ($p < 0.05$, represented by b). Quantification of the percentage of cells in the centre of the wound (C): significant increase observed with GM vs CM ($p < 0.01$, represented by *), GM vs DM ($p < 0.001$, represented by a) and GM vs SF ($p < 0.0001$, represented by b); significant increases were observed with CM vs SF ($p < 0.01$, represented by #). Data are representative of 3 experiments performed in duplicate. (p-values were obtained by using a One-way repeated measures ANOVA).

In order to consolidate these data and to decrease the potential of subjectivity, a tracking methodology was established to monitor the migration of individual cells

into the wound area (described in methods chapter 3.4.2) and under the influence of the selected culture media. Cell tracking analyses support the results presented above, regarding the potency of culture media and the impact on cellular migration (Figure 3.9). Morphological tracking (Figure 3.9A) suggested GM to be most potent at promoting migration from the wound edge to the centre, followed by CM, DM and SF. Analyses of cell tracking, illustrated in Figure 3.9(B), demonstrated significant increases in migration distance with GM vs CM ($580 \pm 60\mu\text{m}$ vs $392 \pm 21\mu\text{m}$, $p < 0.05$, equivalent to 48% increase), GM vs DM ($580 \pm 60\mu\text{m}$ vs $329 \pm 20\mu\text{m}$, $p < 0.01$, equivalent to 76% increase) and GM vs SF ($580 \pm 60\mu\text{m}$ vs $219 \pm 3.5\mu\text{m}$, $p < 0.001$, equivalent to 264% increase). Migration distance was also increased with CM vs SF ($392 \pm 21\mu\text{m}$ vs $219 \pm 3.5\mu\text{m}$, $p < 0.05$, equivalent to 79% increase). No significant difference was observed between CM vs DM or between DM and SF, using ANOVA analysis for all 4 groups, however, when DM and SF were directly compared in a paired t-test significance was achieved with DM vs SF ($329 \pm 20\mu\text{m}$ vs $219 \pm 3.5\mu\text{m}$, $p = 0.03$, equivalent to 50% increase). These analyses confirm the observational, morphological assessments above.

Wishing to determine the impact of cell death on migration capacity, dying cells per arbitrary field of view were quantified. As shown on Figure 3.9(C), percentage dead cells was significantly increased in SF vs CM ($12.2 \pm 1.3\%$ vs $1.77 \pm 1\%$, $p < 0.0001$), SF vs DM ($12.2 \pm 1.3\%$ vs $0.18 \pm 0.13\%$, $p < 0.0001$) and SF vs GM ($12.2 \pm 1.3\%$ vs $0 \pm 0\%$, $p < 0.0001$). No significant differences were found between CM, GM and DM.

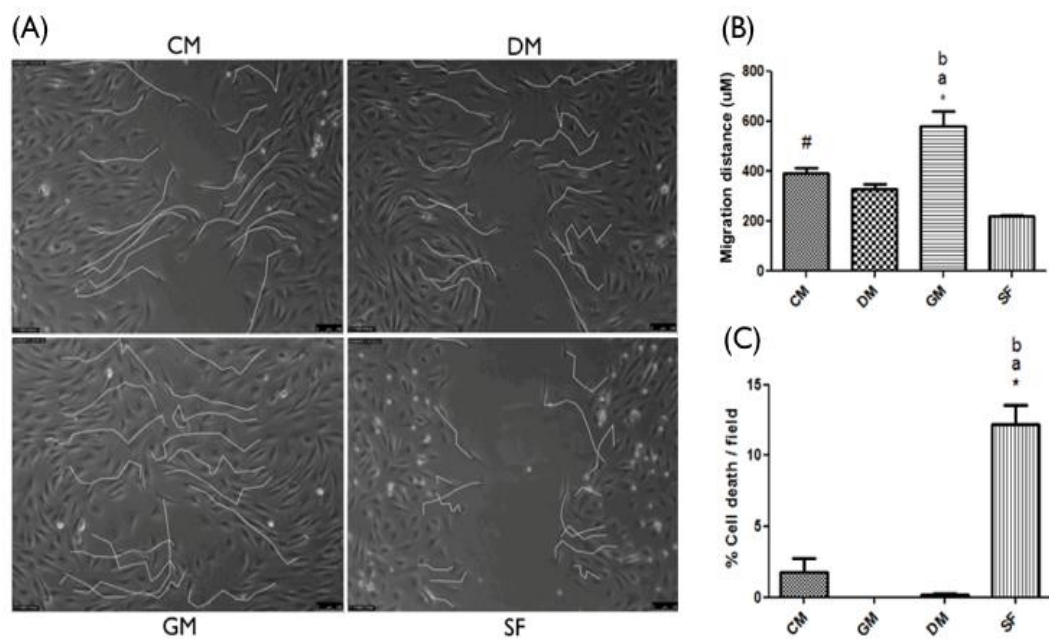


Figure 3.9. Cell tracking and cell death analysis (CM, DM, GM, SF). Cell tracking comparing the effects of CM, DM, GM and SF. (A) (10x magnification). Quantification of cell migration distance (B). Significant increases were observed with GM vs CM ($p < 0.05$, represented by #), GM vs DM ($p < 0.01$, represented by a) and GM vs SF ($p < 0.001$, represented by b). Significant increase was also observed with CM vs SF ($p < 0.05$, represented by #). Cell death quantification (C). Significant increases in cell death were evident with SF vs CM ($p < 0.0001$, represented by #), SF vs GM ($p < 0.0001$, represented by a) and SF vs DM ($p < 0.0001$, represented by b). No significant difference in cell death was found between CM, GM and DM. Data are representative of 3 experiments performed in duplicate. (p-values obtained by One-way repeated measures ANOVA)

3.5.3. IMPACT OF CULTURE CONDITIONS ON CHEMOTAXIS.

Having determined differential effects of culture conditions on the capacity of cells to migrate into wound sites and to remain adherent to the extracellular matrix (ECM) coating the culture dishes, it was further planned to also ascertain the impact of culture conditions on chemotaxis of cells through transwell membranes, in order to substantiate culture conditions for future experimentation. Therefore, chemotaxis in the presence of CM, DM, GM or SF was examined using transwell inserts (Figure 3.10). Following transfer of equivalent cell numbers to the upper chambers of the transwell inserts in SF culture medium, cells were incubated for 4 hours in CM, DM, GM or SF before experimentation was terminated. Cells adherent to the underside of the transwell membrane were stained and examined.

As is evident in Figure 3.10, CM (A) and DM (B) induced greater chemotaxis than SF (D) and, surprisingly, than GM (C).

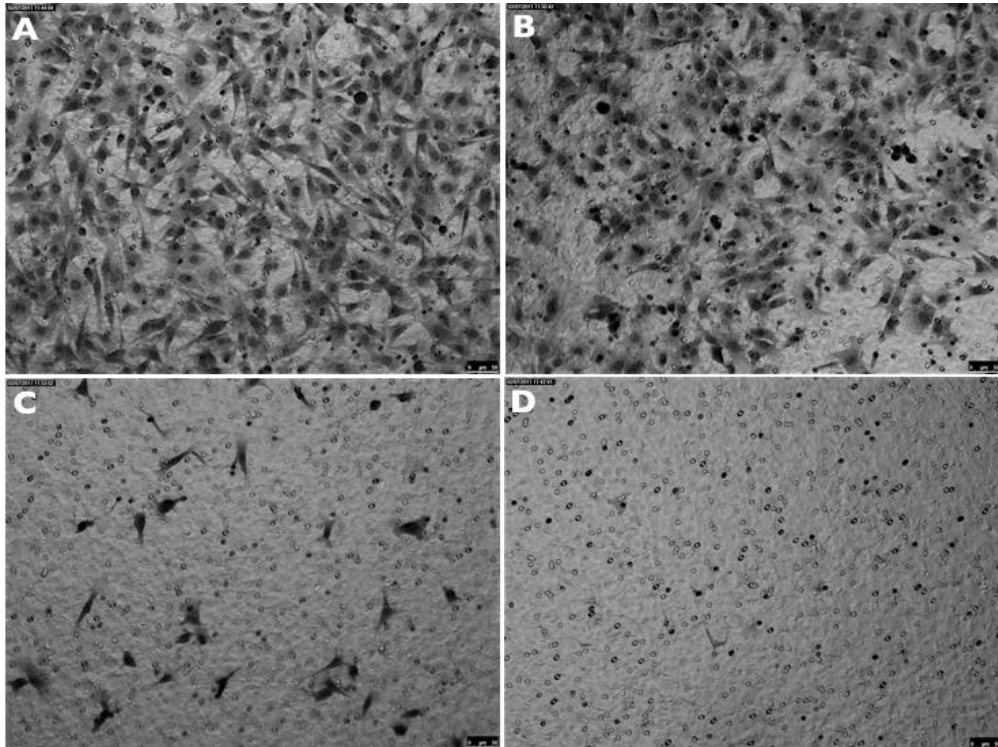


Figure 3.10. Examination of chemotaxis by transwell inserts (CM, DM, GM, SF). Images are representative of the underside of the transwell following 4 hours of incubation. Cells were seeded on the top of the transwells in SF culture medium, with CM (A), DM (B), GM (C) and SF (D) in the lower chambers. Following 4 hrs of incubation, CM (A) and DM (B) induced increased chemotaxis compared to GM (C) and SF (D). (10x magnification, 1.6x zoom). Data are representative of 3 experiments performed in duplicate.

Quantifications and analysis of the number of cells on the bottom surface of the porous membranes (Figure 3.11), demonstrated significant increases in chemotaxis with CM vs SF (253 +/-42 vs 4 +/-2.5, $p<0.01$, equivalent to 6325% increase) and with DM vs SF (199 +/-8 vs 4 +/-2.5, $p<0.01$, equivalent to 4975% increase). Increases were also observed with CM vs GM ($p<0.01$, 253 +/-42 vs 22 +/-2, equivalent to 1150% increase) and DM vs GM ($p<0.01$, 199 +/-8 vs 22 +/- 2, equivalent to 905% increase). No significant differences were observed between GM and SF or between CM and DM.

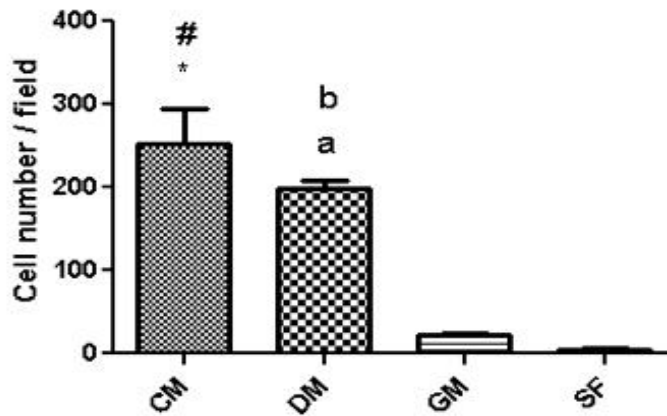


Figure 3.11. Transwell inserts cell quantifications (CM, DM, GM, SF). Significant increases were observed with CM vs SF ($p < 0.01$, represented by #) and DM vs SF ($p < 0.01$, represented by b). Increases were also observed with CM vs GM ($p < 0.01$, represented by *) and DM vs GM ($p < 0.01$, represented by a). No significant difference was indicated between GM and SF or between DM and CM. Data are representative of 3 experiments performed in duplicate. (p-values obtained by One-way repeated measures ANOVA)

GM strongly induced wound closure and migration of C2C12 myoblasts, but, surprisingly, did not largely increase their chemotaxis in the transwell migration assay. To examine this discrepancy, the effect of media dilution was examined using transwell inserts. As shown on Figure 3.12, GM diluted in 1:5 ratio with SF media (equivalent to 2% FBS content in the diluted GM), was more potent at inducing chemotaxis through the transwells compared to standard GM containing 10% FBS, suggesting that the inclusion of high-serum in transwell wells, contrary to what was expected and also evident by enhanced cell migration with wound healing, was not inducing cell chemotaxis, but was decreasing it.

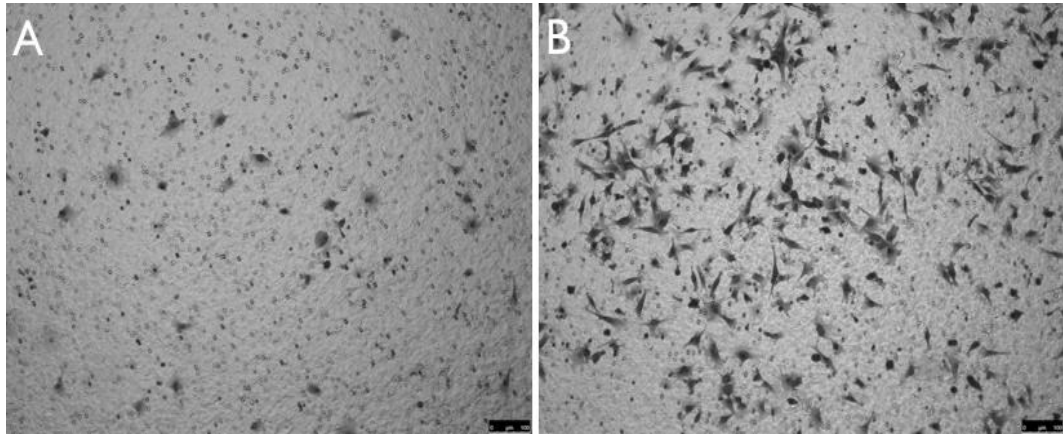


Figure 3.12. Transwell inserts cell quantifications between GM 10% and GM 2%. Standard GM (10% FBS) (A) is less potent at inducing myoblast chemotaxis through transwell inserts, compared to GM diluted 1:5 with SF media (equivalent to 2% FBS) (B).(10x magnification). Data are representative of 3 experiments performed in duplicate.

3.5.4. MEDIA CONDITIONED BY VIABLE OR SERUM STARVED/ATROPHYING MYOTUBES IS MORE POTENT AT INDUCING MIGRATION AND WOUND HEALING COMPARED TO MEDIA CONDITIONED BY INJURED/CRUSHED MYOTUBES

As detailed above, SF media conditioned for 3 days by mature myotubes can induce wound healing, cell survival and transwell chemotaxis. 5 do myotubes incubated for 3 days in SF media display a reduction in the density of the myotubes in culture and increased rates of atrophy (as confirmed morphologically by a decreased myotube size) or death over the 72 h culture period (Figure 3.13).

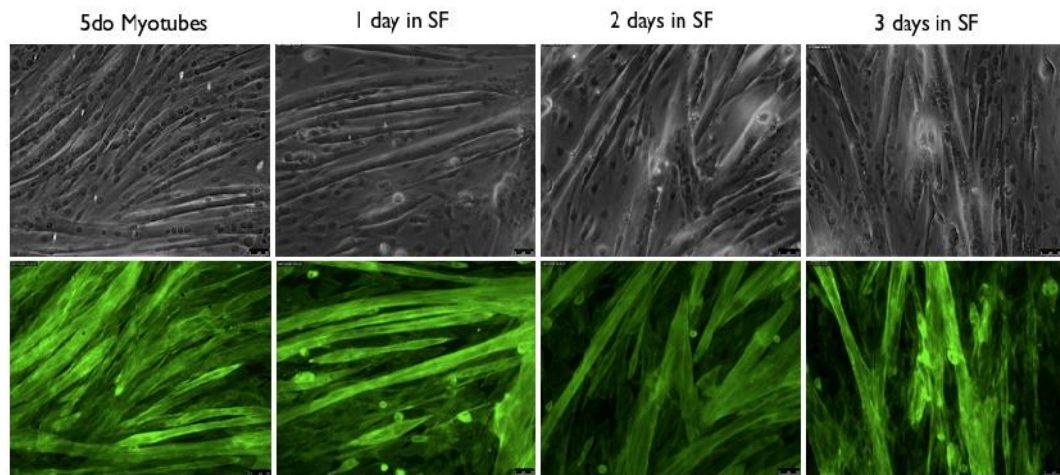


Figure 3.13. Changes in morphology of myotube cultures during conditioning with SF media for 3 days. Atrophy of the 5 day-old myotubes was observed morphologically during the 3 days of incubation with SF media. Top panels show phase-contrast photos (20x objective), while bottom panels - phalloidin-FITC staining (20x objective). Data are representative of 2 experiments performed in duplicate.

It was investigated whether factors released from dead cells, or possibly their cellular contents, were able to induce wound closure and myoblast migration to a degree higher or comparable to the myotubes in CM or to DM. Comparisons were made (by wound healing assay) of the effect of media conditioned for 3 days with well developed 5do myotubes (CM) vs media conditioned for 3 days in the presence of mechanically injured/crushed myotubes (CM-crushed). As shown in Figure 3.14(A) and perhaps in contrast to the expectation that factors from mechanically damaged cells may have enhanced migration compared with CM, wound closure was reduced with CM-crushed vs CM medium.

Quantification of cell counts within the wound site, demonstrated significant decreases in the total number of cells infiltrating the wound (Figure 3.14B) with CM-crushed vs CM (43 ± 5.5 vs 84 ± 5 , $p < 0.05$, equivalent to 95% decrease). Furthermore, the percentage of the cells in the middle of the wound area (Figure 3.14C) was also significantly lower with CM-crushed compared to CM ($1.5 \pm 0.65\%$ vs $15.5 \pm 0.9\%$, $p < 0.001$).

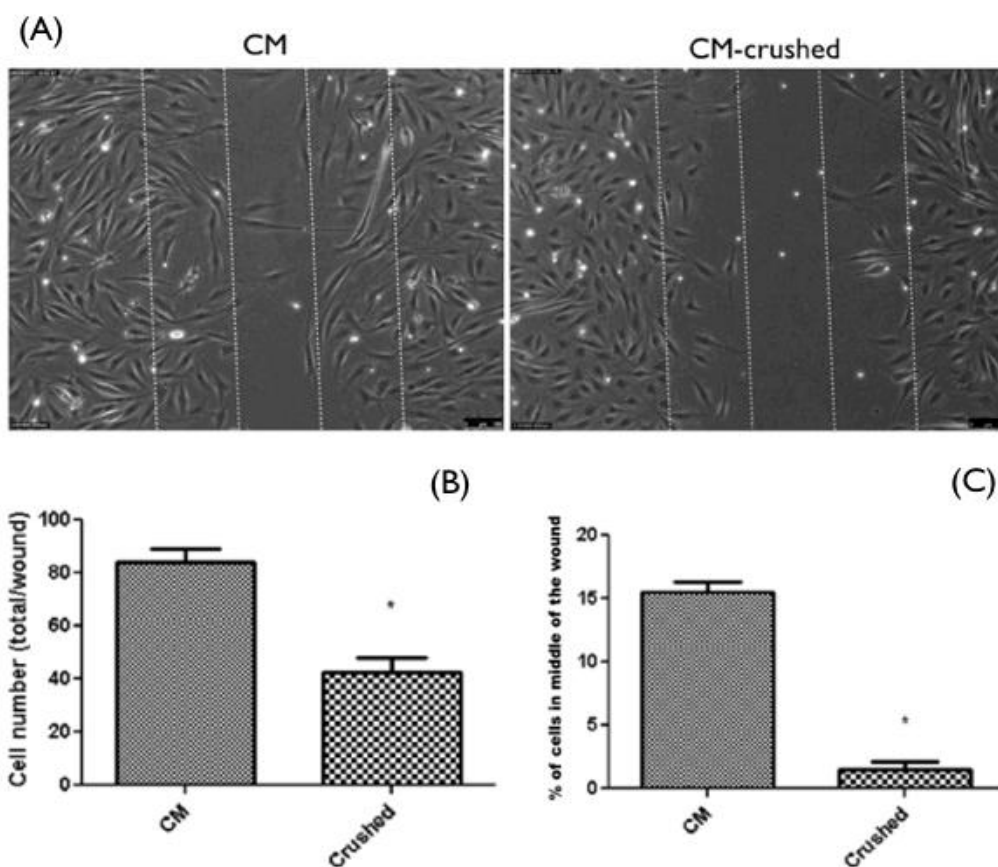


Figure 3.14. Wound healing assay with cell count analysis (CM vs CM-crushed). Wound healing assay comparing the effects on wound closure of media conditioned for 3 days with well developed, 5 day myotubes (CM) vs media conditioned for 3 days with mechanically crushed myotubes (CM-crushed) (A). Wound healing cell migration count quantifications (B). Quantification of the total number of cells infiltrating the wound after 20h: significant decrease observed with CM-crushed compared to CM ($p < 0.05$, represented by *). Quantification of the percentage of cells in the middle of the wound (C): significant decrease observed with CM-crushed vs CM ($p < 0.001$, represented by *). Data are representative of 4 experiments performed in duplicate. (p-values obtained by paired t-test)

Once again, to validate the above observation, cell tracking analyses were performed and visually confirmed the reduction in migration with CM-crushed vs CM as illustrated morphologically (Figure 3.15A) and substantiated by quantification (Figure 3.15B). Cell tracking analyses demonstrated a significant reduction of cell migration distance with CM-crushed vs CM ($213 \pm 21 \mu\text{m}$ vs $380 \pm 10 \mu\text{m}$, $p < 0.01$, equivalent to 78% decrease), following 20h incubation.

Once again, wishing to determine whether culture conditions were impacting on the adherence/survival of migrating cells, dead cell numbers were quantified for

20h post wounding (Figure 3.15C). No significant differences in cell death were observed with CM vs CM-crushed ($2.8 \pm 0.32\%$ vs $3.48 \pm 1.22\%$, $p=0.59$).

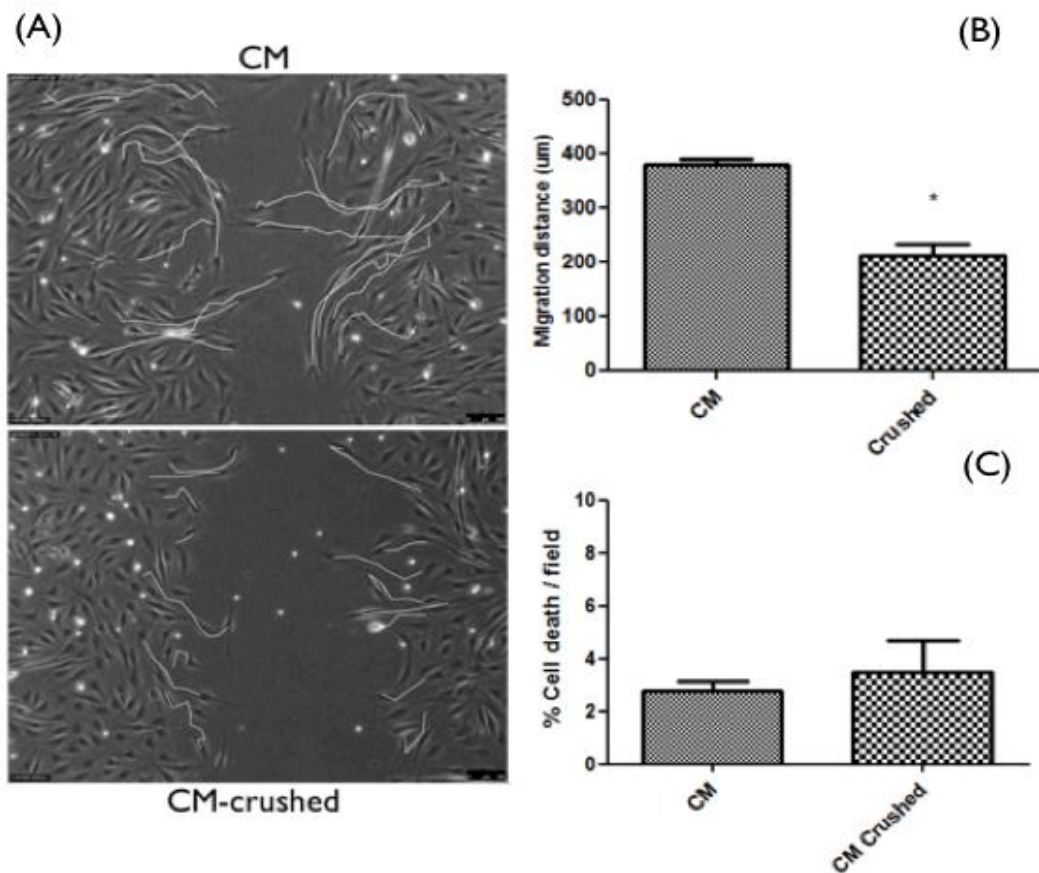


Figure 3.15. Cell tracking and cell death analysis (CM vs CM-crushed). Cell tracking comparing the effects of CM vs CM-crushed on cell migration into a wound area (A). (10x magnification). Quantification of cell migration distance (B). Significant reduction with CM-crushed vs cm ($p<0.01$, represented by *). Cell death quantifications (C). No significant difference was observed between CM and CM-crushed. Data are representative of 3 experiments performed in duplicate. (p-values obtained by paired t-test)

Finally, chemotactic responses of myoblasts to CM and CM-crushed were investigated using transwell inserts (Figure 3.16). Cells moved to the underside of the porous membrane with CM-crushed, however there was a distinctive clustering of cells on the bottom of the membrane, which was not observed with CM.

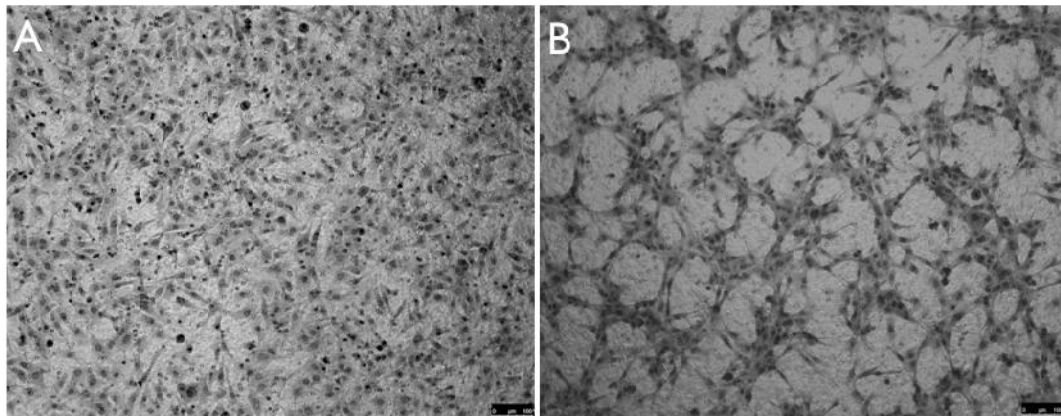


Figure 3.16. Examination of cell chemotaxis by transwell inserts comparing CM vs CM-crushed. Large numbers of cells were present on the underside of the membrane in response to CM (A). Cell chemotaxis was also observed in response to CM-crushed, however cells were clustered in groups of cells (B). (10x magnification). Data are representative of 3 experiments performed in duplicate.

3.5.5. PI3K AND ERK1/2 PATHWAYS ARE ACTIVATED BY CM, GM AND DM, BUT NOT BY SF

In order to determine the impact of culture conditions on signalling pathways, which may be important for cellular migration, cells were cultured as for wound healing assay and at 15 or 30 min following transfer to relevant culture media, lysates were extracted and subsequently subjected to Western blot analyses in order to measure the activation of members of the PI3K and MAPK pathways, in particular pAKT (ser473) and pERK 1/2, in response to GM, DM, SF and CM (Figure 3.17). The data below suggest that both ERK and Akt are not activated by SF. CM does induce more sustained pAkt activation compared to SF, but is not as potent as either GM or DM. Although all 3 triggers (GM, DM, CM) induce potent pERK1/2 activation at 15 min, this is less sustained, as compared to pAkt, and its activation declines at 30 min. with the slope of decline appearing steepest in CM.

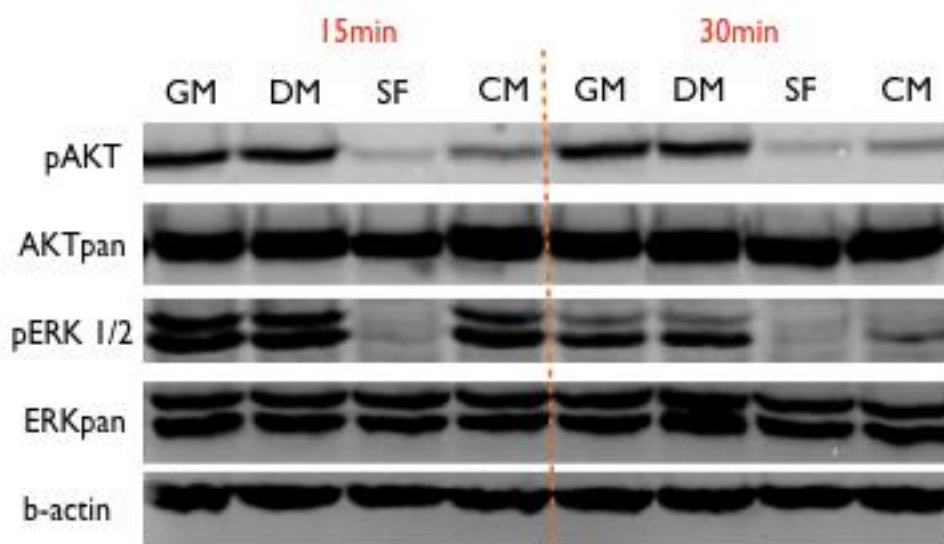


Figure 3.17. Western blots (GM, DM, SF, CM). Western blots examining the activation of members of the PI3K and MAPK signalling pathways in the presence of GM, DM, SF and CM for 15 and 30 min. -Actin, Akt-pan and ERK-pan were included as controls. 30 ug total protein loaded per lane. Data are representative of at least 4 experiments.

Wishing to quantify these apparent observations, blots were subjected to further analysis using Quantity One software. Phospho-Akt levels were first quantified across the 4 different media conditions and the two time points (Figure 3.18). All values are represented as percentage of the calibrator (GM 15m), which was set to 100%. Significantly lower pAKT activity was observed with SF compared to GM at both 15m (4.2 +/-0.86% vs 100%, $p < 0.0001$) and 30m (7.8 +/-4% vs 86.4 +/-7%, $p < 0.0001$). pAkt was also significantly lower in SF vs DM at both 15m (4.2 +/-0.86% vs 67.6 +/-10%, $p < 0.01$) and 30m (7.8 +/-4% vs 66.8 +/-9.9%, $p < 0.0001$). Significantly lower pAKT levels were observed with SF vs CM at both 15m (4.2 +/-0.86% vs 53 +/-13.6%, $p < 0.05$) and 30m (7.8 +/-4% vs 30 +/-8.4%, $p < 0.05$). Levels of pAKT were reduced with CM compared to GM at both 15m (53 +/-13.6% vs 100%, $p < 0.05$) and 30m (30 +/-8.4% vs 86.4 +/-7%, $p < 0.0001$). Significant reduction was observed in pAKT activity with DM vs GM at 30m (66.8 +/-9.9% vs 86.4 +/-7%, $p < 0.05$) and with CM vs DM at 30m (30 +/-8.4% vs 66.8 +/-9.9%, $p < 0.0001$).

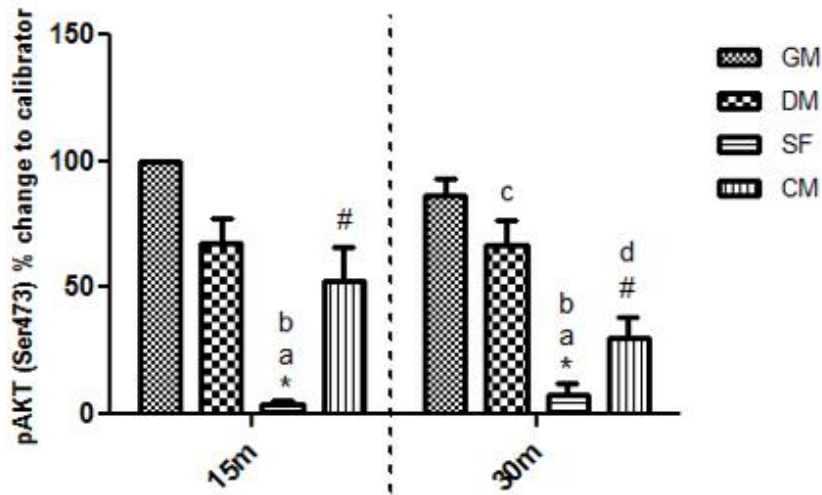


Figure 3.18. pAKT quantification (GM, DM, SF, CM). Following treatments, SDS PAGE and Western blotting, membranes were subjected to quantification for further analyses. Significantly lower pAKT levels were observed with SF vs GM at both 15m ($p < 0.0001$, represented by *) and 30m ($p < 0.0001$, represented by *). Lower pAKT activity was also observed with SF vs DM at both 15m ($p < 0.01$, represented by a) and 30m ($p < 0.0001$, represented by a). Reduced pAKT levels were observed with SF vs CM at both 15m ($p < 0.05$, represented by b) and 30m ($p < 0.01$, represented by b). Lower levels of pAKT activity was present with CM vs GM at both 15m ($p < 0.05$, represented by #) and 30m ($p < 0.0001$, represented by #). pAKT levels were also lower with DM vs GM at 30m ($p < 0.05$) and CM vs DM at 30m ($p < 0.0001$). Data are representative of 5 experiments. (p-values obtained by One-way repeated measures ANOVA)

As for pAkt, phospho-ERK 1/2 levels were quantified following incubation in the 4 different culture media for 15 or 30 min (Figure 3.19). All values are represented as percentage of the calibrator (GM 15m), which was set to be 100%. Significant reductions of pERK1/2 levels were observed with SF vs GM at both 15m ($13.75 \pm 6.36\%$ vs 100% , $p < 0.0001$) and 30m ($3.5 \pm 1.66\%$ vs $73.25 \pm 3.1\%$, $p < 0.0001$), SF vs DM at both 15m ($13.75 \pm 6.36\%$ vs $88.25 \pm 4.68\%$, $p < 0.0001$) and 30m ($3.5 \pm 1.66\%$ vs $59.75 \pm 7.1\%$, $p < 0.001$) and SF vs CM at 15m ($13.75 \pm 6.36\%$ vs $83 \pm 6.1\%$, $p < 0.0001$). Lower pERK1/2 was present with CM vs GM at 30m ($83 \pm 6.1\%$ vs 100% , $p < 0.0001$) and CM vs DM at 30m ($13.25 \pm 5.62\%$ vs $59.75 \pm 7.1\%$, $p < 0.001$). Significant reduction of pERK1/2 levels at 30m vs 15m were observed with GM ($73.25 \pm 3.1\%$ vs 100% , $p < 0.01$), DM ($59.75 \pm 7.1\%$ vs $88.25 \pm 4.68\%$, $p < 0.01$) and CM ($13.25 \pm 5.62\%$ vs $83 \pm 6.1\%$, $p < 0.01$).

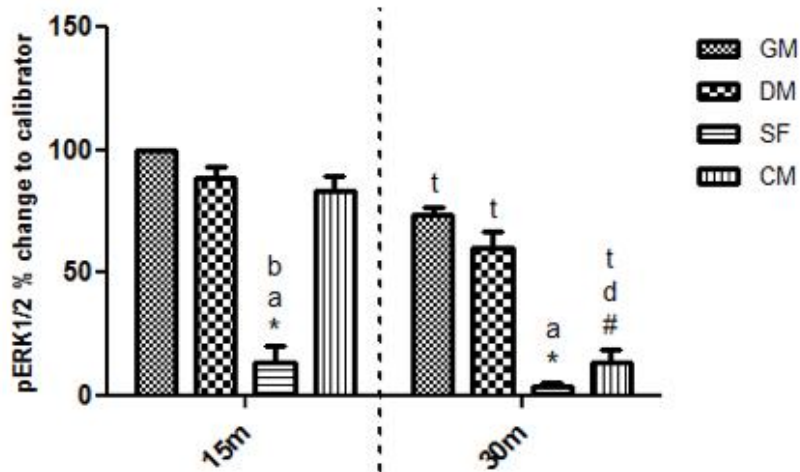


Figure 3.19. pERK 1/2 quantification (GM, DM, SF, CM). Following treatments, SDS PAGE and Western blotting, membranes were subjected to quantification for further analyses. Significantly lower levels of pERK1/2 were observed with SF vs GM at both 15m ($p < 0.0001$, represented by *) and 30m ($p < 0.0001$, represented by *). Lower pERK1/2 activity was also observed with SF vs DM at both 15m ($p < 0.0001$, represented by a) and 30m ($p < 0.001$, represented by a) and SF vs CM at 15m ($p < 0.0001$, represented by b). pERK1/2 activity was lower with CM vs GM at 30m ($p < 0.0001$, represented by #) and with CM vs DM at 30m ($p < 0.001$, represented by d). Significant reduction of pERK1/2 levels at 30m vs 15m was observed with GM ($p < 0.01$, represented by t), DM ($p < 0.01$, represented by t) and CM ($p < 0.01$, represented by t). Data are representative of 4 experiments performed in duplicate. (p-values obtained by One-way repeated measures ANOVA)

3.5.6. REDUCTION OF MYOGENIN EXPRESSION WITH CM VS DM.

Having investigated the impact of culture conditions on cell migration and the potential underlying signalling pathways, the impact of culture conditions on the expression of myogenic regulatory factors, myogenin and myoD, was next questioned. Since investigating positive regulators of migration was of main interest, SF was not included in these studies. RT-PCRs were performed to investigate the expression of MyoD and Myogenin, 24h after treatment with DM, GM or CM. A 24 hour time point was chosen, due to the fact that these myogenic regulatory factors are known to show a peak of expression in the beginning of differentiation, which decreases in later time points. All data are represented in arbitrary units and compared to the calibrator (DM), which was set to 1. As shown in Figure 3.20(A), significant reductions in the expression of Myogenin were

observed with GM vs DM (0.16 +/-0.06 vs 1, $p < 0.001$, equivalent to 6.25 fold decrease) and with CM vs DM (0.5 +/-0.06 vs 1, $p < 0.01$, equivalent to 2 fold decrease). Reductions were also observed with GM vs CM (0.16 +/-0.06 vs 0.5 +/-0.06, $p < 0.05$, equivalent to 3.125 fold decrease). These data suggest that while all three triggers are able to promote migration, GM and CM are more potent at suppressing the myogenic pathway in favour of migration, than DM.

MyoD expression (Figure 3.20B) was less influenced by culture conditions. No significant differences were found between any of the treatments.

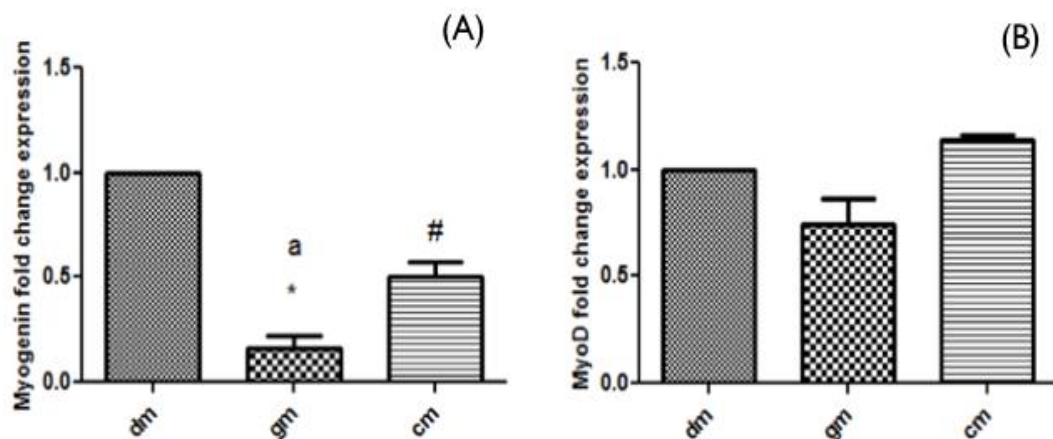


Figure 3.20. Myogenin and MyoD expression (DM, GM, CM). Myogenin expression 24h after treatment with DM, GM and CM (A). All values are represented as fold change to the calibrator (DM), which was set to 1 (mean Ct value (MyoD) = 21.98 +/-0.16; mean Ct value (Myogenin) = 21.79 +/-1.05) Significant reductions were observed with GM vs DM ($p < 0.001$, represented by *), CM vs DM ($p < 0.01$, represented by #) and GM vs CM ($p < 0.05$, represented by a). MyoD expression 24h after treatment with DM, GM and CM (B). No significant difference was observed between any of the treatments. Data are representative of 3 experiments performed in duplicate. (p-values obtained by One-way repeated measures ANOVA)

3.5.7. MYOBLAST MIGRATION, INDUCED BY CONDITIONED MEDIA, IS REDUCED BY INHIBITION OF PI3K/AKT AND MAPK/ERK PATHWAYS WITH LY294002 AND UO126

It was observed that myotube CM was able to induce myoblast migration and to activate signalling pathways, such as PI3K/AKT and MAPK/ERK, which are linked to, among other cellular responses, regulating cellular migration. Inhibitors of PI3K/AKT and MAPK/ERK pathways, respectively LY294002 and UO126, were used to investigate how silencing of these signalling pathways would affect

the migration capacity of myoblasts induced to migrate by CM. In order to confirm the specificity and effect of both inhibitors on levels and activation of these specific proteins, western blots were performed against pAKT (Ser473) and pERK 1/2 (Figure 3.21). Large decreases in the levels of pAKT, as compared to control CM, at both 15m and 30m were obvious in the presence of 10 μ M LY294002, while pERK1/2 levels were not affected. On the contrary, in the presence of 5 μ M UO126, pERK1/2 was largely inhibited, as compared to control CM, at both 15m and 30m, while pAKT levels were not affected. Total Akt, ERK and beta-actin were used as loading controls. As is evident from the figure for Akt and beta-actin, loading was consistent across all samples. The apparent discrepancy evident with pan ERK antibodies e.g. a reduction in ERK levels in the presence of CM and LY at 15 and 30 min. was investigated further and was found to occur as a consequence of competition between the pERK1/2 and pan-ERK antibodies (all pERK1/2 blots were run before membranes being stripped and reprobbed with pan ERK antibodies), with pERK1/2 phosphorylation reducing pan-ERK binding, rather than a reduction in total ERK occurring (data not shown).

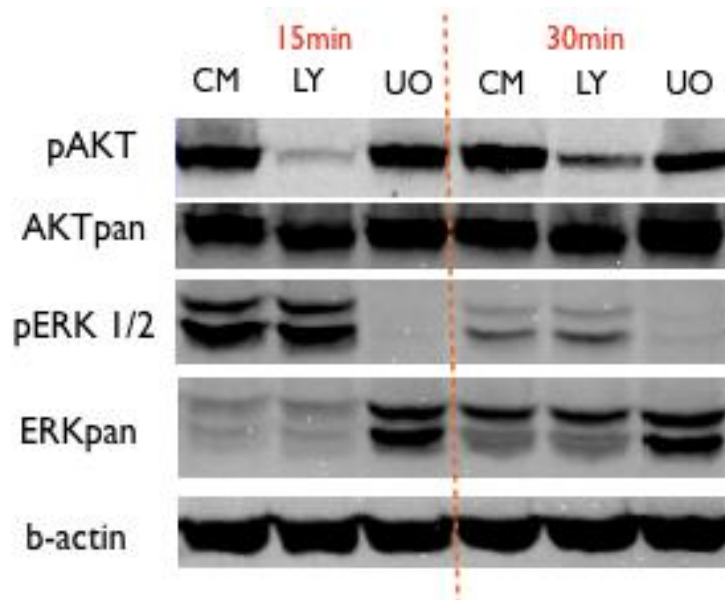


Figure 3.21. Western blots (CM with 10 μ M LY294002 and 5 μ M UO126). Western blots examining the levels of pAKT (Ser473) and pERK 1/2 at 15 and 30 min in response to CM (lanes 1 + 4=CM), CM+10 μ M LY294002 (lanes 2 + 5=LY) and CM+5 μ M UO126 (lanes 3 + 6 =UO). Data are representative of 4 experiments.

Blots were subjected to further analyses using Quantity One software. Phospho-Akt and Phospho-ERK1/2 levels were quantified across the 3 different treatments conditions and the two time points. All values are represented as percentage of the calibrator (CM 15m), which was set to 100%.

Quantification and analyses of pAKT levels (Figure 3.22) indicated significant reductions with CM+10 μ M LY294002 vs CM at both 15m (19.75% \pm 2.36 vs 100%, p <0.001) and 30m (27.25% \pm 2.21 vs 88% \pm 15.56, p <0.05). Significant reductions in pAkt were also observed with CM+10 μ M LY294002 vs CM+5 μ M UO126 at both 15m (19.75% \pm 2.36 vs 91.25% \pm 11.44, p <0.01) and 30m (27.25% \pm 2.21 vs 80% \pm 11.47, p <0.05). No significant reduction in pAKT levels was observed with CM+5 μ M UO126 vs CM.

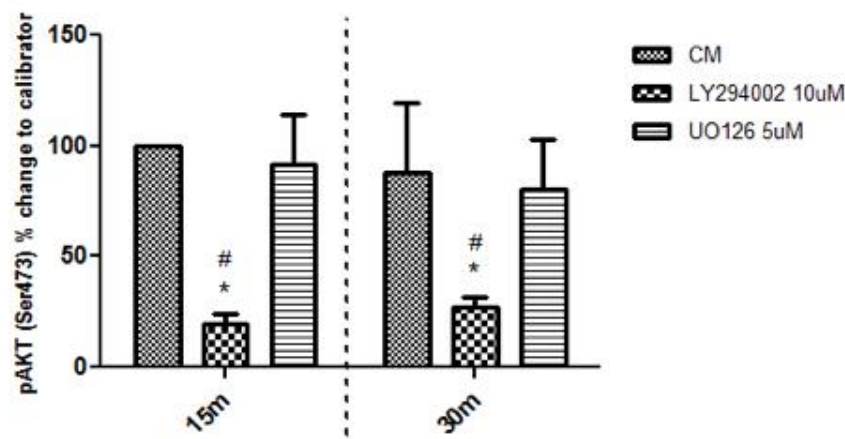


Figure 3.22. Quantification of pAKT (CM with 10 μ M LY294002 and 5 μ M UO126). Quantification of pAKT levels in response to CM, CM+10 μ M LY294002 and CM+5 μ M UO126 indicated significant reductions with CM+10 μ M LY294002 vs CM at both 15m (p <0.001, represented by *) and 30m (p <0.05, represented by *) and with CM+10 μ M LY294002 vs CM+5 μ M UO126 at both 15m (p <0.01, represented by #) and 30m (p <0.05, represented by #). Data are representative of 4 experiments. (p -values obtained by One-way repeated measures ANOVA)

Quantification and analysis of pERK1/2 levels (Figure 3.23) indicated significant reductions in pERK1/2 activation with CM+5 μ M UO126 vs CM at 15m (3% \pm 1.15 vs 100%, p <0.0001) and CM+5 μ M UO126 vs CM+10 μ M LY294002 at 15m (3% \pm 1.15 vs 83.67% \pm 15.45, p <0.001). No significant difference in pERK 1/2 levels was indicated with CM+10 μ M LY294002 vs CM at 15min. No significant change was observed between any of the treatments at 30

min, despite levels of pERK1/2 remaining visually lower with UO126 treatment. Significant reductions of pERK1/2 levels with time was also observed at 30m vs 15m with both CM (17.67% +/-6.33 vs 100%, $p<0.001$) and CM+10 μ M LY294002 (18% +/-2.89 vs 83.67% +/-15.45, $p<0.05$).

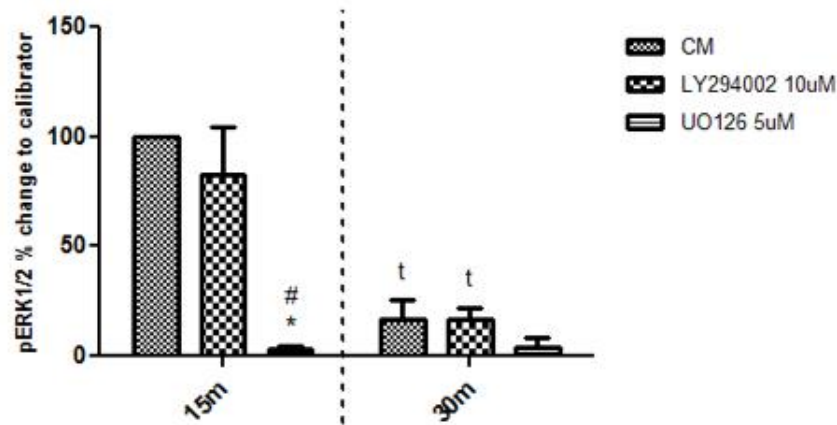


Figure 3.23. Quantification of pERK1/2 (CM with 10 μ M LY294002 and 5 μ M UO126). Quantification of pERK1/2 levels in response to CM, CM+LY294002 and CM+UO126 indicated significant reductions with CM+5 μ M UO126 vs CM at 15m ($p<0.0001$, represented by *) and CM+5 μ M UO126 vs CM+LY294002 at 15m ($p<0.001$, represented by #). Significant reductions in the pERK 1/2 levels were observed at 30m vs 15m with both CM ($p<0.001$, represented by t) and LY ($p<0.05$, represented by t). Data are representative of 4 experiments. (p-values obtained by One-way repeated measures ANOVA)

After observations that both inhibitors were reducing the phosphorylation levels of pAKT and pERK1/2 in a specific manner, wound healing assays were performed in the presence of CM, CM+10 μ M LY294002 and CM+5 μ M UO126, in order to determine the effect of inhibiting these signalling pathways on the migration of myoblasts (Figure 3.24A). Results from these morphological studies, as expected, suggested inhibited migration in the presence of either LY294002 or UO126, compared with CM alone, over 20 h.

Quantifications and statistical analyses of cell counts infiltrating the wound site (Figure 3.24B), indicated significant reductions in the total number of cells when treated with CM+10 μ M LY294002 vs CM (47 +/- 5 vs 71 +/- 4 cells, $p<0.05$, equivalent to 39% decrease) and with CM+5 μ M UO126 vs CM (51 +/- 7 vs 71 +/- 4 cells, $p<0.05$, equivalent to 28% decrease). Significant reductions were also

apparent in the percentage of cells present in the centre of the wound site with CM+10 μ M LY294002 vs CM (3.4 +/-0.5 vs 11.1 +/-1.8 %, $p<0.01$) and with CM+5 μ M UO126 vs CM (4.8 +/-1.36 vs 11.1 +/-1.8 %, $p<0.01$) (Figure 3.24C).

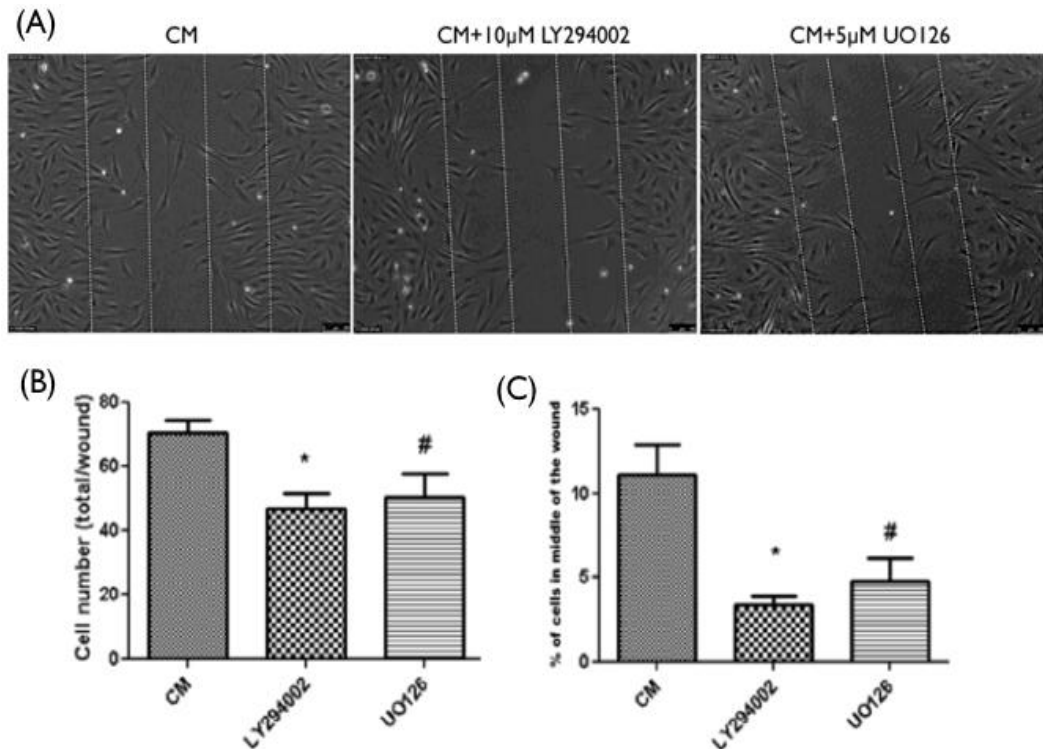


Figure 3.24. Wound healing assay with cell count analysis (CM with 10 μ M LY294002 and 5 μ M UO126). Wound healing assay comparing the effects on wound closure of CM, CM+10 μ M LY294002 and CM+5 μ M UO126 following 20h incubation (A). Quantification of the total number of cells infiltrating the wound after 20h incubation, indicated a significant decrease in the number of cells with both CM+10 μ M LY294002 vs CM ($p<0.05$, represented by *) and CM+5 μ M UO126 vs CM ($p<0.05$, represented by #) (B). Quantification of the percentage of cells in the middle of the wound indicated a significant decrease with both CM+10 μ M LY294002 vs CM ($p<0.01$, represented by *) and CM+5 μ M UO125 vs CM ($p<0.01$, represented by #) (C). All data are representative of 5 experiments performed in duplicate. (p-values obtained by One-way repeated measures ANOVA)

To confirm the cell count quantification data, migration tracking analyses were performed to examine the effect of CM, CM+10 μ M LY294002 and CM+5 μ M UO125 on cell migration distance. Once again, these morphological findings confirmed the observations made above (Figure 3.24) and suggested reductions in migration distance as a consequence of incubations with either inhibitor vs CM alone (Figure 3.25A). Further detailed analyses of the actual cell migration

distance (Figure 3.25B) confirmed that cell migration was inhibited with CM+10 μ M LY294002 vs CM (236 \pm 7 μ m vs 357 \pm 16 μ m, p <0.001, equivalent to 51% decrease) and with CM+5 μ M UO126 vs CM (227 \pm 15.5 μ m vs 357 \pm 16 μ m, p <0.0001, equivalent to 57% decrease), thus strengthening and validating the data obtained in Figure 3.24, above.

Cell death quantifications and analyses (Figure 3.25C) indicated significant increases in the percentage of dead cells with CM+10 μ M LY294002 vs CM (4.16 \pm 1% vs 1.7 \pm 0.4 %, p <0.05) and with CM+10 μ M LY294002 vs CM+5 μ M UO125 (4.16 \pm 1% vs 0.84 \pm 0.2 %, p <0.05). No significant difference in cell death was indicated between CM and CM+5 μ M UO126.

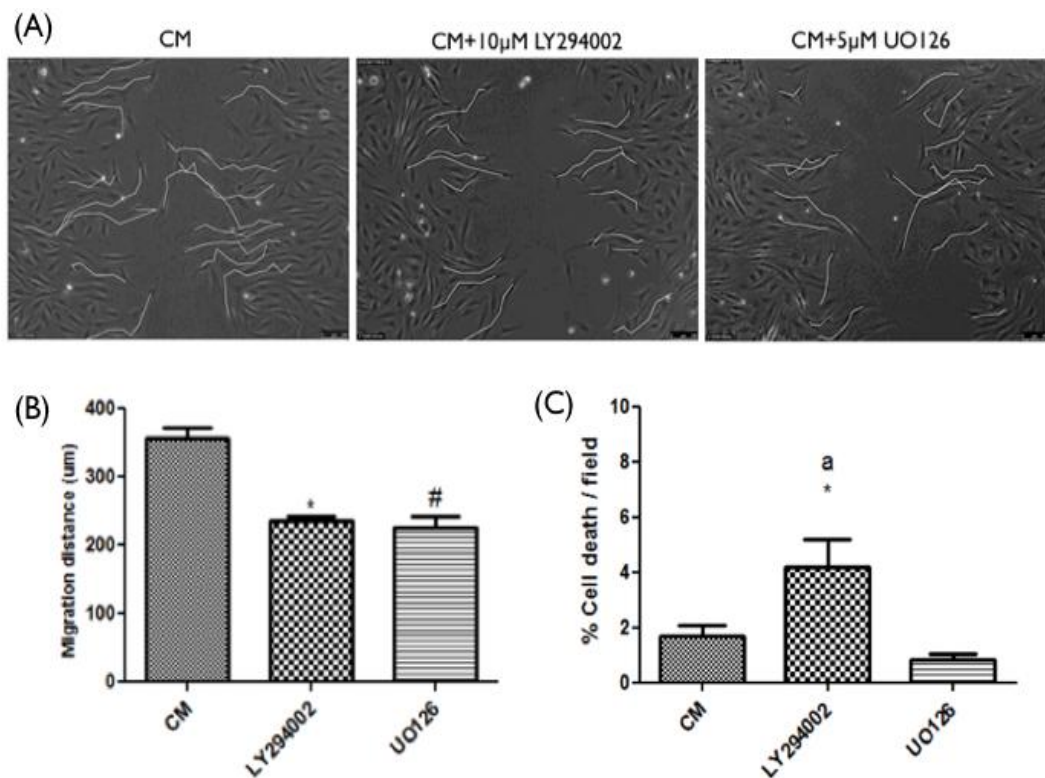


Figure 3.25. Cell tracking and cell death analysis (CM with 10 μ M LY294002 and 5 μ M UO126). Migration tracking comparing the effects of CM, CM+10 μ M LY294002 and CM+5 μ M UO126 on myoblast migration distance following 20h incubation (A). Quantification of cell migration distance indicated significant inhibition of migration with CM+10 μ M LY294002 vs CM (p <0.001, represented by *) and CM+5 μ M UO126 vs CM (p <0.0001, represented by #) (B). Data are representative of 5 experiments performed in duplicate. Cell death quantifications indicated increased cell death with CM+10 μ M LY294002 vs CM (p <0.05, represented by *) and with CM+10 μ M LY294002 vs CM+ 5 μ M UO126 (p <0.05, represented by a) (C). Data are representative of 4 experiments performed in duplicate. (p -values obtained by One-way repeated measures ANOVA)

SUMMARY OF MAJOR FINDINGS

- Myotubes release soluble factors *in vitro*, capable of inducing both migration and chemotaxis of C2C12 myoblasts, as demonstrated by the wound healing assay and the transwell insert assay.
- Enhanced myoblast migration following stimulation by media containing soluble factors released by myotubes (conditioned media), is also associated with activation of PI3K/AKT and MAPK/ERK signalling pathways.
- Migration of myoblasts stimulated by myotube conditioned media is reduced when PI3K/AKT and MAPK/ERK signalling pathways are inhibited with LY294002 or UO126.

3.6. DISCUSSION

3.6.1. MEDIA CONDITIONED BY MATURE MYOTUBES IS ABLE TO INDUCE WOUND HEALING AND MIGRATION OF MYOBLASTS

Media conditioned by 5d mature myotubes was able to induce migration compared to control SF media. This was demonstrated by wound healing assay analysis, resulting in 233% increase in the total number of cells infiltrating the wound, of which nearly 10% more were situated in the middle of the wound, with CM vs SF. These results were also supported by cell tracking analyses, indicating 79% increase in the distance migrated by cells stimulated with CM vs SF. Morphology of the cells stimulated with CM also differed significantly, as compared to the morphology of cells incubated in SF media. Cells in CM possessed more elongated morphology with visible protrusions, such as filopodia, suggestive of their increased migration capacity, compared to the quiescent morphology of cells incubated in SF media. Finally, cell death levels were also increased with SF media, compared to CM. All of these observations suggested that factors, possibly secreted by the myotubes, were responsible for stimulating myoblast migration and survival.

In order to optimise the migration assays and analyses, the effects induced by CM were compared to those of relevant controls, namely GM and DM - both known for their induction of, respectively, proliferation and differentiation of C2C12 cells. It was assessed how these two different media, containing an abundance of growth factors, would compare to the myotube CM in inducing myoblast migration. Both wound healing and transwell insert assays were performed to compare the impact of GM, DM, CM and SF on cell migration or chemotaxis. All three media (GM, DM and CM) induced significantly higher levels of migration, as compared to SF media in the wound healing assays, with GM being most potent and DM and CM equipotent. Transwell inserts, investigating the chemotaxis of myoblasts in response to the 4 different media, however, demonstrated different results. As expected, no chemotaxis was induced by SF media. CM and DM, however, induced extensive levels of chemotaxis of the cells, confirming the hypothesis that factors are released from myotubes that are able to induce myoblast migration and chemotaxis. GM, however, which induced extensive migration in the wound healing assay, surprisingly induced very little chemotaxis through the transwell inserts. It was suggested that this discrepancy

might be due to the very high concentrations of serum growth factors in the media. Previous reports have suggested that growth factors, such as PDGF, HGF, TGF-beta, are less potent at inducing chemotaxis at higher concentration than at lower concentrations (Bischoff, 1997, De Donatis *et al.*, 2008). Therefore, the concentration of serum in the GM used for transwell insert assays was reduced to assess whether chemotaxis of myoblasts would be increased. Diluted GM at a 1:5 ratio with SF media, indeed, induced greater chemotactic response of myoblasts, as compared to non-diluted GM. These results indicated that wound healing assay and transwell inserts should not always be considered as equivalent assays for investigating cell migration and that certain combinations of growth factors and or proteases might exert different effects on adherent cell movement/migration and on chemotactic movement.

3.6.2. MEDIA CONDITIONED BY LIVING MYOTUBES IS MORE POTENT AT INDUCING MIGRATION AND WOUND HEALING, AS COMPARED TO MEDIA CONDITIONED BY FACTORS RELEASED FROM DAMAGED MYOTUBES

It was demonstrated that SF media incubated for 3 days with mature myotubes (CM) was conditioned with factors, capable of inducing myoblast migration. It was visually observed that the myotubes incubated in SF media were decreasing in size with time. As reported by other studies, a cell culture model of serum deprivation/starvation of myotubes mimics to certain extent muscle wasting and atrophy and may increase the levels of myofibrillar proteolysis and apoptosis (Nakashima *et al.*, 2005, Stevenson *et al.*, 2005). Therefore, it was not possible to initially ascertain whether the factors inducing myoblast migration were secreted by the viable myotubes or whether they were being released from the dying or atrophying cells. Although excessive washes were performed before SF media was added to the myotubes for conditioning, the possibility existed that there might also be factors unspecifically bound to the cells or the wells from incubations with media containing serum (during the growth or early differentiation phases of the experiments) and that these factors might subsequently be released into the SF media. In order to check for specificity and also to estimate how the release of potential factors from dead myotubes compared to the myotube CM, the effect on migration of the CM was compared to the effect of media conditioned in the presence of mechanically damaged myotubes. It was demonstrated that media conditioned for 3 days by the living

myotube cultures was significantly more potent at inducing myoblast migration in wound healing assays, as compared to media conditioned by mechanically damaged myotubes over the same period of time. Transwell insert assays demonstrated that chemotaxis of myoblasts was induced by the media conditioned by crushed myotubes, although clustering of the cells crossing the membrane was observed. The data from both assays suggested that the resultant conditioned media from damaged or non-damaged myotubes are two distinct media, composed either of different factors or of different concentrations/combination of factors, hence the altered migration and chemotaxis data, suggesting that secreted factors are indeed capable of manipulating the migration of myoblasts. Previous studies have demonstrated that media conditioned by myocytes at the time of their fusion is capable of inducing their migration (Griffin *et al.*, 2010). Migration itself is important for cell alignment and a prerequisite step for cell fusion. Therefore, it is possible that myogenic cells, upon commencement and progression of the fusion process, release factors, which induce the migration and recruitment of other myogenic cells, which would contribute with their myonuclei during the fusion process. It is proposed that similar situation is observed also with mature or atrophying myotubes - factors inducing myoblast migration are released, capable of recruiting more myogenic cells for fusion enabling the maintenance, the growth or repair of myotubes. These factors could also have effects on other processes or cell types, such as inflammatory cells. Studies investigating the secretome of differentiating muscle have indeed confirmed that a variety of factors are secreted, including factors involved in cell motility (Henningsen *et al.*, 2010). However, further investigation is required into how the combination of these secreted factors is affecting migration of myoblasts and the signalling pathways involved.

3.6.3. PI3K/AKT AND MAPK/ERK SIGNALLING PATHWAYS ARE INDUCED IN RESPONSE TO CM AND THEIR INHIBITION LEADS TO REDUCED MYOBLAST MIGRATION

Following the findings that myotube CM is able to induce migration of myoblasts, the potential signalling pathways involved in this process were investigated. In preliminary studies it was addressed how PI3K/AKT and MAPK/ERK pathways, previously shown to be of importance for myoblast migration (Al-Shanti *et al.*, 2011, Leloup *et al.*, 2007), would be regulated in response to CM. Investigations of these pathways in response to GM and DM

were therefore also assessed. Results showed that all three media, which induced migration (GM, DM and CM), also resulted in increased levels of pAKT and pERK1/2, as compared to SF, which did not induce migration nor activation of these pathways. However, although DM induced a stronger activation of both PI3K/AKT and MAPK/ERK pathways, as compared to CM, migration analyses indicated equivalent, if not slightly greater induction of migration with CM vs DM. It is possible that at later time points, which were not investigated, DM triggered a stronger differentiation response, as compared to cells incubated in CM, the increased expression of myogenin in DM vs. CM underpins this hypothesis. PCRs indeed demonstrated that cells incubated in DM are able to upregulate by 2-fold the expression of Myogenin, an early marker of differentiation, as compared to cells incubated in CM. As suggested by other studies, differentiating myoblasts, although still migrating, do so at a slower pace, as compared to undifferentiated cells (Griffin *et al.*, 2010). Therefore, it is possible that even though signalling pathways important for migration are activated at early time points, triggering of cell differentiation at later time points can override these signals. Furthermore, it must not be forgotten that PI3K and ERK1/2 activation are also key pathways integral for the differentiation process (Foulstone *et al.*, 2004). In order to verify if PI3K/AKT and MAPK/ERK signalling pathways are indeed required for myoblast migration in response to CM, selective inhibitors were used (LY294002 for PI3K/AKT and UO126 for MAPK/ERK pathway). Inhibition of each pathway, not affecting the phosphorylation or total protein levels of the other one, resulted in reduced cell migration. Previous reports in our group demonstrated similar results for PI3K and MAPK pathways, although under different culture conditions (GM) and with different cell types (C2 myoblasts) (Al-Shanti *et al.*, 2011). Current data substantiate these observations and suggest that regardless of the stimulus, these two pathways (as well as others not investigated) are required for unrestricted myoblast migration. An interesting avenue for further investigation would be to study how upregulation of these two pathways would influence the migration of myoblasts and explore potential cross-talk between the two.

3.6.4. CONCLUSIONS AND THESIS DIRECTIONS

It was demonstrated that serum free media conditioned by mature myotubes was able to induce migration of myoblasts in a wound healing model and chemotaxis in transwell inserts. It was suggested that factors secreted by myotubes are inducing this response, although identification of these factors was beyond the scope of this thesis. Involvement of PI3K/AKT and MAPK/ERK pathways was also assessed. Both pathways were shown to be upregulated in response to CM and their inhibition resulted in reduced, if not abolished migration. These studies propose interesting avenues for further research. In particular, it would be interesting to explore the potential links between the contribution of secreted factors and the migration of myoblast to muscle debilitating events or conditions, such as ageing and sarcopenia.

The possibility of age related changes in the way myogenic precursors respond to signals from the local environment, potential alterations in paracrine signalling, associated with signalling pathways activation/reduction in the context of cell migration, was considered as an interesting avenue of investigation. Therefore, in the next chapter, a link was established between the results obtained from media conditioning experiments, the involvement of signalling pathways in myoblast migration and skeletal muscle ageing.

CHAPTER 4

4. SERIALY PASSAGED C2C12 CELLS DEMONSTRATE ALTERED MIGRATION BEHAVIOUR

4.1. INTRODUCTION

Aged skeletal muscle is characterised by a decline in functional properties, including power, strength and endurance, partly due to the overall reduction in size of the muscles and to their intrinsically reduced functional muscle fibres (reviewed in (Brack and Rando, 2008)). The degenerative loss of skeletal muscle mass and strength with age is known as sarcopenia. Both intrinsic and extrinsic factors have been investigated and shown to be altered in aged muscle. The systemic environment is of major importance, as shown by parabiotic murine pairing studies, where rejuvenation of aged progenitor cells (both *in vivo* and *in vitro*) occurred by exposure to a young systemic environment and vice versa – a decline in functionality of young satellite cells exposed to an old systemic environment (Conboy *et al.*, 2005). It is also known that old muscle is able to regenerate when transplanted into young animals, while regeneration of young muscle transplanted in old animals is impaired (Carlson and Faulkner, 1989), further underlying the importance of the extrinsic environment in the process of sarcopenia. However, the potential role of alterations in the intrinsic mechanisms of myogenic precursor cells in ageing is not entirely elucidated. Reports have revealed that expression levels of regulators of muscle differentiation, such as S100B and RAGE, are altered in old vs. young human satellite cells (Beccafico *et al.*, 2010), suggesting that intrinsic mechanisms are also important. It is known that the proliferative potential of isolated satellite cells is reduced with age when they are passaged, coinciding with telomere shortening, resulting in replicative senescence of satellite cells with ageing (Decary *et al.*, 1997, Schultz and Lipton, 1982, Webster and Blau, 1990). Reduced expression of myogenic regulatory factors, such as MyoD and Myogenin, coincide with reduced differentiation of senescent myoblasts (Bigot *et al.*, 2008). However, it has also been suggested that telomerase activity is retained in old muscle and it is only the myoblast progeny, when induced to differentiate, that show deterioration of telomerase activity (O'Connor *et al.*, 2009). Using a C2C12 *in vitro* model of multiple population doublings, which retains telomerase activity, Sharples *et al.* have proposed a model to investigate the impact of cellular divisions on myoblast behavior. They reported that myoblasts subjected to multiple divisions displayed intrinsic

differences in their growth and differentiation potential, as compared to low passage of cells, including altered IGF-I, myogenin, IGFBP-5 and IGFBP-2 expression and changes in the levels of Akt and JNK1/2 phosphorylation (Sharples *et al.*, 2011). Thus, in the absence of senescence and the presence of retained telomerase activity, C2C12 myoblasts subjected to serial passaging are still demonstrating characteristics that mimic the molecular regulation of atrophy seen in elderly skeletal muscle.

It is not well known how migration of myoblasts is affected during the process of ageing. Reports have indicated that migration is retarded in myoblasts isolated from aged vs young mice and rats (Dumke and Lees, 2011, Siriatt *et al.*, 2007). Dumke *et al.* have also demonstrated that myogenic precursors isolated from young, but not from old skeletal muscle, are responsive to chemotactic factors released from activated T cells. To our knowledge, no studies have investigated the effect of multiple divisions on myoblast migration. Sharples *et al.* have demonstrated that intrinsic changes reduced the capacity of C2C12 cells to differentiate and fuse into myotubes, but their migration was not assessed (Sharples *et al.*, 2011). Potential differences in the secretome of serially passaged myogenic cells have not been investigated either.

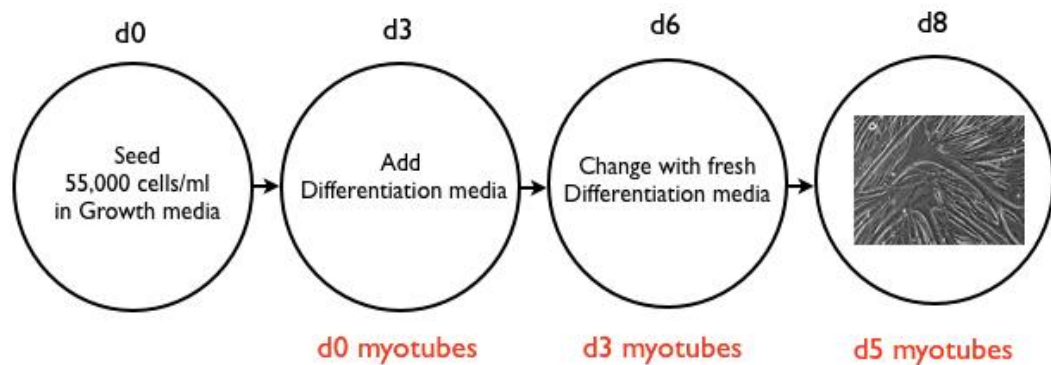
4.2. AIMS, OBJECTIVES AND HYPOTHESIS

The main aim was to reveal the potential changes in migration capacity of myoblasts undergoing multiple divisions and also to identify differences in the impact of CM from aged vs young myotubes on migration, which would provide clues for further investigations in the field of muscle ageing and sarcopenia. Objectives were: 1) to compare, using wound healing assays, the migration capacity of high passage vs low passage C2C12 myoblasts in response to myotube CM and 2) to investigate whether there were differences between media conditioned by low vs high passage C2C12 cells in their ability to induce myoblast migration. It was hypothesized that there would be differences between high and low passage myoblasts and their capacity to migrate and also differences in the ability of media conditioned by low and high passage cells to stimulate cell migration.

4.3. METHODS

4.3.1. CELL CULTURE

C2C12 myoblasts were cultured in a humidified 5% CO₂ atmosphere at 37°C. Cells were grown in the presence of (GM) in T75 flasks until confluent and split into multiwell plates for experiments. In order to initiate differentiation, C2C12 cells were grown in 6 well plates until confluency was achieved, monolayers were washed with PBS and differentiation media (DM) was added to the cell monolayers. When differentiation experiments were performed for 5 days, DM was replaced with fresh media at d3, allowing the replenishment of factors present in the media and maintaining the optimum pH for longer incubation of the cells in the same media type. A schematic representation of performing differentiation experiments and obtaining 5 day old myotubes:



4.3.2. CONDITIONED MEDIA GENERATION

p5 and p50 C2C12 myoblasts were triggered to differentiate into myotubes for 5 days in 6 well plates. For both p5 and p50 cells, conditioned media was generated, as described in section 3.3.2.

4.3.3. WOUND HEALING ASSAY AND LIVE IMAGEING

Cells were grown in pre-gelatinised 12 well plates in GM until ~80-90% confluent. For wound healing assay comparing between p5 and p50 myoblasts, it was established that equal confluencies for migration studies were achieved by seeding 80,000 cells/ml of p5 cells and 100,000 cells/ml of p50 cells in a 12 well plate. Cell monolayers were washed 3 times with PBS and DMEM 0.1% FBS media (quiescent media = QM) was added and incubated for 20h with the cells. In the last 3 hours of incubation with QM, 10µg/ml Mitomycin-C (Sigma-Aldrich)

was added, in order to block proliferation, and monolayers were wounded with a sterile pipette tip, generating a wound of approximately 600µm in size. Wound healing with live imaging microscopy is described in section 2.2.2.1.

4.3.4. ANALYSIS OF CELL MIGRATION

Cell migration was analysed with Keynote'09 software version 5.1.1. (Apple Inc.) and ImageJ v1.45i software, as described in section 3.4.2.

4.3.5. CELL DEATH QUANTIFICATIONS BY LIVE IMAGEING

The numbers of dying cells were counted frame by frame in each area for the duration of the movie, as described in section 2.2.4.

4.3.6. WESTERN BLOTS

Sample collection and preparation for SDS-PAGE was performed as described in section 2.2.8.1. Gel electrophoresis, membrane transfer, blocking and detection steps were performed, as described in sections 2.2.8.2-2.2.8.5. Primary AKTpan, pAKT, b-actin and ERKpan rabbit IgG antibodies were purchased from New England Biolabs (Hertfordshire, UK) and were incubated with membranes overnight at RT in 1:1000 concentration, diluted in 5% BSA/TBST. Primary pERK1/2 rabbit antibody was purchased from Promega and was incubated with membranes overnight at RT in 1:5000 concentration, diluted in 0.1% BSA/TBST. Secondary Goat Anti-rabbit HRP-conjugated antibodies were purchased from MP Biomedicals (United Kingdom) and were incubated with membranes for 1h at RT 1:5000 concentration, diluted in blocking solution. Membranes were blocked for 1h at RT in 5% non-fat dry milk/TBST (for antibodies purchased from New England Biolabs) or in 1% BSA/TBST for pERK1/2.

4.3.7. RNA ISOLATIONS AND REAL-TIME PCR

RNA extraction and TaqMan® Real-time PCR methods were performed as described in sections 2.2.9 and 2.2.10, respectively. The following predesigned primer sets were ordered from Applied Biosystems and were used with the

TaqMan® detection method: Polr2b (Mm00464214_m1), MyoD (mm00440387_m1) and Myogenin (mm00446194_m1).

4.3.8. CREATINE KINASE (CK) ASSAY

Samples for CK assay were prepared by adding 150µL per well (for 6 well plate) of Tris Mes Triton (TMT buffer; composed of: 0.05M Tris/Mes and 1% Triton-X100). Assay was performed, as described in section 2.2.7.2.

4.3.9. SERIAL PASSAGING

C2C12 cells at passage 20 (P20) were seeded in a T75 flasks at a concentration of 500,000cell/ml and allowed to proliferate in GM for 48h before being passaged to a new T75 flask. Upon passaging, total numbers of cells were counted, with approximately 2.5 million cells per flask being yielded at confluency, thus ensuring that 48h was sufficient time for cells to perform 2 full divisions. Cycles of passaging were repeated 30 times until reaching 50 passages (thus, C2C12 cells were designated as p50). Considering that approximately 2.25 cell doublings were initiated over 48h, 30 repeated passaging events would yield approximately 68 cell population doublings.

4.3.10. STATISTICAL ANALYSES

Statistical analyses and significance of data were determined using GraphPad Prism version 5.00 for Mac OS X, GraphPad Software, San Diego California USA, www.graphpad.com. Statistical significance for interactions between two paired groups was determined with a Paired t-test, while unpaired t-test was used for unpaired groups (e.g. when comparing between p5 and p50 groups). Statistical significance for interactions between more than two groups was determined with a one-way ANOVA, or with a one-way repeated measures ANOVA, when matched observations were investigated. All results are presented as mean +/- standard error of the mean (SEM). All values below $p < 0.05$ were considered as significant.

4.4 RESULTS

4.4.1. SERIALY PASSAGED C2C12 MYOBLASTS (P50) DEMONSTRATED AN IMPAIRED CAPACITY TO DIFFERENTIATE COMPARED TO LOW PASSAGE (P5) CELLS

In order to confirm the differences in fusion/differentiation capacity, p5 and p50 myoblasts were incubated until confluent and DM media was added for 3 days. Phase contrast microscopy (Figure 4.1) demonstrated reduced capacity of p50 cells to fuse into myotubes compared with p5.

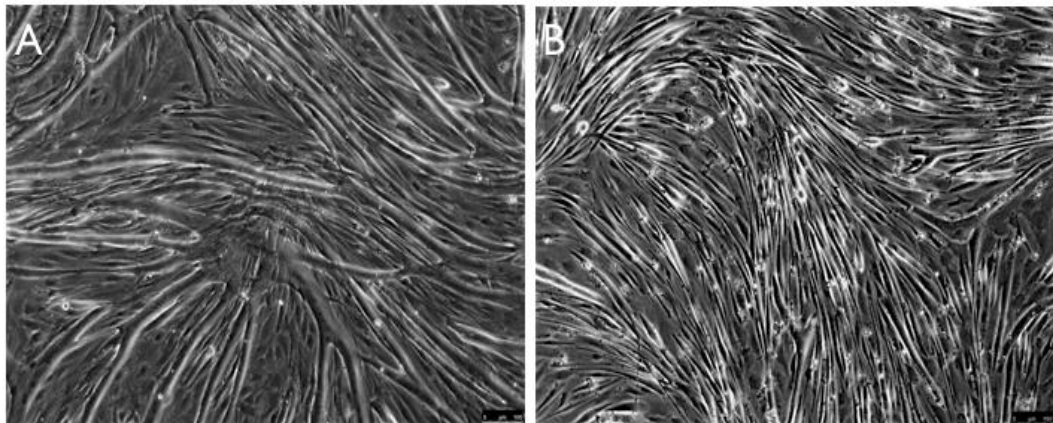


Figure 4.1. Phase-contrast microscopy investigating the effects of DM on p5 or p50 myoblasts. Enhanced myotubes formation was observed with p5 (A) myoblasts vs p50 myoblasts (B), incubated in DM for 3 days. Data are representative of 4 experiments performed in duplicate. 10x objective used.

In order to verify the phase-contrast microscopy observations, CK activity was measured in the two different myoblast passages (Figure 4.2). The data from CK assays supported the phase-contrast microscopy images, showing significant decreases in CK activity with p50 cells treated with DM vs p5 cells treated with DM for 72 hrs (836.75 \pm 90.48 mU/mg vs 1123.2 \pm 66.43 mU/mg, $p < 0.05$, equivalent to 1.34 fold decrease).

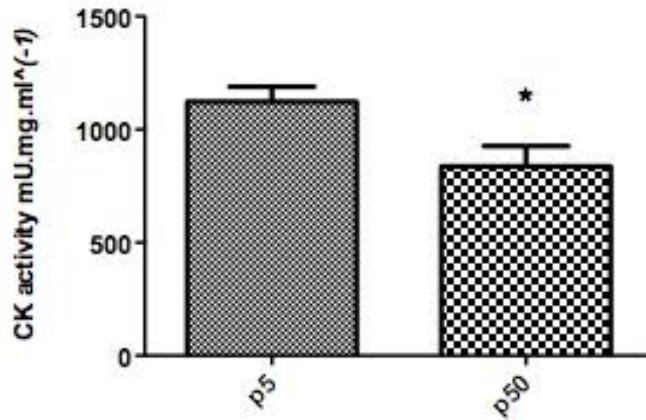


Figure 4.2. CK assay, measuring CK activity between p5 and p50 myoblasts incubated for 3 days with DM. Significant decreases in CK activity were present with p50 in control DM vs p5 cells in control DM ($p < 0.05$, represented by *). Data are representative of 4 experiments performed in duplicate. (p-values obtained by unpaired t-test)

MyoD and Myogenin gene expression were examined in p5 and p50 myoblasts in response to DM (Figure 4.3). Reductions in MyoD expression were observed with passage in p50 myoblasts treated with DM vs p5 myoblasts treated with DM at d1 (0.56 ± 0.01 vs 1, $p < 0.0001$, equivalent to 1.79 fold decrease). Similar to MyoD, passage influenced the expression of Myogenin. Significant decreases were observed with p50 myoblasts vs p5 myoblasts treated with DM at day1 (0.43 ± 0.02 vs 1, $p < 0.0001$, equivalent to 2.33 fold decrease).

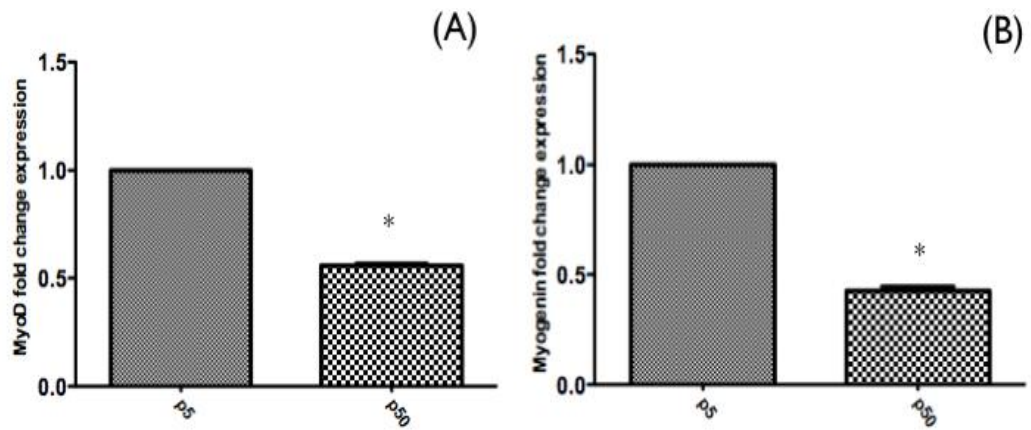


Figure 4.3. Examining the gene expression of MyoD and Myogenin between p5 and p50 myoblasts at d1 following treatment with DM. MyoD gene expression indicated significant decrease with p50 myoblasts vs p5 myoblasts ($p < 0.0001$, represented by *). Values are represented as fold change to the calibrator (p5 d1), which was set to 1 (mean Ct value = 24.54 \pm 0.24). (A). Myogenin gene expression indicated significant decrease with p50 myoblasts vs p5 myoblasts ($p < 0.0001$, represented by *). Values are represented as fold change to the calibrator (p5 d1), which was set to 1 (mean Ct value = 19.21 \pm 0.06). (B). Data are representative of 4 experiments performed in duplicate. (p-values obtained by unpaired t-test)

4.4.2. SIGNIFICANTLY HIGHER LEVELS OF P-ERK1/2 AND ELEVATED LEVELS OF P-AKT WITH P50 MYOBLASTS VS P5 MYOBLASTS IN RESPONSE TO CM

Western blots were performed to investigate the potential altered activation of PI3K/AKT and MAPK/ERK between p5 and p50 cells in response to myotube CM (Figure 4.4). The levels of pAKT and pERK1/2 appeared to increase in response to CM with high passage vs low passage cells. Importantly, temporal differences were apparent, particularly for pERK1/2, where at 30 and 45 minutes ERK1/2 phosphorylation was reduced in p5 cells, but remained elevated in p50 cells.

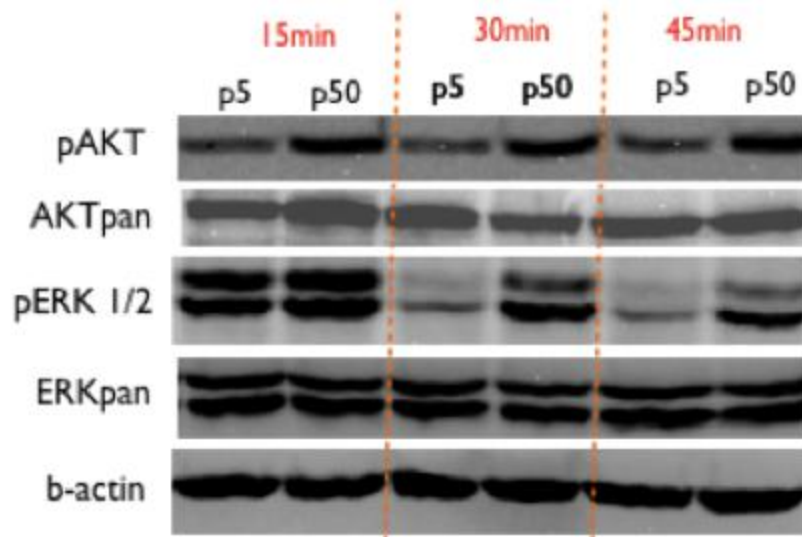


Figure 4.4. Western blots (p5 vs p50 myoblasts in CM). Westerns blots were performed to investigate the activation of PI3K/AKT and MAPK/ERK between p5 and p50 cells in response to CM. Data are representative of at least 4 experiments.

In order to statistically evaluate the western blot results, images of the exposed membranes were subjected to further analyses using Quantity One software. Phospho-Akt and Phospho-ERK1/2 levels were quantified between the 2 different passages and the 3 time points. All values are represented as percentage of the calibrator (p5 15m), which was set to 100%.

Analysis of pAKT (Ser 473) was performed in response to CM between p5 and p50 cells (Figure 4.5). pAKT levels were elevated in p50 vs p5 myoblasts at all time points examined, however, statistical significance was not achieved across the 11 repetitions performed.

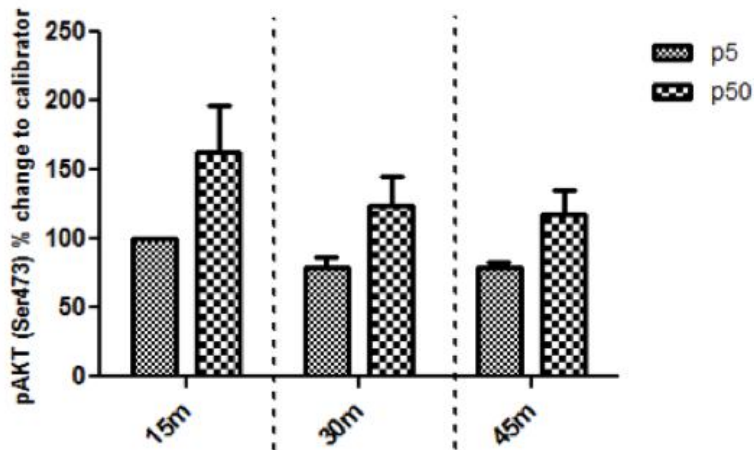


Figure 4.5. Quantification of pAKT levels (p5 vs p50 myoblasts in CM). No significant increases were observed with p50 vs p5 myoblasts in response to CM. Data are representative of 11 experiments. (p-values obtained by unpaired t-test)

Analyses of pERK1/2 data (Figure 4.6) revealed significant increases in ERK1/2 phosphorylation between p50 and p5 cells at 30m ($48.73 \pm 5.42\%$ vs $18.82 \pm 2.28\%$, $p < 0.001$) and at 45m ($38.45 \pm 6\%$ vs $16.37 \pm 3.3\%$, $p < 0.01$). Significant reductions with time were also observed with p5 at 30m vs 15m ($18.82 \pm 2.28\%$ vs 100% , $p < 0.0001$) and at 45m vs 15m ($16.37 \pm 3.3\%$ vs 100% , $p < 0.0001$), confirming the observations made based on the blots above. Reduction with time was observed also with p50 at 30m vs 15m ($48.73 \pm 5.42\%$ vs $134.73 \pm 17.68\%$, $p < 0.0001$) and at 45m vs 15m ($38.45 \pm 6\%$ vs $134.73 \pm 17.68\%$, $p < 0.0001$).

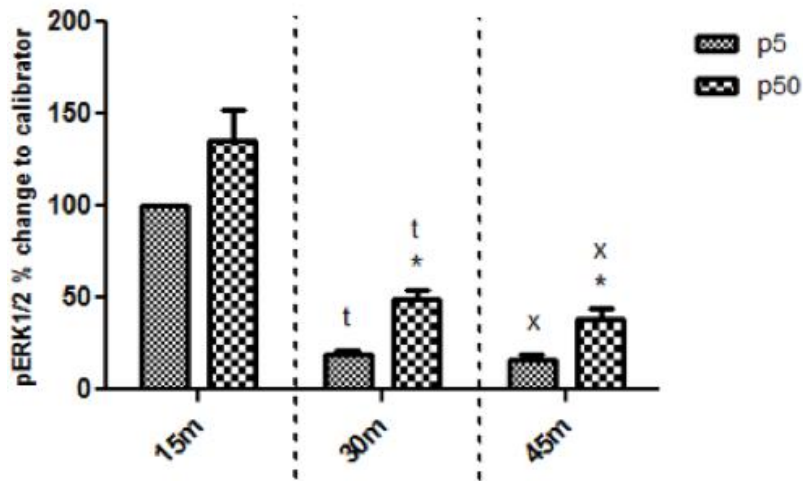


Figure 4.6. Quantification of pERK1/2 levels (p5 vs p50 myoblasts in CM).

Quantification of pERK1/2 levels in response to CM between p5 and p50 myoblasts indicated significant increases with p50 vs p5 at 30m ($p < 0.001$, represented by *) and 45m ($p < 0.01$, represented by *). Reductions with time were observed with both p5 and p50 at 30m vs 15m ($p < 0.0001$ for both p5 and p50, represented by t) and at 45m vs 15m ($p < 0.0001$ for both p5 and p50, represented by x). Data are representative of 11 experiments. (p-values obtained by unpaired t-test)

4.4.3. SERIALY PASSAGED (P50) C2C12 MYOBLASTS DEMONSTRATED HIGHER MIGRATION CAPACITY, AS COMPARED TO LOW PASSAGE (P5) MYOBLASTS, IN RESPONSE TO MEDIA CONDITIONED BY P5 MYOTUBES

Previous studies have investigated the capacity of serially passaged C2C12 cells to differentiate, fuse and form myotube cultures (Sharples *et al.*, 2011), however their ability to migrate was not addressed. It was hypothesized that the ability of myoblasts to migrate would also be altered as a consequence of artificial ageing through serial passaging. Furthermore, elevated levels of pAKT and pERK1/2, as demonstrated in Figure 4.5 and Figure 4.6, suggested that differences in the migration between cells of high and low passage could be expected, based on the data derived from the previous chapter. In order to investigate this, the migration capacity of serially passaged (p50) C2C12 myoblasts was compared to that of low passage myoblasts (p5) in response to media conditioned by p5 myotubes. Wound healing assays were performed to investigate the rate of wound closure between myoblasts of high and low passage (Figure 4.7). Visual observations suggested that p50 cells migrated more rapidly to the centre of the wounds, compared to p5 cells (Figure 4.7A). Although subsequent quantification and analyses of the total number of cells infiltrating the wound as a whole indicated no significant

difference between p5 and p50 cells (Figure 4.7B), significant increases in the percentage of cells in the middle of the wound were however, observed with p50 vs p5 cells (22.5% \pm 1.66 vs 9.75% \pm 2.25, $p < 0.01$), confirming the morphological observations made below and suggesting higher capacity of serially passaged myoblasts to migrate and spread across the wound area (Figure 4.7C).

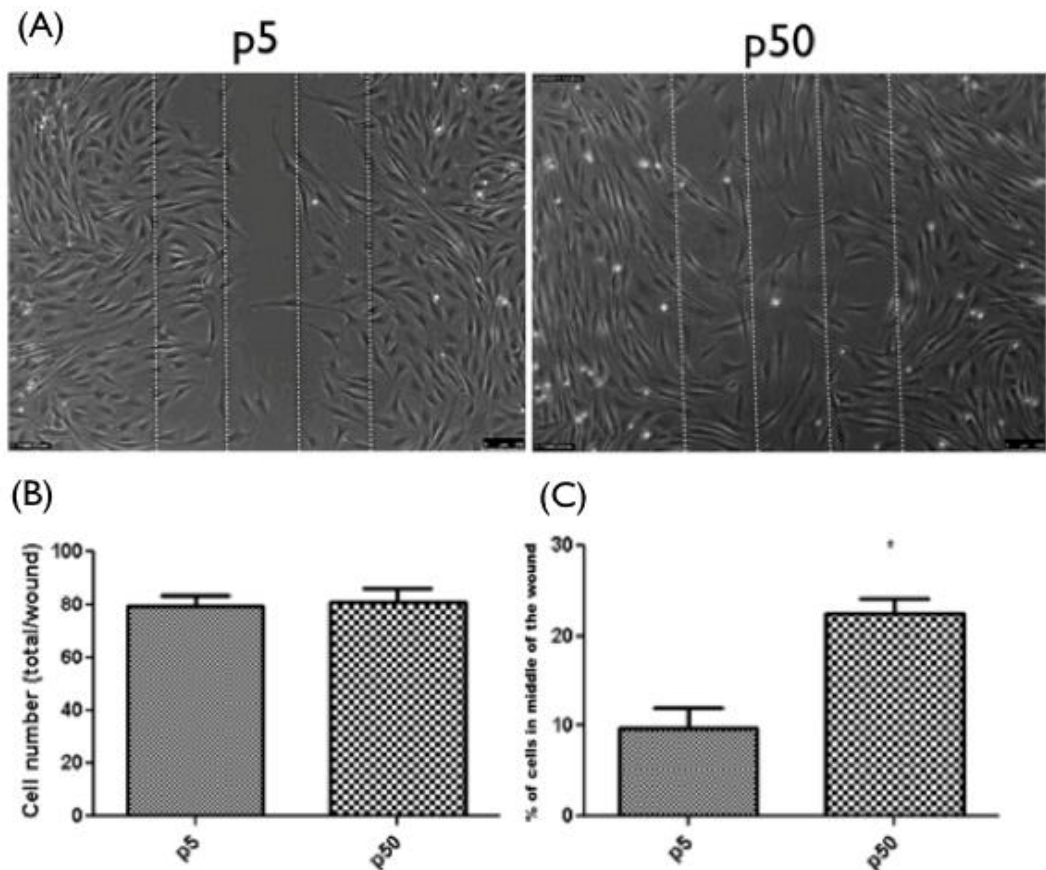


Figure 4.7. Wound healing assay with cell count analysis (p5 vs p50 myoblasts in CM). Wound healing assay comparing the morphological differences between high passage (p50) and low passage (p5) C2C12 myoblasts infiltrating the wound over 20h in response to media conditioned by p5 myotubes (A). Quantification of the total number of cells infiltrating the wound indicated no significant difference between high passage (p50) vs low passage (p5) of myoblasts (B). Quantification of the percentage of cells infiltrating the central area of the wound indicated significant increase with p50 vs p5 ($p < 0.01$, represented by *) (C). Data are representative of 4 experiments performed in duplicate. (p-values obtained by unpaired t-test)

Migration tracking was performed to compare the migration distance of p5 and p50 myoblasts in response to p5-CM (Figure 4.8A). These studies indicated quite

clearly that migration distance over a fixed period of time was enhanced in P50 vs p5 cells. Indeed, further analyses indicated significant increases in migration distance with p50 vs p5 myoblasts (409 \pm 32.6 μ M vs 300 \pm 23.8 μ M, $p < 0.05$, equivalent to 36% increase; Figure 4.8B). Cell death quantification and analyses indicated no differences between p5 and p50 myoblasts (Figure 4.8C).

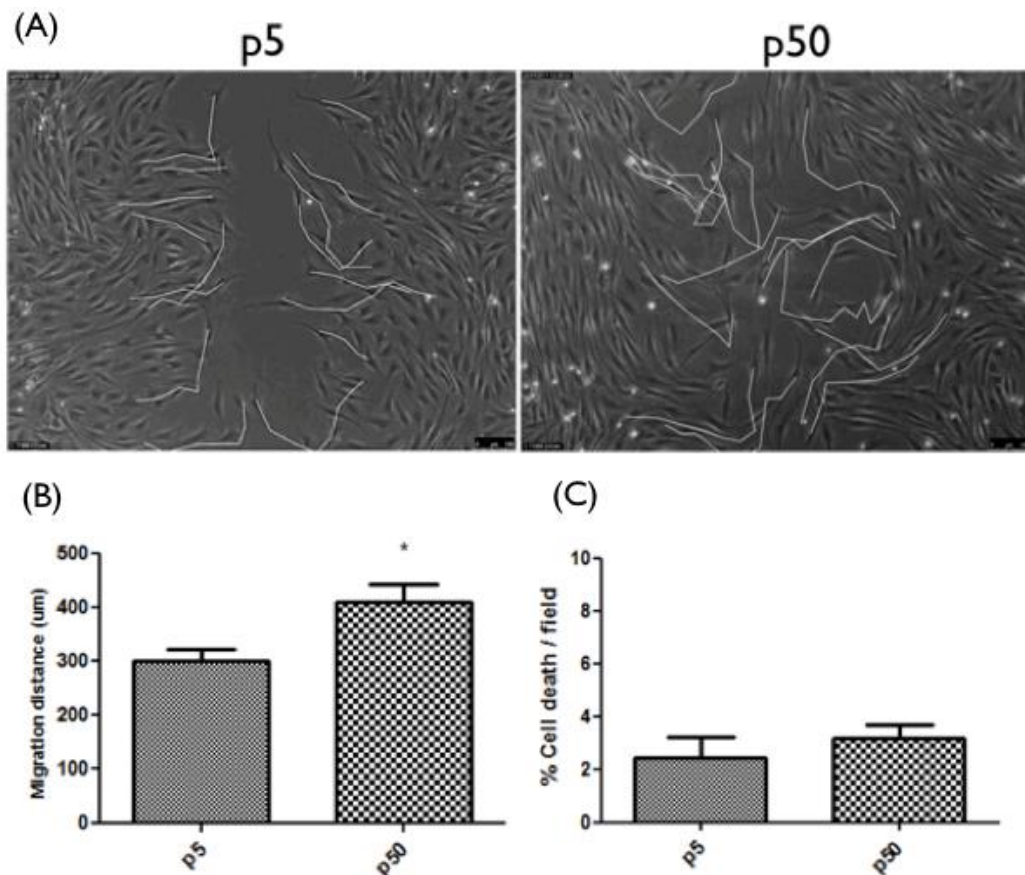


Figure 4.8. Cell tracking and cell death analysis (p5 vs p50 myoblasts in CM). Migration tracking comparing the distance migrated between p5 vs p50 myoblasts (A). Analysis indicated significant increase in the migration distance with p50 vs p5 ($p < 0.05$, represented by *) (B). Analysis of cell death indicated no significant difference between p5 vs p50 myoblasts (C). Data are representative of 5 experiments performed in duplicate. (p-values obtained by unpaired t-test)

4.4.4. MEDIA CONDITIONED BY P50 CELLS ARE LESS POTENT IN INDUCING MIGRATION IN WOUND HEALING ASSAY THAN MEDIA CONDITIONED BY P5 CELLS

Having determined that p50 cells are less potent at morphological, biochemical and associated molecular (reduced myoD and myogenin expression) differentiation than p5 cells and that this was associated with an improved

migration capacity of p50 vs p5 cells in response to media conditioned by p5 myotubes, it was also determined whether there were potential alterations in the secretome of cells following serial passaging. To achieve this end, it was investigated whether media conditioned by serially passaged C2C12 cells would enable improved migration in p5 cells to the same extent as media conditioned by p5 myotubes. Similar to the media conditioning experiments performed in chapter 3, p5 or p50 C2C12 myoblasts were grown to confluence and transferred to DM for 5 days, before being transferred to SF media for a further 3 days. The CM from p5 myotubes was compared to CM from p50 myotubes in migration assays using wounded p5 cells. Morphological assessment suggested that p50 CM when added to p5 cells reduced migration, compared to p5 CM being added to p5 cells (Figure 4.9A). Further analyses of the wound healing assay investigated the total number of cells infiltrating the wound and consolidated the observations, indicating significant decreases with p50 CM vs p5 CM on p5 migration (43 +/- 4 vs 78 +/-9, $p < 0.05$; Figure 4.9B). Furthermore, the percentage of cells in the middle of the wound was also significantly reduced with P50 CM vs P5 CM (12.33% +/-1.76 vs 2% +/-1, $p < 0.01$; Figure 4.9C).

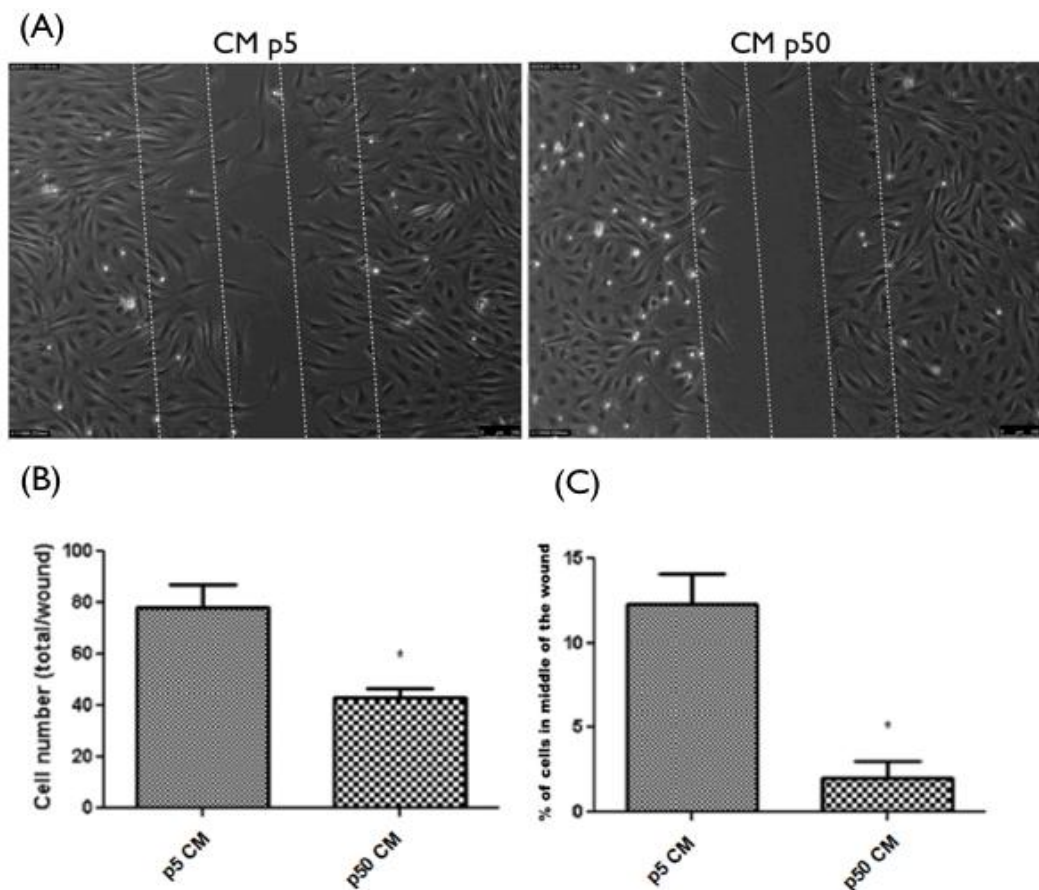


Figure 4.9. Wound healing assay with cell count analysis (p5 myoblasts with p5 CM or p50 CM). Wound healing assay comparing the number of p5 C2C12 myoblasts infiltrating the wound after 20h, in response to media conditioned by p5 cells (p5 CM) and media conditioned by p50 cells (p50 CM) (A). Quantification of the total number of cells infiltrating the wound indicated significant decreases with p50 CM vs p5 CM ($p < 0.05$, represented by *) (B). Quantification of the percentage of cells infiltrating the central area of the wound indicated significant decrease with p50 CM vs p5 CM ($p < 0.01$, represented by *) (C). Data are representative of 3 experiments performed in duplicate. (p-values obtained by paired t-test)

To confirm these observations, cell tracking of p5 cells was performed between P5 CM and P50 CM cultures and data again suggested that migration distance by p5 cells, in the presence of p50 CM was reduced when compared to p5 cells in the presence of p5 CM (Figure 4.10A). Further analyses indicated significant decreases in p5 migration, with p50 vs p5 CM ($224\mu\text{M} \pm 40.7$ vs $342\mu\text{M} \pm 32.1$, $p < 0.05$; Figure 4.10B). Percentage cell death analyses indicated significant increases in p5 dead cell numbers with p50 CM vs p5 CM ($6.43\% \pm 0.78$ vs $1.35\% \pm 0.42$, $p < 0.05$; Figure 4.10C), however, values are still low and would

likely not account for the reduction in migration potential in the presence of p50 CM.

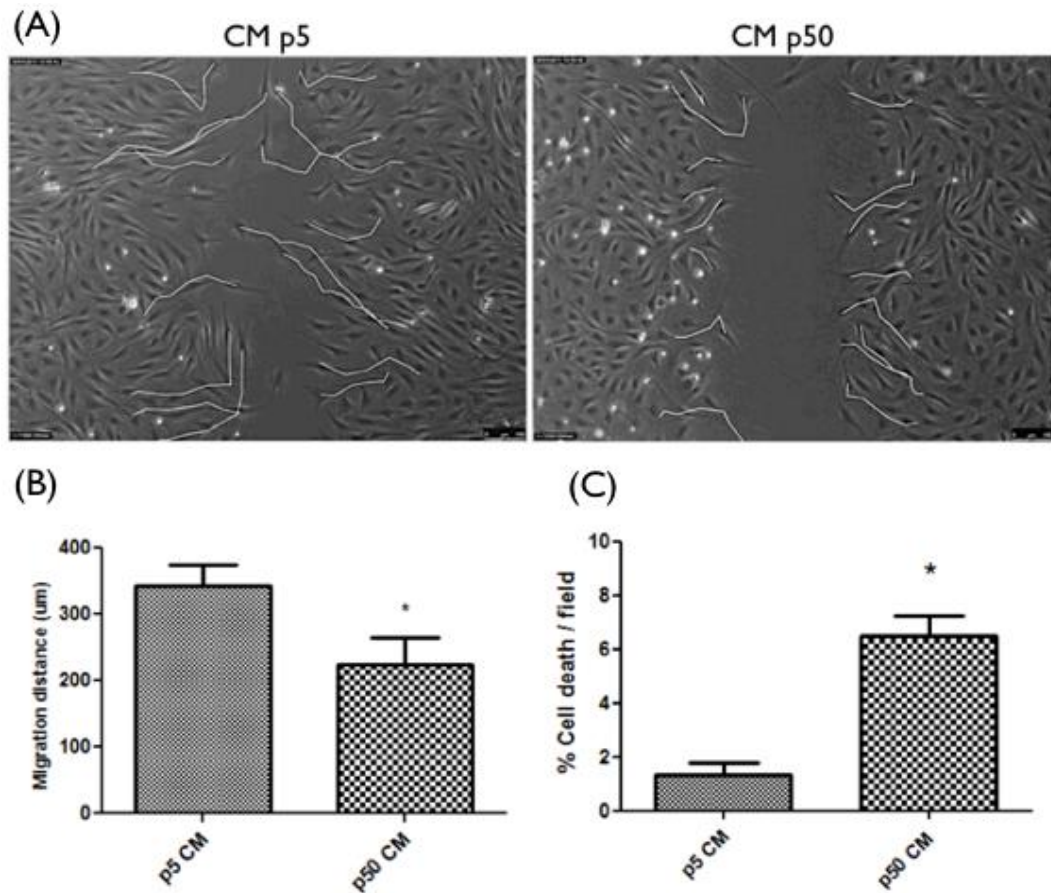


Figure 4.10. Cell tracking and cell death analysis (p5 myoblasts with p5 CM or p50 CM). Cell tracking analysis demonstrating the migration potential of p5 C2C12 myoblasts induced to migrate with p5 CM or p50 CM (A). Analysis indicated significant decreases in cell migration distance with p50 CM vs p5 ($p < 0.05$, represented by *) (B). Cell death analyses indicated significant increases with p50 CM vs p5 CM ($p < 0.05$, represented by *) (C). Data are representative of 3 experiments performed in duplicate. (p-values obtained by paired t-test)

SUMMARY OF MAJOR FINDINGS:

- Serially passaged C2C12 myoblasts (p50) demonstrate impaired capacity to differentiate, as compared to low passage myoblasts (p5), but p50 myoblasts demonstrate enhanced migration capacity in response to myotube conditioned media, as compared to p5 myoblasts.
- Increased migration capacity of p50 vs p5 myoblasts, stimulated by myotube conditioned media, is associated with enhanced PI3K/AKT and MAPK/ERK signalling.
- Media conditioned by p50 myoblasts is less potent in inducing C2C12 cell migration, as compared to media conditioned by p5 myoblasts.

4.5. DISCUSSION

4.5.1. SERIALY PASSAGED C2C12 MYOBLASTS (P50) DEMONSTRATED IMPAIRED CAPACITY TO DIFFERENTIATE COMPARED TO LOW PASSAGE C2C12 MYOBLASTS (P5)

In order to verify the effect of multiple divisions on myoblast differentiation capacity, C2C12 cells were serially passaged until reaching 50 passages (p50) and were compared with low passage of cells (p5). Visually, p50 cells formed much smaller myotubes, as compared to p5 cells. The reduced differentiation of p50 cells was confirmed by the reduced CK activity and reduced gene expression levels of MyoD and Myogenin. These data were confirmed in a recent article, which further demonstrated significant reduction in IGF-1 transcript expression, decreased phosphorylation of Akt and increased phosphorylation of JNK1/2 in myoblasts of high vs low passage (Sharples *et al.*, 2011). Thus, intrinsic changes following multiple divisions were obviously affecting the ability of murine myoblasts to differentiate, even in the absence of proliferative senescence.

4.5.2. SERIALY PASSAGED (P50) C2C12 MYOBLASTS DEMONSTRATED ELEVATED LEVELS OF P-AKT AND P-ERK1/2 IN RESPONSE TO CM, AS COMPARED TO LOW PASSAGE (P5) OF MYOBLASTS, WHICH WAS ASSOCIATED WITH HIGHER MIGRATION CAPABILITY OF P50 VS P5 MYOBLASTS

Having observed reduced differentiation ability of high (p50) vs low (p5) passage of myoblasts, it was investigated whether intrinsic differences between these cells would also lead to changes in their migration ability. Firstly, it was investigated how PI3K/AKT and MAPK/ERK pathways were affected by p5 myotube CM. Surprisingly, elevated levels of pAKT and pERK1/2 in p50 vs p5 myoblasts were found, in response to myotube CM. This was associated with increased migration distance by p50 vs p5 cells, while treatment with LY294002 and UO126 inhibitors, as expected, resulted in visually reduced migration of p50 myoblasts (results not shown), suggesting that PI3K/AKT and MAPK/ERK pathways are required for their migration. Increased levels of pAKT and pERK1/2, accompanied with increased migration of p50 cells were unexpected, considering previous studies by Sharples *et al.*, demonstrating no changes in pERK1/2 levels and decreased levels of pAKT with high vs low passage of C2C12 myoblasts, in response to DM (Sharples *et al.*, 2011), however, the cells

compared in that manuscript were p20 vs p5 myoblasts and were cultured in DM, not CM. Furthermore, myoblasts isolated from old mice and rats were reported to have retarded migration, as compared to myoblasts isolated from young species (Dumke and Lees, 2011, Siriatt *et al.*, 2007). The regulation of signalling pathways, therefore, seems to be altered depending on the external factors, possibly paracrine signals as well as potentially, the numbers of doublings completed. These results, to our knowledge, are the first to report an enhanced migration ability of myoblasts, artificially aged by serial passaging. The observations of reduced differentiation capacity, but increased migration, suggests a potential link between these two processes, which seem to be inversely related - with migration being increased when differentiation capacity is impaired, however, the differential culture conditions must be respected and differentiation studies of p5 vs p50 cells, both in p5 CM should be performed. Another concept worth considering is the potential difference in paracrine signalling of myogenic cells, which can be altered following multiple divisions of these cells.

4.5.3. MEDIA CONDITIONED BY P50 CELLS ARE LESS POTENT IN WOUND HEALING ASSAYS THAN MEDIA CONDITIONED BY P5 CELLS

In chapter 3, it was demonstrated that media conditioned by myotubes is able to enhance myoblast migration, compared to the non-conditioned serum free medium. The question was asked whether there would be differences in the factors secreted by myoblasts of high vs low passage. P50 myoblasts, as previously discussed, mimic to a certain extent the molecular regulation of atrophy seen in elderly skeletal muscle. It was investigated whether media conditioned by p50 myotubes would exert different migratory response in myoblasts, as compared to media conditioned by p5 myotubes. Using a wound healing assay, it was reported that p5 myoblasts indeed have significantly retarded migration when stimulated by media conditioned by p50 myotubes, as compared to media conditioned by p5 myotubes. It must be noted, however, that p50 myotubes were significantly smaller in size, as compared to p5 myotubes. This difference in morphology, therefore, could have contributed to the difference in secreted factors conditioning the media. Further studies would be required to compare between the secretome of both cell passages and reveal whether there are differences in the expression of factors, which might influence the migration of

cells. These initial studies, however, propose interesting avenues for further research. The potential alterations in the secretome and paracrine signalling of aged skeletal muscle or myogenic precursors is an unexplored field and investigating these events in more details could improve our knowledge of muscle regeneration and sarcopenia.

4.5.4. CONCLUSIONS

The effect of serial passaging on the behavior of C2C12 myoblasts was investigated. It was confirmed that high passages of myoblasts have impaired potential to differentiate and to fuse into multinucleated myotubes, as seen by morphological examination, as well as by reduced levels of CK activity and lowered expression of MyoD and Myogenin genes. However, high passage myoblasts demonstrated elevated levels of pAKT and pERK1/2, in response to p5 myotube CM, as compared to low passage of myoblasts. This was associated with increased migration distance, as examined by wound healing assay. It was also proposed that there are differences in the factors secreted by high vs low passage of myoblasts. Media conditioned by p50 myotubes induced significantly less migration, as examined by wound healing assay with p5 myoblasts, compared to media conditioned by p5 myotubes. These initial studies suggest intrinsic differences in myoblasts undergoing multiple divisions, even in the absence of senescence and propose interesting avenues for future research into the field of molecular regulation of muscle ageing, migration and sarcopenia.

4.5.5. THESIS DIRECTIONS

P5 and p50 myoblasts demonstrated significant differences in their migration behavior. PI3K/AKT and MAPK/ERK pathways were activated more strongly with p50 cells, as compared to p5 cells, which was associated with increased migration with the serially passaged myoblasts. In chapter 3, it was also demonstrated that PI3K/AKT and MAPK/ERK pathways were required for myoblast migration in response to myotube CM, thus further supporting their importance for the process. Here, it was also demonstrated that media conditioned by p50 C2C12 cells was less potent in inducing p5 migration, as compared to media conditioned by p5 cells. In order to further investigate in sufficient detail the expression profile and secreted factors between myogenic cells of low and

high passage, various approaches were required, including PCR arrays to investigate the expression of a list of selected genes related to migration, or mass spectrometry, which would reveal the secreted proteins into the supernatant. Due to time and cost constraints, it was decided that these studies should be the topic for future projects and were unfortunately beyond the scope of this thesis.

As a consequence and considering the results obtained for the link between the PI3K/AKT and MAPK/ERK signalling pathways and myoblast migration, it was decided that the focus of the next chapter of the thesis would be given to studies investigating the importance of signalling pathways to myoblast migration. P5 myoblasts, with p5 myotube CM to stimulate their migration, were therefore further used as a model to investigate how modulation of signalling pathways by different inhibitors would affect the migration of myoblasts in response to signals released from myogenic cells.

CHAPTER 5

5. MAPK/ERK AND PI3K/AKT PATHWAYS ARE REQUIRED FOR BPV(HOPIC)-INDUCED C2C12 MYOBLAST MIGRATION. REQUIREMENT OF FAK PATHWAY FOR MYOBLAST MIGRATION

5.1. INTRODUCTION

In chapter 3, it was demonstrated that serum free media conditioned by myotubes (CM) was able to enhance myoblast migration, resulting in the activation of PI3K/AKT and MAPK/ERK pathways and that inhibition of these pathways results in decreased migration. Activation of these pathways, in response to myotube CM, was also associated with increased migration of p50 vs p5 cells, incubated with p5 CM, as demonstrated in chapter 4. Various studies have linked cell migration to PI3K and MAPK pathways. Pharmacological inhibition of MAPK/ERK pathway by PD98059 or UO126 has been demonstrated to reduce cell migration, not only here, but also in various other studies and cell types (Huang *et al.*, 2004b, Lind *et al.*, 2006, Teranishi *et al.*, 2009, Webb *et al.*, 2000). Furthermore, dominant negative ERK and MEK1 are demonstrated to inhibit cell migration, while active MEK1 can promote it (Jo *et al.*, 2002, Lai *et al.*, 2001, Webb *et al.*, 2000). PI3K has been implicated in regulating cell migration and polarity (Cain and Ridley, 2009, Stephens *et al.*, 2002). PI3K involvement in migration has been investigated in various cell types and has been demonstrated to be required for this process (Goncharova *et al.*, 2002a, Hannigan *et al.*, 2002, Irani *et al.*, 2002, Kusch *et al.*, 2000, Vanhaesebroeck *et al.*, 1999, Ye *et al.*, 2008). Few articles, however, have investigated the intracellular regulation of myoblast migration. Kawamura *et al.* have demonstrated that PI3K activity is necessary for the HGF-induced lamellipodial formation in C2C12 myoblasts and for their chemotactic migration (Kawamura *et al.*, 2004). This is supported by a recent study, showing that PI3K-inhibitors reduce the rate of cell migration (Kim *et al.*, 2011). Previous reports from our group have demonstrated that migration of C2 myoblasts, triggered by 20% serum, is reduced by treatments with PI3K and MEK inhibitors, respectively LY294002 and PD98059 (Al-Shanti *et al.*, 2011). Ranzato *et al.* have also demonstrated a decreased myoblast migration, in both wound healing and transwell inserts, in response to platelet lysate, after treatment with PI3K inhibitor wortmannin, but not with MEK inhibitor PD98059 (Ranzato *et al.*, 2009). Others, however, have suggested that PI3K and ERK pathways may not be responsible for chemotaxis in C2C12 cells, as inhibitors of PI3K and MEK

did not affect the chemotactic migration of C2C12 cells toward bFGF, HGF and IGF-1 (Suzuki *et al.*, 2000). Leloup *et al.* have shown that ERK/MAPK signalling pathway is required for IGF-I, TGF- β 1 and insulin mediated migration, as inhibition of this pathway by PD98059 resulted in reduced migration (Leloup *et al.*, 2007). However, as opposed to other articles, they found no inhibition of migration after inhibiting the PI3K/AKT pathways with LY294002. Thus, results on the PI3K and MAPK pathways regulation of myogenic migration have not been entirely unanimous. It seems that regulation of myoblast migration by these two pathways may depend on the extracellular environment, the trigger and the type of cell movement. Furthermore, it is not entirely clear whether crosstalk or any redundancy between these pathways may exist in regulating myoblast migration, as has been demonstrated for smooth muscle cells (Campbell *et al.*, 2004). Revealing in more details, the involvement of PI3K and MAPK pathways in myoblast migration, might not only contribute to our understanding of muscle myogenesis, but it could also be applied in proposed treatments for muscular dystrophies. Limited spreading/migration, along with low survival of transplanted cells and immune rejection, has been known to be one of the limiting factors in proposed therapies of Duchenne muscular dystrophy (Fan *et al.*, 1996, Gussoni *et al.*, 1997, Moens *et al.*, 1996, Skuk *et al.*, 2004, Smythe *et al.*, 2001). Although, following recent publications it remains debatable whether migration is indeed a major limiting factor (Lafreniere *et al.*, 2009, Skuk *et al.*, 2011), enhancing it may still propose a possibility for improving the results from proposed therapies for DMD and, therefore, further research in this area is needed. Investigating myogenic cell migration is not only important for proposed DMD therapies, but, migration being important for repair, it may have implications post surgery and also vast implications for athletes. Thus, finding factors to improve the migration of myoblasts might be of particular interest. Such factors would ideally improve migration without affecting the capacity of myoblasts to differentiate.

The negative effects of PTEN on cell migration have been widely investigated, due to its mutations in cancer, and studies have demonstrated that its downregulation results in enhanced migration of a variety of cell types (Dasari *et al.*, 2010, Liliental *et al.*, 2000, Tamura *et al.*, 1998). PTEN is known to regulate cell migration by its lipid phosphatase activity - catalysing the dephosphorylation of PIP3 to PIP2, thus inhibiting the PI3K/AKT pathway - and also via its protein phosphatase activity and its C2 domain (Dey *et al.*, 2008, Leslie *et al.*, 2007,

Raftopoulou *et al.*, 2004, Zhao, 2007). MAPK/ERK and FAK pathways are also reported to be regulated by PTEN (Cully *et al.*, 2006, Gu *et al.*, 1998, Gu *et al.*, 1999, Yamada and Araki, 2001). BpV compounds, acting as PTEN inhibitors, have been demonstrated to enhance cell migration in epithelial cells (Lai *et al.*, 2007, Mihai *et al.*, 2012, Zhao, 2007). Castaldi *et al.*, to our knowledge the only publication investigating the effects of BpV compounds on skeletal muscle myoblasts, have demonstrated that C2C12 cells treated with high concentrations (10 μ M) of BpV, were able to reach muscle tissue via the circulation and contribute to muscle repair with higher efficiency compared to untreated cells (Castaldi *et al.*, 2007). They also demonstrated that high concentrations of BpV reduced myoblast differentiation, although in a reversible manner. Its effect on myoblast migration, however, was not investigated. Given the effects of BpV compounds on epithelial cells, the data from PTEN inhibition in other cell types and the link between PTEN and PI3K/AKT and MAPK/ERK signalling, it was proposed that using lower concentrations of BpV compounds may be an attractive approach for enhancing myoblast migration thus providing a tool for investigating the pathways regulating this process.

5.2. AIMS, OBJECTIVES AND HYPOTHESIS

The main aim was to reveal the roles of the PI3K signalling pathways in the regulation of myoblast migration. The objectives were to investigate how BpV compounds, in particular BpV(Hopic), at different concentrations would affect the migration of C2C12 myoblasts. Its effect on differentiation would also be examined. PTEN has been known to affect other pathways, such as FAK/Src (Gu *et al.*, 1998, Gu *et al.*, 1999), and therefore the potential involvement of the FAK pathway in regulating myoblast migration would also be investigated. Further objectives were also to reveal whether MAPK/ERK and PI3K/AKT pathways would be upregulated by BpV(Hopic) and whether their inhibition by LY294002 and UO126 would still lead to reduced migration, even if the other pathway remained activated. It was hypothesised that BpV(Hopic) would affect the migration of myoblasts and that PI3K, MAPK and FAK pathways could demonstrate certain levels of redundancy in regulating C2C12 cells migration.

5.3. METHODS

5.3.1. CELL CULTURE

C2C12 myoblasts were cultured in a humidified 5% CO₂ atmosphere at 37°C. Cells were grown in the presence of GM in T75 flasks until confluent and split into multidish plates for experiments. In order to initiate differentiation, C2C12 cells were grown in 6 well plates until confluency was achieved, monolayers were washed with PBS and differentiation media (DM) was added to the cell monolayers. When differentiation experiments were performed for 5days, DM was changed with a fresh media at d3.

5.3.2. CONDITIONED MEDIA GENERATION

C2C12 myoblasts in 6 well plates were triggered to differentiate into myotubes, in the presence of DM. Conditioned media was generated, as described in section 3.3.2.

5.3.3. CELL TREATMENTS AND RECONSTITUTION OF INHIBITORS

All inhibitors were purchased from Merck-Calbiochem (Darmstadt, Germany). Inhibitors were diluted, according to manufacturer's instructions, in either DMSO or H₂O and stored at -20°C. FAK II inhibitor PF-228 was stored at 4°C. All inhibitors were kept in mM concentration stocks which were diluted to working concentrations in appropriate DMEM media before cell treatments. For cell treatments, where appropriate, equivalent concentrations of DMSO or H₂O were added to control wells.

5.3.4. WOUND HEALING ASSAY AND LIVE IMAGEING

Cells were grown in pre-gelatinised 12 well plates in GM until ~80-90% confluent. Cell monolayers were washed 3 times with PBS and DMEM 0.1% FBS media (quiescent media = QM) was added and incubated for 20h with the cells. In the last 3 hours of incubation with QM, 10µg/ml Mitomycin-C (Sigma-Aldrich) was added, in order to block proliferation, and monolayers were wounded with a sterile pipette tip, generating a wound of approximately 600µm in size. Wound healing with live imaging microscopy is described in section 2.2.2.1.

5.3.5. ANALYSIS OF CELL MIGRATION

Cell migration was analysed with Keynote'09 software version 5.1.1. (Apple Inc.) and ImageJ v1.45i software, as described in section 3.4.2.

5.3.6. CELL DEATH QUANTIFICATIONS BY LIVE IMAGEING

The numbers of dying cells were counted frame by frame in each area for the duration of the movie, as described in section 2.2.4.

5.3.7. WESTERN BLOTS

Sample collection and preparation for SDS-PAGE was performed as described in section 2.2.8.1. Gel electrophoresis, membrane transfer, blocking and detection steps were performed, as described in sections 2.2.8.2-2.2.8.5. Primary AKTpan, pAKT, b-actin, pFAK, FAKpan and ERKpan rabbit IgG antibodies were purchased from New England Biolabs (Hertfordshire, UK) and were incubated with membranes overnight at RT in a 1:1000 dilution in 5% BSA/TBST. Primary pERK1/2 rabbit antibody was purchased from Promega and was incubated with membranes overnight at RT at a 1:5000 dilution in 0.1% BSA/TBST. Secondary Goat Anti-rabbit HRP-conjugated antibodies were purchased from MP Biomedicals (United Kingdom) and were incubated with membranes for 1h at RT 1:5000 concentration, diluted in blocking solution. Membranes were blocked for 1h at RT in 5% non-fat dry milk/TBST (for antibodies purchased from New England Biolabs) or in 1% BSA/TBST for pERK1/2. Primary py20 mouse monoclonal antibody was purchased from Santa Cruz and was incubated with membranes overnight at RT at a 1:500 dilution in TBST. Secondary anti-mouse antibody, raised in Goat, was purchased from Millipore and diluted in blocking solution (0.25% gelatin/TBST).

5.3.8. RNA ISOLATIONS AND REAL-TIME PCR

RNA extraction and Real-time PCR methods were performed as described in sections 2.2.9 and 2.2.10, respectively. Both SYBR® Green detection and TaqMan® detection were performed. The following predesigned primer sets were

ordered from Quiagen and were used with the SYBR-Green detection method: Polr2b (QT00154602), MyoD (QT00101983) and Myogenin (QT00112378). The following predesigned primer sets were ordered from Applied Biosystems and were used with the TaqMan® detection method: Polr2b (Mm00464214_m1), MyoD (mm00440387_m1), Myogenin (mm00446194_m1).

5.3.9. CREATINE KINASE (CK) ASSAY

Samples for CK assay were prepared by adding 150µL per well (for 6 well plate) of Tris Mes Triton (TMT buffer; composed of: 0.05M Tris/Mes and 1% Triton-X100). Assay was performed, as described in section 2.2.7.2.

5.3.10. FLOW CYTOMETRY

For investigating cell cycle, cells were collected 20hrs post treatment. Sample preparation and Propidium iodide method for FACS are described in section 2.2.11.

5.3.11. STATISTICAL ANALYSES

Statistical analyses and significance of data were determined using GraphPad Prism version 5.00 for Mac OS X, GraphPad Software, San Diego California USA, www.graphpad.com. Statistical significance for interactions between two paired groups was determined with a Paired t-test, while unpaired t-test was used for unpaired groups. Statistical significance for interactions between more than two groups was determined with a one-way ANOVA, or with a one-way repeated measures ANOVA, when matched observations were investigated. When more than one factor was present, two-way ANOVA was performed to investigate for significances of factors or interactions, or two-way repeated measures (mixed model) ANOVA, when matched observations were investigated. When significances of factors were indicated by two-way ANOVA, these were followed up by examining the statistical significance for interactions between more than two groups within the factor with a One-way ANOVA with Bonferroni post-hoc analysis, or with a t-test for examination between two groups. All results are presented as mean +/- standard error of the mean (SEM). All values below $p < 0.05$ were considered as significant.

5.4 RESULTS

5.4.1. DIFFERENTIATION OF C2C12 MYOBLASTS IS SIGNIFICANTLY AFFECTED BY 10 μ M, BUT NOT BY 1 μ M BPV(HOPIC)

First, it was investigated whether the differentiation of myoblasts was affected by Bpv(Hopic) treatment, as suggested by other studies demonstrating inhibition of C2C12 differentiation using 10 μ M BpV (Castaldi *et al.*, 2007). Three different concentrations of Bpv(Hopic), 1 μ M, 2 μ M and 10 μ M in DM were incubated for 3 days with confluent myoblasts. Phase-contrast microscopy was used to visually estimate the fusion of myoblasts into multinucleated myotubes (Figure 5.1). As seen in the figure, myoblasts incubated in control DM for 3 days, had comparable morphology to cells incubated with DM+1 μ M Bpv(Hopic) and DM+2 μ M Bpv(Hopic), with all of these treatments inducing differentiation and visible myotube formation. By contrast, DM+10 μ M Bpv(Hopic), inhibited the formation of myotubes.

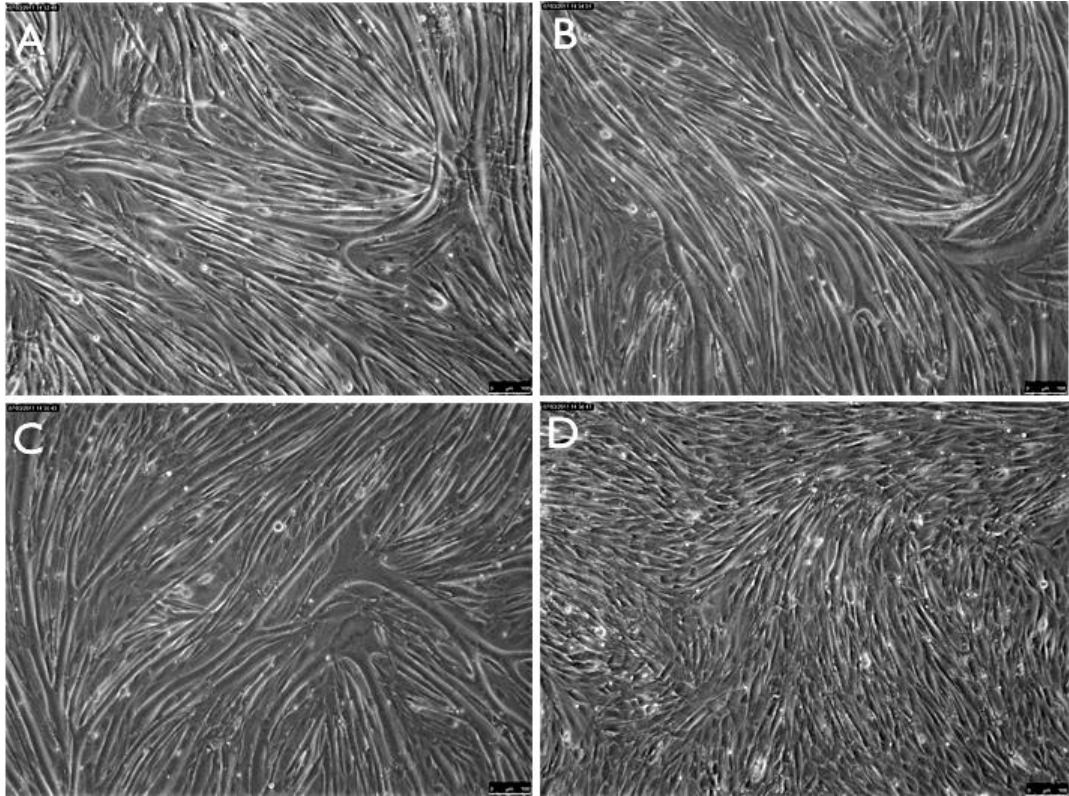


Figure 5.1. Effects of different concentrations of BpV(Hopic) on myotube formation. Phase-contrast microscopy images comparing the effects of 3 days incubation with DM (A), DM+1 μ M Bpv(Hopic) (B), DM+2 μ M Bpv(Hopic) (C) and DM+10 μ M Bpv(Hopic) (D) on the fusion of myoblasts into multinucleated myotubes. DM, DM+1 μ M Bpv(Hopic) and DM+2 μ M Bpv(Hopic) do not demonstrate visual differences in morphology, while DM+10 μ M Bpv(Hopic) completely blocked fusion/differentiation. Data are representative of 5 experiments performed in duplicate.

In order to verify the phase-contrast microscopy data, CK assays were performed, measuring the activity of the CK enzyme (a marker for myoblast differentiation *in vitro*) at 72 hrs following the 4 different treatment regimes (Figure 5.2). Analyses demonstrated significant reductions in CK activity and hence myotube formation, with DM+10 μ M Bpv(Hopic) vs DM (352.6 \pm 15.17 vs 791.8 \pm 37.12, $p < 0.001$, equivalent to 2.25 fold decrease) and a small, but statistically significant decrease with CM+2 μ M Bpv(Hopic) vs DM (712 \pm 33.68 vs 791.8 \pm 37.12, $p < 0.05$, equivalent to 1.11 fold decrease).

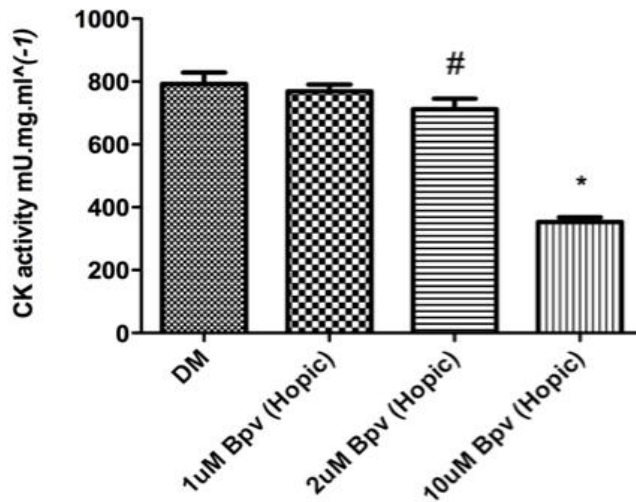


Figure 5.2. CK assay (DM with different concentrations of BpV(Hopic)). CK assay, measuring the CK activity after treatment of C2C12 cells for 3 days with DM, DM+1µM Bpv(Hopic), DM+2µM Bpv(Hopic) and DM+10µM Bpv(Hopic), indicated significant reductions with DM+10µM Bpv(Hopic) vs DM ($p < 0.001$, represented by *) and with DM+2µM Bpv(Hopic) vs DM ($p < 0.05$, represented by #). Data are representative of 5 experiments performed in duplicate. (p-values obtained by One-way repeated measures ANOVA)

To investigate the differentiation inhibitory effect of Bpv(Hopic) at a transcriptional level, RT-PCRs were performed to examine the expression of 2 key genes involved in regulating myogenesis, myoD and myogenin (Figure 5.3). Expression levels of myoD and myogenin were examined 24h post addition of DM, DM+1µM Bpv(Hopic), DM+2µM Bpv(Hopic) or DM+10µM Bpv(Hopic). As seen in Figure 5.3(A), significant reductions in MyoD expression levels were detected with DM+10µM Bpv(Hopic) vs DM (0.44 ± 0.08 vs 1 , $p < 0.0001$, equivalent to 2.27 fold decrease), vs DM+1µM Bpv(Hopic) (0.44 ± 0.08 vs 0.92 ± 0.07 , $p < 0.0001$, equivalent to 2.09 fold decrease) and vs DM+2µM Bpv(Hopic) (0.44 ± 0.08 vs 0.87 ± 0.08 , $p < 0.0001$, equivalent to 1.98 fold decrease). No significant decreases vs DM were observed with DM+1µM Bpv(Hopic) or DM+2µM Bpv(Hopic), confirming the morphological observations. Analyses of myogenin expression levels (Figure 5.3B) indicated a significant decrease with DM+10µM Bpv(Hopic) vs DM (0.14 ± 0.02 vs 1 , equivalent to 7.14 fold decrease, $p < 0.0001$), vs DM+1µM Bpv(Hopic), (0.14 ± 0.02 vs 0.84 ± 0.06 , equivalent to 6 fold decrease, $p < 0.0001$) and vs DM+2µM Bpv(Hopic) (0.14 ± 0.02 vs 0.72 ± 0.08 , equivalent to 5.14 fold decrease, $p < 0.0001$). Decreases were also detected with DM+2µM Bpv(Hopic) vs DM

(0.72 +/-0.08 vs 1, equivalent to 1.39 fold decrease, $p < 0.01$), substantiating the biochemical analyses above.

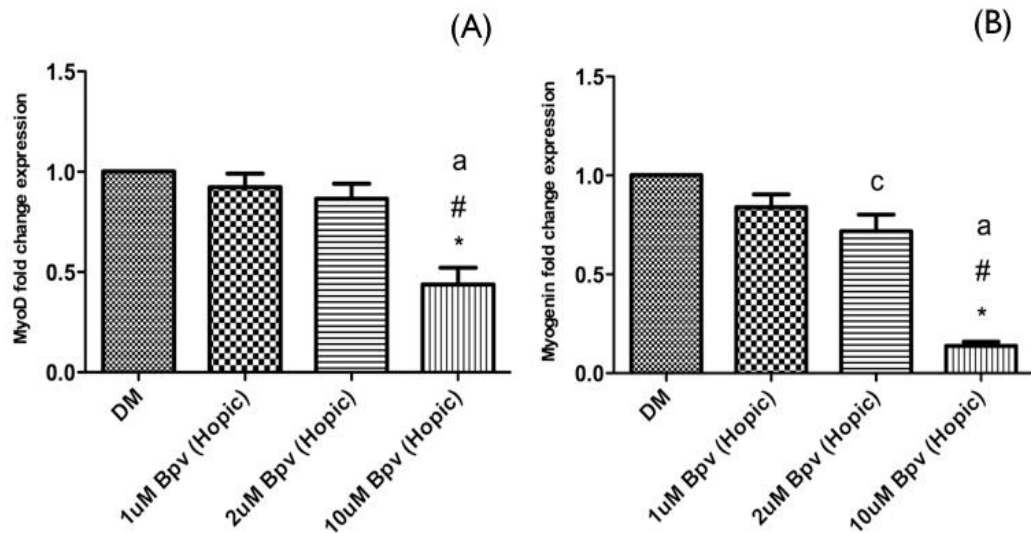


Figure 5.3. RT-PCR analyses of MyoD and Myogenin mRNA expression levels following different concentrations of Bpv(Hopic). Myoblasts were incubated for 24h with DM, DM+1μM Bpv(Hopic), DM+2μM Bpv(Hopic) and DM+10μM Bpv(Hopic) before RNA was collected. All values are represented as fold change to the calibrator (DM d1), which is set to 1 (mean Ct value (MyoD)=25.56 +/- 1.65; mean Ct value(Myogenin)=19.56 +/-0.39). Analysis of MyoD expression levels indicated significant decreases with DM+10μM Bpv(Hopic) vs DM ($p < 0.0001$, represented by *), vs DM+1μM Bpv(Hopic) ($p < 0.0001$, represented by #) and vs DM+2μM Bpv(Hopic) ($p < 0.0001$, represented by a) (A). Analyses of Myogenin expression levels indicate significant decreases with DM+10μM Bpv(Hopic) vs DM ($p < 0.0001$, represented by *), vs DM+1μM Bpv(Hopic) ($p < 0.0001$, represented by #), vs DM+2μM Bpv(Hopic) ($p < 0.0001$, represented by a). and also with DM+2μM Bpv(Hopic) vs DM ($p < 0.01$, represented by c) (B). Data are representative of 5 experiments performed in duplicate. (p-values obtained by One-way repeated measures ANOVA)

5.4.2. INCREASED PERCENTAGE OF C2C12 MYOBLASTS IN S/G2-PHASE OF THE CELL CYCLE AFTER TREATMENT WITH 10 μM BPV(HOPIC)

Previous reports indicated that C2C12 cells treated with high concentrations of BpV displayed a sustained percentage of cells in the s-phase of the cell cycle compared with controls (Castaldi *et al.*, 2007). As permanent withdrawal from the

cell cycle is necessary for progression to myogenic differentiation, an increased percentage of cells in the S/G2-phase of the cell cycle may underpin the inhibited differentiation in the presence of sustained exposure to high dose Bpv(Hopic). To verify this hypothesis, myoblasts were treated and isolated for FLOW cytometric analyses following incubation for 20h in DM or DM+10 μ M Bpv(Hopic) (Figure 5.4). Data indicated significant increases in the percentage of cells in the S/G2-phase with DM+10 μ M Bpv(Hopic) vs DM (42.76 \pm 1.92% vs 17.08 \pm 3.19%, $p < 0.01$), substantiating the theory that continued cell cycle progression may underpin inhibition of differentiation in the presence of high dose Bpv(Hopic).

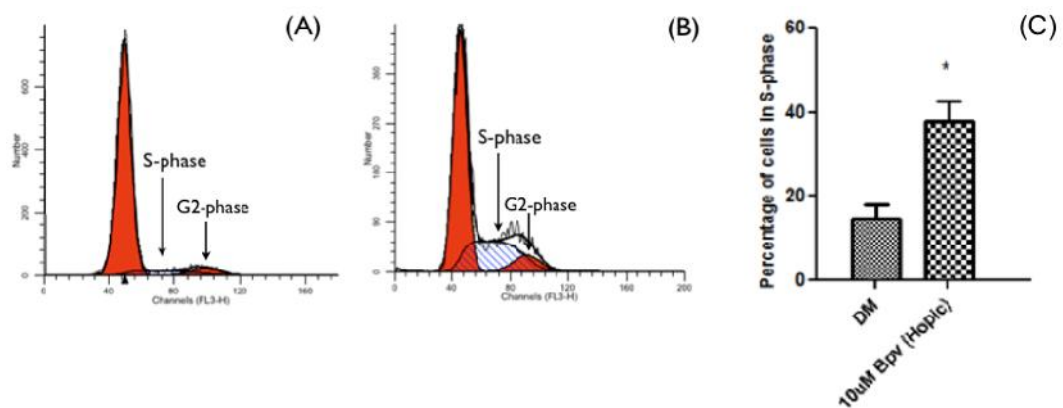


Figure 5.4. Flow cytometric analysis (DM vs DM+10 μ M BpV(Hopic)). Examination of the percentage of C2C12 myoblasts in the S/G2-phase of the cell cycle using FLOW cytometric analyses, following incubation of the cells for 20h with DM (A) or DM+10 μ M Bpv (B). Analyses of the percentage of cells in S-phase of the cell cycle (C) indicate significant increases with DM+10 μ M Bpv(Hopic) vs DM ($p < 0.01$, represented by *). Data are representative of 4 experiments performed in duplicate. (p -values obtained by paired t-test)

5.4.3. THE PHOSPHO-TYROSINE PHOSPHATASE INHIBITOR BPV(HOPIC) IS ABLE TO FURTHER ACTIVATE PI3K/AKT AND MAPK/ERK SIGNALLING PATHWAYS AND TO INCREASE MYOBLAST MIGRATION IN RESPONSE TO CM

It was demonstrated that PI3K/AKT and MAPK/ERK pathways are activated in response to CM and was associated with migration; furthermore, it was demonstrated that their silencing by LY294002 and UO126 resulted in reductions of myoblast migration (Chapter 3.5.7). The action of Bpv(Hopic), reported to act as a PTEN inhibitor (at lower concentrations) and thus suggested to activate PI3K and MAPK pathways in different cell types, was further explored in our model. It

was initially investigated whether Bpv(Hopic) could activate PI3K/AKT and MAPK/ERK pathways in C2C12 myoblasts and whether myoblast migration would subsequently be affected.

Three different concentrations of Bpv(Hopic) were again initially examined - 1 μ M, 2 μ M and 10 μ M. Western blots were performed using anti-phospho-tyrosine antibody (py20) in an attempt to evaluate the specificity of these BpV(Hopic) concentrations. As shown on Figure 5.5, 10 μ M Bpv (Hopic) is highly non-specific, generically phosphorylating multiple tyrosine residues. Specificity of Bpv(Hopic) increased with lowering the concentration, with 1 μ M appearing to be the most specific over time and when compared to CM conditions.

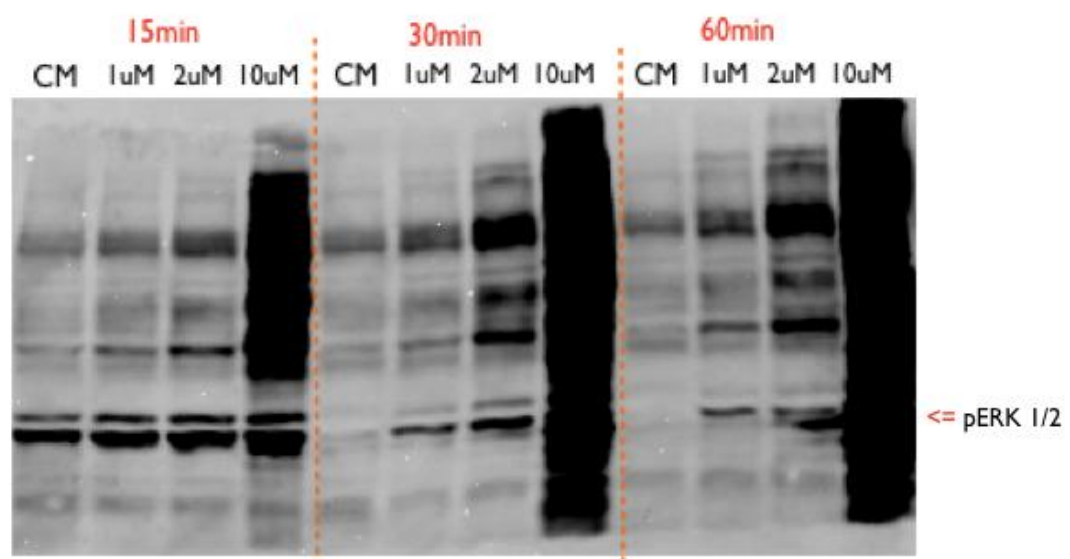


Figure 5.5. Anti-phospho-tyrosine Western blot analyses (py20 antibody) tested the specificity of different concentrations of Bpv(Hopic). As shown, lower concentrations of Bpv(Hopic) are better in maintaining specificity of activity, with 1 μ M being the most specific of the 3 concentrations tested and 10 μ M showing no specificity with regard to tyrosine phosphorylation. Data are representative of 3 experiments.

Western blots were subsequently performed to investigate the effect of 1 μ M, 2 μ M and 10 μ M BpV(Hopic) on activation of PI3K/AKT and MAPK/ERK pathways (Figure 5.6) at 4 different time points (15m, 30m, 45m and 60m) after treatment. Both p-AKT and pERK1/2 appeared to be increased with Bpv(Hopic) vs CM, in a concentration and for higher dose BpV(Hopic), in temporal dependent manner.

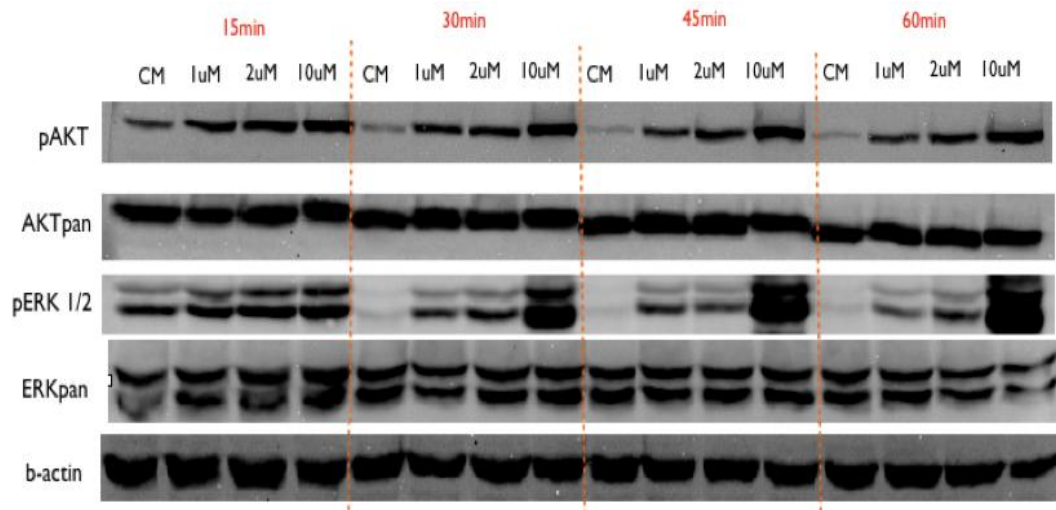


Figure 5.6. Western blot analysis (CM with different concentrations of Bpv(Hopic)). Western blots investigating the effect of 3 different concentrations of Bpv(Hopic) (1 μ M, 2 μ M and 10 μ M) + CM vs CM on the protein and phosphorylation levels of members of the PI3K/AKT and MAPK/ERK pathways over 15m,30m,45m and 60m after cell treatment. Data are representative of 4 experiments.

Further quantification and analyses of the levels of p-AKT and pERK1/2 vs pan-specific controls were performed on 1 μ M and 2 μ M concentrations of Bpv (Hopic). Given the lack of specificity of the 10 μ M concentration (detailed in Figure 5.5 above), for the purposes of these studies, this concentration was included as a positive control only and was not further analysed.

Quantitative analyses of pAKT (Ser 473) activation in response to CM, CM+1 μ M Bpv(Hopic) and CM+2 μ M Bpv(Hopic) were performed (Figure 5.7). pAKT phosphorylation was increased with CM+2 μ M Bpv(Hopic) vs CM at 15m (264.5 \pm 45% vs 100%, $p < 0.001$), 30m (201.25 \pm 27.68% vs 28.5 \pm 3.97%, $p < 0.0001$), 45m (132.5 \pm 18.46% vs 18 \pm 1.22%, $p < 0.01$) and 60m (146 \pm 20.26% vs 23.75 \pm 5.19%, $p < 0.0001$). Significant increases were also evident also with CM+1 μ M Bpv(Hopic) vs CM at 15m (186.5 \pm 14.63% vs 100%, $p < 0.05$), 30m (161.25 \pm 16.78% vs 28.5 \pm 3.97%, $p < 0.001$), 45m (102.25 \pm 7.86% vs 18 \pm 1.22%, $p < 0.01$) and 60m (90.75 \pm 14.27% vs 23.75 \pm 5.19%, $p < 0.01$). Significant increases were also found with CM+2 μ M Bpv(Hopic) vs CM+1 μ M Bpv(Hopic) at 15m (264.5 \pm 45% vs 186.5 \pm 14.63%, $p < 0.01$), at 30m (201.25 \pm 27.68% vs 161.25 \pm 16.78%, $p < 0.05$) and at 60m (146 \pm 20.26% vs 90.75 \pm 14.27%, $p < 0.01$). Reductions of pAKT phosphorylation with time were indicated with CM at 30m vs 15m (28.5 \pm 3.97% vs 100%, $p < 0.0001$), 45m vs 15m (18 \pm 1.22% vs 100%, $p < 0.0001$) and 60m vs 15m (23.75 \pm 5.19%

vs 100%, $p < 0.0001$). Similarly, reductions with time were also evident with CM+1 μ M Bpv(Hopic) at 30m vs 15m (161.25 \pm 16.78% vs 186.5 \pm 14.63%, $p < 0.05$), 45m vs 15m (102.25 \pm 7.86% vs 186.5 \pm 14.63%, $p < 0.001$) and 60m vs 15m (90.75 \pm 14.27% vs 186.5 \pm 14.63%, $p < 0.001$). Reductions with time were also observed with CM+1 μ M Bpv(Hopic) at 45m vs 30m (102.25 \pm 7.86% vs 161.25 \pm 16.78%, $p < 0.01$) and 60m vs 30m (90.75 \pm 14.27% vs 161.25 \pm 16.78%, $p < 0.001$). Reductions in the levels of pAKT with time with CM+2 μ M Bpv(Hopic) were also evident, however, significance was not achieved.

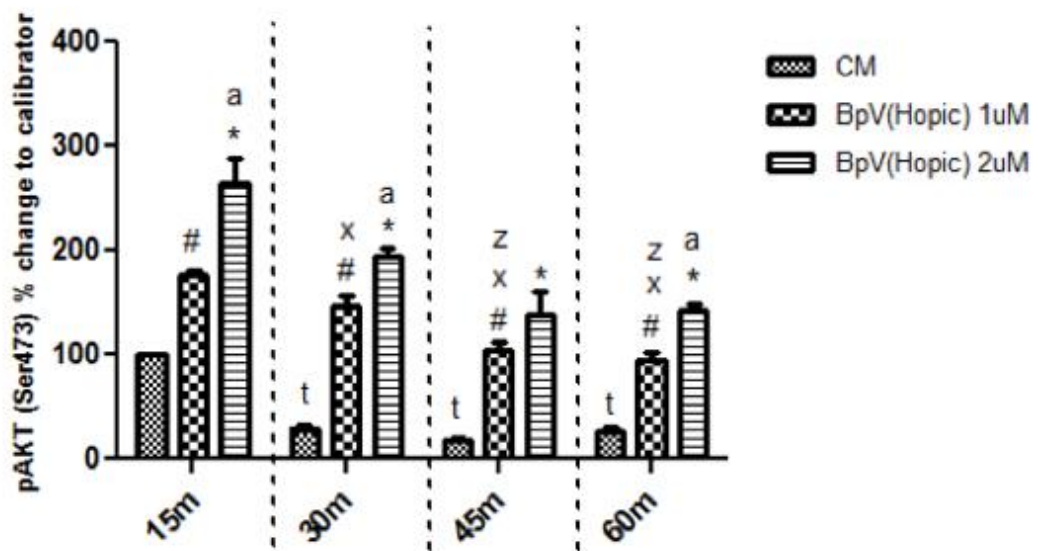


Figure 5.7. Quantification of pAKT levels (CM, CM+1 μ M Bpv(Hopic) and CM+2 μ M Bpv(Hopic)). Quantification of pAKT phosphorylation levels in response to CM, CM+1 μ M Bpv(Hopic) and CM+2 μ M Bpv(Hopic) indicated significant increases with CM+2 μ M BpV(Hopic) vs CM at 15m ($p < 0.001$, represented as *), 30m ($p < 0.0001$, represented as *), 45m ($p < 0.01$, represented as *) and 60m ($p < 0.0001$, represented as *). Significant increases were indicated with CM+1 μ M BpV(Hopic) vs CM at 15m ($p < 0.05$, represented as #), 30m ($p < 0.001$, represented as #), 45m ($p < 0.01$, represented as #) and 60m ($p < 0.01$, represented as #). Significant increase was found with CM+2 μ M Bpv(Hopic) vs CM+1 μ M Bpv(Hopic) at 15m ($p < 0.01$, represented by a), 30m ($p < 0.05$, represented as a) and 60m ($p < 0.01$, represented as a). Significant reductions of pAKT phosphorylation levels with CM were observed at 30m vs 15m, 45m vs 15m and 60m vs 15m (all $p < 0.0001$, represented as t). Significant reductions were observed with CM+1 μ M Bpv(Hopic) at 30m vs 15m ($p < 0.05$, represented by x), at 45m vs 15m ($p < 0.001$, represented by x), at 60m vs 15m ($p < 0.001$, represented by x) and also at 45m vs 30m ($p < 0.01$, represented by z) and 60m vs 30m ($p < 0.001$, represented by z). Data are representative of 4 experiments. (p-values obtained by One-way repeated measures ANOVA)

Analyses of pERK1/2 phosphorylation in response to CM, CM+1 μ M Bpv(Hopic) and CM+2 μ M Bpv(Hopic) were performed (Figure 5.8). Significant increases were observed with CM+2 μ M Bpv(Hopic) vs CM at 15m (172.25 \pm 17.75% vs 100%, $p < 0.05$), 30m (99.5 \pm 8.42% vs 11.75 \pm 3.88%, $p < 0.001$), 45m (53 \pm 2.58% vs 9 \pm 4.92%, $p < 0.001$) and 60m (72.25 \pm 11.19% vs 9.75 \pm 2.21%, $p < 0.001$). An increase was also observed with CM+1 μ M BpV(Hopic) vs CM at 30m (67 \pm 5.73% vs 11.75 \pm 3.88%, $p < 0.01$), 45m (52.25 \pm 3.22% vs 9 \pm 4.92%, $p < 0.001$) and 60m (42.75 \pm 4.25% vs 9.75 \pm 2.21%, $p < 0.05$). Significant increases were indicated with CM+2 μ M Bpv(Hopic) vs CM+1 μ M Bpv(Hopic) at 30m (99.5 \pm 8.42% vs 67 \pm 5.73%, $p < 0.05$) and 60m (72.25 \pm 11.19% vs 42.75 \pm 4.25%, $p < 0.05$). Reductions in pERK1/2 phosphorylation levels with time were observed with CM at 30m vs 15m (11.75 \pm 3.88% vs 100%, $p < 0.0001$), 45m vs 15m (9 \pm 4.92% vs 100%, $p < 0.0001$) and 60m (9.75 \pm 2.21% vs 100%, $p < 0.0001$). Reductions with time were also observed with CM+1 μ M (Bpv(Hopic)) at 30m vs 15m (67 \pm 5.73% vs 154.75 \pm 27.31%, $p < 0.05$), 45m vs 15m (52.25 \pm 3.22% vs 154.75 \pm 27.31%, $p < 0.01$) and 60m vs 15m (42.75 \pm 4.25% vs 154.75 \pm 27.31%, $p < 0.01$). Significant reductions with time were also indicated with CM+2 μ M (Bpv(Hopic)) at 30m vs 15m (99.5 \pm 8.42% vs 172.25 \pm 17.75%, $p < 0.001$), 45m vs 15m (53 \pm 2.58% vs 172.25 \pm 17.75%, $p < 0.001$) and 60m vs 15m (72.25 \pm 11.19% vs 172.25 \pm 17.75%, $p < 0.001$).

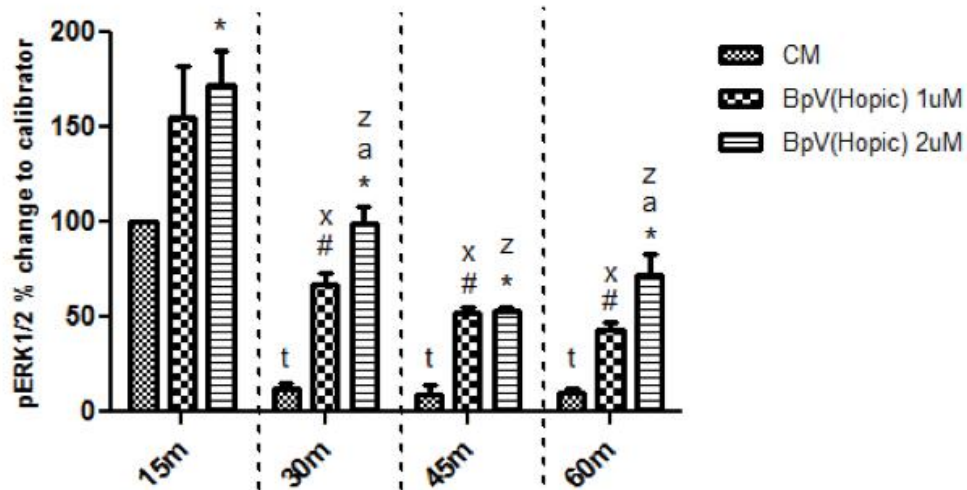


Figure 5.8. Quantification of pERK1/2 levels (CM, CM+1 μ M Bpv(Hopic) and CM+2 μ M Bpv(Hopic)). Quantification of pERK1/2 phosphorylation levels in response to CM, CM+1 μ M Bpv(Hopic) and CM+2 μ M Bpv(Hopic) indicated significant increases with CM+2 μ M BpV(Hopic) vs CM at 15m ($p < 0.05$, represented by *), 30m ($p < 0.001$, represented by *), 45m ($p < 0.001$, represented by *) and 60m ($p < 0.001$, represented by *). Significant increase was indicated with CM+1 μ M BpV(Hopic) vs CM at 30m ($p < 0.01$, represented by #), 45m ($p < 0.001$, represented by #) and 60m ($p < 0.05$, represented by #). Significant increase was observed with CM+2 μ M BpV(Hopic) vs CM+1 μ M BpV(Hopic) at 30m and 60m (for both $p < 0.05$, represented by a). Reduction of pERK1/2 levels at 30m vs 15m, 45m vs 15m and 60m vs 15m with CM was observed (for all $p < 0.0001$, represented by t). Reduction was also observed with CM+1 μ M BpV(Hopic) at 30m vs 15m ($p < 0.05$, represented by x), 45m vs 15m ($p < 0.01$, represented by x) and 60m vs 15m ($p < 0.01$, represented by x). There was a significant reduction with CM+2 μ M BpV(Hopic) at 30m vs 15m, 45m vs 15m and 60m vs 15m (for all $p < 0.001$, represented by z). Data are representative of 4 experiments. (p-values obtained by One-way repeated measures ANOVA)

Having determined the dose responsiveness of Bpv(Hopic) on the C2C12 cells for specificity, as well as activation of ERK and Akt, the action of Bpv(Hopic) on wound closure was assessed in preliminary experiments (Figure 5.9). 10 μ M concentration caused cell contraction and shrinking (illustrated in Figure 5.9 (panel D)), which continued for several hours and this caused a delay in the progress of wound closure. 1 μ M and 2 μ M concentrations also caused cell shrinking/contraction, although this lasted for much shorter time periods compared to the 10 μ M concentration, with 1 μ M causing cells to contract for the shortest period of time. Wound closure was visually improved with both 1 μ M and

2 μ M concentrations of Bpv(Hopic) following 20h incubation, compared to CM alone. CM (Figure 5.9A), despite being more potent at inducing migration compared to SF media (as detailed in chapter 3) was apparently less potent at inducing cell migration over 20h compared to CM+1 μ M Bpv(Hopic) (Figure 5.9B) and CM+2 μ M Bpv(Hopic) (Figure 5.9C). CM+10 μ M Bpv(Hopic) caused cell contraction and shrinking for several hours (Figure 5.9D) and hence migration at 20h (Figure 5.9E) was delayed compared to 1 μ M and 2 μ M concentrations. Following a time lag, wound closure with 10 μ M Bpv(Hopic) did eventually occur, at 40h (Figure 5.9F). As cells migrated in a similar manner with both concentrations (1 μ M and 2 μ M), the differences in migration distance/cell counts was not investigated in detail between these concentrations of Bpv(Hopic).

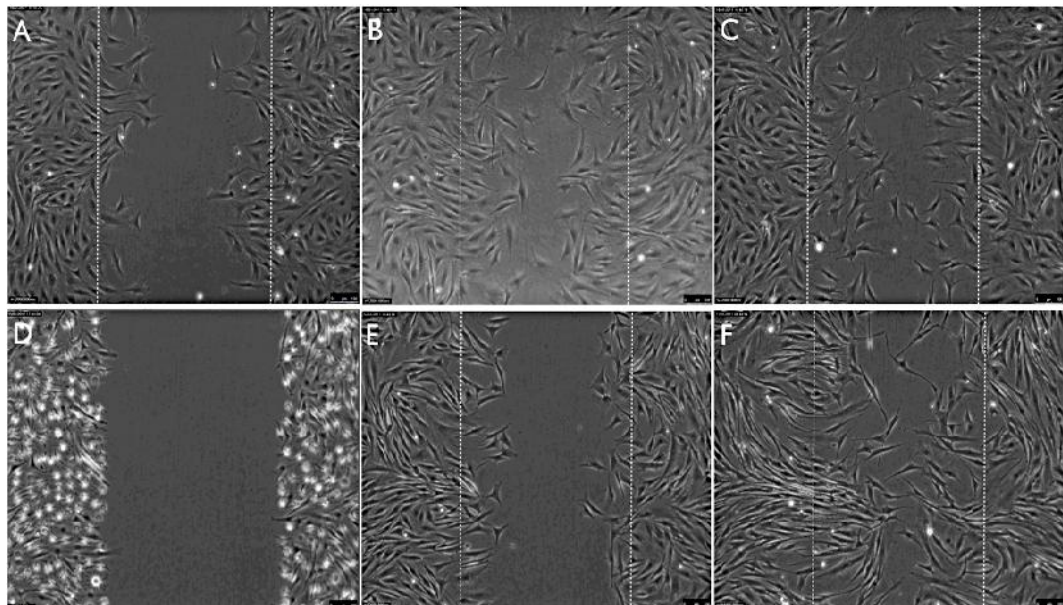


Figure 5.9. Preliminary experiments examining the migration potential between CM and 1 μ M, 2 μ M and 10 μ M concentrations of Bpv(Hopic). CM (A) was less potent in inducing cell migration for 20h compared to CM+1 μ M Bpv(Hopic) (B) and CM+2 μ M Bpv(Hopic) (C). CM+10 μ M Bpv(Hopic) caused cell contraction and shrinking for several hours (D) and migration at 20h (E) was delayed compared to 1 μ M and 2 μ M concentrations (B and C). Wound closure with 10 μ M Bpv(Hopic) was eventually complete with a big delay at 40h (F). Data are representative of 3 experiments performed in duplicate.

Considering the shrinking/contraction of myoblasts, induced by Bpv(Hopic), it was of interest to examine whether adhesion of the cells was affected by the inhibitor. Cells were seeded in CM and the time for cell spreading on the substrate

was examined. As visualized in Figure 5.10, the majority of cells in CM were adherent at 30min., with all cells attached and spreading at 60m. Time for successful adhesion was increased with increasing concentrations of Bpv(Hopic), with poor adhesion even at 60 min. for 2 μ M treatment and 10 μ M application resulting in no evident adhesion even following 60min incubation.

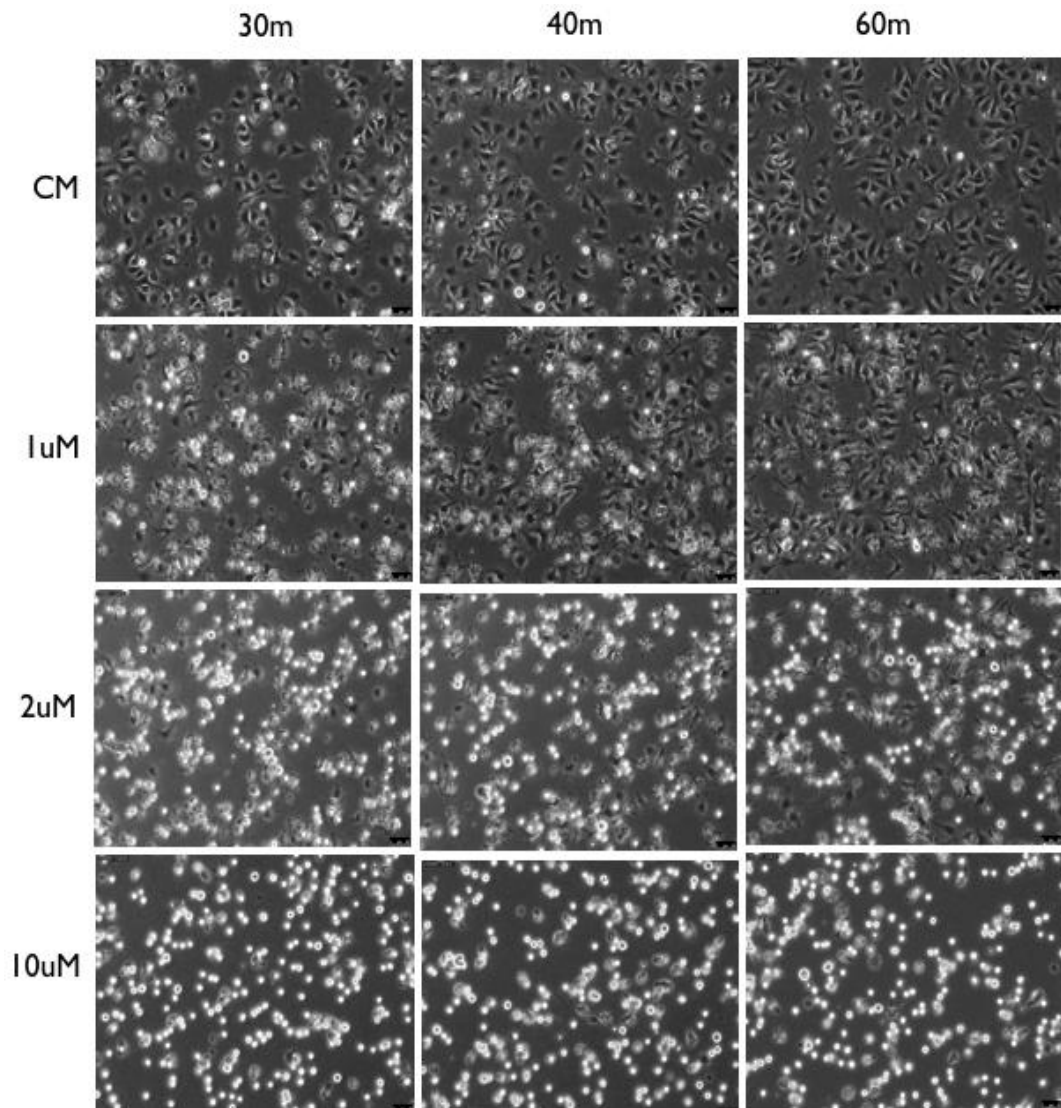


Figure 5.10. Cell adhesion assay examines the time required for cells to adhere to the substratum (0.2% gelatin). The majority of cells in CM were adhering at 30m, and well adhered at 60m. With increasing concentrations of BpV(Hopic), the time required for adhesion was increased. Data are representative of 2 experiments performed in duplicate.

Given the derived data, 1 μ M Bpv(Hopic) demonstrated activation of both PI3K/AKT (Figure 5.7) and MAPK/ERK (Figure 5.8) signalling pathways and

little impact on cell adhesion or death compared to CM, while showing greater specificity than either 2 or 10 μM (Figure 5.5) and no significant impact on differentiation (Figure 5.1-5.3), this dose was therefore chosen for further analyses.

Having examined the appropriate doses of Bpv (Hopic) to be utilized in these studies, the migration of myoblasts with CM vs CM+1 μM Bpv(Hopic) was analyzed in the wound healing assay and indicated that cellular migration was indeed increased following 20hrs incubation with CM+1 μM Bpv(Hopic) vs CM (Figure 5.11). Analyses of the total number of cells migrating into the wound site indicated significant increases in the number of cells with CM+1 μM Bpv(Hopic) vs CM (91 \pm 4 vs 66 \pm 3, $p < 0.0001$, equivalent to 38% increase; (Figure 5.11B). The percentage of cells in the central section of the wound was also significantly greater with CM+1 μM Bpv(Hopic) vs CM (21.87 \pm 1.28% vs 10.13 \pm 1%, $p < 0.0001$; Figure 5.11C), thus confirming the preliminary data derived in Figure 5.9.

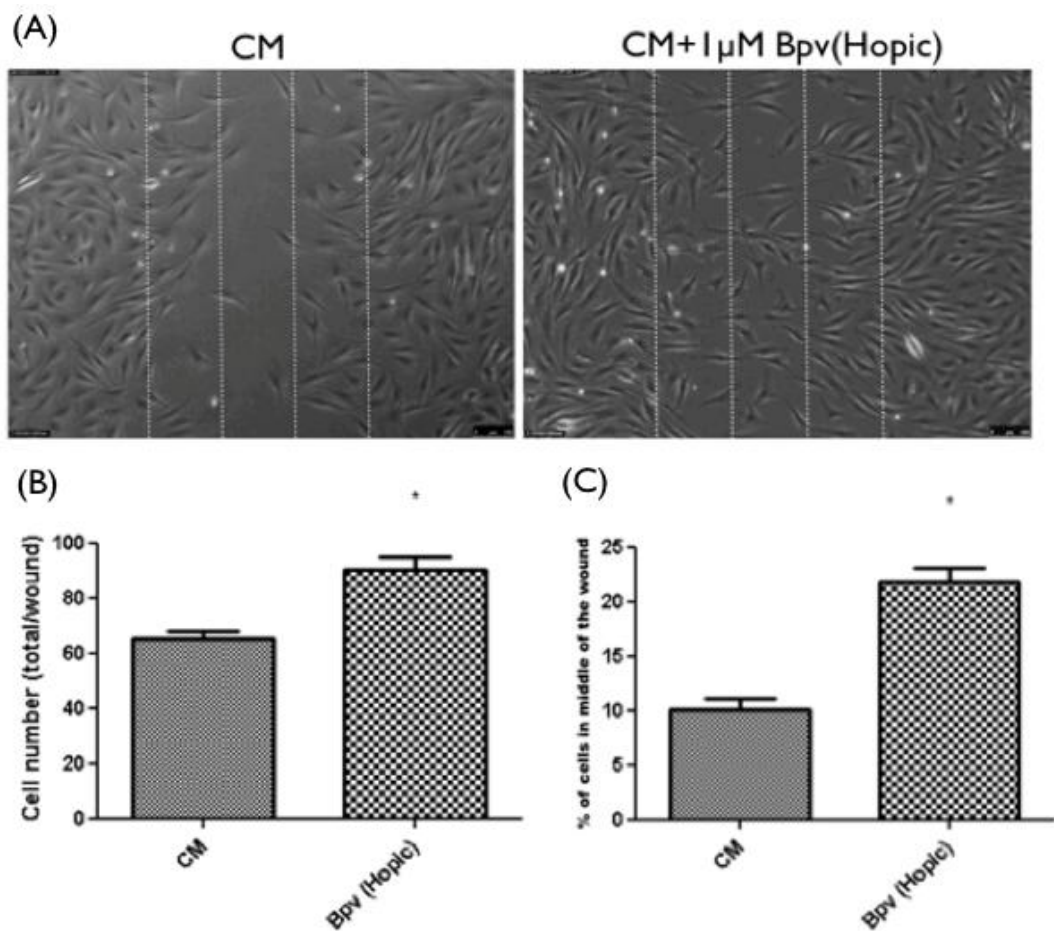


Figure 5.11. Wound healing assay with cell count analysis (CM vs CM+1µM Bpv(Hopic)). Wound healing assay comparing the wound closure between CM and CM+1µM Bpv(Hopic) for 20h (A). Wound healing cell count quantifications between CM and CM+1µM Bpv(Hopic) indicated significant increase with CM+1µM Bpv(Hopic) vs CM ($p < 0.0001$, represented by *) (B). Quantification of the percentage of cells in the middle of the wound indicated significant increase with CM+1µM Bpv(Hopic) vs CM ($p < 0.0001$, represented by *) (C). All data are representative of 15 experiments performed in duplicate. (p-values obtained by paired t-test)

To confirm the quantification data, cell tracking analyses were performed between cells treated with CM and CM+1µM Bpv(Hopic) (Figure 5.12A). The analyses of cell tracking studies revealed significant increases in the migration distances of CM+1µM Bpv(Hopic) vs CM ($598 \pm 47.4 \mu\text{m}$ vs $422 \pm 33.2 \mu\text{m}$, $p < 0.0001$, equivalent to 41% increase; Figure 5.12B). Furthermore, cell death analyses indicated a very small, but significant decrease in the percentage of dead cells with CM+1µM Bpv(Hopic) vs CM ($0.75 \pm 0.13\%$ vs $1.39 \pm 0.3\%$, $p < 0.05$; Figure 5.12C).

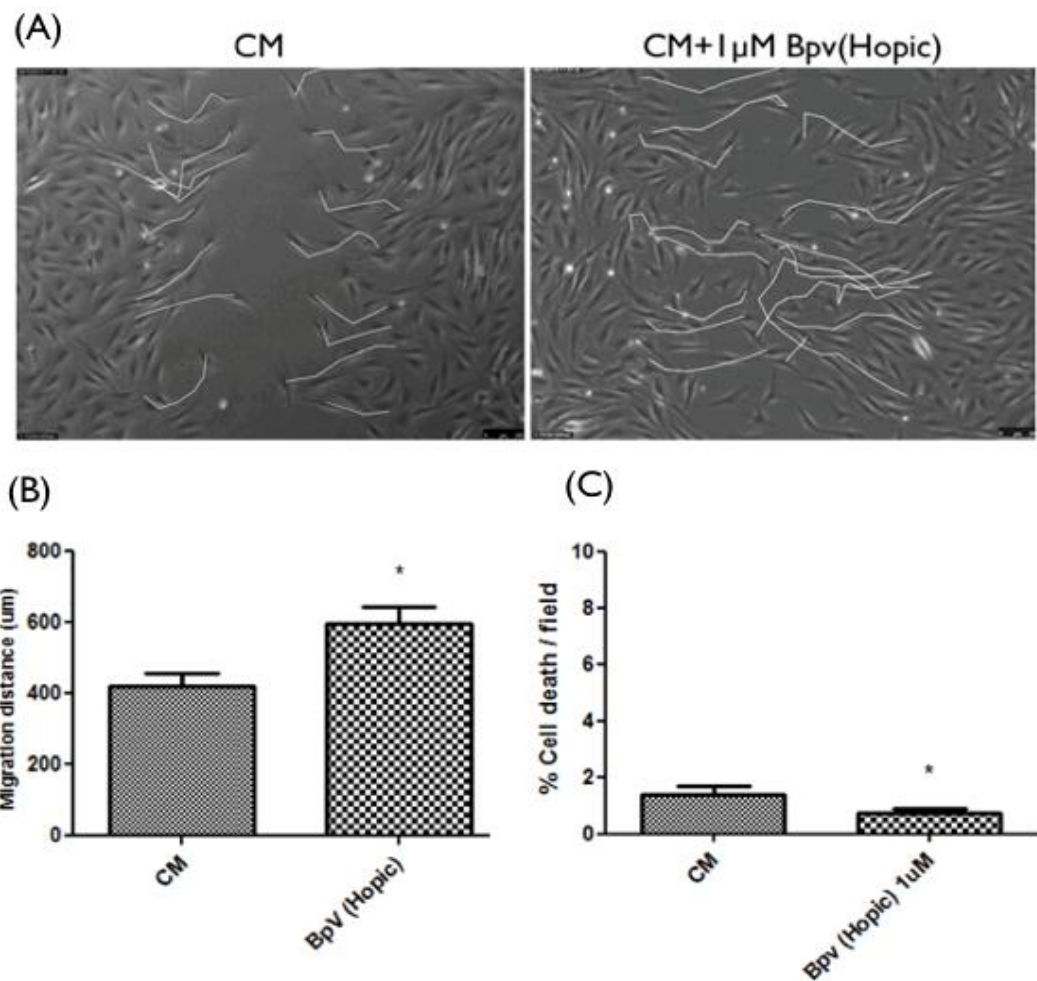


Figure 5.12. Cell tracking and cell death analysis (CM vs CM+1µM Bpv(Hopic)). Morphological photomicrographs of migration tracking comparing the effects of CM and CM+1µM Bpv(Hopic) (A). Quantification of cell migration distance indicated significant increase with CM+1µM Bpv(Hopic) vs CM ($p < 0.0001$, represented by *) (B). Data are representative of 15 experiments performed in duplicate. Cell death quantifications indicated a decrease in cell death with CM+1µM Bpv(Hopic) vs CM ($p < 0.05$) (C). Data are representative of 14 experiments performed in duplicate. (p-values obtained by paired t-test)

5.4.4. THE ACTION OF BPV(HOPIC) ON CELL MIGRATION IS REDUCED BY INHIBITING THE PI3K/AKT PATHWAY WITH LY294002

Here it was demonstrated that Bpv(Hopic) in CM is able to facilitate myoblast migration and to enhance the PI3K/AKT and MAPK/ERK pathways. On the other hand, PI3K/AKT inhibitor LY294002 and MAPK/ERK inhibitor UO126, reduced myoblast migration induced by CM. Wishing to substantiate the specificity of this data using 1µM Bpv(Hopic), an assessment was made on how the myoblast migration, enhanced by Bpv(Hopic), would be affected by co-incubations with

LY294002 or UO126; thus investigating more specifically (in the absence of direct activators of these pathways) whether migration in this model is indeed mediated by either PI3K or MAPK pathways.

Western blotting studies were performed to investigate the effect of CM, CM+1 μ M BpV(Hopic) and CM+1 μ M BpV(Hopic)+10 μ M LY294002 on the levels of p-AKT and pERK1/2 activation over time (Figure 5.13). In the absence of any impact on total Akt, ERK or beta actin levels, it is clear from the blots that Bpv increases pAkt and pERK1/2 phosphorylation, as already demonstrated. Furthermore, the data suggest that in the presence of BpV(Hopic)+10 μ M LY294002, pAkt activation is completely blocked, with no impact on pERK1/2 activity, indicating the specificity of the co-incubations (Figure 5.13).

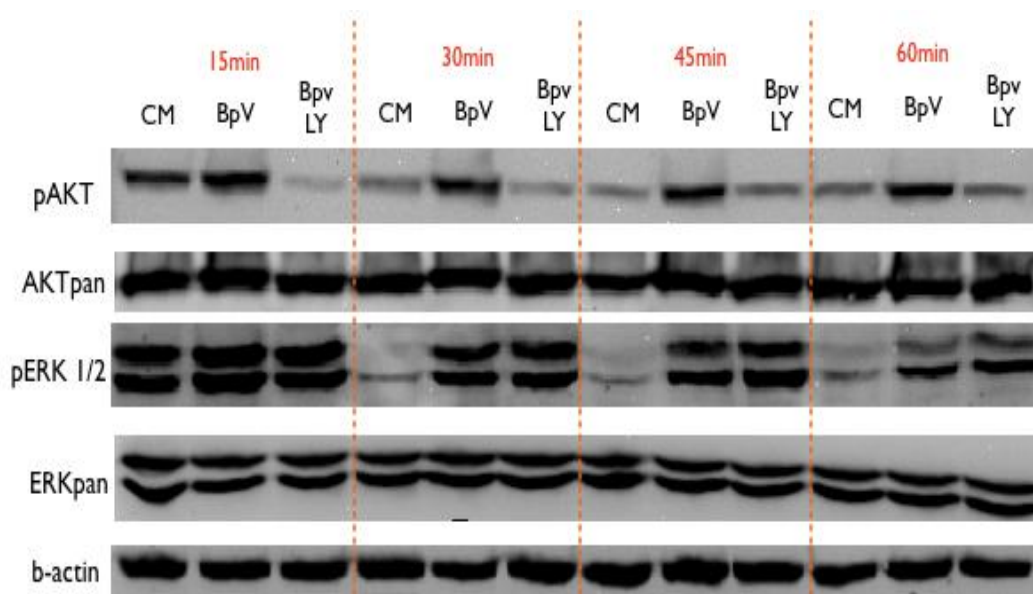


Figure 5.13. Western blots (CM, CM+1 μ M BpV(Hopic) and CM+1 μ M BpV(Hopic)+10 μ M LY294002). Western blots investigating the effects of CM (Lanes 1, 4, 7 and 10=CM), CM+1 μ M BpV(Hopic) (Lane 2, 5, 8 and 11=Bpv) and CM+1 μ M BpV(Hopic)+10 μ M LY294002 (Lane 3, 6, 9 and 12 = BPV LY) with time on the activation levels of p-AKT and pERK1/2. 1 μ M Bpv(Hopic) induced activation of Akt and ERK, while its combination with 10 μ M LY294002 blocked the activation of pAKT, but not of pERK1/2. Data are representative of at least 3 experiments.

Blots were subjected to further analyses using Quantity One software. Phospho-Akt and Phospho-ERK1/2 levels were quantified across the 3 different treatments conditions and the 4 time points. All values are represented as percentage of the calibrator (CM 15m), which was set to 100%.

Analyses of pAKT (Ser 473) were performed in response to CM, CM+1 μ M Bpv(Hopic) and CM+1 μ M Bpv(Hopic)+10 μ M LY294002 (Figure 5.14). Significant increases were observed with CM+1 μ M Bpv(Hopic) vs CM at 15m (153.67 +/-12.23% vs 100%, p<0.01), at 30m (160.33 +/-23.24% vs 60.67 +/-7.83%, p<0.001), at 45m (135.17 +/-17.02% vs 48.67 +/-10.84%, p<0.001) and at 60m (145.5 +/-16.91% vs 66.83 +/-6.58%, p<0.001). A decrease was found with CM+1 μ M Bpv(Hopic)+10 μ M LY294002 vs CM+1 μ M Bpv(Hopic) at 15m (24.67 +/-6.64% vs 153.67 +/-12.23%, p<0.0001), at 30m (46.33 +/-8.18% vs 160.33 +/-23.24%, p<0.001), at 45m (46.17 +/-5.24% vs 135.17 +/-17.02%, p<0.001) and at 60m (59.83 +/-9.89% vs 145.5 +/-16.91%, p<0.0001). Decreases were also indicated with CM+1 μ M Bpv(Hopic)+10 μ M LY294002 vs CM at 15m (24.67 +/-6.64% vs 100%, p<0.001).

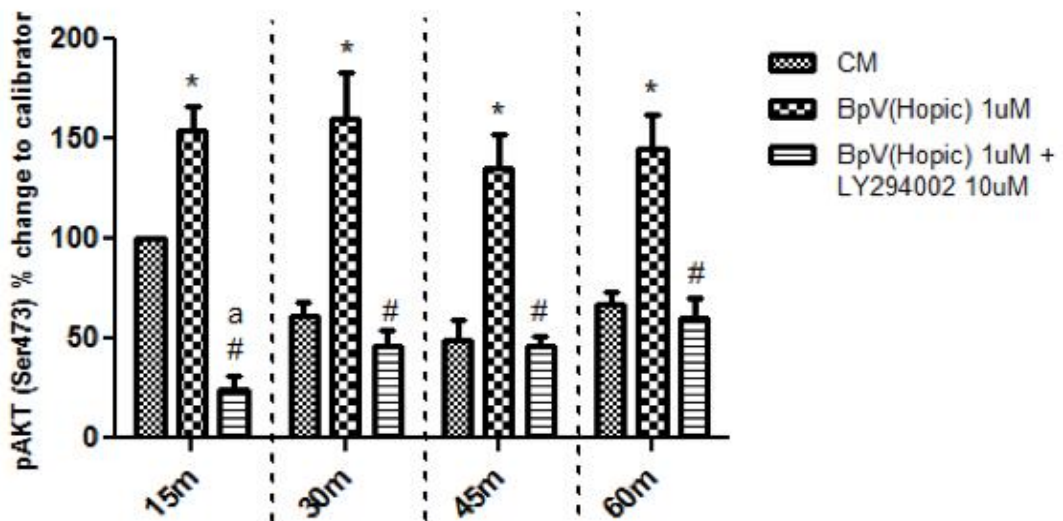


Figure 5.14. Quantification of pAKT levels (CM, CM+1 μ M Bpv(Hopic) and CM+1 μ M Bpv(Hopic)+10 μ M LY294002). Quantification of pAKT levels in response to CM, CM+1 μ M Bpv(Hopic) and CM+1 μ M Bpv(Hopic)+10 μ M LY294002 indicated significant increases with CM+1 μ M Bpv(Hopic) vs CM at 15m (p<0.01, represented by *), at 30m (p<0.001, represented by *), at 45m (p<0.001, represented by *) and at 60m (p<0.001, represented by *). Decreases were indicated with CM+1 μ M Bpv(Hopic)+10 μ M LY294002 vs CM+1 μ M Bpv(Hopic) at 15m (p<0.0001, represented by #), at 30m (p<0.001, represented by #), at 45m (p<0.001, represented by #) and at 60m (p<0.0001, represented by #). Decreases were also found with CM+1 μ M Bpv(Hopic)+10 μ M LY294002 vs CM at 15m (p<0.001, represented by a). Data are representative of 6 experiments. (p-values obtained by One-way repeated measures ANOVA)

Given the visual data above in Figure 5.13 in relation to ERK1/2 phosphorylation, analyses of pERK1/2 were performed to consolidate these findings and to establish the impact of CM, CM+1 μ M Bpv(Hopic) and CM+1 μ M Bpv(Hopic)+10 μ M LY294002 (Figure 5.15) on ERK1/2 phosphorylation. As already described, significant increases in ERK1/2 phosphorylation were evident with CM+1 μ M Bpv(Hopic) vs CM at 30m (88 +/-7.21% vs 8.67 +/-4.33%, $p<0.001$), at 45m (65.33 +/-11.98% vs 7 +/-2.08%, $p<0.05$) and at 60m (41 +/-4.58% vs 6.67 +/-1.76%, $p<0.01$). Similarly, increases with CM+1 μ M Bpv(Hopic)+10 μ M LY294002 vs CM were found at 30m (91 +/-2.08% vs 8.67 +/-4.33%, $p<0.001$), at 45m (68.33 +/-8.67% vs 7 +/-2.08%, $p<0.05$) and at 60m (44.33 +/-3.71% vs 6.67 +/-1.76%, $p<0.01$). Significant reductions in ERK1/2 activation with CM were observed at 30m vs 15m (8.67 +/-4.33% vs 100%, $p<0.001$), 45m vs 15m (7 +/-2.08% vs 100%, $p<0.001$), 60m vs 15m (6.67 +/-1.76% vs 100%, $p<0.001$). Decreases were also found with CM+1 μ M Bpv(Hopic) at 60m vs 15m (41 +/-4.58% vs 123.67 +/-22.64%, $p<0.05$). Similar decreases with time were evident with CM+1 μ M Bpv(Hopic)+10 μ M LY294002, although not statistically significant. Critically, no differences in ERK1/2 phosphorylation were evident between CM+1 μ M Bpv(Hopic) and CM+1 μ M Bpv(Hopic)+10 μ M LY294002 at any of the times investigated, once again confirming the visual data in Figure 5.13.

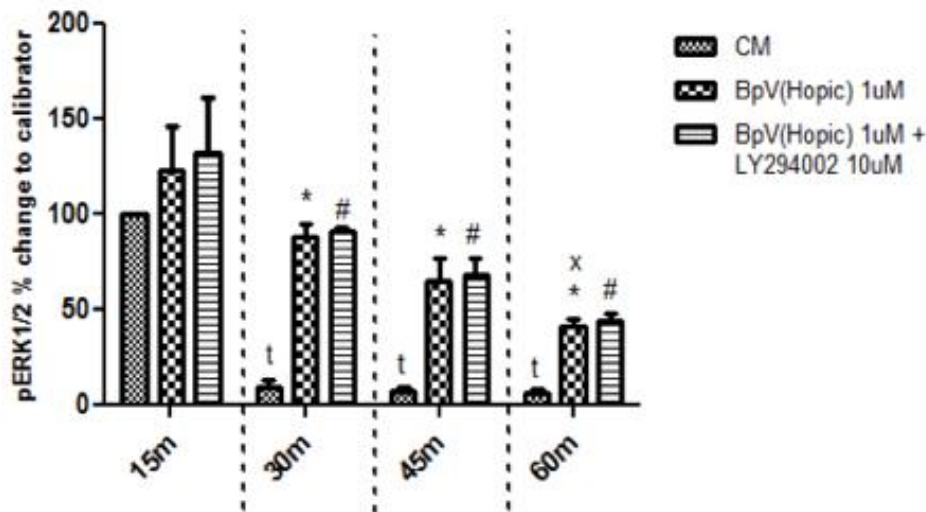


Figure 5.15. Quantification of pERK1/2 levels (CM, CM+1 μ M Bpv(Hopic) and CM+1 μ M Bpv(Hopic)+10 μ M LY294002). Quantification of pERK1/2 activation in response to CM, CM+1 μ M Bpv(Hopic) and CM+1 μ M Bpv(Hopic)+10 μ M LY294002 indicated significant increase with CM+1 μ M Bpv(Hopic) vs CM at 30m ($p < 0.001$, represented by *), at 45m ($p < 0.05$, represented by *) and at 60m ($p < 0.01$, represented by *). Increase was found with CM+1 μ M Bpv(Hopic)+10 μ M LY294002 vs CM at 30m ($p < 0.001$, represented by #), at 45m ($p < 0.05$, represented by #) and at 60m ($p < 0.01$, represented by #). Significant reduction was found with CM at 30m vs 15m ($p < 0.001$, represented by t), at 45m vs 15m ($p < 0.001$, represented by t) and at 60m vs 15m ($p < 0.001$, represented by t). Decrease was indicated with CM+1 μ M Bpv(Hopic) at 60m vs 15m ($p < 0.05$, represented by x). Data are representative of 3 experiments performed. (p-values obtained by One-way repeated measures ANOVA)

After confirming by Western blots that LY294002 induced specific inhibition of the PI3K/Akt pathway, without significantly altering the MAPK/ERK pathway, wound healing studies were performed to investigate the effect on wound closure of CM, CM+1 μ M Bpv(Hopic) and CM+1 μ M Bpv(Hopic)+10 μ M LY294002 (Figure 5.16A); it is evident from these morphological observations the the inclusion of 10 μ M LY294002 in the presence of CM+1 μ M Bpv(Hopic), reduces cellular migration to levels more visually comparable to those seen with CM alone. Analyses of total cell counts in the damaged area (Figure 5.16B) indicated significant increases with CM+1 μ M Bpv(Hopic) vs CM (90 \pm 5 vs 65 \pm 3, $p < 0.001$, equivalent to 38% increase) and a comparable decrease with CM+1 μ M Bpv(Hopic)+10 μ M LY294002 vs CM+1 μ M Bpv(Hopic) (66 \pm 3 vs 90 \pm 5, $p < 0.01$, equivalent to 27% decrease). Analyses of the percentage of cells in the middle of the wound (Figure 5.16C) indicated significant increases with

CM+1 μ M Bpv(Hopic) vs CM (17.33 \pm 2.03% vs 5.17 \pm 0.95%, $p < 0.0001$) and a decrease towards control conditions with CM+1 μ M Bpv(Hopic)+10 μ M LY294002 vs CM+1 μ M Bpv(Hopic) (9.17 \pm 1.28% vs 17.33 \pm 2.03%, $p < 0.0001$). Although no difference was apparent between total cells migrating in the presence of CM vs CM+1 μ M Bpv(Hopic)+10 μ M LY294002 (Figure 5.16B), an increase in the percentage of cells in the middle of the wound was evident with CM+1 μ M Bpv(Hopic)+10 μ M LY294002 vs CM (9.17 \pm 1.28% vs 5.17 \pm 0.95%, $p < 0.01$).

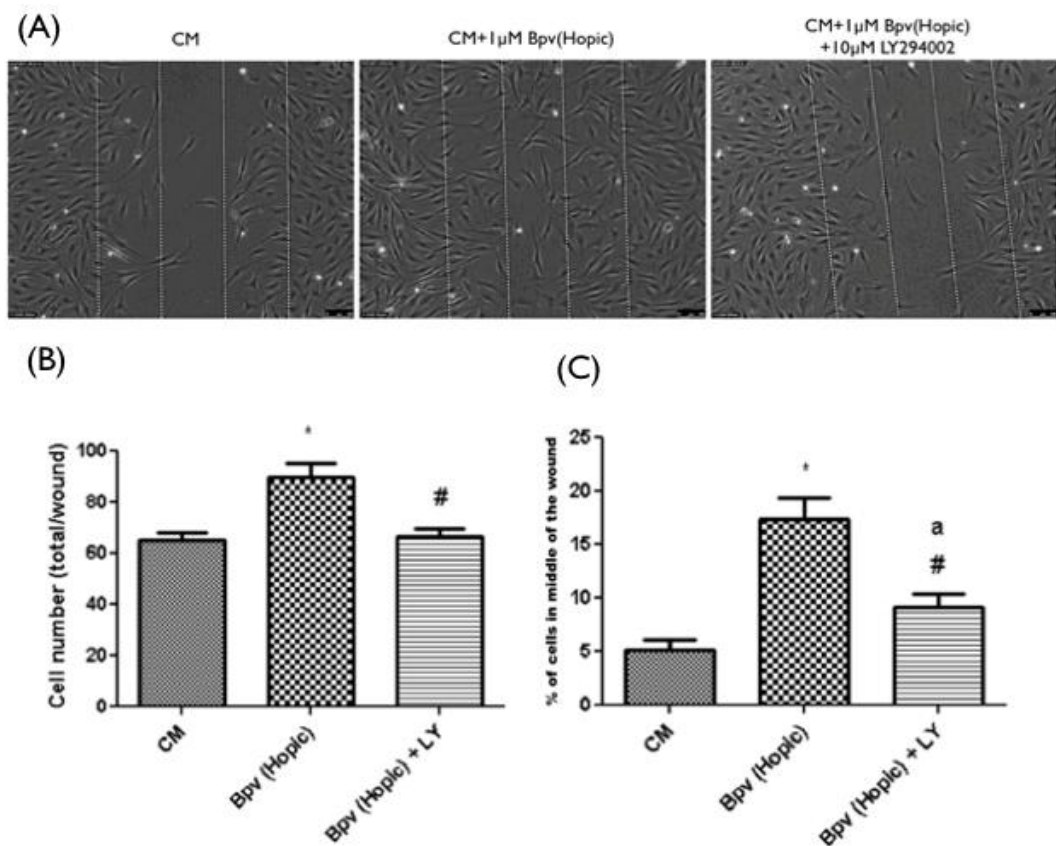


Figure 5.16. Wound healing assay with cell count analyses (CM, CM+1µM Bpv(Hopic) and CM+1µM Bpv(Hopic)+10µM LY294002). Wound healing assay comparing the wound closure between CM, CM+1µM Bpv(Hopic) and CM+1µM Bpv(Hopic)+10µM LY294002 (A). Quantification of the total number of cells infiltrating the wound site following 20h incubation indicated significant increases with CM+1µM Bpv(Hopic) vs CM ($p < 0.001$, represented by *). Significant decreases were indicated with CM+1µM Bpv(Hopic)+10µM LY294002 v CM+1µM Bpv(Hopic) ($p < 0.01$, represented by #) (B). Quantification of the percentage of cells in the middle of the wound indicated significant increases with CM+1µM Bpv(Hopic) vs CM ($p < 0.0001$, represented by *). Significant decreases were observed with CM+1µM Bpv(Hopic)+10µM LY294002 v CM+1µM Bpv(Hopic) ($p < 0.0001$, represented by #). Increases were also indicated with CM+1µM Bpv(Hopic)+10µM LY294002 vs CM ($p < 0.01$, represented by a) (C). All data are representative of 6 experiments performed in duplicate. (p-values obtained by One-way repeated measures ANOVA)

To consolidate the quantification investigations, cell tracking analyses were performed (Figure 5.17A). Statistical analyses of the derived data indicated significant increases in cell migration distance with CM+1µM Bpv(Hopic) vs CM ($678 \pm 63.1\mu\text{m}$ vs $463 \pm 49.4\mu\text{m}$, $p < 0.0001$, equivalent to 46% increase). Significant decreases were observed with CM+1µM Bpv(Hopic)+10µM

LY294002 vs CM+1 μ M Bpv(Hopic) (521 \pm 54.3 μ m vs 678 \pm 63.1 μ m, $p < 0.001$, equivalent to 23% decrease; Figure 5.17B), substantiating the data obtained from Figure 5.16 and suggesting that migration itself was affected and not simply directionality of migration. No significant increase/decrease in cell death was observed between any of the treatments (Figure 5.17C).

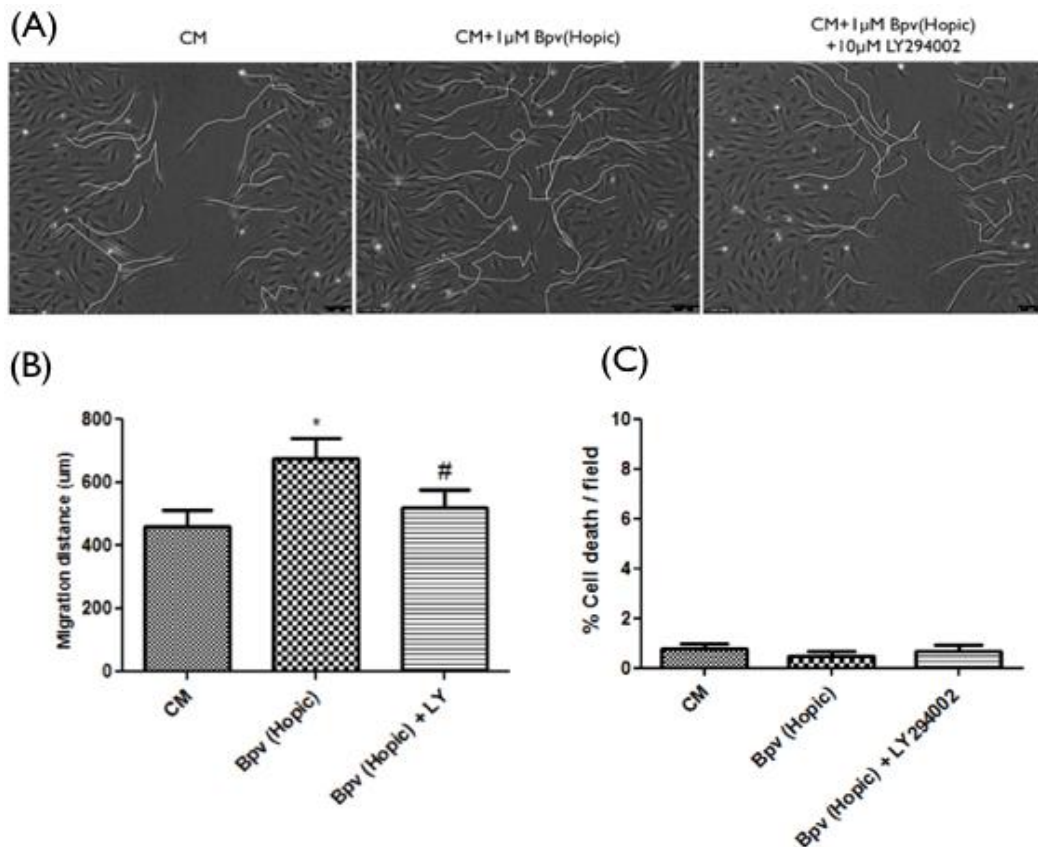


Figure 5.17. Cell tracking and cell death analysis (CM, CM+1 μ M Bpv(Hopic) and CM+1 μ M Bpv(Hopic)+10 μ M LY294002). Migration tracking comparing the effects of CM, CM+1 μ M Bpv(Hopic) and CM+1 μ M Bpv(Hopic)+10 μ M LY294002 (A). Quantification of cell migration distance indicated significant increases with CM+1 μ M Bpv(Hopic) vs CM ($p < 0.0001$, represented by *). Significant decreases were observed with CM+1 μ M Bpv(Hopic)+10 μ M LY294002 vs CM+1 μ M Bpv(Hopic) ($p < 0.001$, represented by #) (B). Cell death quantifications and analyses found no significant difference between CM, CM+1 μ M Bpv(Hopic) and CM+1 μ M Bpv(Hopic)+10 μ M LY294002 (C). All data are representative of 6 experiments performed in duplicate. (p -values obtained by One-way repeated measures ANOVA)

5.4.5. THE ACTION OF BPV(HOPIC) ON CELL MIGRATION IS REDUCED BY INHIBITING THE MAPK/ERK PATHWAY WITH UO126

Similar to the experiments performed in Section 5.4.4, in order to verify the specificity of the MAPK/ERK signalling pathway inhibition by UO126 in the presence of Bpv(Hopic), western blots were performed to investigate the effect of CM, CM+1 μ M BpV(Hopic) and CM+1 μ M BpV(Hopic)+5 μ M UO126 on PI3K/AKT and MAPK/ERK pathways (Figure 5.18). As is evident from representative blots below, UO in the presence of Bpv(Hopic) was with little impact on Akt phosphorylation, compared to Bpv(hopic) alone. By contrast and in line with expectations, UO126 blocked the activation of ERK1/2 when added in combination with and when compared to Bpv(Hopic) alone. Internal controls (pan Akt, pan ERK and beta actin) were unaffected by any of the treatments.

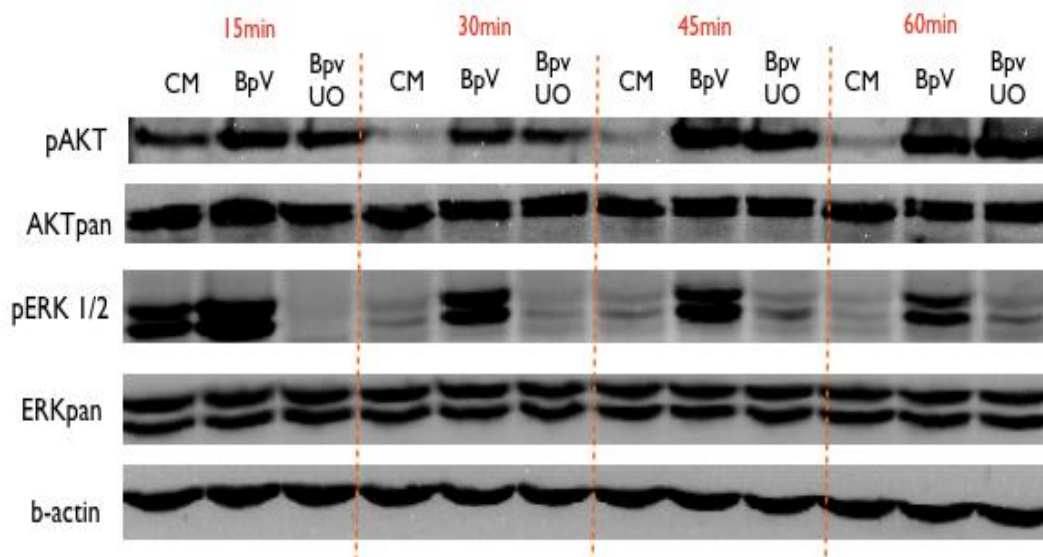


Figure 5.18. Western blots (CM, CM+1 μ M Bpv(Hopic) and CM+1 μ M Bpv(Hopic)+5 μ M UO126). Western blots investigating the effect of CM (Lanes 1, 4, 7 and 10=CM), CM+1 μ M BpV(Hopic) (Lanes 2, 5, 8 and 11=Bpv) and CM+1 μ M BpV(Hopic)+5 μ M UO126 (Lanes 3, 6, 9 and 12=Bpv UO) on the activation levels of p-AKT and pERK1/2. 1 μ M Bpv(Hopic) induced activation of Akt and ERK1/2, while its combination with 5 μ M UO126 blocked the activation of pERK1/2, but not pAKT. Data are representative of 4 experiments.

Blots were subjected to further analyses using Quantity One software. Phospho-Akt and Phospho-ERK1/2 levels were quantified across the 3 different treatments and the 4 time points. All values are represented as percentage of the calibrator (CM 15m), which was set to 100%.

Analyses of pAKT (Ser 473) was performed in response to CM, CM+1 μ M Bpv(Hopic) and CM+1 μ M Bpv(Hopic)+5 μ M UO126 (Figure 5.19). Significant increases were found in pAKT activation levels with CM+1 μ M Bpv(Hopic) vs CM at 15m (143.75% +/-18.79 vs 100%, p<0.01), at 30m (138 +/-38.66% vs 45.5 +/-17.2%, p<0.05), at 45m (230.25 +/-37.14% vs 47.75 +/-19.3%, p<0.0001) and at 60m (177.5 +/-41% vs 54.5 +/-19.27%, p<0.01). Significant increase in pAkt were also observed with CM+1 μ M Bpv(Hopic)+5 μ M UO126 vs CM at 30m (133.5 +/-38.7% vs 45.5 +/-17.2%, p<0.05), at 45m (210.5 +/-29.4% vs 47.75 +/-19.3%) and at 60m (184.25 +/-37.95% vs 54.5 +/-19.27%, p<0.01). As anticipated from the raw data in the blots, there were no differences in Akt activation in the presence of Bpv(Hopic) in the absence or presence of UO126.

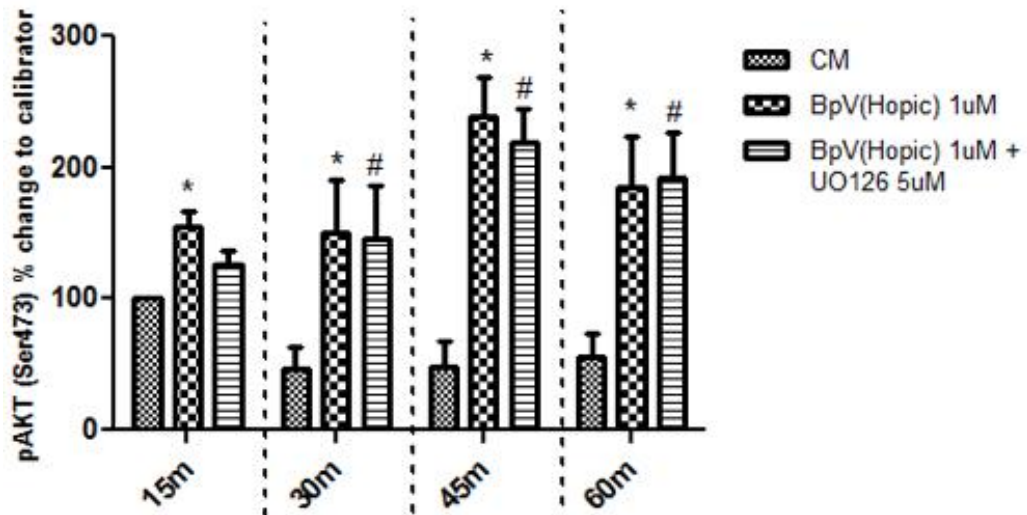


Figure 5.19. Quantification of pAKT levels (CM, CM+1 μ M Bpv(Hopic) and CM+1 μ M Bpv(Hopic)+5 μ M UO126). Quantification of pAKT levels in response to CM, CM+1 μ M Bpv(Hopic) and CM+1 μ M Bpv(Hopic)+5 μ M UO126 indicated significant increases with CM+1 μ M Bpv(Hopic) vs CM at 15m (p<0.01, represented by *), at 30m (p<0.05, represented by *), at 45m (p<0.0001, represented by *) and at 60m (p<0.01, represented by *). Significant increase were also found with CM+1 μ M Bpv(Hopic)+5 μ M UO126 vs CM at 30m (p<0.05, represented by #), at 45m (p<0.001, represented by #) and at 60m (p<0.01, represented by #). No differences were found between CM+1 μ M Bpv(Hopic) and CM+1 μ M Bpv(Hopic)+5 μ M UO126. Data are representative of 4 experiments performed in duplicate. (p-values obtained by One-way repeated measures ANOVA)

Wishing to substantiate the specificity of these findings, analyses of pERK1/2 activation were performed in response to CM, CM+1 μ M Bpv(Hopic) and CM+1 μ M Bpv(Hopic)+5 μ M UO126 (Figure 5.20). Confirming our earlier data, significant increases were found with CM+1 μ M Bpv(Hopic) vs CM at 30m (58.25 \pm 2.59% vs 13.5 \pm 4.33%, $p < 0.0001$), at 45m (44.5 \pm 6.81% vs 8 \pm 1.47%, $p < 0.001$) and at 60m (39.75 \pm 6.09% vs 4 \pm 1.35%, $p < 0.01$). Significant decreases in ERK1/2 activation were observed with CM+1 μ M Bpv(Hopic)+5 μ M UO126 vs CM+1 μ M Bpv(Hopic) at 15m (8.25 \pm 3.04% vs 115 \pm 12.02%, $p < 0.0001$), at 30m (10.5 \pm 2.18% vs 58.25 \pm 2.59%, $p < 0.0001$), at 45m (9.25 \pm 1.93% vs 44.5 \pm 6.81%, $p < 0.001$) and at 60m (8.25 \pm 3.92% vs 39.75 \pm 6.09%, $p < 0.01$). Decreases were also observed with CM+1 μ M Bpv(Hopic)+5 μ M UO126 vs CM at 15m (8.25 \pm 3.04% vs 100%, $p < 0.001$). Furthermore, decreases with time were evident with CM at 30m vs 15m (13.5 \pm 4.33% vs 100%, $p < 0.001$), at 45m vs 15m (8 \pm 1.47% vs 100%, $p < 0.001$) and at 60m vs 15m (4 \pm 1.35% vs 100%, $p < 0.001$), as also detailed previously in this chapter. Reductions in pERK1/2 activation with time were also observed with CM+1 μ M Bpv(Hopic) at 30m vs 15m (58.25 \pm 2.59% vs 115 \pm 12.02%, $p < 0.01$), at 45m vs 15m (44.5 \pm 6.81% vs 115 \pm 12.02%, $p < 0.01$) and at 60m vs 15m (39.75 \pm 6.09% vs 115 \pm 12.02%, $p < 0.01$). Suppression of ERK1/2 activation in the presence of CM+1 μ M Bpv(Hopic)+5 μ M UO126 was complete at 15 min and was not further impacted by time (Figure 5.20). Together these studies suggest that activation of ERK1/2 and PI3K is essential for myoblast migration in the presence of Bpv(Hopic) and that suppression of one is sufficient to block the enhanced migration, despite maintained signalling of the other signalling pathway.

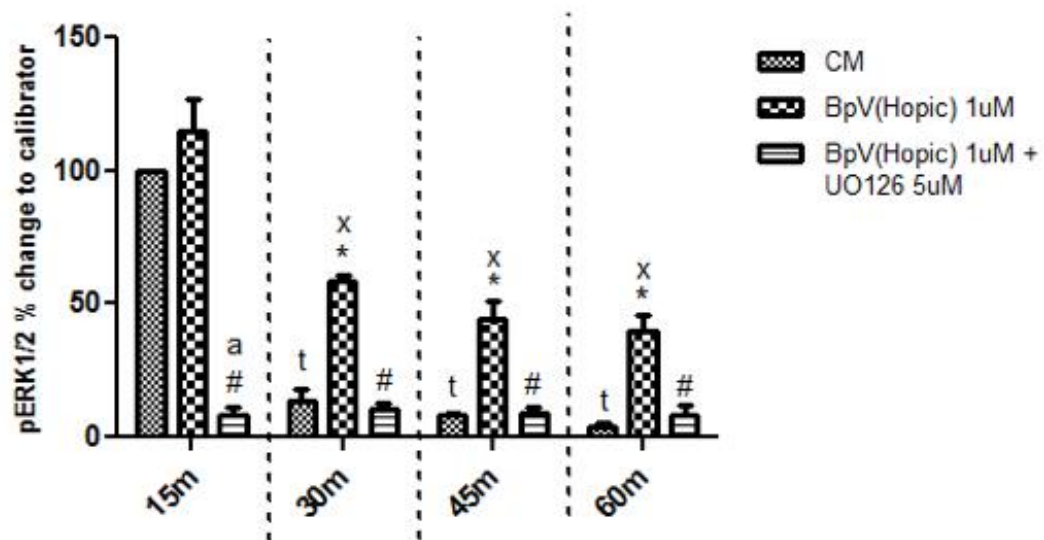


Figure 5.20. Quantification of pERK1/2 levels (CM, CM+1 μ M Bpv(Hopic) and CM+1 μ M Bpv(Hopic)+5 μ M UO126). Quantification of pERK1/2 activation levels in response to CM, CM+1 μ M Bpv(Hopic) and CM+1 μ M Bpv(Hopic)+5 μ M UO126 indicated significant increases with CM+1 μ M Bpv(Hopic) vs CM at 30m ($p < 0.0001$, represented by *), at 45m ($p < 0.001$, represented by *) and at 60m ($p < 0.01$, represented by *). Significant decrease were indicated with CM+1 μ M Bpv(Hopic)+5 μ M UO126 vs CM+1 μ M Bpv(Hopic) at 15m ($p < 0.0001$, represented by #), at 30m ($p < 0.0001$, represented by #), at 45m ($p < 0.001$, represented by #) and at 60m ($p < 0.01$, represented by #). Significant decreases were found with CM+1 μ M Bpv(Hopic)+5 μ M UO126 vs CM at 15m ($p < 0.001$, represented by a). Significant reductions with time were observed with CM at 30m vs 15m ($p < 0.001$, represented by t), at 45m vs 15m ($p < 0.001$, represented by t) and at 60m vs 15m ($p < 0.001$, represented by t). Reductions with time were also observed with CM+1 μ M Bpv(Hopic) at 30m vs 15m ($p < 0.01$, represented by x), at 45m vs 15m ($p < 0.01$, represented by x) and at 60m vs 15m ($p < 0.01$, represented by x). Data are representative of 4 experiments performed in duplicate. (p-values obtained by One-way repeated measures ANOVA)

Having determined that inhibition of Pi3K was able to reduce migration in the face of activated ERK1/2, it was investigated whether inhibition of the MAPK/ERK pathway by 5 μ M UO126 would affect the migration induced by Bpv(Hopic). Wound healing studies were initially performed (Figure 5.21A), which demonstrated decreases in cell migration, towards control levels (CM), with CM+1 μ M Bpv(Hopic)+5 μ M UO126 vs CM+1 μ M Bpv(Hopic). To confirm these observations, quantification of the total cell number infiltrating the wound

site was performed (Figure 5.21B). Analyses demonstrated significant increases with CM+1 μ M Bpv(Hopic) vs CM (97 \pm 7 vs 68 \pm 3, $p < 0.0001$, equivalent to 43% increase) and a comparable decrease with CM+1 μ M Bpv(Hopic)+5 μ M UO126 vs CM+1 μ M Bpv(Hopic) (68 \pm 3 vs 97 \pm 7, $p < 0.0001$, equivalent to 30% decrease). Quantification of the percentage of cells in the centre of the wounds (Figure 5.21C), demonstrated increases with CM+1 μ M Bpv(Hopic) vs CM (23.83 \pm 1.58% vs 11.33 \pm 1.5%, $p < 0.0001$), whereas decreases in cell numbers in the centre of the wound site were observed with CM+1 μ M Bpv(Hopic)+5 μ M UO126 vs CM+1 μ M Bpv(Hopic) (7.17 \pm 1.99% vs 23.83 \pm 1.58%, $p < 0.0001$) and vs CM (7.17 \pm 1.99% vs 11.33 \pm 1.5%), thus once again substantiating the data depicted in the photomicrographs (Figure 5.21(A)).

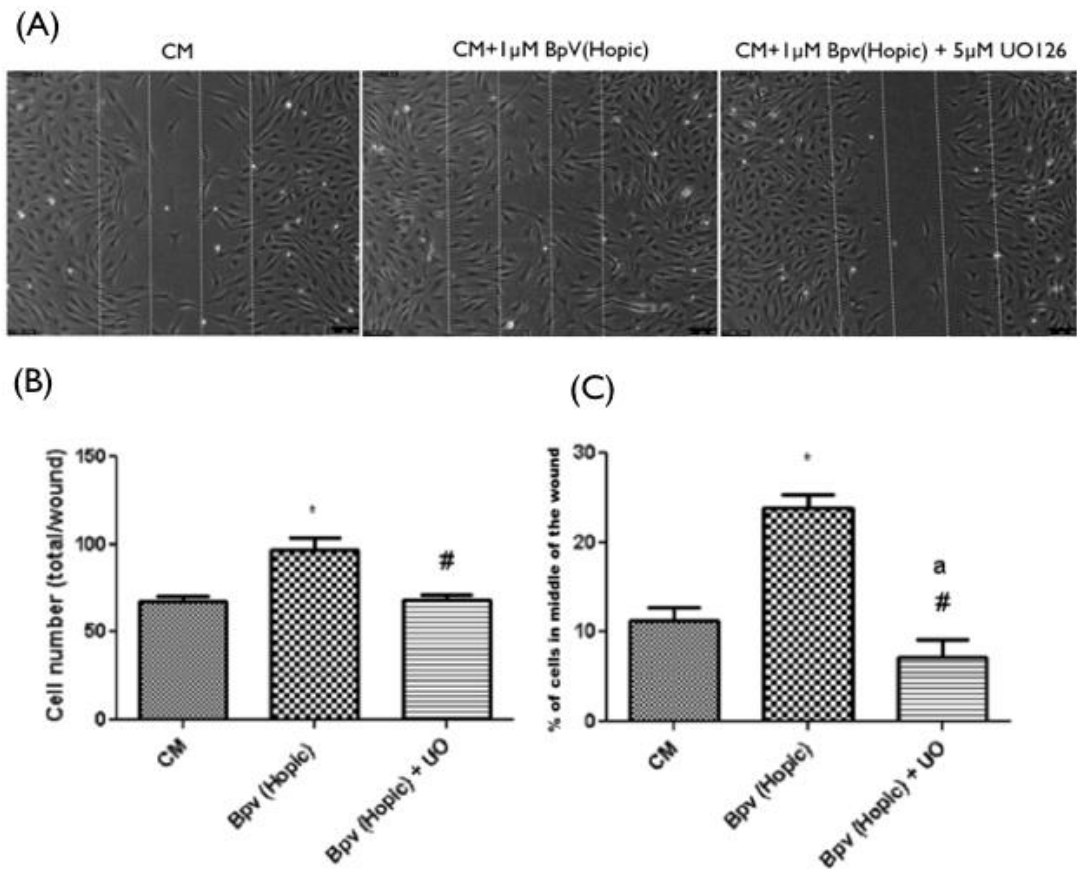


Figure 5.21. Wound healing assay with cell count analysis (CM, CM+1µM Bpv(Hopic) and CM+1µM Bpv(Hopic)+5µM UO126). Wound healing assay comparing the wound closure between CM , CM+1µM Bpv(Hopic) and CM+1µM Bpv(Hopic)+5µM UO126 (A). Quantification of the total number of cells infiltrating the wound demonstrated significant increase with CM+1µM Bpv(Hopic) vs CM ($p < 0.0001$, represented by *). Significant decreases were observed with CM+1µM Bpv(Hopic)+UO126 vs CM+1µM Bpv(Hopic) ($p < 0.0001$, represented by #) (B). Quantification of the percentage of cells in the middle of the wound revealed significant increases with CM+1µM Bpv(Hopic) vs CM ($p < 0.0001$, represented by *). A decrease was also observed with CM+1µM Bpv(Hopic)+5µM UO126 vs CM+1µM Bpv(Hopic) ($p < 0.0001$, represented by #) and vs CM ($p < 0.05$, represented by a) (C). Data are representative of 6 experiments performed in duplicate. (p-values obtained by One-way repeated measures ANOVA)

Cell tracking analyses were again performed to support the quantification data (Figure 5.22A) and indicated clearly that migration was greater with CM+1µM Bpv(Hopic) vs CM and that this increase in migration was suppressed by the co-incubation of 5µM UO126. Analyses of these images demonstrated significant increases in migration distance with CM+1µM Bpv(Hopic) vs CM ($573 \pm 72.6\mu\text{m}$ vs $413 \pm 44.4\mu\text{m}$, $p < 0.01$, equivalent to 39% increase) and a decreases

with CM+1 μ M Bpv(Hopic)+5 μ M UO126 vs CM+1 μ M Bpv(Hopic) (346 +/- 42.1 μ m vs 573 +/-72.6 μ m, $p < 0.0001$, equivalent to 40% decrease). No differences in migration distance were evident between CM and CM+1 μ M Bpv(Hopic)+5 μ M UO126 (Figure 5.22B). Cell death quantifications revealed no significant differences in cell death between CM+1 μ M Bpv(Hopic) and CM, however, surprisingly, there was a small but significant decrease in percentage dead cells with CM+1 μ M Bpv(Hopic)+5 μ M UO126 vs CM (0.46 +/-0.29% vs 2.07 +/-0.28%, $p < 0.05$), but no difference between CM+1 μ M Bpv(Hopic)+5 μ M UO126 and CM+1 μ M Bpv(Hopic) (Figure 5.22C).

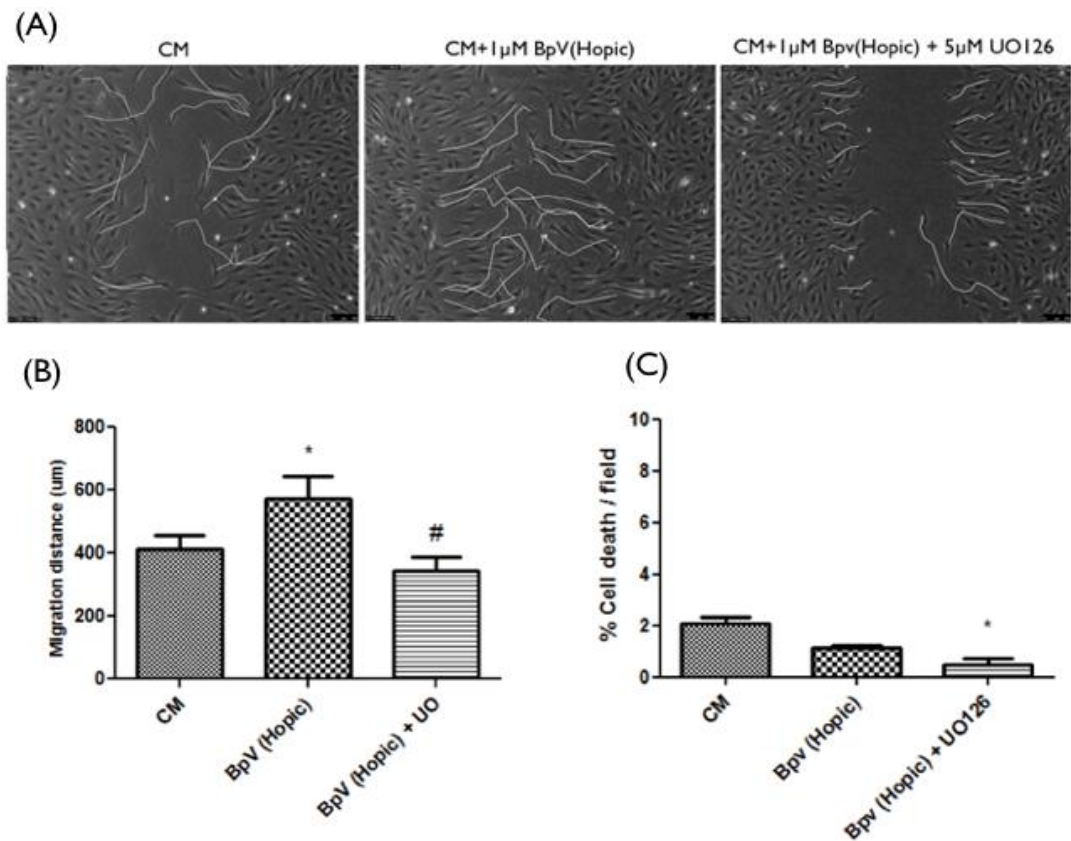


Figure 5.22. Cell tracking and cell death analyses (CM, CM+1 μ M Bpv(Hopic) and CM+1 μ M Bpv(Hopic)+5 μ M UO126). Migration tracking comparing the effects of CM, CM+1 μ M Bpv(Hopic) and CM+1 μ M Bpv(Hopic)+5 μ M UO126 (A). Quantifications of the data tracking, showing significant increases in migration with CM+1 μ M Bpv(Hopic) vs CM ($p < 0.01$, represented by *) and a decrease with CM+1 μ M Bpv(Hopic)+5 μ M UO126 vs CM+1 μ M Bpv(Hopic) ($p < 0.0001$, represented by #) (B). Data are representative of 6 experiments performed in duplicate. Cell death quantifications indicated decreased cell death with CM+1 μ M Bpv(Hopic)+5 μ M UO126 vs CM ($p < 0.05$, represented by *) (C). Data are representative of 4 experiments performed in duplicate. (p-values obtained by One-way repeated measures ANOVA)

5.4.6. THE ACTION OF BPV(HOPIC) ON CELL MIGRATION IS REDUCED BY INHIBITING THE FAK PATHWAY WITH PF-228, DESPITE ONGOING PI3K/AKT AND MAPK/ERK ACTIVATION

Bpv(Hopic) was shown to activate PI3K and MAPK pathways, but at μM concentrations it is possible that it also activates other protein targets, which might be involved in the regulation of myoblast migration. Integrin signalling is important for cell matrix interactions and the fact that Bpv(Hopic) impacts on cellular adhesion warranted further investigation. Furthermore, FAK is known to be regulated by PTEN and its tyrosine phosphorylated site may also be targeted by the phospho-tyrosine phosphatase activity of Bpv(Hopic). It was therefore investigated how FAK phosphorylation at tyrosine 397 was affected by Bpv(Hopic) and whether inhibition of the FAK pathway using the FAK inhibitor PF-228 would also affect myoblast migration induced by CM and by Bpv(Hopic).

Initially, preliminary western blots were performed to investigate the effect of increasing concentrations of BpV(Hopic) on the levels of p-FAK activation (Figure 5.23). No consistent differences in pFAK activation were visually observed between CM and CM+1 μM Bpv(Hopic). However, increased FAK phosphorylation was evident with 2 μM Bpv(Hopic) vs CM and FAK phosphorylation was increased further in the presence of 10 μM Bpv(Hopic). The lack of specificity of high dose Bpv(Hopic), as previously suggested in this report for tyrosine phosphorylated proteins, was again evident with an increased phosphorylation of FAK at tyrosine 397.

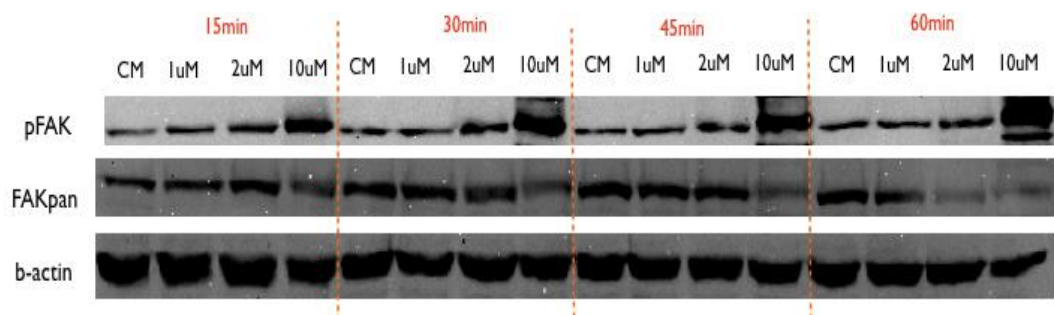


Figure 5.23. Western blots investigating the effect of 1 μM , 2 μM and 10 μM concentrations of Bpv(Hopic) on p-FAK(Tyr397) activation. An increase in pFAK levels, as compared to CM, was obvious with 2 μM and 10 μM , but not with 1 μM concentration of Bpv(Hopic). Data are representative of at least 3 experiments.

Although 1 μ M Bpv(Hopic) facilitated migration (as detailed above), it was without impact on FAK phosphorylation compared with CM. As it was wished to assess whether silencing the FAK pathway using PF-228 would influence the enhanced migration of myoblasts induced by Bpv(Hopic), 2 μ M dose was chosen for further assessment, where FAK was activated above control levels. It was also investigated whether the PI3K and MAPK pathways would remain activated despite the FAK pathway being silenced and whether their activation would impact on any migration changes affected by the FAK pathway inhibition.

Western blot analyses were performed to compare the effects of CM, CM+2 μ M PF-228, CM+2 μ M Bpv(Hopic) and CM+2 μ M Bpv(Hopic)+2 μ M PF-228 on protein activation levels of p-AKT, pERK1/2 and p-FAK (Figure 5.24). 2 μ M of PF-228 reduced the levels of pFAK activation (although not completely when co-incubated with 2 μ M Bpv(Hopic)), but did not appear to significantly affect the levels of pAkt or pERK1/2 (Figure 5.24).

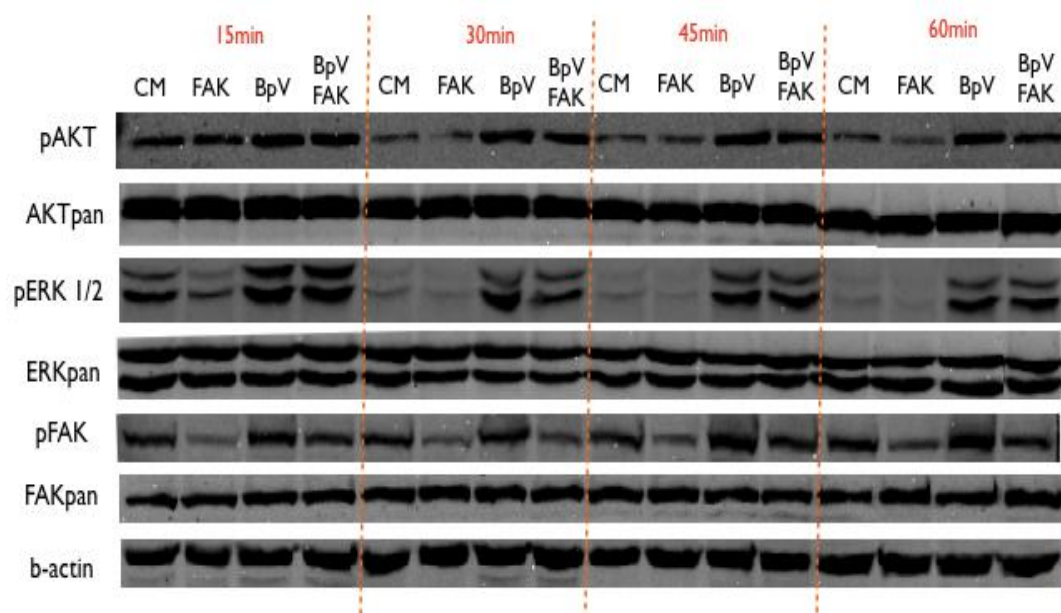


Figure 5.24. Western blots (CM, CM+2 μ M PF-228, CM+2 μ M Bpv(Hopic), CM+2 μ M Bpv(Hopic)+2 μ M PF-228). Western blot comparing the effects of CM (Lane 1, 5, 9, and 13=CM), CM+2 μ M PF-228 (Lane 2, 6, 8 and 14=FAK), CM+2 μ M Bpv(Hopic) (Lane 3, 7, 9 and 15=BpV) and CM+2 μ M Bpv(Hopic)+2 μ M PF-228 (Lane 4, 8, 10 and 16=Bpv+FAK) on Akt, ERK1/2 and FAK activation. Obvious increases in pAKT, pERK1/2 and pFAK activation were observed with 2 μ M Bpv(Hopic). A decrease was observed in pFAK levels in the presence of 2 μ M of PF-228, while pAKT and pERK1/2 levels did not seem to be significantly affected by the FAK inhibitor. Data are representative of at least 3 experiments.

Blots (Figure 5.24) were subsequently subjected to further analyses using Quantity One software. Phospho-FAK, Phospho-Akt and Phospho-ERK1/2 levels were quantified across the 4 different treatments and the 4 time points. All values are represented as percentage of the calibrator (CM 15m), which was set to 100% (Figure 5.25).

Analysis of pFAK (Tyr397) was performed in response to CM, CM+2 μ M PF-228, CM+2 μ M Bpv(Hopic) and CM+2 μ M Bpv(Hopic)+2 μ M PF-228 (Figure 5.25). Significant increases were found with CM+2 μ M Bpv(Hopic) vs CM at 15m (150.25 \pm 10.81% vs 100%, $p < 0.01$), at 30m (170.75 \pm 18.33% vs 124.75 \pm 6.91%, $p < 0.05$), at 45m (186 \pm 17.5% vs 134.5 \pm 21.2%, $p < 0.05$) and at 60m (176.25 \pm 20.65% vs 124 \pm 8.65%, $p < 0.05$), suggesting that 2 μ M Bpv(Hopic) is upregulating the levels of phosphorylated FAK. On the other hand, PF-228 inhibitor treatment, caused decreases in pFAK phosphorylation, as compared to CM: decreases were observed with CM+2 μ M PF-228 vs CM at 15m (40.74 \pm 7.32% vs 100%, $p < 0.001$), at 30m (58 \pm 9.65% vs 124.75 \pm 6.91%, $p < 0.05$), at 45m (72.25 \pm 12.74% vs 134.5 \pm 21.2%, $p < 0.01$) and at 60m (66.75 \pm 12.55% vs 124 \pm 8.65%, $p < 0.01$). Furthermore, PF-228 treatment, eliminated the increase observed with 2 μ M Bpv(Hopic) treatment: decreases were observed with CM+2 μ M Bpv(Hopic)+2 μ M PF-228 vs CM+2 μ M Bpv(Hopic) at 15m (78.25 \pm 4.64% vs 150.25 \pm 10.81%, $p < 0.0001$), at 30m (100.75 \pm 12.34% vs 170.75 \pm 18.33%, $p < 0.01$), at 45m (125.25 \pm 12.87% vs 186 \pm 17%, $p < 0.01$) and at 60m (103.25 \pm 13% vs 176.25 \pm 20.65%, $p < 0.01$). Greater decreases were observed with CM+2 μ M PF-228 vs CM+2 μ M Bpv(Hopic) at 15m (40.74 \pm 7.32% vs 150.25 \pm 10.81%, $p < 0.0001$), at 30m (58 \pm 9.65% vs 170.75 \pm 18.33%, $p < 0.0001$), at 45m (72.25 \pm 12.74% vs 186 \pm 17.5%, $p < 0.0001$) and at 60m (66.75 \pm 12.55% vs 176.25 \pm 20.65%, $p < 0.0001$). Significant decreases were also found with CM+2 μ M PF-228 vs CM+2 μ M Bpv(Hopic)+2 μ M PF-228 at 15m (40.74 \pm 7.32% vs 78.25 \pm 4.64%, $p < 0.05$) and at 45m (72.25 \pm 12.74% vs 125.25 \pm 12.87%, $p < 0.05$). Overall, these observations indicate an increase in the phosphorylation of FAK at Tyr397 in response to 2 μ M Bpv(Hopic) treatment. Treatment with 2 μ M PF-228 inhibitor either caused a decrease in the base levels of pFAK (CM), or eliminated the increase observed with 2 μ M Bpv(Hopic) treatment.

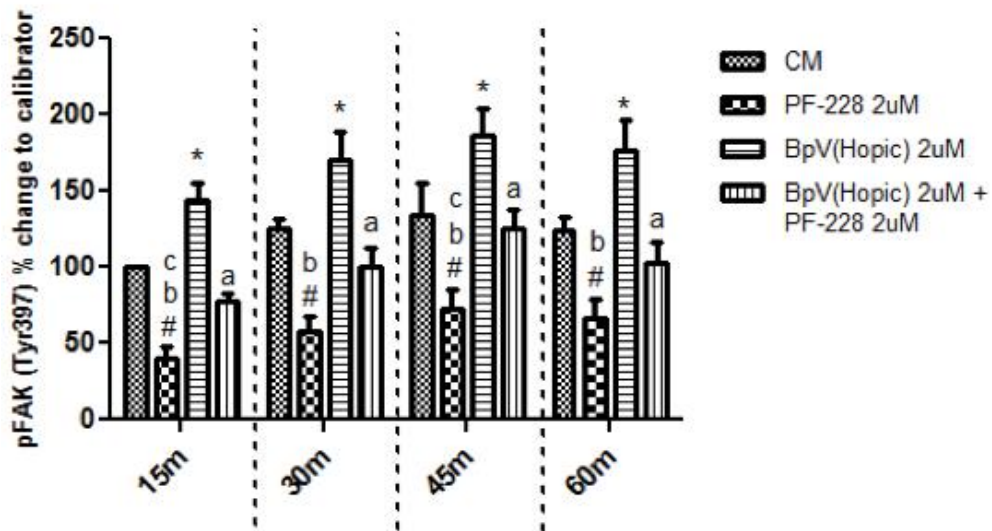


Figure 5.25. Quantification of pFAK levels (CM, CM+2µM PF-228, CM+2µM Bpv(Hopic), CM+2µM Bpv(Hopic)+2µM PF-228). Quantification of pFAK levels in response to CM, CM+2µM PF-228, CM+2µM Bpv(Hopic) and CM+2µM Bpv(Hopic)+2µM PF-228 indicated significant increases with CM+2µM Bpv(Hopic) vs CM at 15m ($p < 0.01$, represented by *), at 30m ($p < 0.05$, represented by *), at 45m ($p < 0.05$, represented by *) and at 60m ($p < 0.05$, represented by *). Decreases with CM+2µM PF-228 vs CM was found at 15m ($p < 0.001$, represented by #), at 30m ($p < 0.05$, represented by #), at 45m ($p < 0.01$, represented by #) and at 60m ($p < 0.01$, represented by #). Decreases with CM+2µM PF-228 vs CM+2µM Bpv(Hopic) were found at 15m ($p < 0.0001$, represented by b), at 30m ($p < 0.0001$, represented by b), at 45m ($p < 0.0001$, represented by b) and at 60m ($p < 0.0001$, represented by b). Decreases were observed with CM+PF-228 vs CM+2µM Bpv(Hopic)+2µM PF-228 at 15m ($p < 0.05$, represented by c) and at 45m ($p < 0.05$, represented by c). Decreases with CM+2µM Bpv(Hopic)+PF-228 vs CM+2µM Bpv(Hopic) was found at 15m ($p < 0.0001$, represented as a), at 30m ($p < 0.01$, represented as a), at 45m ($p < 0.01$, represented by a) and at 60m ($p < 0.01$, represented by a). Data are representative of 4 experiments. (p-values obtained by One-way repeated measures ANOVA)

In order to verify whether pFAK inhibition resulted in changes in the levels of pAKT, analyses of pAKT (Ser473) were performed in response to CM, CM+2µM PF-228, CM+2µM Bpv(Hopic) and CM+2µM Bpv(Hopic)+2µM PF-228 (Figure 5.26). What is evident from these data, as indicated previously, is that Bpv(Hopic) treatment significantly increased pAkt phosphorylation over the full time course, relative to CM and that a co-incubation with PF-228 had not impact on this increase. PF-228 alone was also without significant effect on CM treatment alone when pAkt activation was investigated (Figure 5.26).

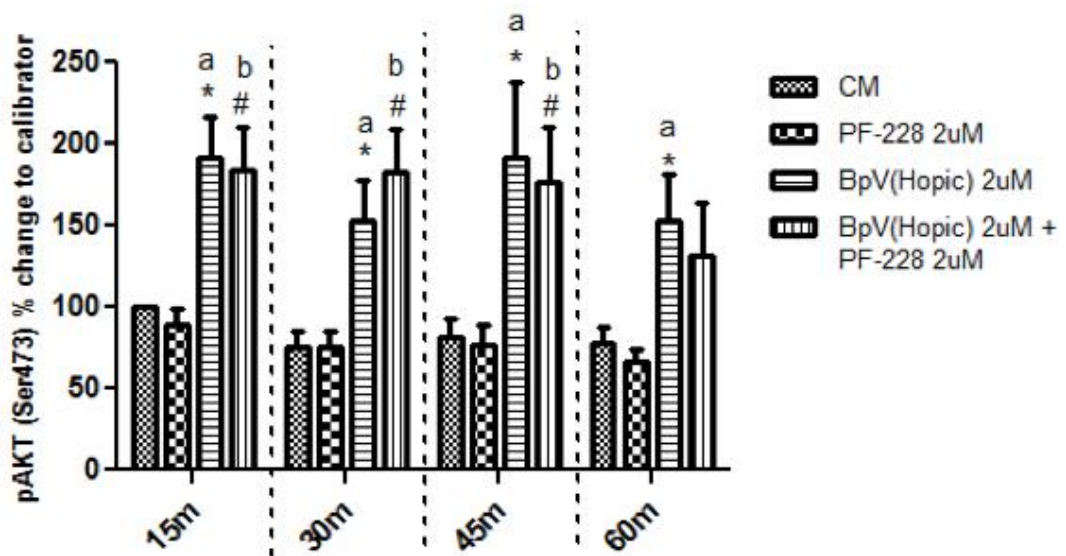


Figure 5.26. Quantification of pAKT levels (CM, CM+2 μ M PF-228, CM+2 μ M Bpv(Hopic), CM+2 μ M Bpv(Hopic)+2 μ M PF-228). Quantification of pAKT levels in response to CM, CM+2 μ M PF-228, CM+2 μ M Bpv(Hopic) and CM+2 μ M Bpv(Hopic)+2 μ M PF-228 indicated significant increases with CM+2 μ M Bpv(Hopic) vs CM at 15m ($p < 0.05$, presented by *), at 30m ($p < 0.05$, presented by *), at 45m ($p < 0.01$, represented by *) and at 60m ($p < 0.05$, presented by *). Significant increases were found with CM+2 μ M Bpv(Hopic)+2 μ M PF-228 vs CM at 15m ($p < 0.05$, represented by #), at 30m ($p < 0.01$, represented by #) and at 45m ($p < 0.05$, represented by #). Significant increases with CM+2 μ M Bpv(Hopic) vs CM+2 μ M PF-228 were found at 15m ($p < 0.01$, represented by a), at 30m ($p < 0.05$, represented by a), at 45m ($p < 0.01$, represented by a) and at 60m ($p < 0.05$, represented by a). Significant increases were found with CM+2 μ M Bpv(Hopic)+2 μ M PF-228 vs CM+2 μ M PF-228 at 15m ($p < 0.01$, represented by b), at 30m ($p < 0.05$, represented by b) and at 45m ($p < 0.05$, represented by b). Data are representative of 5 experiments. (p-values obtained by One-way repeated measures ANOVA)

Analyses of pERK1/2 were performed in response to CM, CM+2 μ M PF-228, CM+2 μ M Bpv(Hopic) and CM+2 μ M Bpv(Hopic)+2 μ M PF-228 (Figure 5.27). As previously reported, Bpv (Hopic) induced a significantly increased activation of pERK1/2, which was not altered in the presence of PF-228, regardless of time. Similarly, PF228 was without impact on ERK1/2 phosphorylation when compared to CM at any given time. There were, however, significant decreases in ERK1/2 phosphorylation over time in the presence of CM and Bpv(Hopic). These declines were not, however, further decreased by PF-228. Therefore, while PF-

228 was able to decrease pFAK activation, it was without direct effect on Akt or ERK1/2 phosphorylation under basal or Bpv(Hopic) conditions.

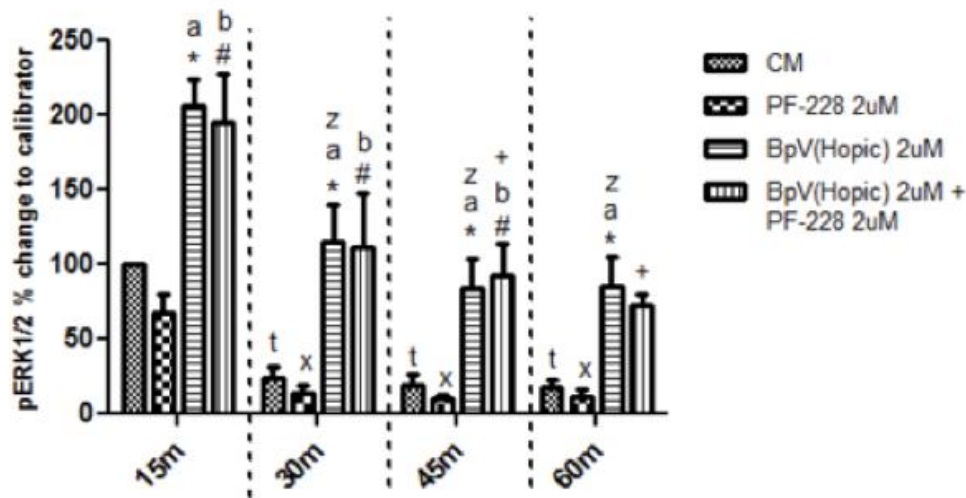


Figure 5.27. Quantification of pERK1/2 levels (CM, CM+2 μ M PF-228, CM+2 μ M Bpv(Hopic), CM+2 μ M Bpv(Hopic)+2 μ M PF-228). Quantification of pERK1/2 activation levels in response to CM, CM+2 μ M PF-228, CM+2 μ M Bpv(Hopic) and CM+2 μ M Bpv(Hopic)+2 μ M PF-228 indicated significant increases with CM+2 μ M Bpv(Hopic) vs CM at 15m ($p < 0.05$, represented by *), at 30m ($p < 0.05$, represented by *), 45m ($p < 0.05$, represented by *) and at 60m ($p < 0.05$, represented by *). Significant increases were also found with CM+2 μ M Bpv(Hopic)+2 μ M PF-228 vs CM at 15m ($p < 0.05$, represented by #), at 30m ($p < 0.05$, represented by #) and at 45m ($p < 0.05$, represented by #). Significant increase was observed with CM+2 μ M Bpv(Hopic) vs CM+2 μ M PF-228 at 15m ($p < 0.01$, represented by a), at 30m ($p < 0.05$, represented by a), at 45m ($p < 0.05$, represented by a) and at 60m ($p < 0.05$, represented by a). Significant increases were found with CM+2 μ M Bpv(Hopic)+2 μ M PF-228 vs CM+2 μ M PF-228 at 15m ($p < 0.01$, represented by b), at 30m ($p < 0.05$, represented by b) and at 45m ($p < 0.05$, represented by b). Significant reductions with time were observed: with CM at 30m vs 15m ($p < 0.001$, represented by t), at 45m vs 15m ($p < 0.001$, represented by t) and at 60m vs 15m ($p < 0.001$, represented by t). Reductions were also observed with CM+2 μ M PF-228 at 30m vs 15m ($p < 0.01$, represented by x), at 45m vs 15m ($p < 0.01$, represented by x) and at 60m vs 15m ($p < 0.01$, represented by x). Decreases were observed with CM+2 μ M Bpv(Hopic) at 30m vs 15m ($p < 0.05$, represented by z), at 45m vs 15m ($p < 0.01$, represented by z) and at 60m vs 15m ($p < 0.01$, represented by z). Significant reductions were also observed with time with CM+2 μ M Bpv(Hopic)+2 μ M PF-228 at 45m vs 15m ($p < 0.05$, represented as c) and 60m vs 15m ($p < 0.05$, represented as c). Data are representative of 3 experiments. (p-values obtained by One-way repeated measures ANOVA)

Wound healing assays were performed in C2C12 cells investigating the effect of FAK inhibition using 2 μ M PF-228 in combination with CM (Figure 5.28A). Four different treatments were compared: CM, CM+2 μ M PF-228, CM+2 μ M Bpv(Hopic) and CM+2 μ M Bpv(Hopic)+2 μ M PF-228. As is evident from the photomicrographs, PF-228 decreased migration vs CM, while Bpv(Hopic) alone increased cellular migration vs. CM. In combination with PF-228, Bpv(Hopic)-induced migration was reduced back to CM levels. Wishing to confirm these findings, quantification of the total number of cells infiltrating the wound was performed (Figure 5.28B) and indicated significant increases with CM+2 μ M Bpv(Hopic) vs CM (111 \pm 8 vs 83 \pm 1 cells, $p < 0.01$, equivalent to 34% increase). Decreases were observed with CM+2 μ M PF-228 vs CM (49 \pm 5 vs 83 \pm 1, $p < 0.001$, equivalent to 41% decrease) and vs CM+2 μ M Bpv(Hopic) (49 \pm 5 vs 111 \pm 8, $p < 0.0001$, equivalent to 56% decrease). A decrease was also detected with CM+2 μ M Bpv(Hopic)+2 μ M PF-228 vs CM+2 μ M Bpv(Hopic) (67 \pm 7 vs 111 \pm 8, $p < 0.001$, equivalent to 40% decrease). Quantification of the percentage of cells in the middle of the wound (Figure 5.28C) indicated significant increases with CM+2 μ M Bpv(Hopic) vs CM (19.75 \pm 2.25% vs 7 \pm 1.15%, $p < 0.001$). Decreases were observed with CM+2 μ M PF-228 vs CM (1 \pm 0.58% vs 7 \pm 1.15%, $p < 0.05$) and vs CM+2 μ M Bpv(Hopic) (1 \pm 0.58% vs 19.75 \pm 2.25%, $p < 0.0001$). A decrease was indicated with CM+2 μ M Bpv(Hopic)+2 μ M PF-228 vs CM+2 μ M Bpv(Hopic) (3.5 \pm 1.04% vs 19.75 \pm 2.25%, $p < 0.0001$).

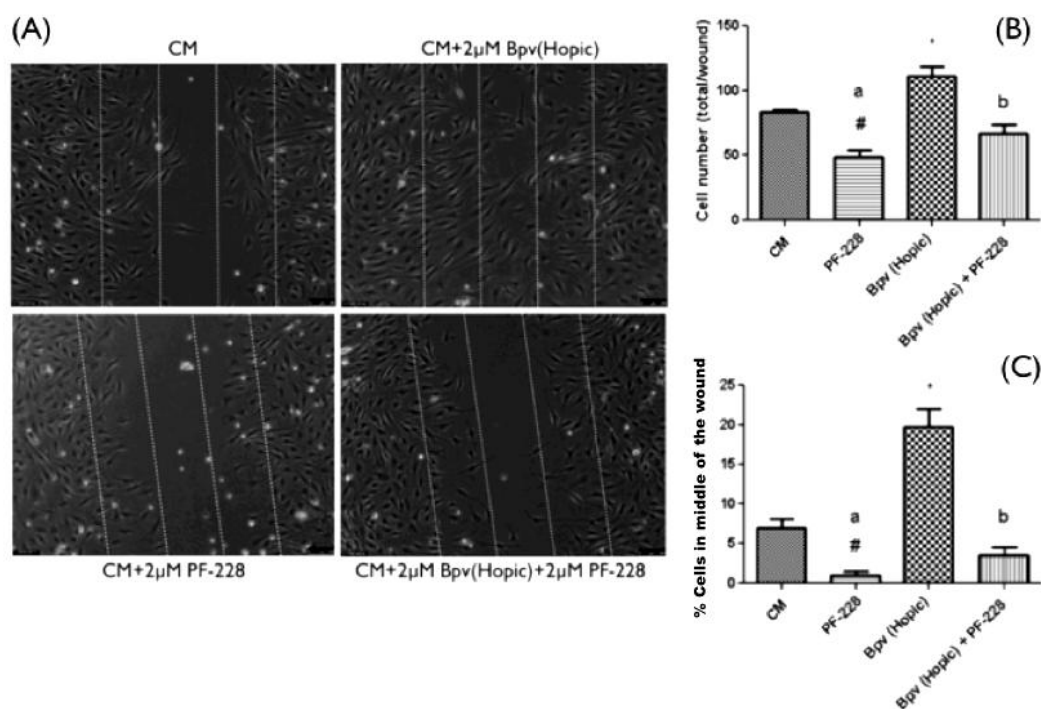


Figure 5.28. Wound healing assay with cell count analysis (CM, CM+2µM PF-228, CM+2µM Bpv(Hopic), CM+2µM Bpv(Hopic)+2µM PF-228). Wound healing assays comparing the effects of CM, CM+2µM PF-228, CM+2µM Bpv(Hopic) and CM+2µM Bpv(Hopic)+2µM PF-228 (A). Quantification of the number of cells infiltrating the wound indicates significant increases with CM+2µM Bpv(Hopic) vs CM ($p < 0.01$, represented by *). A decrease was observed with CM+2µM PF-228 vs CM ($p < 0.001$, represented by #) and vs CM+2µM Bpv(Hopic) ($p < 0.0001$, represented by a). Decreases were indicated with CM+2µM Bpv(Hopic)+2µM PF-228 vs CM+2µM Bpv(Hopic) ($p < 0.001$, represented by b) (B). Quantification of percentage of cell in the centre of the wound indicated increases with CM+2µM Bpv(Hopic) vs CM ($p < 0.001$, represented by *). A decrease was found with CM+2µM PF-228 vs CM ($p < 0.05$, represented by #) and vs CM+2µM Bpv(Hopic) ($p < 0.0001$, represented by a). Decreases were observed with CM+2µM Bpv(Hopic)+2µM PF-228 vs CM+2µM Bpv(Hopic) ($p < 0.0001$, represented by b) (C). All data are representative of 4 experiments performed in duplicate. (p-values obtained by One-way repeated measures ANOVA)

Subsequently, cell tracking was performed to support the quantification data (Figure 5.29A). As images indicate, supporting the quantification data, PF-228 decreased migration distance vs CM, Bpv(Hopic) increased migration vs CM and PF-228 in the presence of Bpv(Hopic) decreased Bpv-induced migration to CM levels. Analyses of cell migration distances (Figure 5.29B) confirmed the morphological findings and indicated significant increases in migration distances

with CM+2 μ M Bpv(Hopic) vs CM (481 \pm 12.8 μ m vs 352 \pm 11.6 μ m, p <0.0001, equivalent to 37% increase). A decrease was found with CM+2 μ M PF-228 vs CM (195 \pm 8.18 μ m vs 352 \pm 11.6 μ m, p <0.0001, equivalent to 45% decrease), vs CM+2 μ M Bpv(Hopic) (195 \pm 8.18 μ m vs 481 \pm 12.8 μ m, p <0.0001, equivalent to 247% increase) and vs CM+2 μ M Bpv(Hopic)+2 μ M PF-228 (195 \pm 8.18 μ m vs 262 \pm 5 μ m, p <0.01, equivalent to 26% decrease). A decrease was also observed with CM+2 μ M Bpv(Hopic)+PF-228 vs CM (262 \pm 5 μ m vs 352 \pm 11.6 μ m, p <0.001, equivalent to 26% decrease) and vs CM+2 μ M Bpv(Hopic) (262 \pm 5 μ m vs 481 \pm 12.8 μ m, p <0.0001, equivalent to 46% decrease).

Cell death analyses (Figure 5.29C) indicated an increase in cell death with CM+2 μ M PF-228 vs CM (3.48 \pm 1.03% vs 1.14 \pm 0.43%, p <0.05), vs CM+2 μ M Bpv(Hopic) (3.48 \pm 1.03% vs 0.66 \pm 0.19%, p <0.01) and vs CM+2 μ M Bpv(Hopic)+PF-228 (3.48 \pm 1.03% vs 1.58 \pm 0.58%, p <0.05).

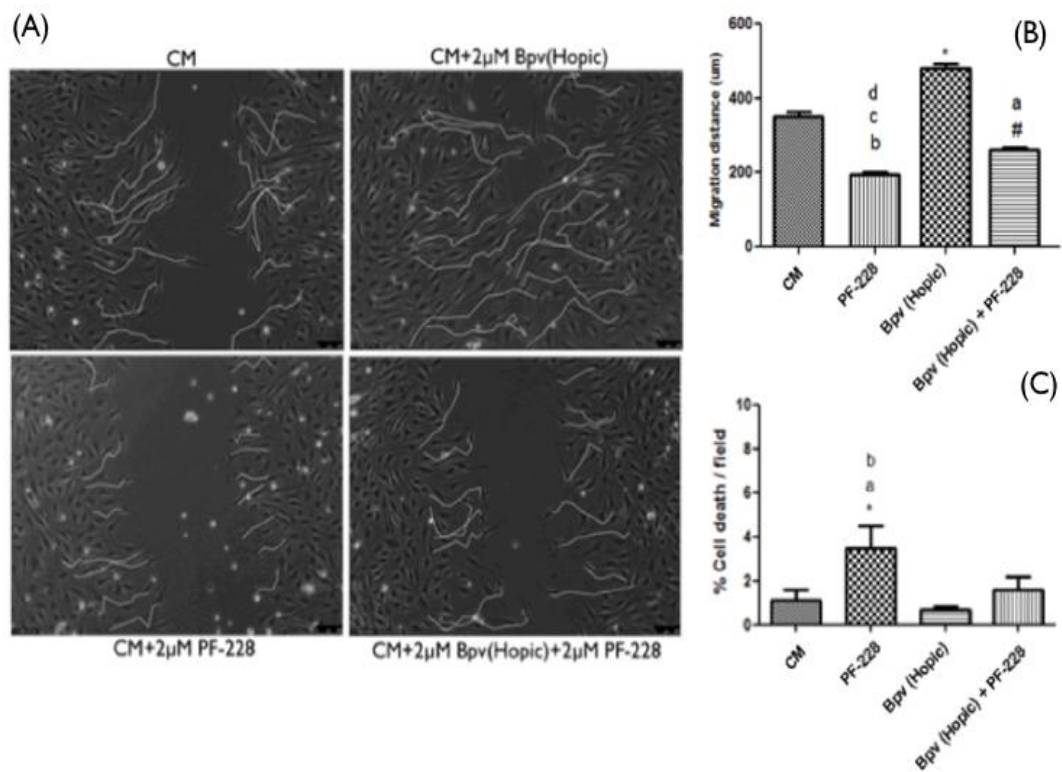


Figure 5.29. Cell tracking and cell death analysis (CM, CM+2µM PF-228, CM+2µM Bpv(Hopic), CM+2µM Bpv(Hopic)+2µM PF-228). Cell tracking comparing the effects of CM, CM+2µM PF-228, CM+2µM Bpv(Hopic) and CM+2µM Bpv(Hopic)+2µM PF-228 (A). Analyses of cell tracking indicated significant increases with CM+2µM Bpv(Hopic) vs CM ($p < 0.0001$, represented by *). A decrease was found with CM+2µM PF-228 vs CM ($p < 0.0001$, represented by b), vs CM+2µM Bpv(Hopic) ($p < 0.0001$, represented by c) and vs CM+2µM Bpv(Hopic)+2µM PF-228 ($p < 0.01$, represented by d). A significant decrease was observed with CM+2µM Bpv(Hopic)+2µM PF-228 vs CM ($p < 0.001$, represented by #) and vs CM+2µM Bpv(Hopic) ($p < 0.0001$, represented by a) (B). Cell death quantifications indicated increased death with CM+PF-228 vs CM ($p < 0.05$, represented as *), vs CM+2µM Bpv(Hopic) ($p < 0.01$, represented as a) and vs CM+2µM Bpv(Hopic)+PF-228 ($p < 0.05$, represented as b) (C). All data are representative of 4 experiments performed in duplicate. (p-values obtained by One-way repeated measures ANOVA)

SUMMARY OF MAJOR FINDINGS:

- 1 μ M Bpv(Hopic) is capable of increasing migration of myoblasts, stimulated by myotube conditioned media, without significantly affecting their capacity to differentiate and fuse into multinucleated myotubes.
- Increased migration of myoblasts following 1 μ M Bpv(Hopic) treatment is associated with enhanced PI3K/AKT and MAPK/ERK signalling and inhibition of each of these pathways with either LY294002 or UO126 leads to reduced myoblast migration.
- Inhibition of FAK signalling by PF-228 leads to reduced myoblast migration, regardless of the activity of PI3K/AKT and MAPK/ERK signalling.

5.5. DISCUSSION

5.5.1. MYOBLAST DIFFERENTIATION IS REDUCED BY 10 μ M, BUT NOT BY 1 μ M BPV(HOPIC)

Previous reports have demonstrated a significant reduction in the ability of C2C12 cells to differentiate and fuse into myotubes following 10 μ M of BpV treatment (Castaldi *et al.*, 2007). It was here confirmed that 10 μ M Bpv(Hopic) significantly reduced the differentiation capability of myoblasts grown in 2% HS DM, which was characterised by delayed exit from the cell cycle, as shown by the significantly higher percentage of cells in S/G2-phase. However, lower concentrations of 1 μ M and 2 μ M Bpv(Hopic) did not seriously affect the fusion of myoblasts into multinucleated myotubes. 2 μ M Bpv(Hopic) showed a slight, but significant, reduction in the activity of CK and the expression levels of Myogenin, although myotube formation was still evident. 1 μ M Bpv(Hopic) treatment did not cause any statistically significant changes in CK activity, or in the expression of MyoD or Myogenin, and myotube formation was visually unchanged, as compared to control CM. These data demonstrate that the ability of BpV compounds to affect myoblast differentiation is only exerted with higher concentrations, or at least in the current *in vitro* model studied. Furthermore, as demonstrated by Castaldi *et al.* and confirmed by our investigation (results not shown), even the effects of high concentrations of Bpv(Hopic) on myoblast differentiation were completely reversible, as upon withdrawal of the inhibitor from the system, differentiation potential of myoblasts was restored and they were able to fuse into myotubes (Castaldi *et al.*, 2007). This effect of Bpv(Hopic) may be important when considering its potential applications, as a tool for enhancing cell migration, without seriously affecting the ability of myoblasts to differentiate and fuse into myotubes. 1 μ M Bpv(Hopic) was therefore considered as an attractive tool for further studies on its effect on myoblast migration.

5.5.2. BPV(HOPIC) INCREASED C2C12 MYOBLAST MIGRATION AND ENHANCED ACTIVATION OF MAPK/ERK AND PI3K/AKT PATHWAYS

BpV compounds are reported to act as a PTEN inhibitors (Schmid *et al.*, 2004). However, this specificity is not retained with increasing concentrations. Using anti-phosphotyrosine (py20) antibodies, the phosphorylation of tyrosines under increasing concentrations of BpV(Hopic) was examined by western blots. Non-

specific phosphorylation of tyrosines with 10 μ M Bpv(Hopic) was observed and reduced specificity decreased with decreasing concentrations of Bpv(Hopic). This increased non-specific tyrosine phosphorylation coincided with cell shrinking and loss of cell adhesion, along with decreased myoblast differentiation, as previously reported. Thus, non-specific activation of many signalling pathways and downstream target proteins was probably present when cells were stimulated with 10 μ M concentration. Furthermore, 10 μ M Bpv(Hopic) caused significant delays in the initiation of migration, due to cell shrinking. Therefore, for further studies, it was decided to explore in more detail the effects of lower concentrations of Bpv(Hopic) on migration. Semi-quantitative analyses of Western blots demonstrated activation of PI3K/AKT and MAPK/ERK pathways with 1 μ M Bpv(Hopic), as compared to control CM. These pathways have previously been suggested to be important for myoblast migration, although articles have not been completely unanimous on this topic, with some suggesting either PI3K or MAPK pathway inhibition not affecting migration (Leloup *et al.*, 2007, Ranzato *et al.*, 2009, Suzuki *et al.*, 2000), while others reporting their requirement for migration of myogenic cells (Al-Shanti *et al.*, 2011, Kawamura *et al.*, 2004, Kim *et al.*, 2011). When migration of myoblasts was examined, it was reported that 1 μ M Bpv(Hopic) treatment induced ~40% more migration in myoblasts, compared with controls. These data were in agreement with the hypothesis that BpV was capable of activating PI3K/AKT and MAPK/ERK pathways and was able to further enhance the migration of myoblasts. At the same time, the same dose of BpV did not significantly affect the differentiation potential of myoblasts. These effects of BpV(Hopic) on myoblasts proposes interesting avenues for further research, in order to investigate whether it can also promote myoblast migration *in vivo* and how this would impact on the regeneration of muscle.

5.5.3. INHIBITION OF EITHER MAPK/ERK OR PI3K/AKT PATHWAYS RESULTED IN INHIBITION OF MYOBLAST MIGRATION TO BASAL CONTROL LEVELS

Despite PI3K/AKT and MAPK/ERK pathways being activated by BpV(Hopic), it is possible that the enhanced migration is mediated by other signalling pathways affected by the inhibitor. In order to reveal whether PI3K/AKT and MAPK/ERK pathways are required for Bpv(Hopic)-induced migration, these pathways were inhibited by LY294002 and UO126 in the presence of BpV and migration was

assessed. Results showed that inhibition of PI3K/AKT pathway by 10 μ M LY294002 did not affect the MAPK/ERK pathway, while migration of myoblasts dropped to basal control levels. Similarly, inhibition of MAPK/ERK pathway with 5 μ M UO126 did not affect the PI3K/AKT pathway, while migration was inhibited to the levels of control CM. Cell death levels were not greatly affected by any of the inhibitors, although, due to the high number of repetitions in section 5.4.3, a slight, but statistically significant decrease of less than 1% was detected following Bpv(Hopic) treatment. A decrease in the percentage of dead cells would be expected following PTEN inhibition and PI3K/Akt activation, a known pathway involved in cell survival (Sun *et al.*, 1999, Yamada and Araki, 2001). However, basal cell death was very low and differences between treatments were also extremely small and on the whole non-significant, therefore, it was concluded that cell death does not influence the migratory capacity of cells.

The above findings are novel within the muscle field. However, a recent article, published during the writing of this thesis, demonstrated very similar findings using epithelial cells (Mihai *et al.*, 2012). They also confirmed activation of PI3K/AKT and MAPK/ERK pathways in response to phospho-tyrosine phosphatase inhibitor Bpv(Phen), suggesting involvement of these pathways in regulating cell migration in response to the inhibitor, and that silencing of each pathway resulted in reduction of cell migration to basal control levels. It was further suggested that alterations in biomechanical properties of cells is what triggers the migration by Bpv. The similarity between our results and the findings by Mihai *et al.* strengthen our findings and also suggest similar migration mechanisms of action between different cell types.

5.5.4. FAK IS NOT AFFECTED BY BPV(HOPIC) AT CONCENTRATIONS BELOW 2 μ M, BUT ITS INHIBITION REDUCES MYOBLAST MIGRATION WITH OR WITHOUT BPV(HOPIC)

Cell shrinking and reduced ability of myoblasts to adhere following treatment with increasing concentration of Bpv(Hopic) was observed. Focal adhesion kinase (FAK) is known to be of major importance for the regulation of cell adhesion (Michael *et al.*, 2009). It is a protein tyrosine kinase, known for its recruitment at the focal adhesion sites of cells and also for mediating downstream signals regulating processes such as survival, cell spreading and migration. Clustering of integrins leads to the recruitment of FAK to the focal adhesion sites and to its

activation by tyrosine phosphorylation, a key site being tyrosine 397 (Parsons *et al.*, 2000). Phosphorylation at tyr397 allows the binding of Src and the subsequent activation of the FAK-Src complex, which is central to the regulation of downstream signals, for processes including cell migration (Hamadi *et al.*, 2005, Siesser and Hanks, 2006). The involvement of FAK in cell migration has been reported in a number of studies: FAK deficient cells migrate poorly, while overexpression of FAK enhances cell migration (Cary *et al.*, 1996, Desai *et al.*, 2009, Sieg *et al.*, 1999). Inhibitor studies have also reported the importance of FAK on cell migration (Slack-Davis *et al.*, 2007). The FAK-Src complex promotes migration by its association with several signalling pathways, including JNK, paxillin and by changes in adhesion dynamics (Hanks *et al.*, 2003, Schlaepfer and Mitra, 2004, Schlaepfer *et al.*, 2004). Furthermore, the level of tyrosine phosphorylation of FAK is reportedly inversely correlated to the level of PTEN protein in hepatoma cells (Zhang *et al.*, 2004). PTEN has been reported to directly associate with FAK resulting in FAK dephosphorylation, thus regulating cell migration and spreading (Gu *et al.*, 1999). Taking this into consideration, a potential involvement of FAK in the Bpv(Hopic)-induced migration of myoblasts was suggested. It was suggested that the protein tyrosine phosphatase activity of Bpv might influence FAK activation and thus cell migration. Initial studies, however, revealed no observational differences with 1 μ M Bpv(Hopic) on pFAK (tyr397). Recent studies, investigating the effect of Bpv(Phen) inhibitor on epithelial cells, suggested that BpV might in fact affect the FAK activity, however only in migrating cells and not in confluent ones (Mihai *et al.*, 2012). Thus, as protein lysates were obtained from a confluent monolayer of myoblasts, the potential activation of FAK in migrating cells might not have been accounted for in these studies. It was observed that increasing concentrations of Bpv(Hopic), such as 2 μ M, which have demonstrated to enhance the phosphorylation of tyrosine residues, also increased the phosphorylation of FAK on tyr397 and induced myoblast migration. To begin to assess the specificity of this response, cells were also co-incubated with the FAK inhibitor PF-228. The purpose was to investigate how myoblasts would migrate following activation of FAK and how its inhibition would affect the levels of pAKT, pERK1/2 (e.g. specificity of the inhibitor) and subsequently the capacity of the cells to migrate. Results here suggested that inhibition of the FAK pathway by the inhibitor PF-228 (2 μ M) resulted in reduced migration and enhanced cell death, concomitant with the role

of FAK in mediating cell survival (Huang *et al.*, 2007, Parsons *et al.*, 2000). Interestingly, a reduction in the PI3K/AKT pathway following FAK inhibition, as reported by others, was not observed (Xia *et al.*, 2004). As suggested by others, it is possible that FAK inhibition mediates cell death via other pathways, independent of PI3K, involving JNK, RIP or p53 (Almeida *et al.*, 2000, Ilic *et al.*, 1998, Kurenova *et al.*, 2004). Inhibition of FAK in the presence of Bpv(Hopic) did not result in significant changes in the PI3K/AKT and MAPK/ERK pathways, although a tendency for a small reduction in the levels of active ERK1/2 following PF-228 treatment in CM was observed. Interestingly, the rates of migration followed the same trend as the levels of pFAK, regardless of the activity of pERK1/2 and pAKT. Migration was enhanced with cells incubated in Bpv(Hopic) vs all other conditions. At the same time, despite pAKT and pERK1/2 levels being activated, the migration distance of cells incubated in Bpv+PF-228 was reduced, compared to cells in CM. Similarly, despite greater activation of pAKT and pERK1/2 levels, only slight increase in migration distance was observed with cells incubated in Bpv+PF-228, as compared to cells in CM+PF-228, which coincided with the slight increase in pFAK levels in cells incubated with Bpv+PF-228. These observations could probably be explained, as suggested by Mihai *et al* (Mihai *et al.*, 2012), by the action of FAK on migrating, but not confluent cells: similarly, FAK inhibition by PF-228 may affect the migrating cells more than non-migrating, confluent cells. Migrating cells would require constant focal adhesion turnover, in which FAK participates, and the presence of FAK inhibitor may thus affect migrating cells more than confluent, non-migrating ones. Furthermore, other pathways not investigated in our studies, such as JNK, might be involved in the reduction of myoblast migration following FAK inhibition in migrating cells (Desai *et al.*, 2009, Liu *et al.*, 2007). In preliminary experiments it was observed that inhibition of JNK by SP600125, indeed, led to decreased migration of myoblasts in wound healing assays (see Appendix 1). Overall, the data suggest that inhibition of FAK results in significant reductions in migration, regardless of the activity of MAPK and PI3K pathways. The possibility that other pathways, beyond the scope of these studies, might also contribute to the regulation of migration following 2 μ M Bpv(Hopic) or PF-228 treatments, cannot be excluded.

5.5.5. CONCLUSION

In summary, the phospho-tyrosine phosphatase inhibitor Bpv(Hopic) at low concentrations (1 μ M) did not significantly affect the differentiation potential of myoblasts in DM, while being capable of inducing their migration in the presence of myotube CM. The induced migration of myoblasts following Bpv(Hopic) treatment was accompanied with activation of the PI3K/AKT and MAPK/ERK pathways and inhibition of these pathways by 10 μ M LY294002 or 5 μ M UO126 resulted in decreased cell migration. At the same time, inhibition of the FAK pathway using PF-228, following 2 μ M Bpv(Hopic) treatment, resulted in a reduction of cell migration below basal levels, even in the presence of activated PI3K/AKT and MAPK/ERK pathways. Overall, these data suggest that for migration to be sustained, at least PI3K, ERK and FAK signalling pathways must be constitutively active over the time frame studied. The reduced migration following disruption by any one of these signalling pathway is not entirely compensated for by the other pathways.

Given the results obtained from media conditioning experiments and inhibitor treatments, a better idea was obtained on the regulation of myogenic precursors migration by soluble factors released by myogenic cells themselves and also on the requirement of signalling pathways, such as PI3K/AKT, MAPK/ERK and FAK. Migration of myogenic cells, however, might also depend on the regulation of different genes, some of them regulating migration by indirectly affecting other cellular processes as well, such as myoblast fusion. In the last chapter of this thesis, preliminary examination was performed on 4 genes, previously unexplored in skeletal muscle, which were hypothesised to be involved in the processes of myoblast migration or fusion. This examination was performed based on the previous findings that both serial passaging (Chapter 4) and treatment with high concentrations of BpV(Hopic) (Chapter 5) negatively affect the differentiation and fusion of skeletal muscle myoblasts. Thus, a link was established between these observations and the potential involvement of different genes in the regulation of myoblast migration and fusion, which could serve as a base for future experiments.

CHAPTER 6

6. SPIRE AND FORMIN GENES ARE EXPRESSED IN C2C12 MYOBLASTS

6.1. THESIS DIRECTIONS

In chapters 4 and 5, in addition to the influence of Bpv(Hopic) and serial passaging on migration, it was also demonstrated that fusion of myoblasts into multinucleated myotubes was blocked by treatment with high dose (10 μ M) Bpv(Hopic) and was also reduced in serially passaged myoblasts. This provides two distinct models for investigating the potential involvement of genes involved in myoblast fusion, which could also be responsible for regulating their migration. Numerous articles have reported a link between myoblast fusion and migration, with many of the factors important for fusion, influencing migration as well (Becciolini *et al.*, 2006, Donati *et al.*, 2005, Griffin *et al.*, 2009, Lafreniere *et al.*, 2006, Louis *et al.*, 2008, Makarenkova *et al.*, 2009, Olguin *et al.*, 2003). Therefore, exploring the genetic regulators of myoblast fusion, might provide important clues of regulators of myoblast migration and thus improve our knowledge of the molecular regulators of myogenesis.

6.2. BACKGROUND

The actin cytoskeleton is essential for many cellular functions, including cell migration, shape determination, intracellular transport and also for myoblast fusion (Guerin and Kramer, 2009, Kim *et al.*, 2007). Due to a high kinetic barrier, actin monomers present in the cytoplasm cannot spontaneously polymerise therefore, for actin filaments to be formed, a catalyst, or actin nucleation factor is required (Pollitt and Insall, 2009). Three classes of nucleation factors have been discovered: the Arp2/3 complex, forming branched actin filaments, FH2 domain containing nucleation factors of the Formin superfamily and the recently discovered WH2 domain containing nucleation factors (including the Spire subfamily), with the latter two being involved in nucleating unbranched actin filaments (Pechlivanis *et al.*, 2009, Quinlan *et al.*, 2005). As reviewed in Guerin *et al.*, studies in *Drosophila* have revealed many genes involved in myoblast fusion and the importance of the actin cytoskeleton for this process (Guerin and Kramer, 2009). Members of the Wiskott-Aldrich syndrome protein family (WASPs and SCAR/WAVES) and the Arp2/3 complexes they regulate, which initiate the

polymerization of actin filaments (Pollitt and Insall, 2009), have been demonstrated to be important for myoblast fusion in several studies (Gildor *et al.*, 2009, Mukherjee *et al.*, 2011, Richardson *et al.*, 2007, Schafer *et al.*, 2007). However, to our knowledge, no studies have investigated the potential roles of Spire and Formins in skeletal muscle. Spire and Formin actin nucleators have been implicated in regulating intracellular vesicle transport and have been demonstrated to co-localize with the Rab11 GTPase (Kerkhoff, 2010, Kerkhoff *et al.*, 2001, Morel *et al.*, 2009, Schuh, 2011). Furthermore, it is known that endocytic recycling and intracellular trafficking are important for myoblast fusion (Doherty *et al.*, 2008, Rochlin *et al.*, 2010). Rab11 is known to mediate endosome recycling (Ullrich *et al.*, 1996) and it has been shown to be required for myoblast fusion (Bhuin and Roy, 2009). Intriguingly, Rab11 is also associated with cell migration, which is known to be mediated by integrin recycling (Caswell and Norman, 2006, Pellinen and Ivaska, 2006).

It has been shown that both mammalian Spire proteins, Spire-1 and Spire-2, interact with mammalian Formin-1 and Formin-2 to form a regulatory complex, with the interaction blocking Formin nucleation activity, while enhancing the activity of Spire (Pechlivanis *et al.*, 2009, Quinlan *et al.*, 2007). However, their expression profiles and the individual contribution of each gene in different cell types is not widely explored. Formin-2 and Spire1 gene expression have been detected in both the developing and adult nervous system (Schumacher *et al.*, 2004), while Formin-2 has also been shown to be important for mouse oogenesis (Azoury *et al.*, 2011, Dumont *et al.*, 2007, Leader *et al.*, 2002). Spire-1 and Spire-2, although primarily expressed in central nervous system, have also been shown to be expressed in many embryonic tissues (Schumacher *et al.*, 2004). However, little is known about their biological functions in different cell types. Furthermore, no studies, to our knowledge, have investigated their expression or potential functions in skeletal muscle.

6.3. AIMS, OBJECTIVES AND HYPOTHESIS

The aim of these studies was to reveal the involvement of Spire and Formin genes in skeletal muscle myogenesis. The objectives were: 1) to investigate by RT-PCR whether there was detectable expression of Spire-1, Spire-2, Formin-1 and Formin-2 genes and 2) whether expression of any of these genes would be

altered following inhibition of fusion by 10 μ M Bpv(Hopic) and serial passaging of C2C12 myoblasts. It was hypothesised that detectable expression levels of Spire and Formin genes, implicated in actin nucleation and intracellular trafficking, would be present in C2C12 cells and that their expression would be altered during myoblast fusion. If the hypothesis is accepted, this research could provide a basis for future studies into the specific functions of these genes in skeletal muscle and their potential involvement in myoblast fusion and migration.

6.4. METHODS

6.4.1. CELL CULTURE

C2C12 myoblasts were cultured in a humidified 5% CO₂ atmosphere at 37°C. Cells were grown in the presence of GM in T75 flasks until confluent and split into multidish plates for experiments. In order to initiate differentiation, C2C12 cells were grown in 6 well plates until confluency was achieved, monolayers were washed with PBS and differentiation media (DM) was added to the cell monolayers. When differentiation experiments were performed for 5days, DM was changed with a fresh media at d3.

6.4.2. RNA ISOLATIONS AND REAL-TIME PCR

RNA extraction and TaqMan® Real-time PCR methods were performed as described in sections 2.2.9 and 2.2.10, respectively. The following predesigned primer sets were ordered from Applied Biosystems and were used with the TaqMan® detection method: Polr2b (Mm00464214_m1), MyoD (mm00440387_m1), Myogenin (mm00446194_m1), Spire1 (mm01258168_m1), Spire2 (mm00552235_m1), Formin1 (mm00439021_m1) and Formin2 (mm00444598_m1).

6.4.3. CREATINE KINASE (CK) ASSAY

Samples for CK assay were prepared by adding 150µL per well (for 6 well plate) of Tris Mes Triton (TMT buffer; composed of: 0.05M Tris/Mes and 1% Triton-X100). Assay was performed, as described in section 2.2.7.2.

6.4.4. FLOW CYTOMETRY

For investigating cell cycle, cells were collected 20hrs post treatment. Sample preparation and Propidium iodide method for FACS are described in section 2.2.11.

6.4.5. SERIAL PASSAGING

C2C12 cells of passage 20 (P20) were seeded in a T75 flasks at concentration of 500,000cell/ml and allowed to proliferate in GM for 48h before being passaged to a new T75 flask. Upon passaging, total number of cells was counted, and on average equated to 2,5 million cells per flask, confirming that 48h was enough time for cells to perform at least 2 doublings (average doublings in 48 hrs was 2.4). Cycles of passaging were repeated 30 times until reaching 50 passages (thus, C2C12 cells were designated as p50).

6.4.6. CELL TREATMENTS AND RECONSTITUTION OF INHIBITORS

All inhibitors were purchased from Merck-Calbiochem (Darmstadt, Germany). Bpv(Hopic) inhibitor was diluted, according to manufacturer's instructions, in H2O and stored at -20°C. It was kept in mM concentration stock and part of the stock was diluted to working concentration in appropriate DMEM media before cell treatments.

6.4.7. STATISTICAL ANALYSES

Statistical analyses and significance of data were determined using GraphPad Prism version 5.00 for Mac OS X, GraphPad Software, San Diego California USA, www.graphpad.com. Statistical significance for interactions between two paired groups was determined with a Paired t-test, while unpaired t-test was used for unpaired groups (e.g. between p5 and p50 groups). Statistical significance for interactions between more than two groups was determined with a one-way ANOVA, or with a one-way repeated measures ANOVA, when matched observations were investigated. When more than one factor was present, two-way ANOVA was performed to investigate for significances of factors or interactions, or two-way repeated measures (mixed model) ANOVA, when matched observations were investigated. When significances of factors were indicated by two-way ANOVA, this was followed up by examining the statistical significance for interactions between more than two groups within the factor with a One-way ANOVA with Bonferroni post-hoc analysis, or with a t-test for examination between two groups. All results are presented as mean +/- standard error of the mean (SEM). All values below $p < 0.05$ were considered as significant.

For determining the significances of the PCR results, 4x2x2 ANOVA was performed to determine whether there were significances for any of the factors (time, passage, inhibitor treatment). When significance was indicated for time, one way ANOVA was performed to investigate the significances between the different time points within one group. When significances were indicated for passage/inhibitor treatment, 2x2 ANOVA was performed to determine the significances of these factors individually for each time point. When significance was indicated by 2x2 ANOVA for either passage or inhibitor treatment within a time point, this was followed up by performing a paired t-test to determine the significance between paired groups (e.g. p5 vs p5-bpv or p50 vs p50-bpv) or unpaired t-test for significances between unpaired groups (e.e.g p5 vs p50, p5 vs p50-bpv or p5-bpv vs p50).

6.5. RESULTS

6.5.1. SERIALY PASSAGED C2C12 MYOBLASTS (P50) DEMONSTRATED IMPAIRED CAPACITY TO DIFFERENTIATE COMPARED TO LOW PASSAGE CELLS (P5), WHICH WAS FURTHER REDUCED BY TREATMENT WITH 10 μ M BPV(HOPIC)

Previous studies have addressed the decrease in fusion/differentiation capacity of C2C12 myoblasts subjected to multiple population doublings. This work was expanded by further exploring the differentiation capacity of C2C12 cells after 50 population doublings and examined the effect of 10 μ M BpV(Hopic) treatment on differentiation of p50 vs p5 myoblasts. The findings coincide with a recent article, using the same model of approx. 50 population doublings (passage 20) of C2C12 myoblasts (Sharples *et al.*, 2011). In order to investigate the differences in fusion/differentiation capacity, p5 and p50 myoblasts were incubated until confluent and subsequently transferred to DM media with and without 10 μ M Bpv(Hopic) for 3 days. Phase contrast microscopy (Figure 6.1) demonstrated reduced capacity of p50 cells to fuse into myotubes compared with p5, which was further decreased by Bpv(Hopic). Bpv (Hopic) also decreased the fusion capacity of p5 cells.

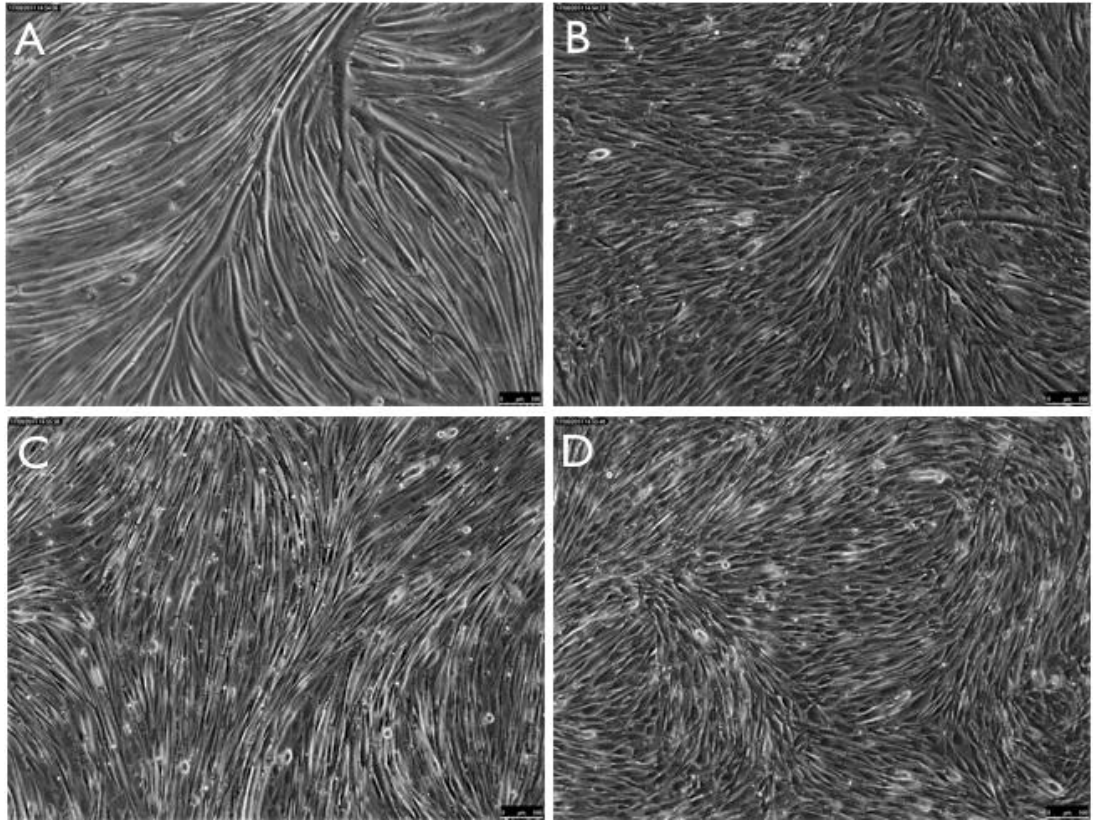


Figure 6.1. Effects of Bpv(Hopic) and serial passaging on myotube formation.

Phase-contrast microscopy investigating the effects of DM on p5 C2C12 myoblasts (A), DM+10µM Bpv(Hopic) on p5 myoblasts (B), DM on p50 myoblasts (C) and DM+10µM Bpv(Hopic) on p50 myoblasts (D). Reduction in myotubes formation was observed with p50 myoblasts vs p5 myoblasts, with further reduction after 10µM Bpv(Hopic) treatment in both p5 and p50. Data are representative of 4 experiments performed in duplicate. 10x objective used.

In order to verify the phase-contrast microscopy observations, CK activity was measured in the two different myoblast passages with and without 10µM Bpv(Hopic) treatment (Figure 6.2). The data from CK assay supported the phase-contrast microscopy images, showing significant decreases in CK activity with p50 cells treated with DM vs p5 cells treated with DM (836.75 +/-90.48 vs 1123.2 +/-66.43 mU/mg, $p < 0.05$, equivalent to 1.34 fold decrease). Decreases were also found in p5 cells treated with DM+10µM Bpv(Hopic) vs DM (343.75 +/-29.92 vs 1123.2 +/-66.43 mU/mg, $p < 0.001$, equivalent to 3.27 fold decrease) and in p50 cells treated with DM+10µM Bpv(Hopic) vs DM (154.5 +/-24.19 vs 836.75 +/-90.48 mU/mg, $p < 0.01$, equivalent to 5.42 fold decrease).

Greater decreases were observed with p50 myoblasts treated with DM+10µM Bpv(Hopic) vs p5 myoblasts treated with DM (154.5 +/-24.19 vs 1123.2 +/-66.43

mU/mg, $p < 0.0001$, equivalent to 7.27 fold decrease). The CK activity values suggested that Bpv(Hopic) treatment was able to further reduce the differentiation potential caused by serial passaging. Decreased CK activity was identified in p50 cells treated with 10 μ M Bpv(Hopic) vs p5 cells treated with 10 μ M Bpv(Hopic) (154.5 \pm 24.19 vs 343.75 \pm 29.92 mU/mg, $p < 0.01$, equivalent to 2.22 fold decrease). Increases were observed with p50 myoblasts treated with DM vs p5 myoblasts treated with DM+10 μ M Bpv(Hopic) (836.75 \pm 90.48 vs 343.75 \pm 29.92 mU/mg, $p < 0.01$, equivalent to 2.43 fold increase), suggesting the greater inhibition effect that BpV(Hopic) treatment has on differentiation, as compared to serial passaging alone. Overall, these observations indicate a reduced CK activity after treatment with 10 μ M Bpv(Hopic), which is compounded by serial passaging of myoblasts.

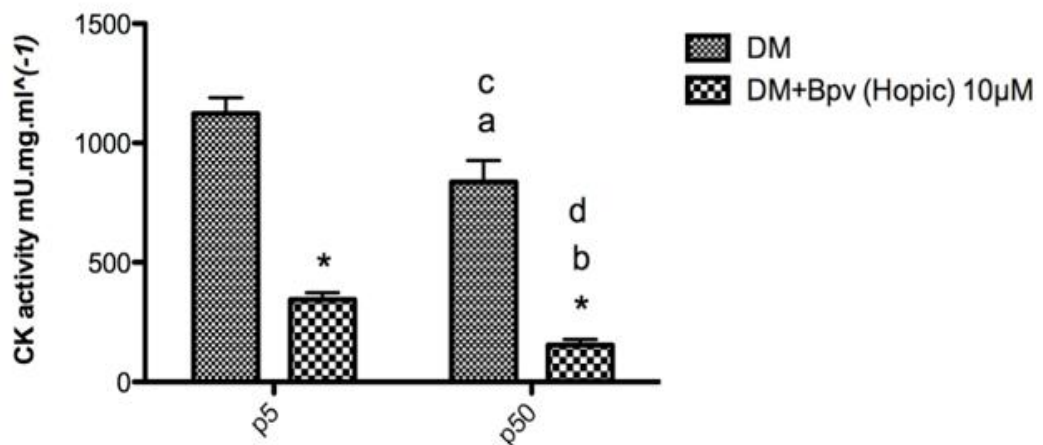


Figure 6.2. CK assay, measuring CK activity between p5 and p50 myoblasts incubated for 3 days in DM with and without 10 μ M Bpv(Hopic). Significant decreases in CK activity were present with p50 in control DM vs p5 cells in control DM ($p < 0.05$, represented by a). Reductions were observed with p5 cells treated with DM+10 μ M Bpv(Hopic) vs DM-treated p5 cells ($p < 0.001$, represented by *) and with p50 cells treated with DM+10 μ M Bpv(Hopic) vs DM-treated p50 cells ($p < 0.01$, represented by *). Reductions were also identified with p50 cells treated with 10 μ M Bpv(Hopic) vs p5 cells treated with 10 μ M Bpv(Hopic) ($p < 0.01$, represented by b) and with p50 cells treated with DM+10 μ M Bpv(Hopic) vs p5 cells treated with DM ($p < 0.0001$, represented by d). An increase was found with p50 myoblasts treated with DM vs p5 myoblasts treated with DM+10 μ M Bpv(Hopic) ($p < 0.01$, represented by c). Data are representative of 4 experiments performed in duplicate. (p-values obtained by paired t-test (within the same passage) and unpaired t-test (between different passages))

6.5.2. CELL CYCLE PROGRESSION: IMPACT OF PASSAGING AND BPV (HOPIC)

As fusion/differentiation was reduced in p50 vs p5 myoblasts, it was investigated whether this occurred as a consequence of increased proliferation and cells in the S-phase of the cell cycle were examined by FACS. Permanent withdrawal from the cell cycle is necessary for progression to myogenic differentiation. Previous studies have demonstrated increases percentages of cells in S-phase of the cell cycle at early time points after the initiation of differentiation (Sharples *et al.*, 2011). As a consequence, the percentage of myoblasts in the S-phase of the cell cycle at 20hr after addition of DM or DM+10 μ M Bpv(Hopic) in p5 or p50 myoblasts was examined and it was ascertained that BpV (Figure 6.3 B & D) appears to actively move cells to the S phase of the cell cycle, regardless of passage (Figure 6.3 A & C).

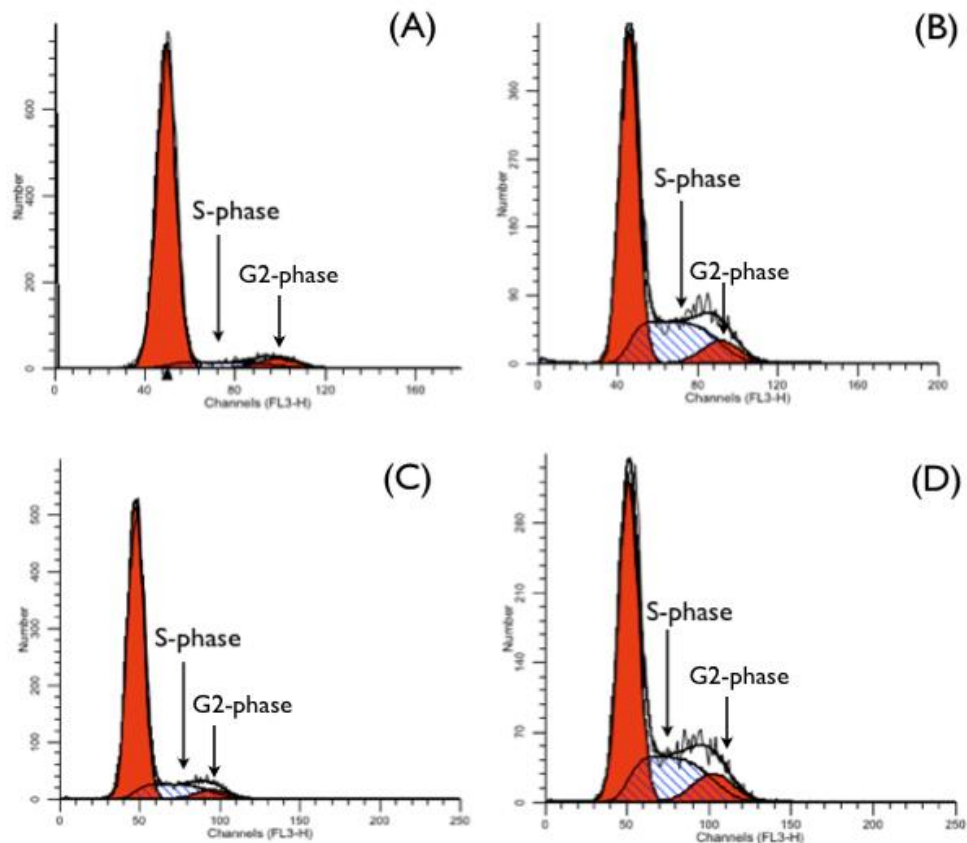


Figure 6.3. Flow cytometric analysis (p5 and p50 myoblasts incubated in DM with and without 10µM Bpv(Hopic)). Examination of the percentage of C2C12 myoblasts in the S/G2-phases of the cell cycle by FLOW cytometry, after incubation for 20h of p5 cells with DM (A), p5 cells with DM+10µM Bpv (B), p50 cells with DM (C) and p50 cells with DM+10µM Bpv (D). Data are representative of 4 experiments.

Analyses (Figure 6.4) indicated significant increases of the percentage of cells in the S/G2-phases of the cell cycle with p5 cells treated with DM+10µM Bpv(Hopic) vs DM only (42.76 +/-1.92% vs 17.08 +/-3.19%, $p < 0.01$) and with p50 cells treated with DM+10µM Bpv(Hopic) vs DM only (44.2 +/-6.1% vs 17.59% +/-2.4, $p < 0.01$) (Figure 6.4). However, no significant differences were found between p5 and p50 in the absence or presence of Bpv (Hopic), 20hr after differentiation was initiated.

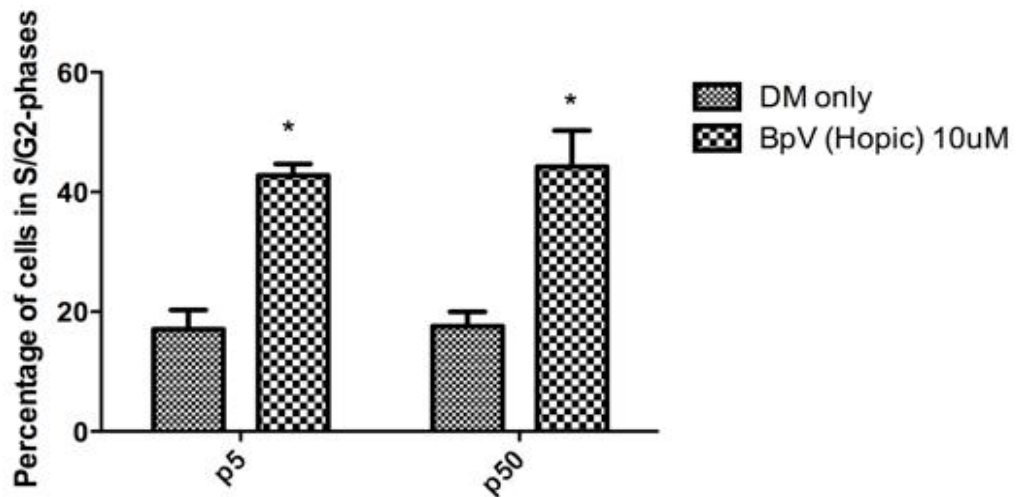


Figure 6.4. Analysis of the percentage of p5 and p50 cells in S/G2-phases of the cell cycle after treatment with DM or DM+10µM Bpv for 20h. Significant increases were observed with p5 cells treated with DM+10µM Bpv(Hopic) vs p5 cells treated with DM ($p < 0.01$, represented by *). Significant increases were also observed with p50 cells treated with DM+10µM Bpv(Hopic) vs p50 cells treated with DM ($p < 0.01$, represented by *). Data are representative of 4 experiments. (p-values obtained by paired t-test (within the same passage) and unpaired t-test (between different passages))

6.5.3. DIFFERENTIAL EXPRESSION OF MYOGENIC REGULATORY FACTORS IN RESPONSE TO BPV(HOPIC) AND SERIAL PASSAGING

Having confirmed that multiple population doublings reduces the differentiation potential of C2C12 cells and that this phenotype is worsened by the incubation with Bpv(Hopic), further investigations aimed to explore how Spire1, Spire2, Formin1 and Formin2 genes were influenced in response to serial passaging of C2C12 myoblasts with and without Bpv(Hopic) treatment. Temporal investigations were performed at 4 different time points (0 (d0), 24 (d1), 48 (d2) and 72 (d3) hr) in both p5 and p50 myoblasts treated with either DM or DM+10µM Bpv(Hopic). 4 different time points, unlike previous RT-PCR results in this thesis, were used due to the fact that this chapter investigates the expression of genes, which are previously not investigated in skeletal muscle and it is not known how their expression is regulated during myogenesis. Nevertheless, MyoD and Myogenin expression were also investigated at 4 different time points in this chapter, in order to examine how the combination of serial passaging and inhibitor treatments influenced the expression of myogenic regulatory factors in these models.

MyoD gene expression was examined in p5 and p50 myoblasts in response to DM or DM+10 μ M Bpv(Hopic) (Figure 6.5). Reductions in MyoD expression were observed with passage under basal conditions in p50 myoblasts treated with DM vs p5 myoblasts treated with DM at d1 (0.56 \pm 0.01 vs 1, p <0.0001, equivalent to 1.79 fold decrease), at d2 (0.55 \pm 0.04 vs 0.93 \pm 0.06, p <0.01, equivalent to 1.69 fold decrease) and at d3 (0.62 \pm 0.04 vs 0.89 \pm 0.06, p <0.01, equivalent to 1.44 fold decrease). Reductions with time were observed with p5 myoblasts treated with DM at d1 vs d0 (1 vs 1.56 \pm 0.17, p <0.01, equivalent to 1.56 fold decrease), at d2 vs d0 (0.93 \pm 0.03 vs 1.56 \pm 0.17, p <0.01, equivalent to 1.68 fold decrease) and at d3 vs d0 (0.89 \pm 0.06 vs 1.56 \pm 0.17, p <0.01, equivalent to 1.75 fold decrease) and also with p50 myoblasts treated with DM at d1 vs d0 (0.56 \pm 0.001 vs 1.13 \pm 0.05, p <0.001, equivalent to 2.02 fold decrease), at d2 vs d0 (0.55 \pm 0.04 vs 1.13 \pm 0.05, p <0.001, equivalent to 2.05 fold decrease) and at d3 vs d0 (0.62 \pm 0.04 vs 1.13 \pm 0.05, p <0.001, equivalent to 1.82 fold decrease).

Inhibitor treatment was also found to have significant effect on MyoD expression levels. Significant decreases in gene expression levels were observed in p5 myoblasts treated with DM+10 μ M Bpv(Hopic) vs DM at d1 (0.52 \pm 0.03 vs 1, p <0.001, equivalent to 1.92 fold decrease) and at d2 (0.65 \pm 0.07 vs 0.93 \pm 0.06, p <0.001, equivalent to 1.43 fold decrease). Decreases in expression with time were observed with p5 myoblasts treated with DM+10 μ M Bpv(Hopic) at d1 vs d0 (0.52 \pm 0.03 vs 1.56 \pm 0.17, p <0.001, equivalent to 3 fold decrease), d2 vs d0 (0.65 \pm 0.07 vs 1.56 \pm 0.17, p <0.001, equivalent to 2.4 fold decrease) and at d3 vs d0 (0.85 \pm 0.05 vs 1.56 \pm 0.17, p <0.01, equivalent to 1.84 fold decrease). Although not statistically significant, a gradual increase with time was also evident with p5 myoblasts treated with DM+10 μ M Bpv(Hopic), indicating that myoblasts slowly recover the MyoD gene expression levels following a single dose of 10 μ M Bpv(Hopic) at d0. Similarly, expression of MyoD was reduced when p50 myoblasts were treated with DM+10 μ M Bpv(Hopic) vs DM at d1 (0.27 \pm 0.02 vs 0.56 \pm 0.01, p <0.001, equivalent to 2.07 fold decrease) and at d2 (0.39 \pm 0.04 vs 0.55 \pm 0.04, p <0.05, equivalent to 1.41 fold decrease). Decreases with time were observed with p50 myoblasts treated with DM+10 μ M Bpv(Hopic) at d1 vs d0 (0.27 \pm 0.02 vs 1.13 \pm 0.05, p <0.001, equivalent to 4.19 fold decrease), at d2 vs d0 (0.39 \pm 0.04 vs 1.13 \pm 0.05, p <0.001, equivalent to 2.9 fold decrease) and at d3 vs d0 (0.51 \pm 0.03 vs 1.13 \pm 0.05, p <0.001, equivalent to

2.22 fold decrease). Increases with time were found with p50 myoblasts treated with DM+10 μ M Bpv(Hopic) at d3 vs d1 (0.51 +/-0.03 vs 0.27 +/-0.02, p<0.01, equivalent to 1.89 fold increase) and at d3 vs d2 (0.51 +/-0.03 vs 0.39 +/-0.04, p<0.05, equivalent to 1.3 fold increase) and at d2 vs d1 (0.39 +/-0.04 vs 0.27 +/-0.02, p<0.05, equivalent to 1.44 fold increase). These observations, similar to p5 myoblasts, suggest a gradual recovery with time of MyoD gene expression levels in the presence of a single dose of 10 μ M Bpv(Hopic) at d0.

Significant decreases were also observed with p50 myoblasts treated with DM+10 μ M Bpv(Hopic) vs p5 myoblasts treated with DM+10 μ M Bpv(Hopic) at d1 (0.27 +/-0.02 vs 0.52 +/-0.03, p<0.001, equivalent to 1.93 fold decrease), at d2 (0.39 +/-0.04 vs 0.65 +/-0.07, p<0.05, equivalent to 1.67 fold decrease) and at d3 (0.51 +/-0.03 vs 0.85 +/-0.05, p<0.01, equivalent to 1.67 fold decrease), suggesting that as with morphological and biochemical differentiation, serial passaging reduces MyoD expression, which is further dampened by BpV(Hopic) treatment. Not surprisingly, given the data above, an even greater reduction in MyoD expression was found with p50 myoblasts treated with DM+10 μ M Bpv(Hopic) vs p5 myoblasts treated with DM at d1 (0.27 +/-0.02 vs 1, p<0.0001, equivalent to 3.7 fold decrease), at d2 (0.39 +/-0.04 vs 0.93 +/-0.06, p<0.001, equivalent to 2.38 fold decrease) and at d3 (0.51 +/-0.03 vs 0.89 +/-0.06, p<0.01, equivalent to 1.75 fold decrease), indicating that combination of serial passaging and BpV(Hopic) treatment further decreases the MyoD expression of the cells, as compared to either of these conditions alone.

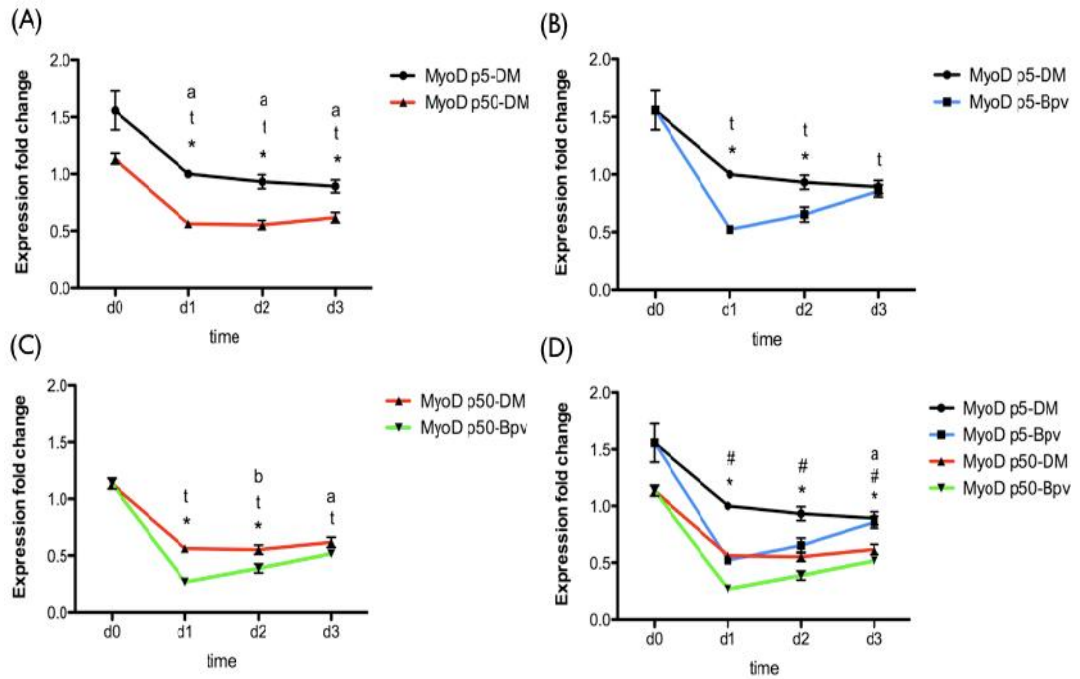


Figure 6.5. MyoD gene expression levels in p5 and p50 myoblasts incubated for 3 days in DM with and without 10 μ M Bpv(Hopic). MyoD gene expression levels examining the difference between p5 and p50 C2C12 myoblasts at d0, d1, d2 and d3 following treatment with DM or DM+10 μ M Bpv(Hopic). All values are represented as fold change to the calibrator (p5 DM d1), which was set to 1 (mean Ct value =24.54 +/-0.24). Effect of passage (p5-DM vs p50-DM): Decreases in MyoD expression were found with p50 myoblasts vs p5 myoblasts at d1 (p<0.0001, represented by *), d2 (p<0.01, represented by *) and d3 (p<0.01, represented by *). Decreases in expression with time were observed with p5 myoblasts treated with DM at d1 vs d0 (p<0.01, represented by t), at d2 vs d0 (p<0.01, represented by t) and at d3 vs d0 (p<0.01, represented by t). Decreases with time were also observed with p50 myoblasts treated with DM at d1 vs d0 (p<0.001, represented by a), d2 vs d0 (p<0.001, represented by a) and d3 vs d0 (p<0.001, represented by a) (p-values obtained by One-way repeated measures ANOVA (changes in gene expression with time) and unpaired t-test (changes in expression with p5 vs p50)) (A). Effect of Bpv(Hopic) treatment on p5 myoblasts (p5-DM vs p5-Bpv): Significant decreases in MyoD expression were observed in p5 myoblasts treated with DM+10 μ M Bpv(Hopic) vs DM at d1 (p<0.001, represented by *) and at d2 (p<0.001, represented by *). Decreases in expression with time were observed with p5 myoblasts treated with DM+10 μ M Bpv(Hopic) at d1 vs d0 (p<0.001, represented by t), d2 vs d0 (p<0.001, represented by t) and d3 vs d0 (p<0.01, represented by t) (p-values obtained by One-way repeated measures ANOVA (changes in gene expression with time) and paired t-test (changes in expression with DM vs BpV)) (B). Effect of Bpv(Hopic) treatment on p50 myoblasts (p50-DM vs p50-Bpv): Decreases in MyoD

expression were found also in p50 myoblasts treated with DM+10 μ M Bpv(Hopic) vs DM at d1 (p<0.001, represented by *) and at d2 (p<0.05, represented by *). Decreases in expression with time were found with p50 myoblasts treated with DM+10 μ M Bpv(Hopic) at d1 vs d0 (p<0.001, represented by t), d2 vs d0 (p<0.001, represented by t) and d3 vs d0 (p<0.001, represented by t). Increases in expression with time were found with p50 myoblasts treated with DM+10 μ M Bpv(Hopic) at d3 vs d1 (p<0.01, represented by a) and d3 vs d2 (p<0.05, represented by a). Increases were also found with p50 myoblasts treated with DM+10 μ M Bpv(Hopic) at d2 vs d1 (p<0.05, represented by b) (p-values obtained by One-way repeated measures ANOVA (changes in gene expression with time) and paired t-test (changes in expression with DM vs BpV)) (C). Interactions between groups: Reductions in MyoD expression were indicated with p50 myoblasts treated with DM+10 μ M Bpv(Hopic) vs p5 myoblasts treated with DM at d1 (p<0.0001, represented by *), at d2 (p<0.001, represented by *) and at d3 (p<0.01, represented by *). Decreases in expression were indicated with p50 myoblasts treated with DM+10 μ M Bpv(Hopic) vs p5 myoblasts treated with DM+10 μ M Bpv(Hopic) at d1 (p<0.001, represented by #), at d2 (p<0.05, represented by #) and at d3 (p<0.01, represented by #). Decreases were also found with p50 myoblasts treated with DM vs p5 myoblasts treated with DM+10 μ M Bpv(Hopic) at d3 (p<0.01, represented by a) (p-values obtained by unpaired t-test (D). Data are representative of 4 experiments performed in duplicate.

Myogenin gene expression was examined in p5 and p50 myoblasts in response to DM or DM+10 μ M Bpv(Hopic) (Figure 6.6). Similar to MyoD, passage influenced the expression of Myogenin. Significant decreases were observed with p50 myoblasts vs p5 myoblasts treated with DM at d1 (0.43 +/-0.02 vs 1, p<0.0001, equivalent to 2.33 fold decrease), at d2 (0.44 +/-0.04 vs 0.86 +/-0.06, p<0.01, equivalent to 1.95 fold decrease) and at d3 (0.41 +/-0.03 vs 0.78 +/-0.06, p<0.01, equivalent to 1.9 fold decrease). Increases with time were found with p5 myoblasts treated with DM at d1 vs d0 (1 vs 0.38 +/-0.05, p<0.001, equivalent to 2.63 fold increase), at d2 vs d0 (0.86 +/-0.06 vs 0.38 +/-0.05, p<0.001, equivalent to 2.26 fold increase) and at d3 vs d0 (0.78 +/-0.06 vs 0.38 +/-0.05, p<0.01, equivalent to 2.05 fold increase). Similarly, although to a smaller extent, increases were found with p50 myoblasts treated with DM at d1 vs d0 (0.43 +/-0.02 vs 0.26 +/-0.03, p<0.05, equivalent to 1.65 fold increase), d2 vs d0 (0.44 +/-0.04 vs 0.26 +/-0.03, p<0.01, equivalent to 1.69 fold increase) and d3 vs d0 (0.41 +/-0.03 vs 0.26 +/-0.03, p<0.05, equivalent to 1.58 fold increase). These observations clearly demonstrate the upregulation of Myogenin after differentiation is triggered. It also shows that serially passaged p50 myoblasts

were able to upregulate Myogenin upon differentiation to a smaller, but perhaps more sustained extent, as compared to p5 myoblasts.

Similar to MyoD, treatment with Bpv(Hopic) influenced the expression of Myogenin in both p5 and p50 cells. Significant decreases were observed with p5 myoblasts treated with DM+10 μ M Bpv(Hopic) vs p5 myoblasts treated with DM at d1 (0.18 \pm 0.01 vs 1, $p < 0.001$, equivalent to 5.56 fold decrease), at d2 (0.32 \pm 0.03 vs 0.86 \pm 0.06, $p < 0.01$, equivalent to 2.69 fold decrease) and at d3 (0.57 \pm 0.07 vs 0.78 \pm 0.06, $p < 0.05$, equivalent to 1.37 fold decrease). A decrease in Myogenin expression with time was found with p5 myoblasts treated with DM+10 μ M Bpv(Hopic) at d1 vs d0 (0.18 \pm 0.01 vs 0.38 \pm 0.05, $p < 0.05$, equivalent to 2.11 fold decrease). On the other hand, increases with time were found with p5 myoblasts treated with DM+10 μ M Bpv(Hopic) at d3 vs d1 (0.57 \pm 0.07 vs 0.18 \pm 0.01, $p < 0.001$, equivalent to 3.17 fold increase) and at d3 vs d2 (0.57 \pm 0.07 vs 0.32 \pm 0.03, $p < 0.05$, equivalent to 1.78 fold increase), suggesting, similar to myoD, recovery of Myogenin expression following prolonged Bpv(Hopic) treatment. Similarly, decreases in expression were observed with p50 myoblasts treated with DM+10 μ M Bpv(Hopic) vs DM at d1 (0.04 \pm 0.01 vs 0.43 \pm 0.02, $p < 0.001$, equivalent to 10.75 fold decrease), at d2 (0.08 \pm 0.01 vs 0.44 \pm 0.04, $p < 0.01$, equivalent to 5.5 fold decrease) and at d3 (0.15 \pm 0.02 vs 0.41 \pm 0.03, $p < 0.01$, equivalent to 2.73 fold decrease). Increases with time were found with p50 myoblasts treated with DM+10 μ M Bpv(Hopic) at d3 vs d1 (0.15 \pm 0.02 vs 0.04 \pm 0.01, $p < 0.01$, equivalent to 3.75 fold increase) and at d3 vs d2 (0.15 \pm 0.02 vs 0.08 \pm 0.01, $p < 0.05$, equivalent to 1.88 fold increase). These observations again indicated a tendency for myoblasts to gradually increase their Myogenin gene expression in to the face of Bpv(Hopic) treatment, after an initial drop at d1. Further decreases were found with p50 myoblasts treated with DM+10 μ M Bpv(Hopic) at d1 vs d0 (0.04 \pm 0.01 vs 0.26 \pm 0.03, $p < 0.001$, equivalent to 6.5 fold decrease), d2 vs d0 (0.08 \pm 0.01 vs 0.26 \pm 0.03, $p < 0.001$, equivalent to 3.25 fold decrease) and d3 vs d0 (0.15 \pm 0.02 vs 0.26 \pm 0.03, $p < 0.01$, equivalent to 1.73 fold decrease). These observations show that Myogenin levels after treatment with 10 μ M Bpv(Hopic) decrease to levels even lower than those evident at the d0 time point, before differentiation was triggered.

Decreases were found with p50 myoblasts treated with DM+10 μ M Bpv(Hopic) vs p5 myoblasts treated with DM+10 μ M Bpv(Hopic) at d1 (0.04 \pm 0.01 vs 0.18

+/-0.01, $p < 0.0001$, equivalent to 4.5 fold decrease), at d2 (0.08 +/-0.01 vs 0.32 +/-0.03, $p < 0.0001$, equivalent to 4 fold decrease) and d3 (0.15 +/-0.02 vs 0.57 +/-0.07, $p < 0.01$, equivalent to 3.8 fold decrease). A greater decrease was found with p50 myoblasts treated with 10 μ M Bpv(Hopic) vs p5 myoblasts treated with DM at d1 (0.04 +/-0.01 vs 1, $p < 0.0001$, equivalent to 25 fold decrease), at d2 (0.08 +/-0.01 vs 0.86 +/-0.06, $p < 0.0001$, equivalent to 10.75 fold decrease) and at d3 (0.15 +/-0.02 vs 0.78 +/-0.06, $p < 0.0001$, equivalent to 5.2 fold decrease). These observations, similar to the MyoD expression studies, indicated that the combination of serial passaging and Bpv(Hopic) treatment reduced the expression of Myogenin to a greater extent than any of the treatments alone. An increase in expression was indicated with p50 myoblasts treated with DM vs p5 myoblasts treated with DM+10 μ M Bpv(Hopic) at d1 (0.43 +/-0.02 vs 0.18 +/-0.01, $p < 0.0001$, equivalent to 2.39 fold increase), suggesting that Bpv(Hopic) treatment induced stronger inhibition of Myogenin expression than serial passaging alone.

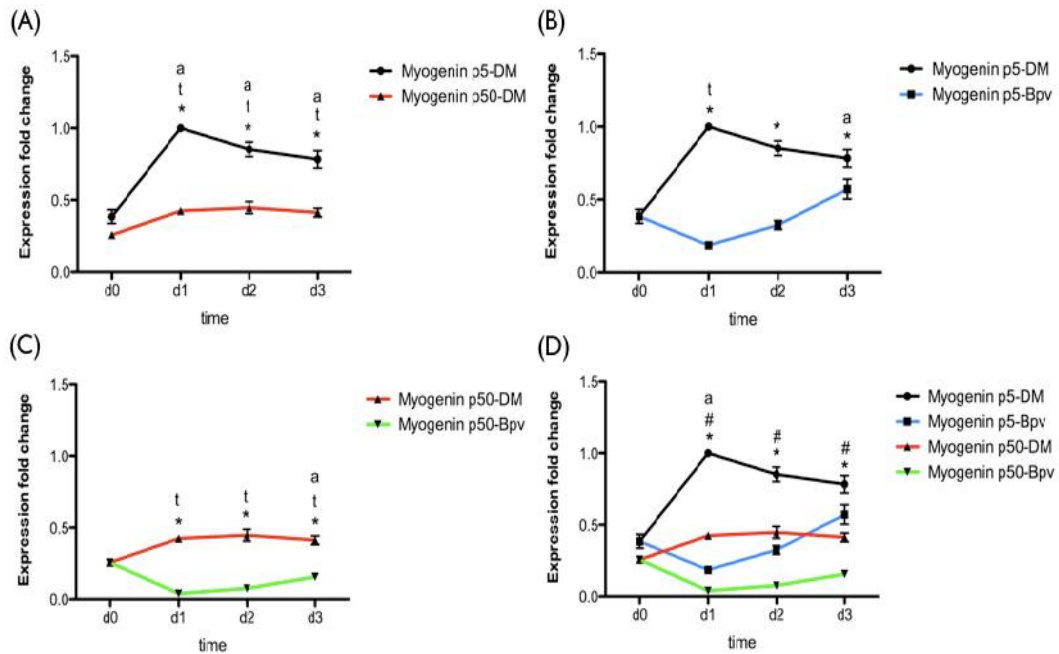


Figure 6.6. Myogenin gene expression levels in p5 and p50 myoblasts incubated for 3 days in DM with and without 10 μ M Bpv(Hopic). Myogenin gene expression levels examining the difference between p5 and p50 C2C12 myoblasts at d0, d1, d2 and d3 following treatment with DM or DM+10 μ M Bpv(Hopic). All values are represented as fold change to the calibrator (p5 DM d1), which was set to 1 (mean Ct value =19.21 +/-0.06). Effect of passage (p5-DM vs p50-DM): Significant decreases in Myogenin expression were observed with p50 myoblasts vs p5 myoblasts at d1 ($p < 0.0001$, represented by *), at d2 ($p < 0.01$, represented by *) and at d3 ($p < 0.01$, represented by *). Increases of expression with time were found with p5 myoblasts treated with DM at d1 vs d0 ($p < 0.001$, represented by *), at d2 vs d0 ($p < 0.001$, represented by *) and at d3 vs d0 ($p < 0.01$, represented by *). Increases were also found with p50 myoblasts treated with DM at d1 vs d0 ($p < 0.05$, represented by a), d2 vs d0 ($p < 0.01$, represented by a) and d3 vs d0 ($p < 0.05$, represented by a) (p-values obtained by One-way repeated measures ANOVA (changes in gene expression with time) and unpaired t-test (changes in expression with p5 vs p50)) (A). Effect of Bpv(Hopic) treatment on p5 myoblasts (p5-DM vs p5-Bpv): Significant decreases in Myogenin expression with time were observed with p5 myoblasts treated with 10 μ M Bpv(Hopic) vs p5 myoblasts treated with DM at d1 ($p < 0.001$, represented by *), at d2 ($p < 0.01$, represented by *) and at d3 ($p < 0.05$, represented by *). Reductions in expression of Myogenin with time were found with p5 myoblasts treated with DM+10 μ M Bpv(Hopic) at d1 vs d0 ($p < 0.05$, represented by t). Increases in expression were found with time with p5 myoblasts treated with DM+10 μ M Bpv(Hopic) at d3 vs d1 ($p < 0.001$, represented by a) and at d3 vs d2 ($p < 0.05$, represented by a) (p-values obtained by One-way repeated measures ANOVA (changes in gene expression with time) and unpaired t-test (changes in

expression with p5 vs p50)) (B). Effect of Bpv(Hopic) treatment on p50 myoblasts (p50-DM vs p50-Bpv): Decreases in expression with time were observed with p50 myoblasts treated with DM+10 μ M Bpv(Hopic) vs DM at d1 ($p<0.001$, represented by *), at d2 ($p<0.01$, represented by *) and at d3 ($p<0.01$, represented by *). Decreases were found with p50 myoblasts treated with DM+10 μ M Bpv(Hopic) at d1 vs d0 ($p<0.001$, represented by t), d2 vs d0 ($p<0.001$, represented by t) and d3 vs d0 ($p<0.01$, represented by t). Increases in expression of Myogenin with time were found with p50 myoblasts treated with DM+10 μ M Bpv(Hopic) at d3 vs d1 ($p<0.01$, represented by a) and at d3 vs d2 ($p<0.05$, represented by a) (p-values obtained by One-way repeated measures ANOVA (changes in gene expression with time) and paired t-test (changes in expression with DM vs BpV)) (C). Interactions between groups: Decreases in Myogenin expression were found with p50 myoblasts treated with DM+10 μ M Bpv(Hopic) vs p5 myoblasts treated with DM at d1 ($p<0.0001$, represented by *), at d2 ($p<0.0001$, represented by *) and at d3 ($p<0.0001$, represented by *). Decreases in expression were found with p50 myoblasts treated with DM+10 μ M Bpv(Hopic) vs p5 myoblasts treated with DM+10 μ M Bpv(Hopic) at d1 ($p<0.0001$, represented by #), at d2 ($p<0.0001$, represented by #) and d3 ($p<0.01$, represented by #). Increases were indicated with p50 myoblasts treated with DM vs p5 myoblasts treated with DM+10 μ M Bpv(Hopic) at d1 ($p<0.0001$, represented by a) (p-values obtained by unpaired t-test (D). Data are representative of 4 experiments performed in duplicate.

6.5.4. DIFFERENTIAL EXPRESSION OF SPIRE AND FORMIN GENES IN RESPONSE TO BPV(HOPIC) AND SERIAL PASSAGING

Spire1 gene expression was examined in p5 and p50 myoblasts in response to DM or DM+10 μ M Bpv(Hopic) (Figure 6.7). Similar to MyoD and Myogenin expression, decreases were observed in Spire1 gene expression with passage. Decreases were found with p50 myoblasts vs p5 myoblasts treated with DM at d1 (0.7 \pm 0.06 vs 1, $p<0.01$, equivalent to 1.43 fold decrease) and, although not statistically significant, the same tendency was observed at d2 (0.61 \pm 0.04 vs 0.8 \pm 0.07, $p=0.051$, equivalent to 1.31 fold decrease). A slight, but significant increase with time was observed with p5 myoblasts treated with DM at d1 vs d0 (1 vs 0.84 \pm 0.06, $p<0.05$, equivalent to 1.19 fold increase), while a decrease was observed at d3 vs d0 (0.66 \pm 0.04 vs 0.84 \pm 0.06, $p<0.05$, equivalent to 1.27 fold decrease). A decrease with time was also found with p5 myoblasts treated with DM at d3 vs d1 (0.66 \pm 0.04 vs 1, $p<0.001$, equivalent to 1.52 fold decrease) and at d2 vs d1 (0.8 \pm 0.07 vs 1, $p<0.05$, equivalent to 1.25 fold decrease). These

data suggest a gradual decrease in Spire1 gene expression after differentiation has been triggered. Similar observations were made with p50 myoblasts. Decreases with time were found with p50 myoblasts treated with DM at d3 vs d0 (0.54 +/- 0.03 vs 0.73 +/- 0.02, $p < 0.001$, equivalent to 1.35 fold decrease) and at d2 vs d0 (0.61 +/- 0.04 vs 0.73 +/- 0.02, $p < 0.05$, equivalent to 1.20 fold decrease), but not at d1 vs d0, while a decrease was also observed with p50 myoblasts between d3 vs d1 (0.54 +/- 0.03 vs 0.7 +/- 0.06, $p < 0.01$, equivalent to 1.30 fold decrease).

Similar to MyoD and Myogenin expression, decreases were observed in Spire1 gene expression following Bpv(Hopic) treatment. Decreases were indicated with p5 myoblasts treated with DM+10 μ M Bpv(Hopic) vs DM at d1 (0.4 +/- 0.04 vs 1, $p < 0.001$, equivalent to 2.5 fold decrease) and at d2 (0.66 +/- 0.07 vs 0.8 +/- 0.07, $p < 0.05$, equivalent to 1.21 fold decrease). Decreases with time were indicated with p5 myoblasts treated with DM+10 μ M Bpv(Hopic) at d1 vs d0 (0.4 +/- 0.04 vs 0.84 +/- 0.06, $p < 0.01$, equivalent to 2.1 fold decrease) and at d2 vs d0 (0.66 +/- 0.07 vs 0.84 +/- 0.06, $p < 0.05$, equivalent to 1.27 fold decrease). Increases in Spire1 expression with time were found with p5 myoblasts treated with DM+10 μ M Bpv(Hopic) at d3 vs d1 (0.7 +/- 0.08 vs 0.4 +/- 0.04, $p < 0.001$, equivalent to 1.75 fold increase) and at d2 vs d1 (0.66 +/- 0.07 vs 1, $p < 0.01$, equivalent to 1.52 fold decrease), indicating the same tendency, observed with MyoD and Myogenin, of myoblasts to gradually increase their Spire1 gene expression in the presence of Bpv(Hopic) treatment after an initial drop at d1. Decreases were also observed with p50 myoblasts treated with DM+10 μ M Bpv(Hopic) vs p50 myoblasts treated with DM at d1 (0.37 +/- 0.03 vs 0.7 +/- 0.06, $p < 0.001$, equivalent to 1.89 fold decrease) and at d2 (0.47 +/- 0.03 vs 0.61 +/- 0.04, $p < 0.01$, equivalent to 1.30 fold decrease). Similar trend of time decrease, as with p5 myoblasts, was observed with p50 myoblasts treated with DM+10 μ M Bpv(Hopic): a decrease at d1 vs d0 (0.37 +/- 0.03 vs 0.73 +/- 0.02, $p < 0.001$, equivalent to 1.97 fold decrease), at d2 vs d0 (0.47 +/- 0.03 vs 0.73 +/- 0.02, $p < 0.001$, equivalent to 1.55 fold decrease) and d3 vs d0 (0.49 +/- 0.05 vs 0.73 +/- 0.02, $p < 0.001$, equivalent to 1.49 fold decrease), followed by an increase with at d2 vs d1 (0.47 +/- 0.03 vs 1, $p < 0.01$, equivalent to 2.12 fold increase) and at d3 vs d1 (0.49 +/- 0.05 vs 1, $p < 0.001$, equivalent to 2.04 fold increase). These data also show that expression levels of Spire1, following treatment with the inhibitor, are reduced below the expression levels evident at d0.

Decreases were indicated with p50 myoblasts treated with DM+10 μ M Bpv(Hopic) vs p5 myoblasts treated with DM at d1 (0.37 +/-0.03 vs 1, p<0.0001, equivalent to 2.7 fold decrease) and at d2 (0.47 +/-0.03 vs 0.8 +/-0.07, p<0.01, equivalent to 1.7 fold decrease). Decreases were also evident with p50 myoblasts treated with DM+10 μ M Bpv(Hopic) vs p5 myoblasts treated with DM+10 μ M Bpv(Hopic) at d2 (0.47 +/-0.03 vs 0.66 +/-0.07, p<0.05, equivalent to 1.4 fold increase). These observations indicate, similarly to MyoD and Myogenin expression, a negative regulation of both serial passaging and Bpv(Hopic) treatment on the expression of Spire1 gene. However, the combination of serial passaging and Bpv(Hopic) did not reduce Spire1 gene expression to the extent which it did with MyoD and Myogenin. An increase was found with p50 myoblasts treated with DM vs p5 myoblasts treated with DM+10 μ M Bpv(Hopic) at d1 (0.7 +/-0.06 vs 0.4 +/-0.04, p<0.01, equivalent to 1.75 fold increase), suggesting that the Bpv(Hopic) inhibitor is a more potent regulator of Spire1 at d1, compared to serial passaging alone.

Overall, these observations indicate a similar expression pattern of Spire1 to MyoD and Myogenin, following serial passaging and Bpv(Hopic) treatment.

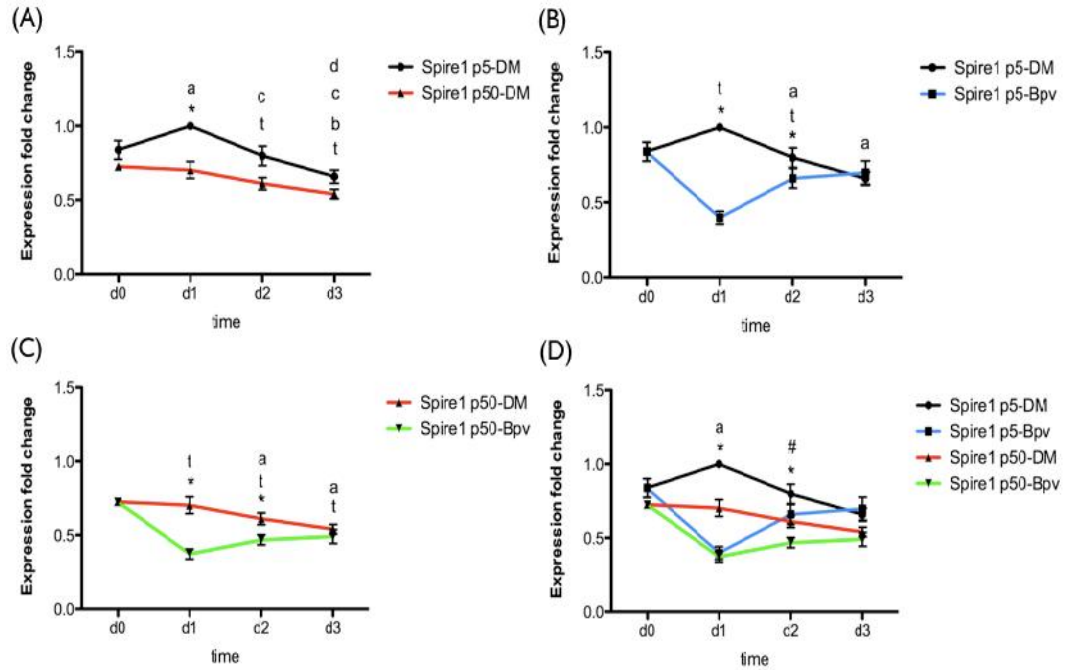


Figure 6.7. Spire1 gene expression levels in p5 and p50 myoblasts incubated for 3 days in DM with and without 10 μ M Bpv(Hopic). Spire1 gene expression levels examining the difference between p5 and p50 C2C12 myoblasts at d0, d1, d2 and d3 following treatment with DM or DM+10 μ M Bpv(Hopic). All values are represented as fold change to the calibrator (p5 DM d1), which was set to 1 (mean Ct value =25 +/- 0.49). Effect of passage (p5-DM vs p50-DM): Decreases in Spire1 expression were found with p50 myoblasts vs p5 myoblasts at d1 ($p < 0.01$, represented by *) and, although not significant, tendency of decrease was also observed at d2 ($p = 0.05$). Decreases in expression of Spire1 with time were found with p5 myoblasts treated with DM at d2 vs d1 ($p < 0.05$, represented by t) and at d3 vs d1 ($p < 0.001$, represented by t). Increases in Spire1 expression with time were found with p5 myoblasts treated with DM at d1 vs d0 ($p < 0.05$, represented by a), while expression decreased at d3 vs d0 ($p < 0.05$, represented by b). Decreases were found with p50 myoblasts at d3 vs d0 ($p < 0.001$, represented by c), at d2 vs d0 ($p < 0.05$, represented by c) and at d3 vs d1 ($p < 0.01$, represented by d) (p -values obtained by One-way repeated measures ANOVA (changes in gene expression with time) and unpaired t-test (changes in expression with p5 vs p50)) (A). Effect of Bpv(Hopic) treatment on p5 myoblasts (p5-DM vs p5-Bpv): Decreases in Spire1 expression were observed with p5 myoblasts treated with DM+10 μ M Bpv(Hopic) vs myoblasts treated with DM at d1 ($p < 0.001$, represented by *) and at d2 ($p < 0.05$, represented by *). Decreases in expression with time were indicated with p5 myoblasts treated with DM+10 μ M Bpv(Hopic) at d1 vs d0 ($p < 0.01$, represented by t) and at d2 vs d0 ($p < 0.05$, represented by t). Increases in expression were found with p5 myoblasts treated with DM+10 μ M Bpv(Hopic) at d3 vs d1 ($p < 0.001$, represented by a) and at d2 vs

d1 ($p < 0.01$, represented by a) (p-values obtained by One-way repeated measures ANOVA (changes in gene expression with time) and unpaired t-test (changes in expression with p5 vs p50)) (B). Effect of Bpv(Hopic) treatment on p50 myoblasts (p50-DM vs p50-Bpv): Decreases in Spire1 expression were observed with p50 myoblasts treated with DM+10 μ M Bpv(Hopic) vs p50 myoblasts treated with DM at d1 ($p < 0.001$, represented by *) and at d2 ($p < 0.01$, represented by *). Decreases in expression with time were found with p50 myoblasts treated with DM+10 μ M Bpv(Hopic) at d1 vs d0 ($p < 0.001$, represented by t), d2 vs d0 ($p < 0.001$, represented by t) and d3 vs d0 ($p < 0.001$, represented by t). Increases with time were found with p50 myoblasts treated with DM+10 μ M Bpv(Hopic) at d2 vs d1 ($p < 0.01$, represented by a) and at d3 vs d1 ($p < 0.001$, represented by a) (p-values obtained by One-way repeated measures ANOVA (changes in gene expression with time) and paired t-test (changes in expression with DM vs BpV)) (C). Interactions between groups: Decreases in Spire1 expression were indicated with p50 myoblasts treated with DM+10 μ M Bpv(Hopic) vs p5 myoblasts treated with DM at d1 ($p < 0.0001$, represented by *) and at d2 ($p < 0.01$, represented by *). Reductions in expression were observed with p50 myoblasts treated with DM+10 μ M Bpv(Hopic) vs p5 myoblasts treated with DM+10 μ M Bpv(Hopic) at d2 ($p < 0.05$, represented by #). Increases were found with p50 myoblasts treated with DM vs p5 myoblasts treated with DM+10 μ M Bpv(Hopic) at d1 ($p < 0.01$, represented by a) (p-values obtained by unpaired t-test (D). Data are representative of 4 experiments performed in duplicate.

Spire2 gene expression was examined in p5 and p50 myoblasts in response to DM or DM+10 μ M Bpv(Hopic) (Figure 6.8). Contrary to what was observed with MyoD, Myogenin and Spire1, no significant changes in gene expression of Spire2 were observed with passage. However, expression of Spire2 was altered with time. Increases were evident with p5 myoblasts treated with DM at d1 vs d0 (1 vs 0.35 \pm 0.07, $p < 0.01$, equivalent to 2.86 fold increase), at d2 vs d0 (1.18 \pm 0.06 vs 0.35 \pm 0.07, $p < 0.001$, equivalent to 3.37 fold increase) and at d3 vs d0 (1.43 \pm 0.15 vs 0.35 \pm 0.07, $p < 0.001$, equivalent to 4.09 fold increase). Similar increases were also found with p50 myoblasts at d1 vs d0 (0.98 \pm 0.18 vs 0.48 \pm 0.1, $p < 0.01$, equivalent to 2.04 fold increase), at d2 vs d0 (1.25 \pm 0.1 vs 0.48 \pm 0.1, $p < 0.001$, equivalent to 2.6 fold increase), at d3 vs d0 (1.36 \pm 0.19 vs 0.48 \pm 0.1, $p < 0.001$, equivalent to 2.83 fold increase) and at d3 vs d1 (1.36 \pm 0.19 vs 0.98 \pm 0.18, $p < 0.05$, equivalent to fold 1.39 increase), indicating a gradual increase of Spire2 gene expression after differentiation had been triggered.

Bpv(Hopic) treatment induced changes in Spire2 gene expression, however, contrary to what was previously observed with MyoD, Myogenin and Spire1, no

significant changes were observed at day 1 following DM addition. A decrease was observed with p5 myoblasts treated with DM+10 μ M Bpv(Hopic) vs p5 myoblasts treated with DM at d2 (0.69 +/-0.04 vs 1.18 +/-0.06, p<0.01, equivalent to 1.71 fold decrease) and at d3 (0.66 +/-0.05 vs 1.43 +/-0.15, p<0.01, equivalent to 2.17 fold decrease). Increases with time were indicated with p5 myoblasts treated with DM+10 μ M Bpv(Hopic) at d1 vs d0 (0.98 +/- 0.15 vs 0.35 +/-0.07, p<0.01, equivalent to 2.8 fold increase). Decreases, although not statistically significant, were visible with p5 myoblasts treated with DM+10 μ M Bpv(Hopic) at d2 vs d1 and d3 vs d1. This confirms the inhibitory effect of Bpv(Hopic) on the expression of Spire2 at days 2 and 3 after differentiation has been triggered. Similarly, decreases were observed with p50 myoblasts treated with DM+10 μ M Bpv(Hopic) vs p50 myoblasts treated with DM at d2 (0.72 +/-0.05 vs 1.25 +/-0.1, p<0.05, equivalent to 1.74 fold decrease) and at d3 (0.47 +/-0.05 vs 1.36 +/-0.19, p<0.05, equivalent to 2.89 fold decrease). An increase in expression with time was found with p50 myoblasts treated with DM+10 μ M Bpv(Hopic) at d1 vs d0 (1.26 +/-0.13 vs 0.48 +/-0.1, p<0.001, equivalent to 2.63 fold increase). Decreases were indicated with p50 myoblasts treated with DM+10 μ M Bpv(Hopic) at d2 vs d1 (0.72 +/-0.05 vs 1.26 +/-0.13, p<0.01, equivalent to 1.75 fold decrease) and at d3 vs d1 (0.47 +/-0.05 vs 1.26 +/-0.13, p<0.001, equivalent to 2.68 fold decrease). Taken together with the previous data, these observations suggest identical expression responses of Spire2 to Bpv(Hopic) treatment between p5 and p50 myoblasts.

Further decreases were observed with p5 myoblasts treated with DM+10 μ M Bpv(Hopic) vs p50 myoblasts treated with DM at d2 (0.69 +/-0.04 vs 1.25 +/-0.1, p<0.01, equivalent to 1.81 fold decrease) and at d3 (0.66 +/-0.05 vs 1.36 +/-0.19, p<0.05, equivalent to 2.06 fold decrease) and also with p50 myoblasts treated with DM+10 μ M Bpv(Hopic) vs p5 myoblasts treated with DM at d2 (0.72 +/-0.05 vs 1.18 +/-0.06, p<0.01, 1.63 equivalent to fold decrease) and at d3 (0.47 +/-0.05 vs 1.43 +/-0.15, p<0.001, equivalent to 3.04 fold decrease).

Overall, these observations indicate an increase of Spire2 gene expression after differentiation has been triggered, which is reduced by treatment with 10 μ M Bpv(Hopic) at days 2 and 3, but not at d1, no influence of serial passaging in the absence or presence of Bpv (Hopic), on Spire 2 gene expression was observed, suggesting that unlike other experimental observations in this chapter, Spire 2 is

not involved in the declining differentiation associated with multiple populations doublings.

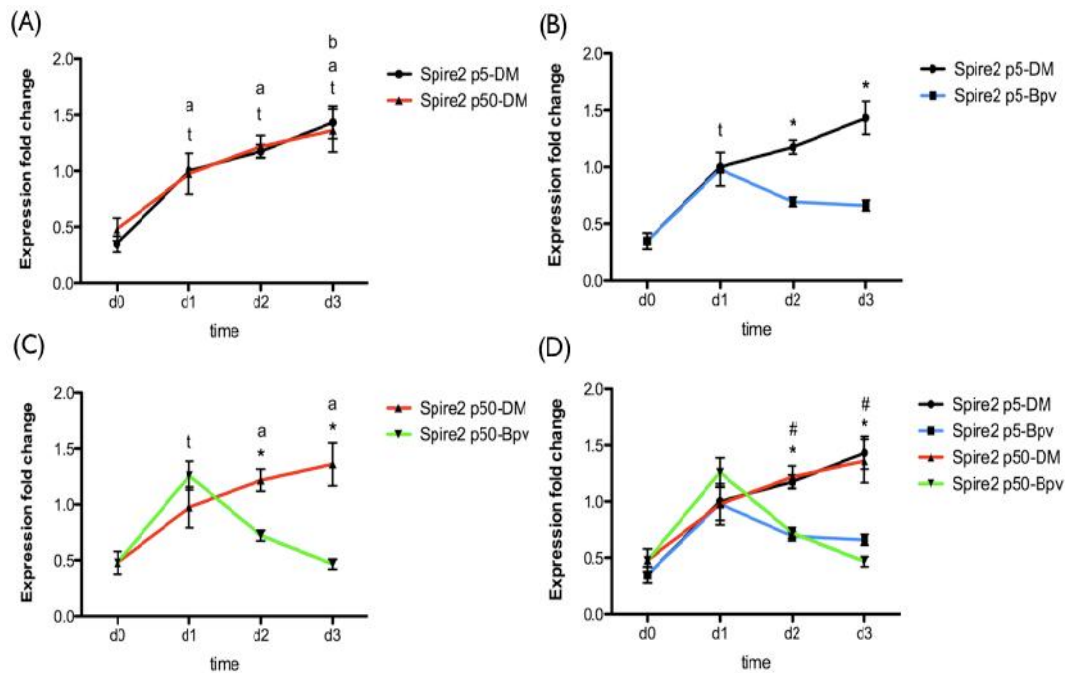


Figure 6.8. Spire2 gene expression levels in p5 and p50 myoblasts incubated for 3 days in DM with and without 10 μ M Bpv(Hopic). Spire2 gene expression levels examining the difference between p5 and p50 C2C12 myoblasts at d0, d1, d2 and d3 following treatment with DM or DM+10 μ M Bpv(Hopic). All values are represented as fold change to the calibrator (p5 DM d1), which was set to 1 (mean Ct value =32.33 +/-0.21). Effect of passage (p5-DM vs p50-DM): No significant effect in expression of Spire2 was observed with passage. However, increases in Spire2 expression with time were found with p5 myoblasts treated with DM at d1 vs d0 ($p < 0.01$, represented by t), at d2 vs d0 ($p < 0.001$, represented by t) and at d3 vs d0 ($p < 0.001$, represented by t). Increases in expression with time were indicated with p50 myoblasts treated with DM at d1 vs d0 ($p < 0.01$, represented by a), at d2 vs d0 ($p < 0.001$, represented by a), at d3 vs d0 ($p < 0.001$, represented by a) and at d3 vs d1 ($p < 0.05$, represented by b) (p-values obtained by One-way repeated measures ANOVA (changes in gene expression with time) and unpaired t-test (changes in expression with p5 vs p50)) (A). Effect of Bpv(Hopic) treatment on p5 myoblasts (p5-DM vs p5-Bpv): Decreases in Spire2 expression were present with p5 myoblasts treated with DM+10 μ M Bpv(Hopic) vs p5 myoblasts treated with DM at d2 ($p < 0.01$, represented by *) and at d3 ($p < 0.01$, represented by *). Increases in expression with time were indicated with p5 myoblasts treated with DM+10 μ M Bpv(Hopic) at d1 vs d0 ($p < 0.01$, represented by t) (p-values obtained by One-way repeated measures ANOVA (changes in gene expression with time) and unpaired t-test (changes in expression with p5 vs p50)) (B). Effect of Bpv(Hopic) treatment on p50

myoblasts (p50-DM vs p50-Bpv): Decreases in Spire2 expression were indicated with p50 myoblasts treated with DM+10 μ M Bpv(Hopic) vs p50 myoblasts treated with DM at d2 ($p < 0.05$, represented by *) and at d3 ($p < 0.05$, represented by *). Increases in expression with time were observed with p50 myoblasts treated with DM+10 μ M Bpv(Hopic) at d1 vs d0 ($p < 0.001$, represented by t). Decreases were found with p50 myoblasts treated with DM+10 μ M Bpv(Hopic) at d2 vs d1 ($p < 0.01$, represented by a) and at d3 vs d1 ($p < 0.001$, represented by a) (p-values obtained by One-way repeated measures ANOVA (changes in gene expression with time) and paired t-test (changes in expression with DM vs BpV)) (C). Interactions between groups: Significant decreases were found with p50 myoblasts treated with DM+10 μ M Bpv(Hopic) vs p5 myoblasts treated with DM at d2 ($p < 0.01$, represented by *) and at d3 ($p < 0.001$, represented by *). Significant decreases were also indicated with p5 myoblasts treated with DM+10 μ M Bpv(Hopic) vs p50 myoblasts treated with DM at d2 ($p < 0.01$, represented by #) and at d3 ($p < 0.05$, represented by #) (p-values obtained by unpaired t-test (D)). Data are representative of 4 experiments performed in duplicate.

Formin1 gene expression was examined in p5 and p50 myoblasts in response to DM or DM+10 μ M Bpv(Hopic) (Figure 6.9). A slight, but significant, increase with passage was discovered with p50 myoblasts vs p5 myoblasts treated with DM at d2 (1.27 \pm 0.02 vs 1.06 \pm 0.07, $p < 0.05$, equivalent to 1.2 fold increase) and at d3 (1.17 \pm 0.09 vs 0.92 \pm 0.04, $p < 0.05$, equivalent to 1.27 fold increase). These observations are the contrary to what was previously observed with MyoD, Myogenin and Spire genes. Reductions with time were found with p5 myoblasts treated with DM at d1 vs d0 (1 vs 1.49 \pm 0.09, $p < 0.01$, equivalent to 1.49 fold decrease), at d2 vs d0 (1.06 \pm 0.07 vs 1.49 \pm 0.09, $p < 0.01$, equivalent to 1.41 fold decrease) and at d3 vs d0 (0.92 \pm 0.04 vs 1.49 \pm 0.09, $p < 0.001$, equivalent to 1.62 fold decrease), showing a decrease in expression levels after differentiation has been triggered. No significant decrease was observed with time when p50 cells were treated with DM and levels remained unchanged during the 4 different time points examined. Changes in Formin1 gene expression were observed after treatment with 10 μ M Bpv(Hopic). An increase was found with p5 myoblasts treated with DM+10 μ M Bpv(Hopic) vs p5 myoblasts treated with DM at d1 (1.33 \pm 0.06 vs 1, $p < 0.05$, equivalent to 1.33 fold increase), at d2 (1.94 \pm 0.05 vs 1.06 \pm 0.07, $p < 0.01$, equivalent to 1.83 fold increase) and at d3 (1.57 \pm 0.05 vs 0.92 \pm 0.04, $p < 0.001$, equivalent to 1.71 fold increase). Once again, these observations are contrary to what was previously observed with MyoD, Myogenin

and Spire genes. Increases with time were found with p5 myoblasts treated with DM+10 μ M Bpv(Hopic) at d2 vs d0 (1.94 \pm 0.05 vs 1.49 \pm 0.09, p <0.01, equivalent to 1.3 fold increase), at d2 vs d1 (1.94 \pm 0.05 vs 1.33 \pm 0.06, p <0.001, equivalent to 1.46 fold increase) and at d2 vs d3 (1.94 \pm 0.05 vs 1.57 \pm 0.05, p <0.01, equivalent to 1.24 fold increase). Thus, Formin1 gene expression seems to be slightly reduced (although not significant) after differentiation is triggered, but Bpv(Hopic) treatment is able to increase the expression, with a peak at 2 days. An increase was also found with p50 myoblasts treated with DM+10 μ M Bpv(Hopic) vs p50 myoblasts treated with DM at d2 (1.46 \pm 0.04 vs 1.27 \pm 0.02, p <0.05, equivalent to 1.15 fold increase) and, although not significant, an increase was also observed at d3 (1.62 \pm 0.08 vs 1.17 \pm 0.09, p =0.06, equivalent to 1.38 fold increase). This once again suggests an effect of Bpv(Hopic), opposite to the one observed previously with MyoD, Myogenin, Spire1 and Spire 2 genes. Gradual increases in Formin1 levels with time were observed when p50 myoblasts were subject to 10 μ M Bpv(Hopic) treatment. An increase was found with p50 myoblasts treated with DM+10 μ M Bpv(Hopic) at d3 vs d0 (1.62 \pm 0.08 vs 1.22 \pm 0.08, p <0.01, equivalent to 1.33 fold increase), at d3 vs d1 (1.62 \pm 0.08 vs 1 \pm 0.04, p <0.001, equivalent to 1.62 fold increase), and at d2 vs d1 (1 \pm 0.04 vs 1.46 \pm 0.04, p <0.001, equivalent to 1.46 fold increase).

Further increases were found with p50 myoblasts treated with DM+10 μ M Bpv(Hopic) vs p5 myoblasts treated with DM at d2 (1.46 \pm 0.04 vs 1.06 \pm 0.07, p <0.01, equivalent to 1.38 fold increase) and at d3 (1.62 \pm 0.08 vs 0.92 \pm 0.04, p <0.001, equivalent to 1.76 fold increase). However, increased expression of Formin1 with p50 vs p5 myoblasts treated with Bpv(Hopic) was not observed, rather a decrease was found with p50 myoblasts treated with DM+10 μ M Bpv(Hopic) vs p5 myoblasts treated with DM+10 μ M Bpv(Hopic) at d2 (1.46 \pm 0.04 vs 1.94 \pm 0.05, p <0.001, equivalent to 1.33 fold decrease). A decrease in Formin 1 expression was also found with p50 myoblasts treated with DM vs p5 myoblasts treated with DM+10 μ M Bpv(Hopic) at d2 (1.27 \pm 0.02 vs 1.94 \pm 0.05, p <0.0001, equivalent to 1.53 fold decrease) and at d3 (1.17 \pm 0.09 vs 1.57 \pm 0.05, p <0.01, equivalent to 1.34 fold decrease).

Overall, these findings indicate a tendency of increased Formin1 expression when myoblasts have been treated with Bpv(Hopic) and displayed reduced differentiation. Serial passaging also elevated the expression of Formin 1 in myoblasts treated with DM, but not in the presence of inhibitor. These

observations suggest that Formin1 expression is affected in an opposite manner to MyoD, Myogenin, Spire1 and Spire2 genes, following Bpv(Hopic) treatment and serial passaging.

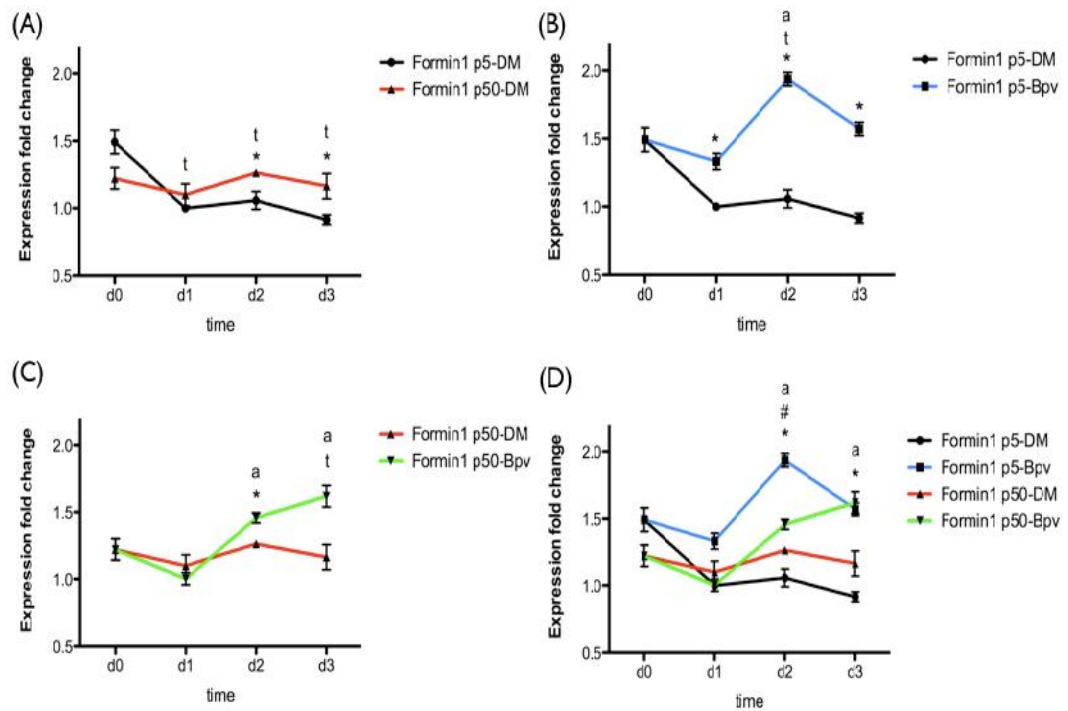


Figure 6.9. Formin1 gene expression levels in p5 and p50 myoblasts incubated for 3 days in DM with and without 10 μ M Bpv(Hopic). Formin1 gene expression levels examining the difference between p5 and p50 C2C12 myoblasts at d0, d1, d2 and d3 following treatment with DM or DM+10 μ M Bpv(Hopic). All values are represented as fold change to the calibrator (p5 DM d1), which was set to 1 (mean Ct value =26.8 +/-0.12). Effect of passage (p5-DM vs p50-DM): Increases in Formin1 expression were observed between p50 cells treated with DM vs p5 cells treated with DM at d2 (p<0.05, represented by *) and at d3 (p<0.05, represented by *). Decreases in expression were found with p5 myoblasts treated with DM at d1 vs d0 (p<0.01, represented by t), at d2 vs d0 (p<0.01, represented by t) and at d3 vs d0 (p<0.001, represented by t) (p-values obtained by One-way repeated measures ANOVA (changes in gene expression with time) and unpaired t-test (changes in expression with p5 vs p50)) (A). Effect of Bpv(Hopic) treatment on p5 myoblasts (p5-DM vs p5-Bpv): Increases in Formin1 expression were found with p5 myoblasts treated with DM+10 μ M Bpv(Hopic) vs p5 myoblasts treated with DM at d1 (p<0.05, represented by *), at d2 (p<0.01, represented by *) and at d3 (p<0.001, represented by *). Increase in expression with time were found with p5 myoblasts treated with DM+10 μ M Bpv(Hopic) at d2 vs d0 (p<0.05, represented by t). Increases were also found with p5 myoblasts treated with DM+10 μ M Bpv(Hopic) at d2 vs d1 (p<0.01, represented by a) and at d2 vs d3 (p<0.05, represented by a) (p-values obtained by One-way repeated measures ANOVA (changes in gene

expression with time) and unpaired t-test (changes in expression with p5 vs p50)) (B). Effect of Bpv(Hopic) treatment on p50 myoblasts (p50-DM vs p50-Bpv): Increase in Formin1 expression were found with p50 myoblasts treated with DM+10 μ M Bpv(Hopic) vs p50 myoblasts treated with DM at d2 ($p < 0.05$, represented by *). Increases in expression with time were found with p50 myoblasts treated with DM+10 μ M Bpv(Hopic) at d3 vs d0 ($p < 0.01$, represented by t). Increase in expression with time were also found with p50 myoblasts treated with DM+10 μ M Bpv(Hopic) at d2 vs d1 ($p < 0.001$, represented by a) and at d3 vs d1 ($p < 0.001$, represented by a) (p-values obtained by One-way repeated measures ANOVA (changes in gene expression with time) and paired t-test (changes in expression with DM vs BpV)) (C). Interactions between groups: Increases in Formin1 expression were found with p50 myoblasts treated with DM+10 μ M Bpv(Hopic) vs p5 myoblasts treated with DM at d2 ($p < 0.01$, represented by *) and at d3 ($p < 0.001$, represented by *). Decreases in expression were found with p50 myoblasts treated with DM+10 μ M Bpv(Hopic) vs p5 myoblasts treated with DM+10 μ M Bpv(Hopic) at d2 ($p < 0.001$, represented by #). Decreases were also found with p50 myoblasts treated with DM vs p5 myoblasts treated with DM+10 μ M Bpv(Hopic) at d2 ($p < 0.0001$, represented by a) and at d3 ($p < 0.01$, represented by a) (p-values obtained by unpaired t-test (D). Data are representative of 4 experiments performed in duplicate.

Formin2 gene expression was examined in p5 and p50 myoblasts in response to DM or DM+10 μ M Bpv(Hopic) (Figure 6.10). Its expression pattern was different to what was previously observed with the other genes examined. Significant increases were observed with p50 myoblasts treated with DM vs p5 myoblasts treated with DM at d1 (4.36 \pm 0.87 vs 1, $p < 0.05$, equivalent to 4.36 fold increase), at d2 (4.91 \pm 0.89 vs 0.82 \pm 0.13, $p < 0.05$, equivalent to 6 fold increase) and at d3 (5.62 \pm 1.11 vs 0.89 \pm 0.36, $p < 0.05$, equivalent to 6.31 fold increase). No significant changes in expression were observed with time. Furthermore, no changes in expression were observed in response to BpV(Hopic) in both p5 and p50 myoblasts. All changes in expression of Formin2 were due to the effect of passage. Increases were indicated with p50 myoblasts treated with DM+10 μ M Bpv(Hopic) vs p5 myoblasts treated with DM at d1 (4.18 \pm 0.81 vs 1, $p < 0.01$, equivalent to 4.18 fold increase), d2 (4.5 \pm 0.78 vs 0.82 \pm 0.13, $p < 0.01$, equivalent to 5.48 fold increase) and d3 (5.3 \pm 1.58 vs 0.89 \pm 0.36, $p < 0.05$, equivalent to 5.96 fold increase). Increases were also observed with p50 myoblasts treated with DM+10 μ M Bpv(Hopic) vs p5 myoblasts treated with DM+10 μ M Bpv(Hopic) at d1 (4.18 \pm 0.81 vs 1.14 \pm 0.19, $p < 0.05$, equivalent to 3.67 fold increase), at d2 (4.5 \pm 0.78 vs 0.8 \pm 0.13, $p < 0.05$, equivalent to 5.63

fold increase) and, while significance was not achieved, the same tendency was evident at d3 (5.3 +/-1.58 vs 0.58 +/-0.21, p=0.057, equivalent to 9.14 fold increase). Increases were further observed with p50 DM vs p5 myoblasts treated with DM+10 μ M Bpv(Hopic) at d1 (4.36 +/-0.87 vs 1.14 +/-0.19, p<0.05, equivalent to 3.82 fold increase) and d2 (4.91 +/-0.89 vs 0.8 +/-0.13, p<0.01, equivalent to 6.14 fold increase) and at d3 (5.62 +/-1.11 vs 0.58 +/-0.21, p<0.01, equivalent to 9.69 fold increase).

Overall, these data indicate increased expression of Formin2 gene in serially passaged p50 cells, as compared to p5 cells, with Bpv(Hopic) treatment not exerting significant effect, suggesting that while Formin 1 was affected by BpV(Hopic), Formin 2 was affected by passage.

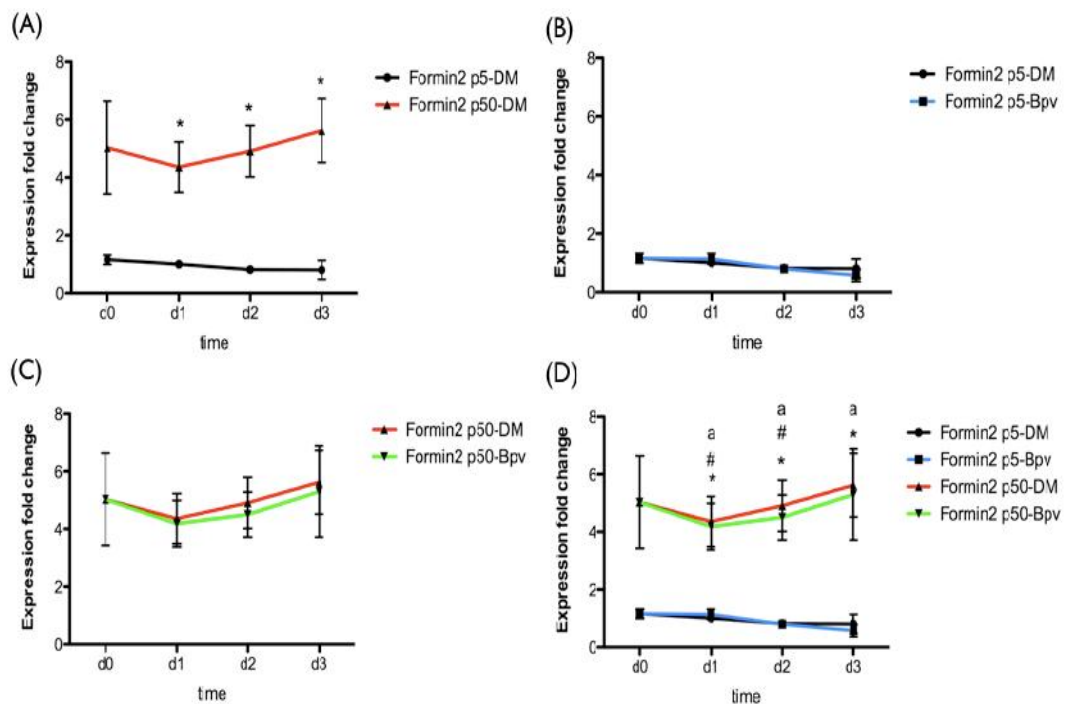


Figure 6.10. Formin2 gene expression levels in p5 and p50 myoblasts incubated for 3 days in DM with and without 10 μ M Bpv(Hopic). Formin2 gene expression levels examining the difference between p5 and p50 C2C12 myoblasts at d0, d1, d2 and d3 following treatment with DM or DM+10 μ M Bpv(Hopic). All values are represented as fold change to the calibrator (p5 DM d1), which was set to 1 (mean Ct value =35.25 +/-0.24). Effect of passage (p5-DM vs p50-DM): Increases in Formin2 expression were observed with p50 myoblasts treated with DM vs p5 myoblasts treated with DM at d1 (p<0.05, represented by *), at d2 (p<0.05, represented by *) and at d3 (p<0.05, represented by *) (p-values obtained by One-way repeated measures ANOVA (changes in gene expression with time) and unpaired t-test (changes in expression with p5 vs p50)) (A). Effect of Bpv(Hopic) treatment on p5 myoblasts (p5-DM vs p5-Bpv): No

significant differences were found between the groups with inhibitor or with time (p-values obtained by One-way repeated measures ANOVA (changes in gene expression with time) and unpaired t-test (changes in expression with p5 vs p50)) (B). Effect of Bpv(Hopic) treatment on p50 myoblasts (p50-DM vs p50-Bpv): No significant differences were found between the groups with inhibitor or with time (p-values obtained by One-way repeated measures ANOVA (changes in gene expression with time) and paired t-test (changes in expression with DM vs BpV)) (C). Interactions between groups: Increases in Formin2 expression were found with p50 myoblasts treated with DM+10 μ M Bpv(Hopic) vs p5 myoblasts treated with DM at d1 (p<0.01, represented by *), at d2 (p<0.01, represented by *) and at d3 (p<0.05, represented by *). Increases in expression were observed with p50 myoblasts treated with DM+10 μ M Bpv(Hopic) vs p5 myoblasts treated with DM+10 μ M Bpv(Hopic) at d1 (p<0.05, represented by #), at d2 (p<0.05, represented by #) and, although not significant, the same tendency was observed also at d3 (p=0.057). Increases were found with p50 myoblasts treated with DM vs p5 myoblasts treated with DM+10 μ M Bpv(Hopic) at d1 (p<0.05, represented by a), at d2 (p<0.01, represented by a) and at d3 (p<0.01, represented by a) (p-values obtained by unpaired t-test (D). Data are representative of 4 experiments performed in duplicate.

SUMMARY OF MAJOR FINDINGS

- Serially passaged (p50) myoblasts are less capable of differentiating, as compared to p5 myoblasts, and demonstrate further reduction in differentiation capacity following 10 μ M Bpv(Hopic) treatment, associated with greater reduction in the gene expression of myogenic regulatory factors, such as MyoD and Myogenin.
- Spire1 gene expression is reduced by serial passaging and by 10 μ M Bpv(Hopic) treatment.
- Spire2 gene expression is reduced by 10 μ M Bpv(Hopic) treatment, notable after d2 post treatment, but is unaffected by serial passaging.
- Formin1 gene expression demonstrates a tendency to increase following serial passaging and is elevated by 10 μ M Bpv(Hopic) treatment, most notable at d2 and d3 post treatment.
- Formin2 gene expression is unaffected by 10 μ M Bpv(Hopic) treatment, but it is significantly increased following serial passaging of myoblasts.

6.6. DISCUSSION

6.6.1. SERIALY PASSAGED C2C12 MYOBLASTS (P50) DEMONSTRATE IMPAIRED CAPACITY TO DIFFERENTIATE COMPARED TO LOW PASSAGE CELLS (P5), WHICH IS FURTHER REDUCED BY TREATMENT WITH 10 μ M BPV(HOPIC).

Previously, reduced differentiation potential was demonstrated by serial passaging (Chapter 4) and following 10 μ M Bpv(Hopic) treatment (Chapter 5). Here, it was demonstrated that inhibition of differentiation was even larger when serially passaged myoblasts were treated with Bpv(Hopic), as compared to any of these treatments alone, demonstrated by reduced levels of CK activity and lower expression of MyoD and Myogenin genes. It must be noted that the reduction of MyoD gene expression after DM addition is not what normally occurs. This is probably due to the high confluency of cells at which differentiation was initiated, which may have triggered high expression of MyoD at d0, committing cells to the myogenic lineage before DM was added to the cells. Never the less, serial passaging and Bpv(Hopic) treatment significantly reduced the expression levels of MyoD, as compared to controls. Sharples *et al.* demonstrated that serially passaged myoblasts (P20), at early time points upon transfer from GM to DM, continue to progress through the cell cycle, with greater percentage of cells in S and G2 phases (Sharples *et al.*, 2011). This, together with the reported decrease in phosphorylation of AKT and decreased IGF-1 transcript levels in DM treated myoblasts, could explain the reduced differentiation of serially passaged myoblasts. It was here demonstrated that 20h following transfer to DM, serially passaged cells no longer have higher percentage of cells in G2/S phases, as compared to low passage of myoblasts. At the same time point, however, both p5 and p50 cells treated with 10 μ M Bpv(Hopic) had a significantly greater percentage of cells in G2/S-phases. This could, at least partly, explain why differentiation is further inhibited by addition of Bpv(Hopic) to serially passaged cells, which even at 20hrs post addition of DM, caused myoblasts to continue to progress through the cell cycle and thus further delayed their differentiation. Thus, myoblast fusion into myotubes is reduced by serial passaging, but completely blocked/delayed in the presence of 10 μ M Bpv(Hopic).

6.6.2. DIFFERENTIAL EXPRESSION OF SPIRE AND FORMIN GENES IN RESPONSE TO BPV(HOPIC) AND SERIAL PASSAGING

Using the expression of MyoD and Myogenin genes as a reference for how the differentiation of myoblasts is affected in response to Bpv(Hopic) treatment, serial passaging and the combination of both, it was next addressed how these stimuli influenced the expression of Spire and Formin genes. As inhibition of myoblast differentiation and fusion by both inhibitor treatment and serial passaging was observed, it was hypothesised that if any of the Spire or Formin genes were involved in the process of myoblast fusion, their expression could also be altered.

With a Ct value of 25 +/-0.49, Spire1 gene was expressed in C2C12 cells. Its expression peaked at day1 following addition of DM, despite this increase being smaller, as compared to Myogenin, and similar to MyoD and Myogenin, decreased at day2 and day3. Expression of Spire1 gene seemed to be similar to that of MyoD and Myogenin in its tendency to reduce its expression after differentiation and fusion were inhibited by Bpv(Hopic) treatment and serial passaging. These data suggest that Spire1 might be involved in the process of myotube formation and promises to be an interesting target for further research into its function in skeletal muscle. On the other hand, Spire2 gene expression was lower in C2C12 cells, with a Ct value of 32.33 +/-0.21. Interestingly, its expression increased 4-fold, as fusion progressed, suggesting its potential involvement in the process, although not clear whether it is involved in its regulation, or whether its expression is influenced by fusion/differentiation. The link between Spire2 expression and fusion/differentiation of myoblasts was supported by observations that its expression was significantly inhibited following 10µM Bpv(Hopic) treatment. However, no difference in Spire2 expression was observed between p5 and p50 myoblasts. Thus, it seems that Spire2 expression is not impacted by changes in basal differentiation, but is reduced globally by 10µM Bpv(Hopic), suggesting it may display delayed suppression as a consequence of global phosphotyrosine activation, independent of differentiation or fusion. Formin1 gene was also expressed in C2C12 cells, with a Ct value of 26.8 +/-0.12. Interestingly, it demonstrated an inverse expression trend in response to serial passaging and 10µM Bpv(Hopic) treatment, as compared to what was previously observed with MyoD, Myogenin and Spire genes. The expression of Formin1 seemed to be reduced with progression of differentiation with p5, but not with p50 myoblasts, and inhibition of differentiation and myoblast fusion was associated

with increases in its expression. Both Bpv(Hopic) and serial passaging, negatively affecting myoblast fusion, seemed to result in increases of Formin1 expression, although this response was delayed and was obvious after day 2 of DM addition. This suggested that Formin1 might be an interesting target for further research. Finally, investigating the expression of Formin2 demonstrated that this gene was very weakly expressed in p5 myoblasts, with Ct value of above 35, however, interestingly, its expression in p50 myoblasts was significantly higher compared to that in p5 myoblasts. Bpv(Hopic) treatment caused no changes in expression pattern of Formin2. Its almost undetectable expression levels and no changes with time or following Bpv(Hopic) question its involvement in myogenesis, although its considerably higher expression in serially passaged cells might be of interest for further studies into its potential functions in skeletal muscle ageing.

Despite reported alterations in expression of Spire and Formin genes with Bpv(Hopic), serial passaging, or both, the function of these genes in skeletal muscle remains unknown. However, knowing that they are expressed in myoblasts and that their expression differs in response to factors affecting myoblast fusion, holds a promise that they might be involved in regulating this process. Of particular interest would be Spire1 and Formin1 genes, whose expression is inversely affected by inhibition of myoblast fusion with both serial passaging and Bpv(Hopic). Despite Spire1 and Spire2 proteins being able to interact with both Formin1 and Formin2 proteins, it is not known whether all of these associations are indeed required for their functions *in vivo*, and in particular in skeletal muscle. Thus, further studies on protein level are required to elucidate the functions of Spires and Formins in skeletal muscle. Considering the involvement of these genes in endocytic recycling and intracellular trafficking (Kerkhoff *et al.*, 2001, Kerkhoff, 2010, Morel *et al.*, 2009, Schuh, 2011), which are also associated with myoblast fusion and migration (Doherty *et al.*, 2008, Rochlin *et al.*, 2010, Caswell and Norman, 2006, Pellinen and Ivaska, 2006), it was suggested that these genes might provide to be interesting targets for future research into their function in skeletal muscle.

6.6.3. CONCLUSIONS

Overall, these studies demonstrate that Spire1, Spire2 and Formin1 genes are expressed in C2C12 myoblasts and that their expression is altered by factors influencing myoblast fusion. To our knowledge, these are the first data to demonstrate the expression of these genes in skeletal muscle myoblasts, but their particular function remains unknown. It was suggested that these genes are involved in myoblast fusion and migration via their involvement in vesicle transport. Of particular interest is the inverse expression of Spire1 and Formin1 genes in response to inhibition of myoblast differentiation and fusion by Bpv(Hopic) and serial passaging. Further studies needed to confirm their expression at a protein level. In addition, it would be interesting to investigate how silencing and overexpression of these genes would affect myogenic precursor cells and their differentiation potential. These studies might reveal in more detail the significance of the actin cytoskeleton in regulating myogenesis and improve our knowledge for muscle development and regeneration, which can ultimately lead to the development of therapies aimed at treating loss of muscle mass associated with injuries, degenerative disorders and ageing.

CHAPTER 7

7. DISCUSSION AND FUTURE DIRECTIONS

7.1. AIMS OF THESIS

Muscle loss can occur due to a variety of conditions, including genetic disorders, traumatic injuries, cancer or ageing, which can ultimately lead to weakness, loss of functional dependence or even death. Improving muscle regeneration for conditions leading to muscle loss is an important area of research, which can improve the lifestyle of millions of people worldwide and reduce the socio-economic burden associated with these symptoms. The studies presented in this thesis were performed in an attempt to elucidate in more details the cellular and molecular regulators of skeletal muscle myogenesis and regeneration. Skeletal muscle progenitor cells, satellite cells and their progeny of myoblasts, are key contributors to the process of muscle regeneration with their ability to migrate to the site of muscle damage, proliferate and fuse with damaged muscle fibres, thus promoting repair (reviewed in (Charge and Rudnicki, 2004, Hawke and Garry, 2001, Turner and Badylak, 2011)). Therefore, in order to develop or improve therapeutic approaches aimed at restoring muscle mass and to facilitate the muscle regeneration process, in depth knowledge into the regulators of muscle progenitor cell functions is required.

Migration of muscle progenitors is a necessary step in the process of muscle regeneration, in order for these cells to reach the site of muscle damage (Hawke and Garry, 2001, Watt *et al.*, 1994). Further, migration is required for the alignment of myoblasts prior to their subsequent fusion into myotubes (Louis *et al.*, 2008, Rochlin *et al.*, 2010). Myoblast migration has also been reported to be one of the limiting steps in proposed therapies of muscular dystrophies, which rely on the introduction of donor myoblasts, in order to repair dystrophic muscles (Fan *et al.*, 1996, Gussoni *et al.*, 1997, Moens *et al.*, 1996, Skuk *et al.*, 2004, Smythe *et al.*, 2001). Thus, improving our knowledge into the field of myoblast migration might not only be important for a better understanding of myogenesis and skeletal muscle regeneration, but might also have therapeutic applications. As discussed, external factors, such as growth factors secreted by infiltrating inflammatory cells or damaged skeletal muscle itself, are implicated in regulating myoblast migration. Internal factors, in particular signalling pathways, are also important for regulating and coordinating the migratory response of myogenic cells in response to the milieu of external factors. Many studies have focused on

investigating the effects of single factors on myoblast migration, but the complexity of interactions between different factors also needs to be considered, in both physiological and pathological conditions. Furthermore, muscle myogenesis and regeneration each comprises a series of events, which need to be strictly coordinated to enable the whole process. Extensive research is still required in order to reveal in full, the complexity of these interactions and how their modulation will culminate in developing therapies for conditions leading to muscle loss. Here, an attempt was made to contribute to this knowledge, by exploring the external and internal regulation of myoblast migration. The first aim was to explore *in vitro* the contribution of factors secreted by myogenic cells themselves by investigating the effect of myotube CM on the migration of myoblasts. A model of serially passaged C2C12 myoblasts was then be used to study how multiple divisions of these cells would affect their migration capacity and whether this could also have impact on their potential ability to secrete factors inducing migration of other myogenic cells. Further, CM inducing migration, enriched with variety of factors, was used as a model to reveal the involvement of biochemical signalling pathways, such as PI3K/AKT and MAPK/ERK, in myoblast migration. The activation of these signalling pathways by phosphotyrosine phosphatase inhibitor Bpv(Hopic) was assessed in the context of myoblast migration. The importance of these pathways, along with the FAK signalling pathway, were explored by selective inhibition of each pathway under conditions when the other pathways were still activated, in an attempt to investigate possible redundancy in intracellular signalling, thus addressing the importance of studying the complexity of factors influencing myoblast migration. Finally, as fusion and migration processes often share similar regulators, the possible involvement of 4 genes involved in actin nucleation was investigated and their expression studied in response to conditions influencing myoblast fusion.

7.2. CONDITIONED MEDIA AND THE IMPORTANCE OF SECRETED FACTORS FOR MYOBLAST MIGRATION

Migration of myogenic cells is regulated by a variety of extracellular factors. Growth factors and cytokines, which can regulate various processes of muscle progenitors, including migration, can both be secreted from inflammatory cells or damaged muscle (Bischoff, 1986, Chen and Quinn, 1992, Merly *et al.*, 1999, Ranzato *et al.*, 2009, Tidball, 2005). *In vitro* studies have investigated and

confirmed that many soluble factors are able to induce migration of satellite cells or myoblasts, including HGF, IL-4, TGF β , TNF α , RANTES, PDGF-A, PDGF-B, FGF, IGF-I (Amano *et al.*, 2002, Bischoff, 1997, Corti *et al.*, 2001, Lafreniere *et al.*, 2004, Lafreniere *et al.*, 2006, Torrente *et al.*, 2003). However, it must be considered that the balance and concentration of soluble factors might be particularly important for the regulation of muscle regeneration *in vivo*, including the migration of myogenic cells. For example, studies from our group have demonstrated that the combination of low doses of IGF-I and TNF α , is able to induce apoptosis of myoblasts, which does not occur in the presence of either of these two factors alone at equivalent concentrations (Saini *et al.*, 2008). Growth factors, such as HGF, TGF β and PDGF, are known to induce migration of myogenic cells, but this response is reduced with increasing growth factor concentrations (Bischoff, 1997, De Donatis *et al.*, 2008). It is therefore, important to reveal the presence and source of soluble factors in both physiological and pathological conditions, the combination of which, may influence muscle repair and hypertrophy. Here, an attempt was made to reveal the contribution of secreted soluble factors by myogenic cells themselves. It was demonstrated that SF media conditioned by myotubes is capable of inducing migration of myoblasts in a wound healing model and chemotaxis in transwell insert assays. Recent articles, published in the course of this thesis work, demonstrated that myoblasts are capable of upregulating the expression of many chemokines, with an expression peak at the time of myoblast fusion and myotube formation (Griffin *et al.*, 2009, Griffin *et al.*, 2010). They have further demonstrated that media conditioned by myoblasts were capable of inducing migration of myocytes. This, together with our data confirms the contribution of myogenic cells in different stages of differentiation in the release of factors stimulating migration of myoblasts, and most likely of other cell types and cellular processes as well. Further, the media conditioned by myotubes, starved in SF media was more potent at inducing migration, as compared to media conditioned by mechanically damaged/crushed myotubes. Thus, although the question remains regarding the specific factors released and their relative concentrations in both media, it is safe to suggest that the soluble factor milieu is different when mechanical damage is present, as opposed to a situation when myotubes are not mechanically damaged. It is possible that starved myotubes, as the ones used in our model, are releasing factors that are capable of stimulating myoblast migration, which can ultimately

lead to recruitment of more myonuclei, which can contribute key proteins enabling repair. In fact, numerous articles have demonstrated that diseased or regenerating muscles are capable of increasing the expression of cytokines, growth factors and chemokines, along with their receptors (Civatte *et al.*, 2005, De Rossi *et al.*, 2000, Griffin *et al.*, 2010, Hirata *et al.*, 2003, Peterson and Pizza, 2009, Porter *et al.*, 2003, Sachidanandan *et al.*, 2002, Summan *et al.*, 2003, Warren *et al.*, 2004). Many of these factors will not only affect muscle regeneration by direct effect on myogenic cells, but also indirectly by triggering inflammatory responses and the recruitment of inflammatory cells. Except migration, many of these factors are likely to be regulating other myogenic cell processes as well, such as proliferation and survival (Nedachi *et al.*, 2009, Vasyutina *et al.*, 2005, Yahiaoui *et al.*, 2008). These findings were substantiated by further demonstrating that myotubes, in the absence of exogenous inflammatory responses, can release factors directly influencing the migration of myoblasts. This model was further used to examine the signalling pathways involved in this process.

7.3. THE IMPACT OF SERIAL PASSAGING ON MYOBLAST MIGRATION AND SECRETOME - IMPLICATIONS FOR AGEING?

Only recently, has research been undertaken, investigating in more detail the secretome of skeletal muscle cells (Chan *et al.*, 2011, Cui *et al.*, 2009, Griffin *et al.*, 2010, Henningsen *et al.*, 2010, Henningsen *et al.*, 2011). Thus, a better understanding can be gained of the contribution of soluble factors released by myogenic cells themselves during both embryonic and adult myogenesis. Critically, different stages of myogenesis or different conditions might trigger the release of different factors by muscle cells. For example, the expression of chemokines can increase in contracting myotubes *in vitro* or at the time of myocyte fusion, while being reduced at later time points (Griffin *et al.*, 2009, Griffin *et al.*, 2010, Nedachi *et al.*, 2009). In addition, pro-inflammatory cytokines are able to trigger the expression of myogenic regulatory factors, which are not constitutively expressed (De Rossi *et al.*, 2000). Together these studies underpin the importance of considering the release of factors under different experimental situations and how this affects the various aspects of muscle regeneration. As it was demonstrated, serum-starved, morphologically atrophying myotubes are capable of releasing factors inducing myoblast migration and it was therefore

asked whether the same model could be used to find potential differences in the secretions between the low passage of myogenic cells used previously vs myoblasts subjected to multiple divisions. The model of serially passaged myoblasts provides a model of atrophy seen in elderly skeletal muscle, as described by Sharples *et al* (Sharples *et al.*, 2011). Serially passaged myoblasts demonstrate decreased differentiation capacity, reduction in IGF-I expression and reduced phosphorylation of Akt, and, as confirmed in this thesis, is also associated with reduced CK activity and lower gene expression levels of myogenic regulatory factors, such as MyoD and Myogenin. However, the migration of serially passaged myogenic cells has not been examined. It was here assessed how migration of these serially passaged myoblasts compares to that of control low passage myoblasts and assessed whether there is a difference in the effect, of soluble factors released by both passages, on migration of myoblasts. CM from p5 myotubes, as previously shown to induce migration, was used with wound healing assays to compare between the migration capacity of p5 and p50 myoblasts. It was demonstrated that p50 myoblasts were capable of migrating greater distances, as compared to p5 myoblasts under these conditions, and increased migration was associated with differences in the activation of signalling pathways, such as PI3K/AKT and MAPK/ERK. Interestingly, significant decreases were found in the migration of cells cultured in media conditioned by high passage vs low passage of myotubes. These results propose different internal or external regulation of migration in myoblasts that have undergone multiple divisions, which might have implications in the field of sarcopenia. However, the increased migration distance of p50 myoblasts vs p5 myoblasts is contrary to what was expected, suggests that given appropriate cues, the older cells are fully capable of extensive migration, potentially at the expense of fusion. It is known that myogenic cells from aged skeletal muscle respond differently to the extracellular environment, as compared to cell isolated from young muscle, with reports suggesting for a reduced functionality of myogenic cells isolated from old muscle (Conboy *et al.*, 2005, Dumke and Lees, 2011, Jump *et al.*, 2009, Lees *et al.*, 2009, Mezzogiorno *et al.*, 1993). Our results are in contrast with previous reports that have demonstrated a reduced migration capacity of myoblasts isolated from old vs young animals (Dumke and Lees, 2011, Siriatt *et al.*, 2007). One would expect a reduced, rather than increased migration with serially passaged myoblasts, which have previously been shown to mimic the molecular regulation of elderly skeletal

muscle (Sharples *et al.*, 2011). A possible explanation is in the response of these cells to paracrine signals released from the muscle environment. Of course, it should also be considered that an *in vitro* model of skeletal muscle ageing might not be the most appropriate one and differences with other models would be present. It was demonstrated that CM of differentiated myotubes from young mice or from saline extracts of muscle from young mice, are capable of greatly inducing proliferation of aged satellite cells, while CM from old muscle was reducing the proliferation of satellite cells isolated from both young and old muscle (Mezzogiorno *et al.*, 1993). It was reported that myotube CM from serially passaged myotubes reduces the migration capacity of myoblasts, as compared to myotube CM from low passage myoblasts. It is possible that the serially passaged myoblasts are responsive to certain paracrine factors, but not other factors, such as serum or mitogenic factors from immune cells (Dumke and Lees, 2011, Siriett *et al.*, 2007). Indeed, preliminary observation of migration behaviour between p5 and p50 myoblasts in the presence of GM (10% FBS DMEM) in wound healing assay, was visually not different between both passages (results not shown), which requires further investigation. Further studies are also required to reveal potential differences in expression of cell surface receptors between p5 and p50 cells. Our data demonstrate that soluble factors released from myotubes are capable of regulating myoblast migration, suggestive of the importance of paracrine mechanisms in the process of muscle regeneration, and that the paracrine mechanisms regulating the migration of myogenic cells are altered following multiple divisions of myoblasts, suggestive of implications in the process of ageing and sarcopenia. Key questions, warranting further investigation.

7.4. SIGNALLING PATHWAYS REGULATING MYOBLAST MIGRATION - CONTRIBUTION OF PI3K/AKT, MAPK/ERK AND FAK PATHWAYS

Following investigation of the impact of soluble factors released by myogenic cells on myoblast migration, the role of intracellular regulators was examined. PI3K/AKT and MAPK/ERK pathways are implicated in regulating migration of various cell types, including skeletal muscle cells, although results from different groups have been divergent. Some have reported that PI3K/AKT is required for myogenic cell migration (Kawamura *et al.*, 2004, Kim *et al.*, 2011, Al-Shanti *et al.*, 2011, Ranzato *et al.*, 2009), while others have reported it is not (Suzuki *et al.*,

2000, Leloup *et al.*, 2007). Similarly, some studies have reported that MAPK/ERK pathway is required for myogenic cell migration (Leloup *et al.*, 2007, Al-Shanti *et al.*, 2011), while others suggest that it is not required (Ranzato *et al.*, 2009, Suzuki *et al.*, 2000). These discrepancies might be due to investigating myoblast migration in different models, conditions or migration inducers. Thus, the aim was to examine whether PI3K/AKT and MAPK/ERK were required for myoblast migration induced by factors released from myotubes. It was reported that both of these pathways were activated in response to CM. Using LY294002 and UO126 for inhibiting PI3K/AKT and MAPK/ERK pathways, respectively, it was demonstrated that both of these pathways were required for myoblast migration induced by myotube CM. It was further demonstrated that the increased migration of p50 myoblasts in response to p5 CM was associated with elevated activity of MAPK/ERK and, to a lesser extent PI3K/AKT.

Myotube CM induced migration was associated with activated PI3K/AKT and MAPK/ERK pathways, while their inhibition led to a reduction in myoblast migration. In addition, treatment of myoblasts with Bpv(Hopic), a phosphotyrosine phosphatase and PTEN inhibitor, led to further activation of PI3K/AKT and MAPK/ERK signalling, which was associated with further increases in myoblast migration. The activation of these two pathways by Bpv(Hopic) can be explained by previously reported effects of PTEN on PI3K and MAPK signalling and their involvement in regulating migration (Cully *et al.*, 2006, Dey *et al.*, 2008, Gu *et al.*, 1998, Gu *et al.*, 1999, Leslie *et al.*, 2007, Raftopoulou *et al.*, 2004, Yamada and Araki, 2001, Zhao, 2007). The individual inhibition of each pathway by LY294002 or UO126 led to an abolition of the effect of Bpv(Hopic) on migration, while not affecting the activity of the other pathway. Very similar results were reported in epithelial cells in an article published during the write up period of this thesis (Mihai *et al.*, 2012). Mihai *et al.* demonstrated an increase in migration of epithelial cells, following incubation with the PTEN inhibitor Bpv(Phen), which was in conjunction with activation of the Akt and ERK signalling pathways. In the same article, it was reported that inhibition of these pathways resulted in reduced migration to levels of the untreated control group. PTEN inhibition resulted in biomechanical properties, such as cell stiffness, mediated by both Akt and ERK pathways. The importance of biomechanical properties, for cell migration is due to its association with lamellipodia ruffling,

focal adhesions and cell contractility (Mihai *et al.*, 2012, Pelham and Wang, 1997, Riveline *et al.*, 2001). As an adherent cell type, it is entirely possible that skeletal muscle myoblasts would be regulated in a similar fashion and that the induced migration by treatment with Bpv(Hopic) would exert similar alterations on biomechanical properties of myoblasts. Further research would be needed to verify this.

It was demonstrated that PI3K/AKT and MAPK/ERK pathways were required for myoblast migration in response to CM, as well as for the Bpv(Hopic)-induced increase in myoblast migration. The action of BpV compounds in other cell types has also been reported to increase cell migration (Lai *et al.*, 2007, Mihai *et al.*, 2012, Zhao, 2007) and PTEN regulation of cell migration is well known, although not investigated in skeletal muscle (Dasari *et al.*, 2010, Liliental *et al.*, 2000, Tamura *et al.*, 1998). PTEN's pleiotropic effect on different signalling pathways and the phospho-tyrosine phosphatase activity of BpV compounds was suggestive of possible activation of other signalling pathways, besides PI3K/AKT and MAPK/ERK, which could contribute to the enhanced migration capacity. Another signalling pathway, which has been reported to be downstream of PTEN, is FAK/Src (Gu *et al.*, 1999). FAK has a known effect on adhesion dynamics (Hanks *et al.*, 2003, Schlaepfer and Mitra, 2004, Schlaepfer *et al.*, 2004) and is also known as a regulator of cell migration (Cary *et al.*, 1996, Desai *et al.*, 2009, Sieg *et al.*, 1999, Slack-Davis *et al.*, 2007). The Bpv(Hopic)-induced effect on cell adhesion and the reported cell shrinking/rounding, possibly associated with loss of contacts with the substratum, was a reason to investigate whether FAK pathway is associated with the Bpv-induced myoblast migration. Low (1 μ M) concentrations of Bpv(Hopic), capable of inducing myoblast migration, did not lead to a global activation of pFAK on tyr397, while increasing the Bpv(Hopic) concentration, in conjunction with the increase of phosphorylated tyrosine residues and decreased specificity to PTEN, also resulted in increased pFAK phosphorylation on tyr397. As suggested by Mihai *et al.* (Mihai *et al.*, 2012), it is possible that the effect of Bpv of FAK is exerted on migrating cells only. However, if migration was compared between 2 μ M and 1 μ M Bpv(Hopic), it was not visually different - both induced an approximate 40% increase, as compared to control CM. This could be due either to limitations of the wound healing assay, or possibly to the "saturation" of the signalling pathways or their downstream targets in response to higher doses Bpv(Hopic). It is also possible that the lack of

specificity of PTEN at greater concentrations affects other signalling pathways or targets, acting negatively on cell migration. The delay caused by cell shrinking must also be considered. In addition, it was observed that pFAK phosphorylation levels were not visually elevated in myoblasts treated with GM or in p50 vs p5 myoblasts treated with CM, despite migration levels being higher (results not shown). Thus, FAK could in fact be activated in migrating cells, even if it is not globally altered, but it is questionable to what extent it actually contributes to the increases in myoblast migration.

FAK activation is, however required for myoblast migration, as shown by its inhibition using the PF-228 inhibitor. Reductions of pFAK (tyr397) activation levels by PF-228 resulted in decreased migration, induced by CM and Bpv(Hopic). Strikingly, myoblast migration capacity seemed to be following the pFAK activation levels and appeared independent on the PI3K/AKT and MAPK/ERK levels. It was proposed that FAK inhibition might have direct effects on migrating muscle cells.

Overall, these data suggest that requirement of PI3K/AKT, MAPK/ERK and FAK pathways for myoblast migration. The possible redundancy between these and other signalling pathways is yet to be examined in more detail, but our observations suggest that even if certain redundancy exists between signalling pathways regulating myoblast migration, each pathway is required for optimal migration to take place and loss of one pathway cannot be compensated for by activation of other pathways. Further investigation is required for elucidating in more detail the coordination between different signalling pathways in regulating myoblast migration.

7.5. CHANGES IN SIGNALLING PATHWAYS MIGHT EXERT EFFECTS NOT ONLY ON MYOGENIC MIGRATION, BUT ALSO ON PROCESSES SUCH AS CELL DEATH, PROLIFERATION OR DIFFERENTIATION

In addition to the examination of myoblast migration, the levels of cell death were also quantified. Increased levels of cell death would contribute to a reduced number of cells available for migration in the wound healing model and this could lead to misleading results. It was found that cell death levels were not greatly increased under most experimental conditions, with the exception of when myoblasts were treated with SF media. The lack of growth factors and the low levels of PI3K/AKT activation in myoblasts treated with SF media resulted in

approximately 10% cell death and this could, in part, indeed contribute to the reduced number of cells migrating into the wound. However, under other experimental conditions, levels of death in cells treated with inhibitors hardly exceeded 4%, with no big differences between conditions and it is therefore unlikely that this contributed to significant differences in cell migration levels. In fact, most death events were detected hours after migration was initiated and frequently cell death was observed suddenly in motile cells, with these cells showing no visible inhibition of migration speed beforehand. These observations, along with the low percentage of dying cells, suggests that cell death would not significantly effect the migration of myoblasts in response to the different conditions examined. The slight increases in cell death levels observed were associated with decreased levels of pAKT, a well known regulator of cell survival (Brunet *et al.*, 1999, Datta *et al.*, 1997, Matsui *et al.*, 2003). This could explain also the slight reductions in cell death levels following PTEN inhibition, which leads to activation of AKT signalling and promotes cell survival (Sun *et al.*, 1999, Yamada and Araki, 2001). Interestingly, not even small increases in cell death were observed when PI3K/AKT signalling was inhibited with LY294002 in the presence of Bpv(Hopic). Possibly, the induction of apoptosis by the inhibition of the PI3K/AKT was compensated for by the effect of Bpv(Hopic) via its effect on other signalling pathways, which were not examined. The potential crosstalk between PI3K/AKT and JNK pathways, for example, is implicated in apoptosis (Zhang *et al.*, 2007) indeed the JNK pathway, which might also be affected has been implicated in both pro- and anti-apoptotic roles (possibly in a cell type and stimulus dependent manner, as discussed in (Liu and Lin, 2005)). This, however, warrants further investigation and is out of the scope of this thesis.

As this thesis focused on investigating the migration of myogenic cells, other events, such as proliferation and differentiation were not examined in detail. PI3K/AKT and MAPK/ERK pathways were demonstrated to be required for myoblast migration, but in addition it would be important to consider how these signalling pathways affect other processes, such as proliferation and differentiation. PI3K/AKT pathway is known to be necessary for myoblast differentiation (Foulstone *et al.*, 2004, Kaliman *et al.*, 1996, Li *et al.*, 2000). The IGF-I/Akt pathway is central in muscle hypertrophy by its association with downstream targets, such as mTOR and GSK-3beta, involved in protein synthesis, and transcription factors of the FoxO family, involved in protein degradation

(reviewed in (Saini *et al.*, 2006, Schiaffino and Mammucari, 2011). On the other hand, the MAPK pathway is a key regulator of myoblast proliferation (Coolican *et al.*, 1997, Foulstone *et al.*, 2004, Johnson and Lapadat, 2002). The balance of these signalling pathways is crucial for the coordination of skeletal muscle myogenesis. It was demonstrated that inhibition of MAPK/ERK pathway, regulating myoblast proliferation, by PD98059 resulted in increased differentiation (Al-Shanti and Stewart, 2008, Coolican *et al.*, 1997). Similarly, FAK has also been shown to be involved in regulating the cell cycle of myoblast and their differentiation and fusion into myotubes (Clemente *et al.*, 2005, Quach *et al.*, 2009). The temporal regulation, coordination and switch between different processes of myogenesis would involve a complex combination of extracellular and intracellular cues and might be context dependent. Thus, although activation of PI3K/AKT signalling is linked to increased hypertrophy and myotube formation (Lai *et al.*, 2004, Morissette *et al.*, 2009) and the PI3K/AKT signalling was demonstrated to be activated by 10 μ M Bpv(Hopic), the treatment of myoblasts with 10 μ M Bpv(Hopic) in the presence of DM resulted in reduced myoblast differentiation, as compared to untreated controls. This was shown to be a result of the activation of NF- κ B activity, upregulation of cyclin D1 expression and decreased differentiation due to inability of cells to withdraw from the cell cycle (Castaldi *et al.*, 2007). Similarly, despite DM inducing more consistent activation of PI3K/AKT and MAPK/ERK signalling, the migration of myoblasts with DM in a wound healing assay was not higher than migration induced by CM. This was associated with a decreased ability of CM to induce Myogenin expression, as compared to DM. Therefore, it is important to reveal how the activation or inhibition of signalling pathways alters the cellular responses, such as migration, proliferation or differentiation, as this will have implications for future therapeutic interventions. However, the activity of these signalling pathways should also be considered in the context of the extracellular environment and the potential crosstalk with or activation of other signalling pathways, which can override their activity and trigger distinct cellular responses.

7.6. POTENTIAL THERAPEUTIC APPLICATIONS FOR BISPEROXOVANADIUM COMPOUNDS IN MUSCLE REGENERATION

Muscular dystrophies are a group of muscle diseases, characterised by gene mutation and muscle protein defects, leading to progressive skeletal muscle

weakness, reduced locomotion and overall reduced quality of life or shortened life span. The most common form, Duchenne muscular dystrophy, is a condition caused by mutation in the dystrophin gene, which participates in maintaining the integrity of a muscle cell, protecting the muscle fibres from injury when they contract and relax (Blake *et al.*, 2002, Petrof, 2002). Missing/mutated dystrophin leads to vulnerability and damage of muscle fibres during contraction and constant damage-repair cycles, ultimately lead to muscle loss, to wheelchair dependency and in many patients, death due to respiratory failure between the ages of 17 and 30 (reviews: (Cossu and Sampaolesi, 2007, Emery, 2002, Nowak and Davies, 2004, Quattrocchi *et al.*, 2010)). Cell therapy, such as myoblast transplantation, has been investigated as a promising approach to deliver normal variants of the gene to dystrophic muscles and to restore at least partially the normal musculature and function. This strategy can also potentially be applied to treating loss of muscle tissue after traumas (review: (Turner and Badylak, 2011)). Although significant improvement of muscle regeneration and functionality was achieved after cell therapy in mdx mice (Morgan *et al.*, 1990, Partridge *et al.*, 1989), clinical trials in humans were far less successful (Mendell *et al.*, 1995, Tremblay *et al.*, 1993). Three main problems were associated with the low success: reduced survival of transplanted cells, limited spreading and migration of transplanted cells and immune rejection (Fan *et al.*, 1996, Gussoni *et al.*, 1997, Moens *et al.*, 1996, Skuk *et al.*, 2004, Smythe *et al.*, 2001).

The significance of migration for the success of myoblast transfer therapy has recently been questioned by articles published from the Tremblay group (Lafreniere *et al.*, 2009, Skuk *et al.*, 2011). Lafreniere *et al.* demonstrated that coinjection of bFGF and IGF-I was able to improve migration of myogenic cells in nonhuman primates, but this did not improve the cell transplantation success, as myoblasts did not fuse with undamaged fibres, but only with fibres injured in the injection trajectories (Lafreniere *et al.*, 2009). In addition, Skuk *et al.* demonstrated using monkey models that transplanted myoblasts were capable of migrating several millimetres, but only fused with regenerating, but not undamaged myofibres (Skuk *et al.*, 2011). Due to ethical reasons, dystrophic primates do not exist and this study could not examine myoblast migration in a model of dystrophic muscle, when more significant muscle damage would occur. These studies argue that even if migration is improved, no improved transplantation success could be achieved until donor myoblasts are able to fuse

with undamaged myofibres. As discussed by Lafreniere *et al.*, this could potentially be achieved by either harming muscle fibres, or by stimulating fibre hypertrophy, which would recruit more of the transplanted myoblasts (Lafreniere *et al.*, 2009). However, one would expect that in dystrophic muscles, where extensive muscle damage occurs, recruitment of myoblasts would be enhanced. Overall, the above mentioned findings do not prove that improving myoblast migration cannot contribute to a better success of cell therapies, but rather underlie the importance of the combination of factors, on which these therapeutic strategies depend. Improving the migration of transplanted myoblasts could indeed lead to an improved transplantation success, but it would need to be combined with other approaches aimed at improving the fusion of these myoblasts with muscle fibres. Improving the migration of myoblasts would also need to be considered along with their ability to degrade and migrate through extracellular matrix (El Fahime *et al.*, 2000).

The effect of phospho-tyrosine phosphatase inhibitor Bpv(Hopic) on the migration of myoblasts was examined and it was demonstrated that it is capable of increasing their motility in a wound healing assay, in response to factors released from starved myotubes. The application of BpV compounds and inhibition of PTEN for inducing cell migration has previously been considered in the context of lung pathogenesis and potential therapies for lung injuries, with PTEN inhibition enhancing epithelial wound healing (Lai *et al.*, 2007, Mihai *et al.*, 2012). In skeletal muscle, Castaldi *et al.* demonstrated that high concentrations (10 μ M) of BpV triggered multi potency in myoblasts and inhibited their differentiation. However, it enhanced the ability of these cells, transplanted intra-arterially in alpha-sarcoglycan-deficient dystrophic mice, to circulate, cross vessel walls and contribute to muscle regeneration, despite showing a delay in the activation of myogenic phenotype (Castaldi *et al.*, 2007). The effect of BpV on migration, however, was not investigated. It was here demonstrated that lower concentrations of Bpv(Hopic) are capable of increasing myoblast migration, without significantly affecting the ability of myoblasts to differentiate and fuse into myotubes. It is proposed that this compound and the inhibition of PTEN might be considered as a potential tool to enhance the migration of grafted myoblasts and improve transplantation success. It is suggested that other agents or strategies to inhibit PTEN in transplanted myogenic cells might provide ways for improving their spreading after muscle injection. It must be considered, however,

that a persistent activation of PTEN would be unwanted in terms of the tumorigenic phenotype it triggers (Stiles *et al.*, 2002). A temporal inactivation of PTEN in donor myoblasts, however, would be an interesting phenomenon to examine *in vivo*. A temporary period of increased migration, proliferation and survival of myogenic precursors following muscle injury would certainly be a promising possibility for enhanced muscle repair. However, for practical reasons this might be a task hard to accomplish with tools other than local or systemic delivery of factors. And as muscle repair involves the coordinated activities of several cell types, it is important to consider the effect of delivered compounds not only on muscle cells, but on other cell types as well. A local delivery of a compound acting as a PTEN inhibitor might exert negative effects on muscle repair, as PTEN is known to inhibit myofibroblast differentiation and its inhibition promotes fibrosis (White *et al.*, 2006). Excessive fibrosis and scar formation is associated with reduced motile and contractile functions of the muscle and is a pathological feature observed in patients suffering with DMD (Mann *et al.*, 2011, Zhou and Lu, 2010). Therefore, the mechanisms of delivering agents aimed at improving the migration of myogenic cells must also be considered in the context of their effects on other cell processes, as well as their general effect on the organ or organism, which is being “treated”. It is suggested that Bpv(Hopic) treatment of myoblasts could provide a useful tool for enhancing the migration of muscle injected donor myoblasts and propose further studies to test this hypothesis *in vivo*. However, any strategies aimed at enhancing donor myoblast migration, in order to improve their transplantation success in future, would need to be considered in combination with other strategies, such as improving the fusion of myoblasts with muscle fibres.

7.7. SPIRE AND FORMIN GENES ARE EXPRESSED IN MYOBLASTS - POSSIBLE IMPLICATIONS FOR MYOBLAST FUSION AND MIGRATION

Improving our knowledge of both myoblast migration and fusion could lead to the development of therapies for conditions, associated with loss of muscle mass, such as DMD. Despite being considered as separate events, myoblast migration and fusion are often affected by the same regulators (Becciolini *et al.*, 2006, Bondesen *et al.*, 2007, Donati *et al.*, 2005, Griffin *et al.*, 2009, Lafreniere *et al.*, 2006, Louis *et al.*, 2008, Makarenkova *et al.*, 2009, Olguin *et al.*, 2003). Myotube

formation depends on the ability of myoblasts to align and establish cell-cell contacts, while increased differentiation and fusion may lead to decreased migration (Griffin *et al.*, 2010, Smythe and Grounds, 2001). Thus, any modulation in the ability of myoblasts to differentiate and to fuse, might exert indirect effects on the process of myoblast migration, and vice versa. As differentiation/fusion potential of myoblasts following 10 μ M Bpv(Hopic) treatment and serial passaging was significantly inhibited, it was hypothesised that these two treatments could be useful in identifying new targets for investigating the mechanisms of myoblast fusion and migration. The expression of 4 genes (Spire1, Spire2, Formin1 and Formin2), was examined using RT-PCR following the inhibition of differentiation/fusion with Bpv(Hopic) treatment or serial passaging. The protein products of Spire and Formin genes are reported to act as actin nucleators, promoting the assembly of new actin filaments (Pechlivanis *et al.*, 2009, Quinlan *et al.*, 2005). Regulators of actin polymerisation, such as WASPs and SCAR/WAVES, have been shown to regulate myoblast fusion (Gildor *et al.*, 2009, Guerin and Kramer, 2009, Kim *et al.*, 2007, Mukherjee *et al.*, 2011, Richardson *et al.*, 2007, Schafer *et al.*, 2007), but the expression of Spire and Formin genes or their protein products in skeletal muscle was not investigated. Our results indicated that Spire1, Spire2 and Formin1 gene are expressed in C2C12 myoblasts, with Formin2 gene expression almost undetectable. Of particular interest is the expression of Spire1 and Formin1 genes, which seemed to be associated with myoblast differentiation/fusion, with Spire1 gene levels decreasing and Formin1 gene levels increasing upon inhibition of differentiation following both 10 μ M Bpv(Hopic) and serial passaging. Spire2 gene expression was affected only by BpV treatment, but not by serial passaging, while Formin 2 gene expression was affected by serial passaging, but not by BpV treatment, suggesting that while signalling pathways may be shared, the gene responses may uncouple. The expression of Formin and Spire genes raises the question of their potential functions in skeletal muscle. Considering their involvement in endocytic recycling and intracellular trafficking (Kerkhoff *et al.*, 2001, Kerkhoff, 2010, Morel *et al.*, 2009, Schuh, 2011), which are associated with both myoblast fusion and cell migration (Doherty *et al.*, 2008, Rochlin *et al.*, 2010, Caswell and Norman, 2006, Pellinen and Ivaska, 2006), it was suggested that these genes might indeed be associated with these processes, either directly or as a consequence of altered fusion/migration. Further investigations, particularly at the

protein level, should provide more details for their roles in skeletal muscle and their potential implication in myoblast fusion or migration.

7.8. NOVELTY OF THE FINDINGS

The present study addressed the external and internal regulation of myoblast migration. The regulation of myogenic cell migration by soluble factors has previously been investigated by a number of studies (Amano *et al.*, 2002, Bischoff, 1997, Corti *et al.*, 2001, Lafreniere *et al.*, 2004, Lafreniere *et al.*, 2006, Torrente *et al.*, 2003), but more attention is needed on how combinations of factors are affecting the process. Additional research is required to address the contribution of individual cell niches and the release of soluble factors that influence the process of myogenesis and muscle regeneration, including migration of myogenic cells. In the course of these studies, articles examined the expression of chemokines in myoblasts and the contribution of factors released from fusing myoblasts to migration of myogenic cells (Griffin *et al.*, 2009, Griffin *et al.*, 2010). A number of other studies have demonstrated the expression of cytokines, growth factors, chemokines and their receptors at different stages of myogenic development (Civatte *et al.*, 2005, De Rossi *et al.*, 2000, Griffin *et al.*, 2010, Hirata *et al.*, 2003, Peterson and Pizza, 2009, Porter *et al.*, 2003, Sachidanandan *et al.*, 2002, Summan *et al.*, 2003, Warren *et al.*, 2004). Here, these studies were substantiated by further demonstrating that starved myotubes were capable of releasing factors, which are capable of stimulating the migration of myoblasts, although these factors were not biochemically identified. In addition, the question was raised whether differences in the release of soluble factors would be observed in myogenic cells during ageing, a topic which has not received enough attention. A model of serially passaged myoblasts was used, which is known to mimic the molecular regulators of aged skeletal muscle (Sharpley *et al.*, 2011) and demonstrated differences in the potency of inducing myoblast migration between media conditioned by passaged and non passaged myotubes. These observations were substantiated by observing an increased capacity of serially passaged myoblasts to migrate in the presence of media conditioned by unpassaged cells, which provides initial cues for the existence of differences in the regulation of myogenic cell migration following multiple divisions, which may be observed during ageing. The release of soluble factors by myogenic cells was linked to the

intracellular regulators, which mediate the response to these factors, which was previously not addressed. PI3K/AKT and MAPK/ERK pathways were demonstrated to be required for migration of myoblasts in response to myotube CM. Reports of the involvement of these two pathways in regulating migration of myogenic cells were not unanimous (Kawamura *et al.*, 2004, Kim *et al.*, 2011, Al-Shanti *et al.*, 2011, Suzuki *et al.*, 2000, Leloup *et al.*, 2007). A more detailed investigation into the involvement of these two pathways in the regulation of myoblast migration was performed. It was demonstrated that further upregulation of PI3K/AKT and MAPK/ERK pathways by phospho-tyrosine phosphatase and PTEN inhibitor Bpv(Hopic) was associated with a larger increase in the migration of myoblasts and that PI3K/AKT and MAPK/ERK pathways were required for this increase. The requirement of the FAK signalling pathway for basal myoblast migration was also demonstrated, which previously was not assessed in this context by other researchers. The involvement of high concentration of BpV was previously investigated in skeletal muscle and shown to decrease the capacity of C2C12 cells to differentiate, induce multipotency in these cells, increase their ability to reach inflamed muscle tissue and contribute to muscle repair (Castaldi *et al.*, 2007). However, this is the first study in skeletal muscle reporting that low dose BpV is capable of increasing migration of myoblasts, without seriously affecting the differentiation capacity of these cells, proposing potential application for increasing myoblast migration in myoblast transfer therapies. Finally, the expression of Spire and Formin genes, previously not investigated in skeletal muscle, was examined in response to inhibited differentiation/fusion by high concentrations of Bpv(Hopic) and following serial passaging. It was demonstrated that Spire1, Spire2 and Formin1 genes were expressed in C2C12 myoblasts, with Formin2 expression being very weak, and that the expression of these genes was altered by either Bpv(Hopic), serial passaging, or both. A potential involvement of Spire1 and Formin1 genes in the process of myoblast fusion/migration was proposed. These data encourage further examination in the potential role of Spire and Formin genes in skeletal muscle.

7.9. SUMMARY AND FUTURE DIRECTIONS

Only recently, research has revealed in more detail the secretagogues of myogenic cells and partly addressed the differential secretion of soluble factors at

different stages of myoblast development (Chan *et al.*, 2011, Cui *et al.*, 2009, Griffin *et al.*, 2010, Henningsen *et al.*, 2010, Henningsen *et al.*, 2011). Little research, however, has focused on the effect of this pool of secreted factors on different processes of myogenesis. Recently, the increased expression of a number of chemokines in differentiating/fusing myoblasts was revealed and it was demonstrated that media conditioned by myoblasts at the time of fusion was capable of inducing migration of myogenic cells (Griffin *et al.*, 2010). Previous reports have also shown that crushed muscle extract, known to contain factors, such as HGF and other soluble ligands, was capable of inducing migration of myogenic cells (Bischoff, 1997, Chen and Quinn, 1992, Griffin *et al.*, 2009, Griffin *et al.*, 2010, Tatsumi *et al.*, 1998). Therefore, research has started addressing the auto/paracrine mechanisms behind the regulation of myogenesis. In this report, it was found that starved/atrophying myotubes are capable of conditioning media with soluble factors inducing migration of myoblasts and that this media is more potent at inducing myoblast migration to a media conditioned by crushed myotubes. The factors present in the media, however, were not revealed. Thus, previous findings were substantiated by showing that living myotubes in a state of potential atrophy are capable of releasing factors inducing migration of myogenic cells and likely influencing other myogenic processes. It is proposed that further investigations should be performed into the expression profile (PCR arrays) and secreted factors (Mass spectrometry) produced by muscle cell cultures, not only at different stages of differentiation, but also under different physiological states. Thus, thorough future studies should address the differences in transcription profile and secreted proteins of quiescent myoblasts, dying myoblasts, differentiating myoblasts, mature myotubes, starving/atrophying myotubes and mechanically injured myotubes. These investigations should be performed to examine how the pool of factors secreted at different stages of muscle development influence different processes of myogenesis, such as migration, proliferation, differentiation and survival. Thus, possible cross-talk or interaction between different factors might be addressed. More detailed studies could start identifying the importance of individual factors present in the conditioned media. The potential identification of novel factors, previously not investigated in the context of myogenesis or myogenic cell migration would provide promising avenues for further research. Establishing the concentrations at which these factors exert most potent action on myogenic progenitors migration,

the potential interaction with other factors and the intracellular targets they affect, would be a logical next step. The co-incubation of myogenic cells with other cell types, such as inflammatory cells, and the subsequent release of factors by these cells is also a necessary experimental model, which could provide more information on the importance of the muscle environment in releasing soluble factors that affect the regeneration process. Identifying and establishing the exact action of soluble factors present in the muscle environment in different physiological conditions could allow the creation of better therapies against muscle wasting or reinforcing the muscle repair process. This could allow the creation of a “cocktail” of factors required for inducing high rates of myoblast migration or muscle regeneration, which could speculatively be a mixture of growth factors, cytokines, matrix metalloproteinases. An important consideration would also be how these soluble factors would affect other cell processes and cell types. Thus, a great amount of research effort would still be required to reveal completely the importance of soluble factors on skeletal muscle myogenesis and regeneration. Based on previous studies, the importance of the systemic environment in the context of skeletal muscle ageing and regeneration is already known (Conboy *et al.*, 2005) and also the paracrine stimulation of aged satellite cells by factors released from young muscle (Mezzogiorno *et al.*, 1993). Changes in the paracrine mechanisms following multiple divisions of myogenic cells, which would occur during ageing, have not received attention. Future studies should address the differences in the secretome between low and high passage myogenic cells in different stages of differentiation. Identifying the change in expression and secretions of serially passaged myogenic cells could give clues of paracrine mechanisms influencing the adaptations of ageing of skeletal muscle. A more thorough investigation would also need to be performed on how the pool of factors secreted by different stages and states of myogenesis would influence not only myogenic cell migration, but other processes of myogenesis, such as cell survival, proliferation, differentiation. The response to these factors of other tissues or cell types participating in muscle repair, such as inflammatory cells, would also need to be addressed. Overall, these studies would contribute to our better understanding of how myogenic cells participate in the regulation of myogenesis and muscle regeneration, which factors are important for this process and identify potentially important cross-talk between factors.

A link was established between the migration induced by soluble factors released from myogenic cells and intracellular pathways, such as PI3K/AKT and MAPK/ERK, and their requirement for the process was demonstrated. BpV(Hopic) treatment further activated these pathways and induced the migration of myoblasts. The requirement of the FAK pathway was also demonstrated. Overall, these studies demonstrated that each of the signalling pathways was required for myoblast migration, regardless of the activation state of the others. However, other pathways and downstream targets were not investigated. It is entirely possible that the migration induced by Bpv(Hopic), despite being dependent on the three signalling pathways investigated, is triggered by other mechanisms, not investigated in this thesis. The phospho-tyrosine phosphatase activity of BpV(Hopic) and the pleiotropic effects of PTEN could be responsible for the activation of multiple intracellular targets. Future studies should address this concept. Rac activation is known to be dependent on PI3K signalling (Royal *et al.*, 2000, Sander *et al.*, 1998) and Rac itself is important for cell migration through its involvement in actin polymerization and formation of membrane protrusions, such as lamellipodia (Nobes and Hall, 1995, Raftopoulou and Hall, 2004). Thus, future investigation into the involvement of Rac in the induced migration of myoblasts must also be performed. Preliminary studies demonstrated that JNK inhibitor SP600125 is capable of inhibiting myoblast migration in response to CM (see Appendix 1). However, a more detailed investigation into how this pathway regulates myoblast migration has not been performed and could also be addressed in future studies. In particular, the crosstalk between different pathways would be an interesting research theme. Of particular interest would be the investigation of the expression profiles of matrix metalloproteinases. MMP9 overexpression has been demonstrated to improve myoblast migration and engraftment (Morgan *et al.*, 2010). At the same time, PI3K/PTEN/AKT/mTOR pathway is implicated in the upregulation of MMP9 in hepatocellular carcinoma, thus involved in the invasion (Chen *et al.*, 2009). The involvement of PTEN in MMP-9 regulation has also been demonstrated in smooth muscle cells (Moon *et al.*, 2004) and warrants investigation in our models. Taken together, these data provide promising prospects for the involvement of BpV compounds in stimulating migration and invasion of donor myoblasts in myoblast transfer therapy. Promising results were obtained with systemically injected myoblasts pre-treated with 10 μ M BpV, which reached inflamed muscle and contributed to

muscle repair (Castaldi *et al.*, 2007). However, studies should be performed to assess the potential of different concentrations of BpV(Hopic) to stimulate myoblast migration *in vivo*, following local muscle injections. A temporary inactivation of PTEN may prove to be a promising tool for enhancing the grafting of donor myoblasts in proposed therapies of DMD, however, this might need to be combined with other strategies, such as enhancing the fusion of these myoblasts with muscle fibres. In a wider context, a more detailed investigation could be performed on how signalling pathways are involved in the stimulation of different cell processes by various mixtures and concentrations of soluble factors and conditioned media, as discussed above. Identification and examining the action of soluble factors, or mixture of factors, enhancing or reducing myoblast migration, could be accompanied with a detailed investigation on the signalling pathways they affect. Further exploration could be performed on which signalling pathways, or combination of signalling pathways actions, exerts positive or negative effects on myoblast migration, which could further lead to examining how knocking down or overexpressing of these pathways affects the process. Thus, for example, an interesting avenue for research might provide overexpressing of signalling pathways acting positively on myogenic cell migration, associated with inhibiting of signalling pathways acting negatively on myogenic cell migration. This would, of course, require examination of other cell processes, as signalling pathways often diverge to regulate several processes. It would also be essential to verify that enhanced myogenic cell migration would lead to beneficial results for skeletal muscle regeneration. Too much migration may lead to reduced fusion, which eventually might lead to less regeneration. Different models, such as *in vivo* cell imaging, could provide extremely useful for revealing how increased/reduced migration of myogenic progenitors contributes to skeletal muscle regeneration and to what extent migrating cells are recruited in regenerating myofibers. This method could also be useful in observing how myoblasts stimulated *in vivo* by BpV(Hopic), for example, are recruited to injured myofibers in both young and old individuals. The tracking of myoblasts or satellite cells in aged muscles *in vivo* and their stimulation by different factors would give invaluable information on the contribution of cell migration to ageing and sarcopenia.

The expression of Spire and Formin genes, previously not investigated in skeletal muscle, suggested a potential involvement of these genes in myogenesis. Inhibited differentiation/fusion by 10 μ M Bpv(Hopic) treatment and serial

passaging revealed that Spire1 and Formin1 gene expression was influenced by both treatments, while Spire2 and Formin2 expression were influenced, respectively, by only BpV treatment or serial passaging. These genes could play a role in skeletal muscle myogenesis and potential association of Spire1 and Formin1 genes in the process of myoblast fusion was proposed, which could subsequently affect migration as well. However, this could not be verified through the use of RT-PCR experiments only. Future studies should address the involvement of Spires and Formins at the protein level and the roles they may play in enabling migration. Spire and Formin proteins have been implicated in intracellular trafficking (Kerkhoff *et al.*, 2001, Kerkhoff, 2010, Morel *et al.*, 2009, Schuh, 2011) and immunostaining experiments should reveal their location in both quiescent and differentiating/fusing myogenic cells. Silencing and overexpression experiments should also reveal the potential functions of these genes in skeletal muscle. In a wider context,, if these genes are indeed involved in regulating skeletal muscle myogenesis and repair, their expression in different physiological or pathological conditions could be examined, together with the expression of their protein products. Thus, biopsies could be taken from individuals with DMD, cancer cachexia, or following exercise induced hypertrophy, and the expression of Spire and Formin genes and protein products assessed. If changes exist, potential implication of these genes as targets of different therapies could be considered.

Overall, these findings contribute to the field of skeletal muscle myogenesis by revealing both intracellular and extracellular mechanisms for regulating myoblast migration. Proposed future studies could provide more detailed data on the regulation of this process, the cross-talk between different factors and the coordination between myoblast migration and other processes, such as proliferation, differentiation and fusion. This knowledge can serve to develop or improve therapeutic approaches for conditions associated with loss of muscle mass following disease, injury or ageing.

CHAPTER 8

8. REFERENCES

- AARTSMA-RUS, A., DEN DUNNEN, J. T. & VAN OMMEN, G. J. 2010. New insights in gene-derived therapy: the example of Duchenne muscular dystrophy. *Ann N Y Acad Sci*, 1214, 199-212.
- AARTSMA-RUS, A., KAMAN, W. E., WEIJ, R., DEN DUNNEN, J. T., VAN OMMEN, G. J. & VAN DEUTEKOM, J. C. 2006. Exploring the frontiers of therapeutic exon skipping for Duchenne muscular dystrophy by double targeting within one or multiple exons. *Mol Ther*, 14, 401-7.
- ABMAYR, S., GREGOREVIC, P., ALLEN, J. M. & CHAMBERLAIN, J. S. 2005. Phenotypic improvement of dystrophic muscles by rAAV/microdystrophin vectors is augmented by Igf1 codelivery. *Mol Ther*, 12, 441-50.
- ADAMS, A. M., HARDING, P. L., IVERSEN, P. L., COLEMAN, C., FLETCHER, S. & WILTON, S. D. 2007. Antisense oligonucleotide induced exon skipping and the dystrophin gene transcript: cocktails and chemistries. *BMC Mol Biol*, 8, 57.
- ADAMS, G. R. 2006. Satellite cell proliferation and skeletal muscle hypertrophy. *Appl Physiol Nutr Metab*, 31, 782-90.
- ADAMS, G. R., CAIOZZO, V. J., HADDAD, F. & BALDWIN, K. M. 2002. Cellular and molecular responses to increased skeletal muscle loading after irradiation. *Am J Physiol Cell Physiol*, 283, C1182-95.
- ADAMS, G. R. & MCCUE, S. A. 1998. Localized infusion of IGF-I results in skeletal muscle hypertrophy in rats. *J Appl Physiol*, 84, 1716-22.
- AL-SHANTI, N., FAULKNER, S. H., SAINI, A., LORAM, I. & STEWART, C. E. 2011. A semi-automated programme for tracking myoblast migration following mechanical damage: manipulation by chemical inhibitors. *Cell Physiol Biochem*, 27, 625-36.
- AL-SHANTI, N. & STEWART, C. E. 2008. PD98059 enhances C2 myoblast differentiation through p38 MAPK activation: a novel role for PD98059. *J Endocrinol*, 198, 243-52.
- ALAMEDDINE, H. S., DEHAUPAS, M. & FARDEAU, M. 1989. Regeneration of skeletal muscle fibers from autologous satellite cells multiplied in vitro. An experimental model for testing cultured cell myogenicity. *Muscle Nerve*, 12, 544-55.
- ALBLAS, J., ULFMAN, L., HORDIJK, P. & KOENDERMAN, L. 2001. Activation of Rhoa and ROCK are essential for detachment of migrating leukocytes. *Mol Biol Cell*, 12, 2137-45.
- ALLEN, D. L., TEITELBAUM, D. H. & KURACHI, K. 2003. Growth factor stimulation of matrix metalloproteinase expression and myoblast migration and invasion in vitro. *Am J Physiol Cell Physiol*, 284, C805-15.
- ALLEN, R. E. & BOXHORN, L. K. 1987. Inhibition of skeletal muscle satellite cell differentiation by transforming growth factor-beta. *J Cell Physiol*, 133, 567-72.
- ALLEN, R. E. & BOXHORN, L. K. 1989. Regulation of skeletal muscle satellite cell proliferation and differentiation by transforming growth factor-beta, insulin-like growth factor I, and fibroblast growth factor. *J Cell Physiol*, 138, 311-5.

- ALLEN, R. E., SHEEHAN, S. M., TAYLOR, R. G., KENDALL, T. L. & RICE, G. M. 1995. Hepatocyte growth factor activates quiescent skeletal muscle satellite cells in vitro. *J Cell Physiol*, 165, 307-12.
- ALMEIDA, E. A., ILIC, D., HAN, Q., HAUCK, C. R., JIN, F., KAWAKATSU, H., SCHLAEPFER, D. D. & DAMSKY, C. H. 2000. Matrix survival signaling: from fibronectin via focal adhesion kinase to c-Jun NH(2)-terminal kinase. *J Cell Biol*, 149, 741-54.
- AMANO, M., FUKATA, Y. & KAIBUCHI, K. 2000. Regulation and functions of Rho-associated kinase. *Exp Cell Res*, 261, 44-51.
- AMANO, O., YAMANE, A., SHIMADA, M., KOSHIMIZU, U., NAKAMURA, T. & ISEKI, S. 2002. Hepatocyte growth factor is essential for migration of myogenic cells and promotes their proliferation during the early periods of tongue morphogenesis in mouse embryos. *Dev Dyn*, 223, 169-79.
- ANANTHAKRISHNAN, R. & EHRLICHER, A. 2007. The forces behind cell movement. *Int J Biol Sci*, 3, 303-17.
- ANASTASI, S., GIORDANO, S., STHANDIER, O., GAMBAROTTA, G., MAIONE, R., COMOGLIO, P. & AMATI, P. 1997. A natural hepatocyte growth factor/scatter factor autocrine loop in myoblast cells and the effect of the constitutive Met kinase activation on myogenic differentiation. *J Cell Biol*, 137, 1057-68.
- ANDERSON, J. E. 2000. A role for nitric oxide in muscle repair: nitric oxide-mediated activation of muscle satellite cells. *Mol Biol Cell*, 11, 1859-74.
- ARAI, K., LEE, S. R. & LO, E. H. 2003. Essential role for ERK mitogen-activated protein kinase in matrix metalloproteinase-9 regulation in rat cortical astrocytes. *Glia*, 43, 254-64.
- ARBER, S., BARBAYANNIS, F. A., HANSER, H., SCHNEIDER, C., STANYON, C. A., BERNARD, O. & CARONI, P. 1998. Regulation of actin dynamics through phosphorylation of cofilin by LIM-kinase. *Nature*, 393, 805-9.
- ARNOLD, L., HENRY, A., PORON, F., BABA-AMER, Y., VAN ROOIJEN, N., PLONQUET, A., GHERARDI, R. K. & CHAZAUD, B. 2007. Inflammatory monocytes recruited after skeletal muscle injury switch into antiinflammatory macrophages to support myogenesis. *J Exp Med*, 204, 1057-69.
- ASSOIAN, R. K. & SPORN, M. B. 1986. Type beta transforming growth factor in human platelets: release during platelet degranulation and action on vascular smooth muscle cells. *J Cell Biol*, 102, 1217-23.
- ATHANASOPOULOS, T., GRAHAM, I. R., FOSTER, H. & DICKSON, G. 2004. Recombinant adeno-associated viral (rAAV) vectors as therapeutic tools for Duchenne muscular dystrophy (DMD). *Gene Ther*, 11 Suppl 1, S109-21.
- AUSTIN, L., BOWER, J. J., BENNETT, T. M., LYNCH, G. S., KAPSA, R., WHITE, J. D., BARNARD, W., GREGOREVIC, P. & BYRNE, E. 2000. Leukemia inhibitory factor ameliorates muscle fiber degeneration in the mdx mouse. *Muscle Nerve*, 23, 1700-5.
- AZOURY, J., LEE, K. W., GEORGET, V., HIKAL, P. & VERLHAC, M. H. 2011. Symmetry breaking in mouse oocytes requires transient F-actin meshwork destabilization. *Development*, 138, 2903-8.

- BAILEY, P., HOLOWACZ, T. & LASSAR, A. B. 2001. The origin of skeletal muscle stem cells in the embryo and the adult. *Curr Opin Cell Biol*, 13, 679-89.
- BARK, T. H., MCNURLAN, M. A., LANG, C. H. & GARLICK, P. J. 1998. Increased protein synthesis after acute IGF-I or insulin infusion is localized to muscle in mice. *Am J Physiol*, 275, E118-23.
- BARNARD, W., BOWER, J., BROWN, M. A., MURPHY, M. & AUSTIN, L. 1994. Leukemia inhibitory factor (LIF) infusion stimulates skeletal muscle regeneration after injury: injured muscle expresses lif mRNA. *J Neurol Sci*, 123, 108-13.
- BARTON-DAVIS, E. R., SHOTURMA, D. I., MUSARO, A., ROSENTHAL, N. & SWEENEY, H. L. 1998. Viral mediated expression of insulin-like growth factor I blocks the aging-related loss of skeletal muscle function. *Proc Natl Acad Sci U S A*, 95, 15603-7.
- BEAUCHAMP, J. R., HESLOP, L., YU, D. S., TAJBAKHSI, S., KELLY, R. G., WERNIG, A., BUCKINGHAM, M. E., PARTRIDGE, T. A. & ZAMMIT, P. S. 2000. Expression of CD34 and Myf5 defines the majority of quiescent adult skeletal muscle satellite cells. *J Cell Biol*, 151, 1221-34.
- BECCAFICO, S., RIUZZI, F., PUGLIELLI, C., MANCINELLI, R., FULLE, S., SORCI, G. & DONATO, R. 2010. Human muscle satellite cells show age-related differential expression of S100B protein and RAGE. *Age (Dordr)*.
- BECCIOLINI, L., MEACCI, E., DONATI, C., CENCETTI, F., RAPIZZI, E. & BRUNI, P. 2006. Sphingosine 1-phosphate inhibits cell migration in C2C12 myoblasts. *Biochim Biophys Acta*, 1761, 43-51.
- BELCASTRO, A. N., ARTHUR, G. D., ALBISSER, T. A. & RAJ, D. A. 1996. Heart, liver, and skeletal muscle myeloperoxidase activity during exercise. *J Appl Physiol*, 80, 1331-5.
- BELCASTRO, A. N., SHEWCHUK, L. D. & RAJ, D. A. 1998. Exercise-induced muscle injury: a calpain hypothesis. *Mol Cell Biochem*, 179, 135-45.
- BENARD, V., BOHL, B. P. & BOKOCH, G. M. 1999. Characterization of rac and cdc42 activation in chemoattractant-stimulated human neutrophils using a novel assay for active GTPases. *J Biol Chem*, 274, 13198-204.
- BENCHAOUIR, R., MEREGALLI, M., FARINI, A., D'ANTONA, G., BELICCHI, M., GOYENVALLE, A., BATTISTELLI, M., BRESOLIN, N., BOTTINELLI, R., GARCIA, L. & TORRENTE, Y. 2007. Restoration of human dystrophin following transplantation of exon-skipping-engineered DMD patient stem cells into dystrophic mice. *Cell Stem Cell*, 1, 646-57.
- BENDALL, A. J., DING, J., HU, G., SHEN, M. M. & ABATE-SHEN, C. 1999. Msx1 antagonizes the myogenic activity of Pax3 in migrating limb muscle precursors. *Development*, 126, 4965-76.
- BERRIER, A. L. & YAMADA, K. M. 2007. Cell-matrix adhesion. *J Cell Physiol*, 213, 565-73.
- BHAGAVATI, S. & XU, W. 2005. Generation of skeletal muscle from transplanted embryonic stem cells in dystrophic mice. *Biochem Biophys Res Commun*, 333, 644-9.
- BHUIN, T. & ROY, J. K. 2009. Rab11 is required for myoblast fusion in *Drosophila*. *Cell Tissue Res*, 336, 489-99.

- BIGOT, A., JACQUEMIN, V., DEBACQ-CHAINIAUX, F., BUTLER-BROWNE, G. S., TOUSSAINT, O., FURLING, D. & MOULY, V. 2008. Replicative aging down-regulates the myogenic regulatory factors in human myoblasts. *Biol Cell*, 100, 189-99.
- BIRESSI, S., TAGLIAFICO, E., LAMORTE, G., MONTEVERDE, S., TENEDINI, E., RONCAGLIA, E., FERRARI, S., CUSELLA-DE ANGELIS, M. G., TAJBAKHS, S. & COSSU, G. 2007. Intrinsic phenotypic diversity of embryonic and fetal myoblasts is revealed by genome-wide gene expression analysis on purified cells. *Dev Biol*, 304, 633-51.
- BISCHOFF, R. 1986. A satellite cell mitogen from crushed adult muscle. *Dev Biol*, 115, 140-7.
- BISCHOFF, R. 1997. Chemotaxis of skeletal muscle satellite cells. *Dev Dyn*, 208, 505-15.
- BISHOP, A. L. & HALL, A. 2000. Rho GTPases and their effector proteins. *Biochem J*, 348 Pt 2, 241-55.
- BLADT, F., RIETHMACHER, D., ISENMANN, S., AGUZZI, A. & BIRCHMEIER, C. 1995. Essential role for the c-met receptor in the migration of myogenic precursor cells into the limb bud. *Nature*, 376, 768-71.
- BLAKE, D. J., WEIR, A., NEWAY, S. E. & DAVIES, K. E. 2002. Function and genetics of dystrophin and dystrophin-related proteins in muscle. *Physiol Rev*, 82, 291-329.
- BLANCO-APARICIO, C., RENNER, O., LEAL, J. F. & CARNERO, A. 2007. PTEN, more than the AKT pathway. *Carcinogenesis*, 28, 1379-86.
- BLAU, H. M., PAVLATH, G. K., HARDEMAN, E. C., CHIU, C. P., SILBERSTEIN, L., WEBSTER, S. G., MILLER, S. C. & WEBSTER, C. 1985. Plasticity of the differentiated state. *Science*, 230, 758-66.
- BODENSTEINER, J. B. & ENGEL, A. G. 1978. Intracellular calcium accumulation in Duchenne dystrophy and other myopathies: a study of 567,000 muscle fibers in 114 biopsies. *Neurology*, 28, 439-46.
- BOKOCH, G. M., VLAHOS, C. J., WANG, Y., KNAUS, U. G. & TRAYNOR-KAPLAN, A. E. 1996. Rac GTPase interacts specifically with phosphatidylinositol 3-kinase. *Biochem J*, 315 (Pt 3), 775-9.
- BONDESEN, B. A., JONES, K. A., GLASGOW, W. C. & PAVLATH, G. K. 2007. Inhibition of myoblast migration by prostacyclin is associated with enhanced cell fusion. *FASEB J*, 21, 3338-45.
- BOWER, J., VAKAKIS, N., NICOLA, N. A. & AUSTIN, L. 1995. Specific binding of leukemia inhibitory factor to murine myoblasts in culture. *J Cell Physiol*, 164, 93-8.
- BRACK, A. S., CONBOY, I. M., CONBOY, M. J., SHEN, J. & RANDO, T. A. 2008. A temporal switch from notch to Wnt signaling in muscle stem cells is necessary for normal adult myogenesis. *Cell Stem Cell*, 2, 50-9.
- BRACK, A. S., CONBOY, M. J., ROY, S., LEE, M., KUO, C. J., KELLER, C. & RANDO, T. A. 2007. Increased Wnt signaling during aging alters muscle stem cell fate and increases fibrosis. *Science*, 317, 807-10.

- BRACK, A. S. & RANDO, T. A. 2007. Intrinsic changes and extrinsic influences of myogenic stem cell function during aging. *Stem Cell Rev*, 3, 226-37.
- BRACK, A. S. & RANDO, T. A. 2008. Age-Dependent Changes in Skeletal Muscle Regeneration. *Skeletal Muscle Repair and Regeneration*. Springer Science+Business Media B.V.
- BRAKEBUSCH, C. & FASSLER, R. 2003. The integrin-actin connection, an eternal love affair. *EMBO J*, 22, 2324-33.
- BROHMANN, H., JAGLA, K. & BIRCHMEIER, C. 2000. The role of Lbx1 in migration of muscle precursor cells. *Development*, 127, 437-45.
- BRUNET, A., BONNI, A., ZIGMOND, M. J., LIN, M. Z., JUO, P., HU, L. S., ANDERSON, M. J., ARDEN, K. C., BLENIS, J. & GREENBERG, M. E. 1999. Akt promotes cell survival by phosphorylating and inhibiting a Forkhead transcription factor. *Cell*, 96, 857-68.
- BRUSSEE, V., MERLY, F., TARDIF, F. & TREMBLAY, J. P. 1998. Normal myoblast implantation in MDX mice prevents muscle damage by exercise. *Biochem Biophys Res Commun*, 250, 321-7.
- BUCKINGHAM, M., BAJARD, L., CHANG, T., DAUBAS, P., HADCHOUEL, J., MEILHAC, S., MONTARRAS, D., ROCANCOURT, D. & RELAIX, F. 2003. The formation of skeletal muscle: from somite to limb. *J Anat*, 202, 59-68.
- CAIN, R. J. & RIDLEY, A. J. 2009. Phosphoinositide 3-kinases in cell migration. *Biol Cell*, 101, 13-29.
- CAMPBELL, M., ALLEN, W. E., SAWYER, C., VANHAESEBROECK, B. & TRIMBLE, E. R. 2004. Glucose-potentiated chemotaxis in human vascular smooth muscle is dependent on cross-talk between the PI3K and MAPK signaling pathways. *Circ Res*, 95, 380-8.
- CANTINI, M. & CARRARO, U. 1995. Macrophage-released factor stimulates selectively myogenic cells in primary muscle culture. *J Neuropathol Exp Neurol*, 54, 121-8.
- CANTINI, M., MASSIMINO, M. L., BRUSON, A., CATANI, C., DALLA LIBERA, L. & CARRARO, U. 1994. Macrophages regulate proliferation and differentiation of satellite cells. *Biochem Biophys Res Commun*, 202, 1688-96.
- CARLSON, B. M. & FAULKNER, J. A. 1989. Muscle transplantation between young and old rats: age of host determines recovery. *Am J Physiol*, 256, C1262-6.
- CAROSIO, S., BERARDINELLI, M. G., AUCELLO, M. & MUSARO, A. 2011. Impact of ageing on muscle cell regeneration. *Ageing Res Rev*, 10, 35-42.
- CARY, L. A., CHANG, J. F. & GUAN, J. L. 1996. Stimulation of cell migration by overexpression of focal adhesion kinase and its association with Src and Fyn. *J Cell Sci*, 109 (Pt 7), 1787-94.
- CASSANO, M., BIRESSI, S., FINAN, A., BENEDETTI, L., OMES, C., BORATTO, R., MARTIN, F., ALLEGRETTI, M., BROCCOLI, V., CUSELLA DE ANGELIS, G., COMOGLIO, P. M., BASILICO, C., TORRENTE, Y., MICHIELI, P., COSSU, G. & SAMPAOLESI, M. 2008. Magic-factor 1, a partial agonist of Met, induces muscle hypertrophy by protecting myogenic progenitors from apoptosis. *PLoS One*, 3, e3223.
- CASTALDI, L., SERRA, C., MORETTI, F., MESSINA, G., PAOLETTI, R., SAMPAOLESI, M., TORGOVNICK, A., BAIOCCHI, M., PADULA,

- F., PISANIELLO, A., MOLINARO, M., COSSU, G., LEVRERO, M. & BOUCHE, M. 2007. Bisperoxovanadium, a phospho-tyrosine phosphatase inhibitor, reprograms myogenic cells to acquire a pluripotent, circulating phenotype. *FASEB J*, 21, 3573-83.
- CASWELL, P. T. & NORMAN, J. C. 2006. Integrin trafficking and the control of cell migration. *Traffic*, 7, 14-21.
- CAU, J. & HALL, A. 2005. Cdc42 controls the polarity of the actin and microtubule cytoskeletons through two distinct signal transduction pathways. *J Cell Sci*, 118, 2579-87.
- CHAKRAVARTHY, M. V., DAVIS, B. S. & BOOTH, F. W. 2000. IGF-I restores satellite cell proliferative potential in immobilized old skeletal muscle. *J Appl Physiol*, 89, 1365-79.
- CHAN, C. Y., MASUI, O., KRAKOVSKA, O., BELOZEROV, V. E., VOISIN, S., GHANNY, S., CHEN, J., MOYEZ, D., ZHU, P., EVANS, K. R., MCDERMOTT, J. C. & SIU, K. W. 2011. Identification of differentially regulated secretome components during skeletal myogenesis. *Mol Cell Proteomics*, 10, M110 004804.
- CHARGE, S. B. & RUDNICKI, M. A. 2004. Cellular and molecular regulation of muscle regeneration. *Physiol Rev*, 84, 209-38.
- CHEN, G. & QUINN, L. S. 1992. Partial characterization of skeletal myoblast mitogens in mouse crushed muscle extract. *J Cell Physiol*, 153, 563-74.
- CHEN, J. S., WANG, Q., FU, X. H., HUANG, X. H., CHEN, X. L., CAO, L. Q., CHEN, L. Z., TAN, H. X., LI, W., BI, J. & ZHANG, L. J. 2009. Involvement of PI3K/PTEN/AKT/mTOR pathway in invasion and metastasis in hepatocellular carcinoma: Association with MMP-9. *Hepatol Res*, 39, 177-86.
- CHEN, X. & LI, Y. 2009. Role of matrix metalloproteinases in skeletal muscle: migration, differentiation, regeneration and fibrosis. *Cell Adh Migr*, 3, 337-41.
- CHOU, F. L., HILL, J. M., HSIEH, J. C., POUYSSEGUR, J., BRUNET, A., GLADING, A., UBERALL, F., RAMOS, J. W., WERNER, M. H. & GINSBERG, M. H. 2003. PEA-15 binding to ERK1/2 MAPKs is required for its modulation of integrin activation. *J Biol Chem*, 278, 52587-97.
- CHRIST, B. & ORDAHL, C. P. 1995. Early stages of chick somite development. *Anat Embryol (Berl)*, 191, 381-96.
- CIVATTE, M., BARTOLI, C., SCHLEINITZ, N., CHETAÏLLE, B., PELLISSIER, J. F. & FIGARELLA-BRANGER, D. 2005. Expression of the beta chemokines CCL3, CCL4, CCL5 and their receptors in idiopathic inflammatory myopathies. *Neuropathol Appl Neurobiol*, 31, 70-9.
- CLARKE, M. S., KHAKEE, R. & MCNEIL, P. L. 1993. Loss of cytoplasmic basic fibroblast growth factor from physiologically wounded myofibers of normal and dystrophic muscle. *J Cell Sci*, 106 (Pt 1), 121-33.
- CLEMENTE, C. F., CORAT, M. A., SAAD, S. T. & FRANCHINI, K. G. 2005. Differentiation of C2C12 myoblasts is critically regulated by FAK signaling. *Am J Physiol Regul Integr Comp Physiol*, 289, R862-70.
- COLEMAN, M. E., DEMAYO, F., YIN, K. C., LEE, H. M., GESKE, R., MONTGOMERY, C. & SCHWARTZ, R. J. 1995. Myogenic vector

- expression of insulin-like growth factor I stimulates muscle cell differentiation and myofiber hypertrophy in transgenic mice. *J Biol Chem*, 270, 12109-16.
- COMER, F. I. & PARENT, C. A. 2007. Phosphoinositides specify polarity during epithelial organ development. *Cell*, 128, 239-40.
- CONBOY, I. M., CONBOY, M. J., SMYTHE, G. M. & RANDO, T. A. 2003. Notch-mediated restoration of regenerative potential to aged muscle. *Science*, 302, 1575-7.
- CONBOY, I. M., CONBOY, M. J., WAGERS, A. J., GIRMA, E. R., WEISSMAN, I. L. & RANDO, T. A. 2005. Rejuvenation of aged progenitor cells by exposure to a young systemic environment. *Nature*, 433, 760-4.
- CONBOY, I. M. & RANDO, T. A. 2002. The regulation of Notch signaling controls satellite cell activation and cell fate determination in postnatal myogenesis. *Dev Cell*, 3, 397-409.
- COOLICAN, S. A., SAMUEL, D. S., EWTON, D. Z., MCWADE, F. J. & FLORINI, J. R. 1997. The mitogenic and myogenic actions of insulin-like growth factors utilize distinct signaling pathways. *J Biol Chem*, 272, 6653-62.
- COOPER, R. N., TAJBAKSH, S., MOULY, V., COSSU, G., BUCKINGHAM, M. & BUTLER-BROWNE, G. S. 1999. In vivo satellite cell activation via Myf5 and MyoD in regenerating mouse skeletal muscle. *J Cell Sci*, 112 (Pt 17), 2895-901.
- CORNELISON, D. D., FILLA, M. S., STANLEY, H. M., RAPRAEGER, A. C. & OLWIN, B. B. 2001. Syndecan-3 and syndecan-4 specifically mark skeletal muscle satellite cells and are implicated in satellite cell maintenance and muscle regeneration. *Dev Biol*, 239, 79-94.
- CORNELISON, D. D., OLWIN, B. B., RUDNICKI, M. A. & WOLD, B. J. 2000. MyoD(-/-) satellite cells in single-fiber culture are differentiation defective and MRF4 deficient. *Dev Biol*, 224, 122-37.
- CORNELISON, D. D. & WOLD, B. J. 1997. Single-cell analysis of regulatory gene expression in quiescent and activated mouse skeletal muscle satellite cells. *Dev Biol*, 191, 270-83.
- CORTI, S., SALANI, S., DEL BO, R., SIRONI, M., STRAZZER, S., D'ANGELO, M. G., COMI, G. P., BRESOLIN, N. & SCARLATO, G. 2001. Chemotactic factors enhance myogenic cell migration across an endothelial monolayer. *Exp Cell Res*, 268, 36-44.
- COSSU, G. & BIRESSI, S. 2005. Satellite cells, myoblasts and other occasional myogenic progenitors: possible origin, phenotypic features and role in muscle regeneration. *Semin Cell Dev Biol*, 16, 623-31.
- COSSU, G. & BORELLO, U. 1999. Wnt signaling and the activation of myogenesis in mammals. *EMBO J*, 18, 6867-72.
- COSSU, G., KELLY, R., TAJBAKSH, S., DI DONNA, S., VIVARELLI, E. & BUCKINGHAM, M. 1996. Activation of different myogenic pathways: myf-5 is induced by the neural tube and MyoD by the dorsal ectoderm in mouse paraxial mesoderm. *Development*, 122, 429-37.
- COSSU, G. & MOLINARO, M. 1987. Cell heterogeneity in the myogenic lineage. *Curr Top Dev Biol*, 23, 185-208.
- COSSU, G. & SAMPAOLESI, M. 2004. New therapies for muscular dystrophy: cautious optimism. *Trends Mol Med*, 10, 516-20.

- COSSU, G. & SAMPAOLESI, M. 2007. New therapies for Duchenne muscular dystrophy: challenges, prospects and clinical trials. *Trends Mol Med*, 13, 520-6.
- COULTON, G. R., MORGAN, J. E., PARTRIDGE, T. A. & SLOPER, J. C. 1988. The mdx mouse skeletal muscle myopathy: I. A histological, morphometric and biochemical investigation. *Neuropathol Appl Neurobiol*, 14, 53-70.
- COX, E. A. & HUTTENLOCHER, A. 1998. Regulation of integrin-mediated adhesion during cell migration. *Microsc Res Tech*, 43, 412-9.
- CREUZET, S., LESCAUDRON, L., LI, Z. & FONTAINE-PERUS, J. 1998. MyoD, myogenin, and desmin-nls-lacZ transgene emphasize the distinct patterns of satellite cell activation in growth and regeneration. *Exp Cell Res*, 243, 241-53.
- CRISCO, J. J., JOKL, P., HEINEN, G. T., CONNELL, M. D. & PANJABI, M. M. 1994. A muscle contusion injury model. Biomechanics, physiology, and histology. *Am J Sports Med*, 22, 702-10.
- CRUZ-JENTOFT, A. J., BAEYENS, J. P., BAUER, J. M., BOIRIE, Y., CEDERHOLM, T., LANDI, F., MARTIN, F. C., MICHEL, J. P., ROLLAND, Y., SCHNEIDER, S. M., TOPINKOVA, E., VANDEWOUDE, M., ZAMBONI, M. & EUROPEAN WORKING GROUP ON SARCOPENIA IN OLDER, P. 2010. Sarcopenia: European consensus on definition and diagnosis: Report of the European Working Group on Sarcopenia in Older People. *Age Ageing*, 39, 412-23.
- CUI, Z., CHEN, X., LU, B., PARK, S. K., XU, T., XIE, Z., XUE, P., HOU, J., HANG, H., YATES, J. R., 3RD & YANG, F. 2009. Preliminary quantitative profile of differential protein expression between rat L6 myoblasts and myotubes by stable isotope labeling with amino acids in cell culture. *Proteomics*, 9, 1274-92.
- CULLY, M., YOU, H., LEVINE, A. J. & MAK, T. W. 2006. Beyond PTEN mutations: the PI3K pathway as an integrator of multiple inputs during tumorigenesis. *Nat Rev Cancer*, 6, 184-92.
- DAFTARY, A. S., CRISANTI, M., KALRA, M., WONG, B. & AMIN, R. 2007. Effect of long-term steroids on cough efficiency and respiratory muscle strength in patients with Duchenne muscular dystrophy. *Pediatrics*, 119, e320-4.
- DAHIA, P. L. 2000. PTEN, a unique tumor suppressor gene. *Endocr Relat Cancer*, 7, 115-29.
- DASARI, V. R., KAUR, K., VELPULA, K. K., GUJRATI, M., FASSETT, D., KLOPFENSTEIN, J. D., DINH, D. H. & RAO, J. S. 2010. Upregulation of PTEN in glioma cells by cord blood mesenchymal stem cells inhibits migration via downregulation of the PI3K/Akt pathway. *PLoS One*, 5, e10350.
- DATTA, S. R., DUDEK, H., TAO, X., MASTERS, S., FU, H., GOTOH, Y. & GREENBERG, M. E. 1997. Akt phosphorylation of BAD couples survival signals to the cell-intrinsic death machinery. *Cell*, 91, 231-41.
- DE ANGELIS, L., BERGHELLA, L., COLETTA, M., LATTANZI, L., ZANCHI, M., CUSELLA-DE ANGELIS, M. G., PONZETTO, C. & COSSU, G. 1999. Skeletal myogenic progenitors originating from embryonic dorsal aorta coexpress endothelial and myogenic

- markers and contribute to postnatal muscle growth and regeneration. *J Cell Biol*, 147, 869-78.
- DE DONATIS, A., COMITO, G., BURICCHI, F., VINCI, M. C., PARENTI, A., CASELLI, A., CAMICI, G., MANAO, G., RAMPONI, G. & CIRRI, P. 2008. Proliferation versus migration in platelet-derived growth factor signaling: the key role of endocytosis. *J Biol Chem*, 283, 19948-56.
- DE ROSSI, M., BERNASCONI, P., BAGGI, F., DE WAAL MALEFYT, R. & MANTEGAZZA, R. 2000. Cytokines and chemokines are both expressed by human myoblasts: possible relevance for the immune pathogenesis of muscle inflammation. *Int Immunol*, 12, 1329-35.
- DECARY, S., MOULY, V., HAMIDA, C. B., SAUTET, A., BARBET, J. P. & BUTLER-BROWNE, G. S. 1997. Replicative potential and telomere length in human skeletal muscle: implications for satellite cell-mediated gene therapy. *Hum Gene Ther*, 8, 1429-38.
- DEDIEU, S., POUSSARD, S., MAZERES, G., GRISE, F., DARGELOS, E., COTTIN, P. & BRUSTIS, J. J. 2004. Myoblast migration is regulated by calpain through its involvement in cell attachment and cytoskeletal organization. *Exp Cell Res*, 292, 187-200.
- DESAI, L. P., WHITE, S. R. & WATERS, C. M. 2009. Mechanical stretch decreases FAK phosphorylation and reduces cell migration through loss of JIP3-induced JNK phosphorylation in airway epithelial cells. *Am J Physiol Lung Cell Mol Physiol*, 297, L520-9.
- DEY, N., CROSSWELL, H. E., DE, P., PARSONS, R., PENG, Q., SU, J. D. & DURDEN, D. L. 2008. The protein phosphatase activity of PTEN regulates SRC family kinases and controls glioma migration. *Cancer Res*, 68, 1862-71.
- DI ROCCO, G., IACHININOTO, M. G., TRITARELLI, A., STRAINO, S., ZACHEO, A., GERMANI, A., CREA, F. & CAPOGROSSI, M. C. 2006. Myogenic potential of adipose-tissue-derived cells. *J Cell Sci*, 119, 2945-52.
- DIETRICH, S., ABOU-REBYEH, F., BROHMANN, H., BLADT, F., SONNENBERG-RIETHMACHER, E., YAMAAI, T., LUMSDEN, A., BRAND-SABERI, B. & BIRCHMEIER, C. 1999. The role of SF/HGF and c-Met in the development of skeletal muscle. *Development*, 126, 1621-9.
- DOHERTY, K. R., CAVE, A., DAVIS, D. B., DELMONTE, A. J., POSEY, A., EARLEY, J. U., HADHAZY, M. & MCNALLY, E. M. 2005. Normal myoblast fusion requires myoferlin. *Development*, 132, 5565-75.
- DOHERTY, K. R., DEMONBREUN, A. R., WALLACE, G. Q., CAVE, A., POSEY, A. D., HERETIS, K., PYTEL, P. & MCNALLY, E. M. 2008. The endocytic recycling protein EHD2 interacts with myoferlin to regulate myoblast fusion. *J Biol Chem*, 283, 20252-60.
- DOHERTY, T. J. 2003. Invited review: Aging and sarcopenia. *J Appl Physiol*, 95, 1717-27.
- DONATI, C., MEACCI, E., NUTI, F., BECCIOLINI, L., FARNARARO, M. & BRUNI, P. 2005. Sphingosine 1-phosphate regulates myogenic differentiation: a major role for S1P2 receptor. *FASEB J*, 19, 449-51.
- DOUMIT, M. E., COOK, D. R. & MERKEL, R. A. 1993. Fibroblast growth factor, epidermal growth factor, insulin-like growth factors, and

- platelet-derived growth factor-BB stimulate proliferation of clonally derived porcine myogenic satellite cells. *J Cell Physiol*, 157, 326-32.
- DOURDIN, N., BALCERZAK, D., BRUSTIS, J. J., POUSSARD, S., COTTIN, P. & DUCASTAING, A. 1999. Potential m-calpain substrates during myoblast fusion. *Exp Cell Res*, 246, 433-42.
- DUMKE, B. R. & LEES, S. J. 2011. Age-related impairment of T cell-induced skeletal muscle precursor cell function. *Am J Physiol Cell Physiol*, 300, C1226-33.
- DUMONT, J., MILLION, K., SUNDERLAND, K., RASSINIER, P., LIM, H., LEADER, B. & VERLHAC, M. H. 2007. Formin-2 is required for spindle migration and for the late steps of cytokinesis in mouse oocytes. *Dev Biol*, 301, 254-65.
- EDEN, S., ROHATGI, R., PODTELEJNIKOV, A. V., MANN, M. & KIRSCHNER, M. W. 2002. Mechanism of regulation of WAVE1-induced actin nucleation by Rac1 and Nck. *Nature*, 418, 790-3.
- EDOM-VOVARD, F., BONNIN, M. A. & DUPREZ, D. 2001. Misexpression of Fgf-4 in the chick limb inhibits myogenesis by down-regulating Fek expression. *Dev Biol*, 233, 56-71.
- EDWALL, D., SCHALLING, M., JENNISCHE, E. & NORSTEDT, G. 1989. Induction of insulin-like growth factor I messenger ribonucleic acid during regeneration of rat skeletal muscle. *Endocrinology*, 124, 820-5.
- EDWARDS, D. C., SANDERS, L. C., BOKOCH, G. M. & GILL, G. N. 1999. Activation of LIM-kinase by Pak1 couples Rac/Cdc42 GTPase signalling to actin cytoskeletal dynamics. *Nat Cell Biol*, 1, 253-9.
- EL FAHIME, E., MILLS, P., LAFRENIERE, J. F., TORRENTE, Y. & TREMBLAY, J. P. 2002. The urokinase plasminogen activator: an interesting way to improve myoblast migration following their transplantation. *Exp Cell Res*, 280, 169-78.
- EL FAHIME, E., TORRENTE, Y., CARON, N. J., BRESOLIN, M. D. & TREMBLAY, J. P. 2000. In vivo migration of transplanted myoblasts requires matrix metalloproteinase activity. *Exp Cell Res*, 258, 279-87.
- EMERY, A. E. 2002. The muscular dystrophies. *Lancet*, 359, 687-95.
- ENGELMAN, J. A., LUO, J. & CANTLEY, L. C. 2006. The evolution of phosphatidylinositol 3-kinases as regulators of growth and metabolism. *Nat Rev Genet*, 7, 606-19.
- ENGERT, J. C., BERGLUND, E. B. & ROSENTHAL, N. 1996. Proliferation precedes differentiation in IGF-I-stimulated myogenesis. *J Cell Biol*, 135, 431-40.
- EPSTEIN, J. A., SHAPIRO, D. N., CHENG, J., LAM, P. Y. & MAAS, R. L. 1996. Pax3 modulates expression of the c-Met receptor during limb muscle development. *Proc Natl Acad Sci U S A*, 93, 4213-8.
- FAN, Y., MALEY, M., BEILHARZ, M. & GROUNDS, M. 1996. Rapid death of injected myoblasts in myoblast transfer therapy. *Muscle Nerve*, 19, 853-60.
- FERRARI, G., CUSELLA-DE ANGELIS, G., COLETTA, M., PAOLUCCI, E., STORNAIUOLO, A., COSSU, G. & MAVILIO, F. 1998. Muscle regeneration by bone marrow-derived myogenic progenitors. *Science*, 279, 1528-30.

- FIELDING, R. A., MANFREDI, T. J., DING, W., FIATARONE, M. A., EVANS, W. J. & CANNON, J. G. 1993. Acute phase response in exercise. III. Neutrophil and IL-1 beta accumulation in skeletal muscle. *Am J Physiol*, 265, R166-72.
- FLETCHER, S., HONEYMAN, K., FALL, A. M., HARDING, P. L., JOHNSEN, R. D., STEINHAUS, J. P., MOULTON, H. M., IVERSEN, P. L. & WILTON, S. D. 2007. Morpholino oligomer-mediated exon skipping averts the onset of dystrophic pathology in the mdx mouse. *Mol Ther*, 15, 1587-92.
- FLORINI, J. R., EWTON, D. Z. & ROOF, S. L. 1991. Insulin-like growth factor-I stimulates terminal myogenic differentiation by induction of myogenin gene expression. *Mol Endocrinol*, 5, 718-24.
- FLOSS, T., ARNOLD, H. H. & BRAUN, T. 1997. A role for FGF-6 in skeletal muscle regeneration. *Genes Dev*, 11, 2040-51.
- FLUCK, M. & HOPPELER, H. 2003. Molecular basis of skeletal muscle plasticity--from gene to form and function. *Rev Physiol Biochem Pharmacol*, 146, 159-216.
- FOULSTONE, E. J., HUSER, C., CROWN, A. L., HOLLY, J. M. & STEWART, C. E. 2004. Differential signalling mechanisms predisposing primary human skeletal muscle cells to altered proliferation and differentiation: roles of IGF-I and TNFalpha. *Exp Cell Res*, 294, 223-35.
- FOURAUX, M. A., DENEKA, M., IVAN, V., VAN DER HEIJDEN, A., RAYMACKERS, J., VAN SUYLEKOM, D., VAN VENROOIJ, W. J., VAN DER SLUIJS, P. & PRUIJN, G. J. 2004. Rabip4' is an effector of rab5 and rab4 and regulates transport through early endosomes. *Mol Biol Cell*, 15, 611-24.
- FUNAMOTO, S., MEILI, R., LEE, S., PARRY, L. & FIRTEL, R. A. 2002. Spatial and temporal regulation of 3-phosphoinositides by PI 3-kinase and PTEN mediates chemotaxis. *Cell*, 109, 611-23.
- GADIANT, R. A. & PATTERSON, P. H. 1999. Leukemia inhibitory factor, Interleukin 6, and other cytokines using the GP130 transducing receptor: roles in inflammation and injury. *Stem Cells*, 17, 127-37.
- GAL-LEVI, R., LESHEM, Y., AOKI, S., NAKAMURA, T. & HALEVY, O. 1998. Hepatocyte growth factor plays a dual role in regulating skeletal muscle satellite cell proliferation and differentiation. *Biochim Biophys Acta*, 1402, 39-51.
- GALLI, R., BORELLO, U., GRITTI, A., MINASI, M. G., BJORNSON, C., COLETTA, M., MORA, M., DE ANGELIS, M. G., FIOCCO, R., COSSU, G. & VESCOVI, A. L. 2000. Skeletal myogenic potential of human and mouse neural stem cells. *Nat Neurosci*, 3, 986-91.
- GENOT, E. M., ARRIEUMERLOU, C., KU, G., BURGERING, B. M., WEISS, A. & KRAMER, I. M. 2000. The T-cell receptor regulates Akt (protein kinase B) via a pathway involving Rac1 and phosphatidylinositide 3-kinase. *Mol Cell Biol*, 20, 5469-78.
- GIBSON, M. C. & SCHULTZ, E. 1982. The distribution of satellite cells and their relationship to specific fiber types in soleus and extensor digitorum longus muscles. *Anat Rec*, 202, 329-37.
- GIBSON, M. C. & SCHULTZ, E. 1983. Age-related differences in absolute numbers of skeletal muscle satellite cells. *Muscle Nerve*, 6, 574-80.

- GILDOR, B., MASSARWA, R., SHILO, B. Z. & SCHEJTER, E. D. 2009. The SCAR and WASp nucleation-promoting factors act sequentially to mediate *Drosophila* myoblast fusion. *EMBO Rep*, 10, 1043-50.
- GLADING, A., BODNAR, R. J., REYNOLDS, I. J., SHIRAHA, H., SATISH, L., POTTER, D. A., BLAIR, H. C. & WELLS, A. 2004. Epidermal growth factor activates m-calpain (calpain II), at least in part, by extracellular signal-regulated kinase-mediated phosphorylation. *Mol Cell Biol*, 24, 2499-512.
- GLADING, A., CHANG, P., LAUFFENBURGER, D. A. & WELLS, A. 2000. Epidermal growth factor receptor activation of calpain is required for fibroblast motility and occurs via an ERK/MAP kinase signaling pathway. *J Biol Chem*, 275, 2390-8.
- GLUND, S., DESHMUKH, A., LONG, Y. C., MOLLER, T., KOISTINEN, H. A., CAIDAHL, K., ZIERATH, J. R. & KROOK, A. 2007. Interleukin-6 directly increases glucose metabolism in resting human skeletal muscle. *Diabetes*, 56, 1630-7.
- GONCHAROVA, E. A., AMMIT, A. J., IRANI, C., CARROLL, R. G., ESZTERHAS, A. J., PANETTIERI, R. A. & KRYMSKAYA, V. P. 2002a. PI3K is required for proliferation and migration of human pulmonary vascular smooth muscle cells. *Am J Physiol Lung Cell Mol Physiol*, 283, L354-63.
- GONCHAROVA, E. A., VOROTNIKOV, A. V., GRACHEVA, E. O., WANG, C. L., PANETTIERI, R. A., JR., STEPANOVA, V. V. & TKACHUK, V. A. 2002b. Activation of p38 MAP-kinase and caldesmon phosphorylation are essential for urokinase-induced human smooth muscle cell migration. *Biol Chem*, 383, 115-26.
- GRIFFIN, C. A., APPONI, L. H., LONG, K. K. & PAVLATH, G. K. 2010. Chemokine expression and control of muscle cell migration during myogenesis. *J Cell Sci*, 123, 3052-60.
- GRIFFIN, C. A., KAFADAR, K. A. & PAVLATH, G. K. 2009. MOR23 promotes muscle regeneration and regulates cell adhesion and migration. *Dev Cell*, 17, 649-61.
- GROS, J., MANCEAU, M., THOME, V. & MARCELLE, C. 2005. A common somitic origin for embryonic muscle progenitors and satellite cells. *Nature*, 435, 954-8.
- GROSS, M. K., MORAN-RIVARD, L., VELASQUEZ, T., NAKATSU, M. N., JAGLA, K. & GOULDING, M. 2000. Lbx1 is required for muscle precursor migration along a lateral pathway into the limb. *Development*, 127, 413-24.
- GROUNDS, M. D. 1987. Phagocytosis of necrotic muscle in muscle isografts is influenced by the strain, age, and sex of host mice. *J Pathol*, 153, 71-82.
- GROUNDS, M. D., GARRETT, K. L., LAI, M. C., WRIGHT, W. E. & BEILHARZ, M. W. 1992. Identification of skeletal muscle precursor cells in vivo by use of MyoD1 and myogenin probes. *Cell Tissue Res*, 267, 99-104.
- GU, J., TAMURA, M., PANKOV, R., DANEN, E. H., TAKINO, T., MATSUMOTO, K. & YAMADA, K. M. 1999. Shc and FAK differentially regulate cell motility and directionality modulated by PTEN. *J Cell Biol*, 146, 389-403.

- GU, J., TAMURA, M. & YAMADA, K. M. 1998. Tumor suppressor PTEN inhibits integrin- and growth factor-mediated mitogen-activated protein (MAP) kinase signaling pathways. *J Cell Biol*, 143, 1375-83.
- GUERIN, C. M. & KRAMER, S. G. 2009. Cytoskeletal remodeling during myotube assembly and guidance: coordinating the actin and microtubule networks. *Commun Integr Biol*, 2, 452-7.
- GUSSONI, E., BENNETT, R. R., MUSKIEWICZ, K. R., MEYERROSE, T., NOLTA, J. A., GILGOFF, I., STEIN, J., CHAN, Y. M., LIDOV, H. G., BONNEMANN, C. G., VON MOERS, A., MORRIS, G. E., DEN DUNNEN, J. T., CHAMBERLAIN, J. S., KUNKEL, L. M. & WEINBERG, K. 2002. Long-term persistence of donor nuclei in a Duchenne muscular dystrophy patient receiving bone marrow transplantation. *J Clin Invest*, 110, 807-14.
- GUSSONI, E., BLAU, H. M. & KUNKEL, L. M. 1997. The fate of individual myoblasts after transplantation into muscles of DMD patients. *Nat Med*, 3, 970-7.
- HALEVY, O., PIESTUN, Y., ALLOUH, M. Z., ROSSER, B. W., RINKEVICH, Y., RESHEF, R., ROZENBOIM, I., WLEKLINSKI-LEE, M. & YABLONKA-REUVENI, Z. 2004. Pattern of Pax7 expression during myogenesis in the posthatch chicken establishes a model for satellite cell differentiation and renewal. *Dev Dyn*, 231, 489-502.
- HALL, A. 2005. Rho GTPases and the control of cell behaviour. *Biochem Soc Trans*, 33, 891-5.
- HAMADI, A., BOUALI, M., DONTENWILL, M., STOECKEL, H., TAKEDA, K. & RONDE, P. 2005. Regulation of focal adhesion dynamics and disassembly by phosphorylation of FAK at tyrosine 397. *J Cell Sci*, 118, 4415-25.
- HANKS, S. K., RYZHOVA, L., SHIN, N. Y. & BRABEK, J. 2003. Focal adhesion kinase signaling activities and their implications in the control of cell survival and motility. *Front Biosci*, 8, d982-96.
- HANNIGAN, M., ZHAN, L., LI, Z., AI, Y., WU, D. & HUANG, C. K. 2002. Neutrophils lacking phosphoinositide 3-kinase gamma show loss of directionality during N-formyl-Met-Leu-Phe-induced chemotaxis. *Proc Natl Acad Sci U S A*, 99, 3603-8.
- HAWKE, T. J. & GARRY, D. J. 2001. Myogenic satellite cells: physiology to molecular biology. *J Appl Physiol*, 91, 534-51.
- HAWKINS, P. T., EGUINO, A., QIU, R. G., STOKOE, D., COOKE, F. T., WALTERS, R., WENNSTROM, S., CLAEISSON-WELSH, L., EVANS, T., SYMONS, M. & ET AL. 1995. PDGF stimulates an increase in GTP-Rac via activation of phosphoinositide 3-kinase. *Curr Biol*, 5, 393-403.
- HENNINGSEN, J., PEDERSEN, B. K. & KRATCHMAROVA, I. 2011. Quantitative analysis of the secretion of the MCP family of chemokines by muscle cells. *Mol Biosyst*, 7, 311-21.
- HENNINGSEN, J., RIGBOLT, K. T., BLAGOEV, B., PEDERSEN, B. K. & KRATCHMAROVA, I. 2010. Dynamics of the skeletal muscle secretome during myoblast differentiation. *Mol Cell Proteomics*, 9, 2482-96.
- HIBI, M., NAKAJIMA, K. & HIRANO, T. 1996. IL-6 cytokine family and signal transduction: a model of the cytokine system. *J Mol Med (Berl)*, 74, 1-12.

- HIRATA, A., MASUDA, S., TAMURA, T., KAI, K., OJIMA, K., FUKASE, A., MOTOYOSHI, K., KAMAKURA, K., MIYAGOE-SUZUKI, Y. & TAKEDA, S. 2003. Expression profiling of cytokines and related genes in regenerating skeletal muscle after cardiotoxin injection: a role for osteopontin. *Am J Pathol*, 163, 203-15.
- HOFFMAN, E. P. & DRESSMAN, D. 2001. Molecular pathophysiology and targeted therapeutics for muscular dystrophy. *Trends Pharmacol Sci*, 22, 465-70.
- HOFFMAN, E. P., FISCHBECK, K. H., BROWN, R. H., JOHNSON, M., MEDORI, R., LOIKE, J. D., HARRIS, J. B., WATERSTON, R., BROOKE, M., SPECHT, L. & ET AL. 1988. Characterization of dystrophin in muscle-biopsy specimens from patients with Duchenne's or Becker's muscular dystrophy. *N Engl J Med*, 318, 1363-8.
- HUANG, C., BORCHERS, C. H., SCHALLER, M. D. & JACOBSON, K. 2004a. Phosphorylation of paxillin by p38MAPK is involved in the neurite extension of PC-12 cells. *J Cell Biol*, 164, 593-602.
- HUANG, C., JACOBSON, K. & SCHALLER, M. D. 2004b. MAP kinases and cell migration. *J Cell Sci*, 117, 4619-28.
- HUANG, D., KHOE, M., BEFEKADU, M., CHUNG, S., TAKATA, Y., ILIC, D. & BRYER-ASH, M. 2007. Focal adhesion kinase mediates cell survival via NF-kappaB and ERK signaling pathways. *Am J Physiol Cell Physiol*, 292, C1339-52.
- HUANG, Z., YAN, D. P. & GE, B. X. 2008. JNK regulates cell migration through promotion of tyrosine phosphorylation of paxillin. *Cell Signal*, 20, 2002-12.
- HUGHES, S. M. & BLAU, H. M. 1990. Migration of myoblasts across basal lamina during skeletal muscle development. *Nature*, 345, 350-3.
- HUSMANN, I., SOULET, L., GAUTRON, J., MARTELLY, I. & BARRITAULT, D. 1996. Growth factors in skeletal muscle regeneration. *Cytokine Growth Factor Rev*, 7, 249-58.
- HYNES, R. O. 2002. Integrins: bidirectional, allosteric signaling machines. *Cell*, 110, 673-87.
- IGNOTZ, R. A. & MASSAGUE, J. 1986. Transforming growth factor-beta stimulates the expression of fibronectin and collagen and their incorporation into the extracellular matrix. *J Biol Chem*, 261, 4337-45.
- IJIMA, M. & DEVREOTES, P. 2002. Tumor suppressor PTEN mediates sensing of chemoattractant gradients. *Cell*, 109, 599-610.
- ILIC, D., ALMEIDA, E. A., SCHLAEPFER, D. D., DAZIN, P., AIZAWA, S. & DAMSKY, C. H. 1998. Extracellular matrix survival signals transduced by focal adhesion kinase suppress p53-mediated apoptosis. *J Cell Biol*, 143, 547-60.
- IRANI, C., GONCHAROVA, E. A., HUNTER, D. S., WALKER, C. L., PANETTIERI, R. A. & KRYMSKAYA, V. P. 2002. Phosphatidylinositol 3-kinase but not tuberin is required for PDGF-induced cell migration. *Am J Physiol Lung Cell Mol Physiol*, 282, L854-62.
- IRINTCHEV, A., ZESCHNIGK, M., STARZINSKI-POWITZ, A. & WERNIG, A. 1994. Expression pattern of M-cadherin in normal, denervated, and regenerating mouse muscles. *Dev Dyn*, 199, 326-37.

- JASPER, H., BENES, V., SCHWAGER, C., SAUER, S., CLAUDER-MUNSTER, S., ANSORGE, W. & BOHMANN, D. 2001. The genomic response of the Drosophila embryo to JNK signaling. *Dev Cell*, 1, 579-86.
- JEJURIKAR, S. S. & KUZON, W. M., JR. 2003. Satellite cell depletion in degenerative skeletal muscle. *Apoptosis*, 8, 573-8.
- JENNISCHE, E., EKBERG, S. & MATEJKA, G. L. 1993. Expression of hepatocyte growth factor in growing and regenerating rat skeletal muscle. *Am J Physiol*, 265, C122-8.
- JO, M., THOMAS, K. S., SOMLYO, A. V., SOMLYO, A. P. & GONIAS, S. L. 2002. Cooperativity between the Ras-ERK and Rho-Rho kinase pathways in urokinase-type plasminogen activator-stimulated cell migration. *J Biol Chem*, 277, 12479-85.
- JOHNSON, G. L. & LAPADAT, R. 2002. Mitogen-activated protein kinase pathways mediated by ERK, JNK, and p38 protein kinases. *Science*, 298, 1911-2.
- JONES, M. C., CASWELL, P. T. & NORMAN, J. C. 2006. Endocytic recycling pathways: emerging regulators of cell migration. *Curr Opin Cell Biol*, 18, 549-57.
- JONES, N. C., FEDOROV, Y. V., ROSENTHAL, R. S. & OLWIN, B. B. 2001. ERK1/2 is required for myoblast proliferation but is dispensable for muscle gene expression and cell fusion. *J Cell Physiol*, 186, 104-15.
- JUMP, S. S., CHILDS, T. E., ZWETSLOOT, K. A., BOOTH, F. W. & LEES, S. J. 2009. Fibroblast growth factor 2-stimulated proliferation is lower in muscle precursor cells from old rats. *Exp Physiol*, 94, 739-48.
- KABLAR, B., KRASTEL, K., YING, C., ASAKURA, A., TAPSCOTT, S. J. & RUDNICKI, M. A. 1997. MyoD and Myf-5 differentially regulate the development of limb versus trunk skeletal muscle. *Development*, 124, 4729-38.
- KADI, F., ERIKSSON, A., HOLMNER, S., BUTLER-BROWNE, G. S. & THORNELL, L. E. 1999. Cellular adaptation of the trapezius muscle in strength-trained athletes. *Histochem Cell Biol*, 111, 189-95.
- KALIMAN, P., VINALS, F., TESTAR, X., PALACIN, M. & ZORZANO, A. 1996. Phosphatidylinositol 3-kinase inhibitors block differentiation of skeletal muscle cells. *J Biol Chem*, 271, 19146-51.
- KANDEL, E. S. & HAY, N. 1999. The regulation and activities of the multifunctional serine/threonine kinase Akt/PKB. *Exp Cell Res*, 253, 210-29.
- KARALAKI, M., FILI, S., PHILIPPOU, A. & KOUTSILIERIS, M. 2009. Muscle regeneration: cellular and molecular events. *In Vivo*, 23, 779-96.
- KASTNER, S., ELIAS, M. C., RIVERA, A. J. & YABLONKA-REUVENI, Z. 2000. Gene expression patterns of the fibroblast growth factors and their receptors during myogenesis of rat satellite cells. *J Histochem Cytochem*, 48, 1079-96.
- KAUFMANN, U., MARTIN, B., LINK, D., WITT, K., ZEITLER, R., REINHARD, S. & STARZINSKI-POWITZ, A. 1999. M-cadherin and its sisters in development of striated muscle. *Cell Tissue Res*, 296, 191-8.

- KAUNAS, R., NGUYEN, P., USAMI, S. & CHIEN, S. 2005. Cooperative effects of Rho and mechanical stretch on stress fiber organization. *Proc Natl Acad Sci U S A*, 102, 15895-900.
- KAWAMURA, K., TAKANO, K., SUETSUGU, S., KURISU, S., YAMAZAKI, D., MIKI, H., TAKENAWA, T. & ENDO, T. 2004. N-WASP and WAVE2 acting downstream of phosphatidylinositol 3-kinase are required for myogenic cell migration induced by hepatocyte growth factor. *J Biol Chem*, 279, 54862-71.
- KAWANO, Y., FUKATA, Y., OSHIRO, N., AMANO, M., NAKAMURA, T., ITO, M., MATSUMURA, F., INAGAKI, M. & KAIBUCHI, K. 1999. Phosphorylation of myosin-binding subunit (MBS) of myosin phosphatase by Rho-kinase in vivo. *J Cell Biol*, 147, 1023-38.
- KELLER, C., KELLER, P., MARSHAL, S. & PEDERSEN, B. K. 2003a. IL-6 gene expression in human adipose tissue in response to exercise--effect of carbohydrate ingestion. *J Physiol*, 550, 927-31.
- KELLER, P., KELLER, C., CAREY, A. L., JAUFFRED, S., FISCHER, C. P., STEENBERG, A. & PEDERSEN, B. K. 2003b. Interleukin-6 production by contracting human skeletal muscle: autocrine regulation by IL-6. *Biochem Biophys Res Commun*, 310, 550-4.
- KERKHOFF, E. 2010. Actin dynamics at intracellular membranes: The Spir/formin nucleator complex. *Eur J Cell Biol*.
- KERKHOFF, E., SIMPSON, J. C., LEBERFINGER, C. B., OTTO, I. M., DOERKS, T., BORK, P., RAPP, U. R., RAABE, T. & PEPPERKOK, R. 2001. The Spir actin organizers are involved in vesicle transport processes. *Curr Biol*, 11, 1963-8.
- KIM, D., KIM, S., KOH, H., YOON, S. O., CHUNG, A. S., CHO, K. S. & CHUNG, J. 2001. Akt/PKB promotes cancer cell invasion via increased motility and metalloproteinase production. *FASEB J*, 15, 1953-62.
- KIM, M. J., FROEHNER, S. C., ADAMS, M. E. & KIM, H. S. 2011. alpha-Syntrophin is required for the hepatocyte growth factor-induced migration of cultured myoblasts. *Exp Cell Res*, 317, 2914-24.
- KIM, S., SHILAGARDI, K., ZHANG, S., HONG, S. N., SENS, K. L., BO, J., GONZALEZ, G. A. & CHEN, E. H. 2007. A critical function for the actin cytoskeleton in targeted exocytosis of pre-fusion vesicles during myoblast fusion. *Dev Cell*, 12, 571-86.
- KIMURA, K., TERANISHI, S., YAMAUCHI, J. & NISHIDA, T. 2008. Role of JNK-dependent serine phosphorylation of paxillin in migration of corneal epithelial cells during wound closure. *Invest Ophthalmol Vis Sci*, 49, 125-32.
- KONING, M., HARMSSEN, M. C., VAN LUYN, M. J. & WERKER, P. M. 2009. Current opportunities and challenges in skeletal muscle tissue engineering. *J Tissue Eng Regen Med*, 3, 407-15.
- KRAYNOV, V. S., CHAMBERLAIN, C., BOKOCH, G. M., SCHWARTZ, M. A., SLABAUGH, S. & HAHN, K. M. 2000. Localized Rac activation dynamics visualized in living cells. *Science*, 290, 333-7.
- KRISHAN, K. & DHOOT, G. K. 1996. Changes in some troponin and insulin-like growth factor messenger ribonucleic acids in regenerating and denervated skeletal muscles. *J Muscle Res Cell Motil*, 17, 513-21.

- KUANG, S., GILLESPIE, M. A. & RUDNICKI, M. A. 2008. Niche regulation of muscle satellite cell self-renewal and differentiation. *Cell Stem Cell*, 2, 22-31.
- KUANG, S., KURODA, K., LE GRAND, F. & RUDNICKI, M. A. 2007. Asymmetric self-renewal and commitment of satellite stem cells in muscle. *Cell*, 129, 999-1010.
- KUREK, J., BOWER, J., ROMANELLA, M. & AUSTIN, L. 1996a. Leukaemia inhibitory factor treatment stimulates muscle regeneration in the mdx mouse. *Neurosci Lett*, 212, 167-70.
- KUREK, J. B., BOWER, J. J., ROMANELLA, M., KOENTGEN, F., MURPHY, M. & AUSTIN, L. 1997. The role of leukemia inhibitory factor in skeletal muscle regeneration. *Muscle Nerve*, 20, 815-22.
- KUREK, J. B., NOURI, S., KANNOURAKIS, G., MURPHY, M. & AUSTIN, L. 1996b. Leukemia inhibitory factor and interleukin-6 are produced by diseased and regenerating skeletal muscle. *Muscle Nerve*, 19, 1291-301.
- KURENOVA, E., XU, L. H., YANG, X., BALDWIN, A. S., JR., CRAVEN, R. J., HANKS, S. K., LIU, Z. G. & CANCE, W. G. 2004. Focal adhesion kinase suppresses apoptosis by binding to the death domain of receptor-interacting protein. *Mol Cell Biol*, 24, 4361-71.
- KUSCH, A., TKACHUK, S., HALLER, H., DIETZ, R., GULBA, D. C., LIPP, M. & DUMLER, I. 2000. Urokinase stimulates human vascular smooth muscle cell migration via a phosphatidylinositol 3-kinase-Tyk2 interaction. *J Biol Chem*, 275, 39466-73.
- KWAK, K. B., CHUNG, S. S., KIM, O. M., KANG, M. S., HA, D. B. & CHUNG, C. H. 1993. Increase in the level of m-calpain correlates with the elevated cleavage of filamin during myogenic differentiation of embryonic muscle cells. *Biochim Biophys Acta*, 1175, 243-9.
- LAFRENIERE, J. F., CARON, M. C., SKUK, D., GOULET, M., CHEIKH, A. R. & TREMBLAY, J. P. 2009. Growth factor coinjection improves the migration potential of monkey myogenic precursors without affecting cell transplantation success. *Cell Transplant*, 18, 719-30.
- LAFRENIERE, J. F., MILLS, P., BOUCHENTOUF, M. & TREMBLAY, J. P. 2006. Interleukin-4 improves the migration of human myogenic precursor cells in vitro and in vivo. *Exp Cell Res*, 312, 1127-41.
- LAFRENIERE, J. F., MILLS, P., TREMBLAY, J. P. & EL FAHIME, E. 2004. Growth factors improve the in vivo migration of human skeletal myoblasts by modulating their endogenous proteolytic activity. *Transplantation*, 77, 1741-7.
- LAFYATIS, R., LECHLEIDER, R., ROBERTS, A. B. & SPORN, M. B. 1991. Secretion and transcriptional regulation of transforming growth factor-beta 3 during myogenesis. *Mol Cell Biol*, 11, 3795-803.
- LAI, C. F., CHAUDHARY, L., FAUSTO, A., HALSTEAD, L. R., ORY, D. S., AVIOLI, L. V. & CHENG, S. L. 2001. Erk is essential for growth, differentiation, integrin expression, and cell function in human osteoblastic cells. *J Biol Chem*, 276, 14443-50.
- LAI, J. P., DALTON, J. T. & KNOELL, D. L. 2007. Phosphatase and tensin homologue deleted on chromosome ten (PTEN) as a molecular target in lung epithelial wound repair. *Br J Pharmacol*, 152, 1172-84.

- LAI, K. M., GONZALEZ, M., POUYMIROU, W. T., KLINE, W. O., NA, E., ZLOTCHENKO, E., STITT, T. N., ECONOMIDES, A. N., YANCOPOULOS, G. D. & GLASS, D. J. 2004. Conditional activation of akt in adult skeletal muscle induces rapid hypertrophy. *Mol Cell Biol*, 24, 9295-304.
- LAUFFENBURGER, D. A. & HORWITZ, A. F. 1996. Cell migration: a physically integrated molecular process. *Cell*, 84, 359-69.
- LE GRAND, F., JONES, A. E., SEALE, V., SCIME, A. & RUDNICKI, M. A. 2009. Wnt7a activates the planar cell polarity pathway to drive the symmetric expansion of satellite stem cells. *Cell Stem Cell*, 4, 535-47.
- LEADER, B., LIM, H., CARABATSOS, M. J., HARRINGTON, A., ECSEDY, J., PELLMAN, D., MAAS, R. & LEDER, P. 2002. Formin-2, polyploidy, hypofertility and positioning of the meiotic spindle in mouse oocytes. *Nat Cell Biol*, 4, 921-8.
- LEES, S. J., ZWETSLOOT, K. A. & BOOTH, F. W. 2009. Muscle precursor cells isolated from aged rats exhibit an increased tumor necrosis factor- alpha response. *Aging Cell*, 8, 26-35.
- LEFAUCHEUR, J. P. & SEBILLE, A. 1995. Muscle regeneration following injury can be modified in vivo by immune neutralization of basic fibroblast growth factor, transforming growth factor beta 1 or insulin-like growth factor I. *J Neuroimmunol*, 57, 85-91.
- LELOUP, L., DAURY, L., MAZERES, G., COTTIN, P. & BRUSTIS, J. J. 2007. Involvement of the ERK/MAP kinase signalling pathway in milli-calpain activation and myogenic cell migration. *Int J Biochem Cell Biol*, 39, 1177-89.
- LELOUP, L., MAZERES, G., DAURY, L., COTTIN, P. & BRUSTIS, J. J. 2006. Involvement of calpains in growth factor-mediated migration. *Int J Biochem Cell Biol*, 38, 2049-63.
- LEPPER, C., CONWAY, S. J. & FAN, C. M. 2009. Adult satellite cells and embryonic muscle progenitors have distinct genetic requirements. *Nature*, 460, 627-31.
- LESCAUDRON, L., PELTEKIAN, E., FONTAINE-PERUS, J., PAULIN, D., ZAMPIERI, M., GARCIA, L. & PARRISH, E. 1999. Blood borne macrophages are essential for the triggering of muscle regeneration following muscle transplant. *Neuromuscul Disord*, 9, 72-80.
- LESLIE, N. R., YANG, X., DOWNES, C. P. & WEIJER, C. J. 2005. The regulation of cell migration by PTEN. *Biochem Soc Trans*, 33, 1507-8.
- LESLIE, N. R., YANG, X., DOWNES, C. P. & WEIJER, C. J. 2007. PtdIns(3,4,5)P(3)-dependent and -independent roles for PTEN in the control of cell migration. *Curr Biol*, 17, 115-25.
- LEVINOVITZ, A., JENNISCHE, E., OLDFORS, A., EDWALL, D. & NORSTEDT, G. 1992. Activation of insulin-like growth factor II expression during skeletal muscle regeneration in the rat: correlation with myotube formation. *Mol Endocrinol*, 6, 1227-34.
- LI, P., AKIMOTO, T., ZHANG, M., WILLIAMS, R. S. & YAN, Z. 2006. Resident stem cells are not required for exercise-induced fiber-type switching and angiogenesis but are necessary for activity-dependent muscle growth. *Am J Physiol Cell Physiol*, 290, C1461-8.

- LI, Y., JIANG, B., ENSIGN, W. Y., VOGT, P. K. & HAN, J. 2000. Myogenic differentiation requires signalling through both phosphatidylinositol 3-kinase and p38 MAP kinase. *Cell Signal*, 12, 751-7.
- LILIENTAL, J., MOON, S. Y., LESCHE, R., MAMILLAPALLI, R., LI, D., ZHENG, Y., SUN, H. & WU, H. 2000. Genetic deletion of the Pten tumor suppressor gene promotes cell motility by activation of Rac1 and Cdc42 GTPases. *Curr Biol*, 10, 401-4.
- LIND, C. R., GRAY, C. W., PEARSON, A. G., CAMERON, R. E., O'CARROLL, S. J., NARAYAN, P. J., LIM, J. & DRAGUNOW, M. 2006. The mitogen-activated/extracellular signal-regulated kinase kinase 1/2 inhibitor U0126 induces glial fibrillary acidic protein expression and reduces the proliferation and migration of C6 glioma cells. *Neuroscience*, 141, 1925-33.
- LIU, J. & LIN, A. 2005. Role of JNK activation in apoptosis: a double-edged sword. *Cell Res*, 15, 36-42.
- LIU, S., XU, S. W., KENNEDY, L., PALA, D., CHEN, Y., EASTWOOD, M., CARTER, D. E., BLACK, C. M., ABRAHAM, D. J. & LEASK, A. 2007. FAK is required for TGFbeta-induced JNK phosphorylation in fibroblasts: implications for acquisition of a matrix-remodeling phenotype. *Mol Biol Cell*, 18, 2169-78.
- LO, S. H., WEISBERG, E. & CHEN, L. B. 1994. Tensin: a potential link between the cytoskeleton and signal transduction. *Bioessays*, 16, 817-23.
- LOUIS, M., ZANOUE, N., VAN SCHOOR, M. & GAILLY, P. 2008. TRPC1 regulates skeletal myoblast migration and differentiation. *J Cell Sci*, 121, 3951-9.
- LU, Q. L., MANN, C. J., LOU, F., BOU-GHARIOS, G., MORRIS, G. E., XUE, S. A., FLETCHER, S., PARTRIDGE, T. A. & WILTON, S. D. 2003. Functional amounts of dystrophin produced by skipping the mutated exon in the mdx dystrophic mouse. *Nat Med*, 9, 1009-14.
- LUND, T. C., GRANGE, R. W. & LOWE, D. A. 2007. Telomere shortening in diaphragm and tibialis anterior muscles of aged mdx mice. *Muscle Nerve*, 36, 387-90.
- MAEKAWA, M., ISHIZAKI, T., BOKU, S., WATANABE, N., FUJITA, A., IWAMATSU, A., OBINATA, T., OHASHI, K., MIZUNO, K. & NARUMIYA, S. 1999. Signaling from Rho to the actin cytoskeleton through protein kinases ROCK and LIM-kinase. *Science*, 285, 895-8.
- MAIER, D., JONES, G., LI, X., SCHONTHAL, A. H., GRATZL, O., VAN MEIR, E. G. & MERLO, A. 1999. The PTEN lipid phosphatase domain is not required to inhibit invasion of glioma cells. *Cancer Res*, 59, 5479-82.
- MAKARENKOVA, H. P., GONZALEZ, K. N., KIOSSES, W. B. & MEECH, R. 2009. Barx2 controls myoblast fusion and promotes MyoD-mediated activation of the smooth muscle alpha-actin gene. *J Biol Chem*, 284, 14866-74.
- MANN, C. J., PERDIGUERO, E., KHARRAZ, Y., AGUILAR, S., PESSINA, P., SERRANO, A. L. & MUNOZ-CANOVES, P. 2011. Aberrant repair and fibrosis development in skeletal muscle. *Skelet Muscle*, 1, 21.

- MANSOURI, A., STOYKOVA, A., TORRES, M. & GRUSS, P. 1996. Dysgenesis of cephalic neural crest derivatives in Pax7^{-/-} mutant mice. *Development*, 122, 831-8.
- MAROTO, M., RESHEF, R., MUNSTERBERG, A. E., KOESTER, S., GOULDING, M. & LASSAR, A. B. 1997. Ectopic Pax-3 activates MyoD and Myf-5 expression in embryonic mesoderm and neural tissue. *Cell*, 89, 139-48.
- MASSIMINO, M. L., RAPIZZI, E., CANTINI, M., LIBERA, L. D., MAZZOLENI, F., ARSLAN, P. & CARRARO, U. 1997. ED2⁺ macrophages increase selectively myoblast proliferation in muscle cultures. *Biochem Biophys Res Commun*, 235, 754-9.
- MATSUI, T., NAGOSHI, T. & ROSENZWEIG, A. 2003. Akt and PI 3-kinase signaling in cardiomyocyte hypertrophy and survival. *Cell Cycle*, 2, 220-3.
- MAURO, A. 1961. Satellite cell of skeletal muscle fibers. *J Biophys Biochem Cytol*, 9, 493-5.
- MCFARLAND, D. C., PESALL, J. E. & GILKERSON, K. K. 1993. The influence of growth factors on turkey embryonic myoblasts and satellite cells in vitro. *Gen Comp Endocrinol*, 89, 415-24.
- MCLENNAN, I. S. & KOISHI, K. 2002. The transforming growth factor-betas: multifaceted regulators of the development and maintenance of skeletal muscles, motoneurons and Schwann cells. *Int J Dev Biol*, 46, 559-67.
- MEJILLANO, M. R., KOJIMA, S., APPLEWHITE, D. A., GERTLER, F. B., SVITKINA, T. M. & BORISY, G. G. 2004. Lamellipodial versus filopodial mode of the actin nanomachinery: pivotal role of the filament barbed end. *Cell*, 118, 363-73.
- MENDELL, J. R., KISSEL, J. T., AMATO, A. A., KING, W., SIGNORE, L., PRIOR, T. W., SAHENK, Z., BENSON, S., MCANDREW, P. E., RICE, R. & ET AL. 1995. Myoblast transfer in the treatment of Duchenne's muscular dystrophy. *N Engl J Med*, 333, 832-8.
- MENETREY, J., KASEMKIJWATTANA, C., FU, F. H., MORELAND, M. S. & HUARD, J. 1999. Suturing versus immobilization of a muscle laceration. A morphological and functional study in a mouse model. *Am J Sports Med*, 27, 222-9.
- MENNERICH, D., SCHAFER, K. & BRAUN, T. 1998. Pax-3 is necessary but not sufficient for lbx1 expression in myogenic precursor cells of the limb. *Mech Dev*, 73, 147-58.
- MERLOT, S. & FIRTEL, R. A. 2003. Leading the way: Directional sensing through phosphatidylinositol 3-kinase and other signaling pathways. *J Cell Sci*, 116, 3471-8.
- MERLY, F., LESCAUDRON, L., ROUAUD, T., CROSSIN, F. & GARDAHAUT, M. F. 1999. Macrophages enhance muscle satellite cell proliferation and delay their differentiation. *Muscle Nerve*, 22, 724-32.
- MESSINA, G. & COSSU, G. 2009. The origin of embryonic and fetal myoblasts: a role of Pax3 and Pax7. *Genes Dev*, 23, 902-5.
- MEZZOGIORNO, A., COLETTA, M., ZANI, B. M., COSSU, G. & MOLINARO, M. 1993. Paracrine stimulation of senescent satellite cell proliferation by factors released by muscle or myotubes from young mice. *Mech Ageing Dev*, 70, 35-44.

- MICHAEL, K. E., DUMBAULD, D. W., BURNS, K. L., HANKS, S. K. & GARCIA, A. J. 2009. Focal adhesion kinase modulates cell adhesion strengthening via integrin activation. *Mol Biol Cell*, 20, 2508-19.
- MIHAI, C., BAO, S., LAI, J. P., GHADIALI, S. N. & KNOELL, D. L. 2012. PTEN inhibition improves wound healing in lung epithelia through changes in cellular mechanics that enhance migration. *Am J Physiol Lung Cell Mol Physiol*, 302, L287-99.
- MILLER, J. B., SCHAEFER, L. & DOMINOV, J. A. 1999. Seeking muscle stem cells. *Curr Top Dev Biol*, 43, 191-219.
- MILLER, K. J., THALLOOR, D., MATTESON, S. & PAVLATH, G. K. 2000. Hepatocyte growth factor affects satellite cell activation and differentiation in regenerating skeletal muscle. *Am J Physiol Cell Physiol*, 278, C174-81.
- MOENS, P. D., VAN-SCHOOR, M. C. & MARECHAL, G. 1996. Lack of myoblasts migration between transplanted and host muscles of mdx and normal mice. *J Muscle Res Cell Motil*, 17, 37-43.
- MONACO, A. P., BERTELSON, C. J., LIECHTI-GALLATI, S., MOSER, H. & KUNKEL, L. M. 1988. An explanation for the phenotypic differences between patients bearing partial deletions of the DMD locus. *Genomics*, 2, 90-5.
- MOON, S. K., KIM, H. M. & KIM, C. H. 2004. PTEN induces G1 cell cycle arrest and inhibits MMP-9 expression via the regulation of NF-kappaB and AP-1 in vascular smooth muscle cells. *Arch Biochem Biophys*, 421, 267-76.
- MOON, S. Y. & ZHENG, Y. 2003. Rho GTPase-activating proteins in cell regulation. *Trends Cell Biol*, 13, 13-22.
- MOREL, E., PARTON, R. G. & GRUENBERG, J. 2009. Annexin A2-dependent polymerization of actin mediates endosome biogenesis. *Dev Cell*, 16, 445-57.
- MORGAN, J., ROUCHE, A., BAUSERO, P., HOUSSAINI, A., GROSS, J., FISZMAN, M. Y. & ALAMEDDINE, H. S. 2010. MMP-9 overexpression improves myogenic cell migration and engraftment. *Muscle Nerve*, 42, 584-95.
- MORGAN, J. E., HOFFMAN, E. P. & PARTRIDGE, T. A. 1990. Normal myogenic cells from newborn mice restore normal histology to degenerating muscles of the mdx mouse. *J Cell Biol*, 111, 2437-49.
- MORGAN, J. E., PAGEL, C. N., SHERRATT, T. & PARTRIDGE, T. A. 1993. Long-term persistence and migration of myogenic cells injected into pre-irradiated muscles of mdx mice. *J Neurol Sci*, 115, 191-200.
- MORISSETTE, M. R., COOK, S. A., BURANASOMBATI, C., ROSENBERG, M. A. & ROSENZWEIG, A. 2009. Myostatin inhibits IGF-I-induced myotube hypertrophy through Akt. *Am J Physiol Cell Physiol*, 297, C1124-32.
- MUKHERJEE, P., GILDOR, B., SHILO, B. Z., VIJAYRAGHAVAN, K. & SCHEJTER, E. D. 2011. The actin nucleator WASp is required for myoblast fusion during adult *Drosophila* myogenesis. *Development*, 138, 2347-57.
- MUNSTERBERG, A. E. & LASSAR, A. B. 1995. Combinatorial signals from the neural tube, floor plate and notochord induce myogenic bHLH gene expression in the somite. *Development*, 121, 651-60.

- MUNTONI, F., TORELLI, S. & FERLINI, A. 2003. Dystrophin and mutations: one gene, several proteins, multiple phenotypes. *Lancet Neurol*, 2, 731-40.
- MUSARO, A., MCCULLAGH, K., PAUL, A., HOUGHTON, L., DOBROWOLNY, G., MOLINARO, M., BARTON, E. R., SWEENEY, H. L. & ROSENTHAL, N. 2001. Localized Igf-1 transgene expression sustains hypertrophy and regeneration in senescent skeletal muscle. *Nat Genet*, 27, 195-200.
- MUSARO, A., MCCULLAGH, K. J., NAYA, F. J., OLSON, E. N. & ROSENTHAL, N. 1999. IGF-1 induces skeletal myocyte hypertrophy through calcineurin in association with GATA-2 and NF-ATc1. *Nature*, 400, 581-5.
- MUSARO, A. & ROSENTHAL, N. 1999. Maturation of the myogenic program is induced by postmitotic expression of insulin-like growth factor I. *Mol Cell Biol*, 19, 3115-24.
- MUSARO, A. & ROSENTHAL, N. 2006. The Critical Role of Insulin-Like Growth Factor-1 Isoforms in the Physiopathology of Skeletal Muscle. *Current Genomics*, 7, 19-32.
- NAGASE, H. & WOESSNER, J. F., JR. 1999. Matrix metalloproteinases. *J Biol Chem*, 274, 21491-4.
- NAKAGAWA, M., KOYANAGI, M., TANABE, K., TAKAHASHI, K., ICHISAKA, T., AOI, T., OKITA, K., MOCHIDUKI, Y., TAKIZAWA, N. & YAMANAKA, S. 2008. Generation of induced pluripotent stem cells without Myc from mouse and human fibroblasts. *Nat Biotechnol*, 26, 101-6.
- NAKASHIMA, K., YAMAZAKI, M. & ABE, H. 2005. Effects of serum deprivation on expression of proteolytic-related genes in chick myotube cultures. *Biosci Biotechnol Biochem*, 69, 623-7.
- NEDACHI, T., HATAKEYAMA, H., KONO, T., SATO, M. & KANZAKI, M. 2009. Characterization of contraction-inducible CXC chemokines and their roles in C2C12 myocytes. *Am J Physiol Endocrinol Metab*, 297, E866-78.
- NGUYEN, D. H., CATLING, A. D., WEBB, D. J., SANKOVIC, M., WALKER, L. A., SOMLYO, A. V., WEBER, M. J. & GONIAS, S. L. 1999. Myosin light chain kinase functions downstream of Ras/ERK to promote migration of urokinase-type plasminogen activator-stimulated cells in an integrin-selective manner. *J Cell Biol*, 146, 149-64.
- NICHOLSON, G. A., GARDNER-MEDWIN, D., PENNINGTON, R. J. & WALTON, J. N. 1979. Carrier detection in Duchenne muscular dystrophy: Assessment of the effect of age on detection-rate with serum-creatine-kinase-activity. *Lancet*, 1, 692-4.
- NISHIMURA, T., NAKAMURA, K., KISHIOKA, Y., KATO-MORI, Y., WAKAMATSU, J. & HATTORI, A. 2008. Inhibition of matrix metalloproteinases suppresses the migration of skeletal muscle cells. *J Muscle Res Cell Motil*, 29, 37-44.
- NOBES, C. D. & HALL, A. 1995. Rho, rac, and cdc42 GTPases regulate the assembly of multimolecular focal complexes associated with actin stress fibers, lamellipodia, and filopodia. *Cell*, 81, 53-62.
- NOBES, C. D. & HALL, A. 1999. Rho GTPases control polarity, protrusion, and adhesion during cell movement. *J Cell Biol*, 144, 1235-44.

- NOWAK, K. J. & DAVIES, K. E. 2004. Duchenne muscular dystrophy and dystrophin: pathogenesis and opportunities for treatment. *EMBO Rep*, 5, 872-6.
- O'CONNOR, M. S., CARLSON, M. E. & CONBOY, I. M. 2009. Differentiation rather than aging of muscle stem cells abolishes their telomerase activity. *Biotechnol Prog*, 25, 1130-7.
- OBERC, M. A. & ENGEL, W. K. 1977. Ultrastructural localization of calcium in normal and abnormal skeletal muscle. *Lab Invest*, 36, 566-77.
- OBERMEIER, A., AHMED, S., MANSER, E., YEN, S. C., HALL, C. & LIM, L. 1998. PAK promotes morphological changes by acting upstream of Rac. *EMBO J*, 17, 4328-39.
- OKUMURA, K., ZHAO, M., DEPINHO, R. A., FURNARI, F. B. & CAVENEE, W. K. 2005. Cellular transformation by the MSP58 oncogene is inhibited by its physical interaction with the PTEN tumor suppressor. *Proc Natl Acad Sci U S A*, 102, 2703-6.
- OLGUIN, H. C., SANTANDER, C. & BRANDAN, E. 2003. Inhibition of myoblast migration via decorin expression is critical for normal skeletal muscle differentiation. *Dev Biol*, 259, 209-24.
- ONTELL, M. & KOZEKA, K. 1984. The organogenesis of murine striated muscle: a cytoarchitectural study. *Am J Anat*, 171, 133-48.
- OTTO, A., COLLINS-HOOPER, H. & PATEL, K. 2009. The origin, molecular regulation and therapeutic potential of myogenic stem cell populations. *J Anat*, 215, 477-97.
- OUSTANINA, S., HAUSE, G. & BRAUN, T. 2004. Pax7 directs postnatal renewal and propagation of myogenic satellite cells but not their specification. *EMBO J*, 23, 3430-9.
- PALECEK, S. P., HUTTENLOCHER, A., HORWITZ, A. F. & LAUFFENBURGER, D. A. 1998. Physical and biochemical regulation of integrin release during rear detachment of migrating cells. *J Cell Sci*, 111 (Pt 7), 929-40.
- PALMIERI, B. & TREMBLAY, J. P. 2010. Myoblast transplantation: a possible surgical treatment for a severe pediatric disease. *Surg Today*, 40, 902-8.
- PALMIERI, B., TREMBLAY, J. P. & DANIELE, L. 2010. Past, present and future of myoblast transplantation in the treatment of Duchenne muscular dystrophy. *Pediatr Transplant*, 14, 813-9.
- PARSONS, J. T., HORWITZ, A. R. & SCHWARTZ, M. A. 2010. Cell adhesion: integrating cytoskeletal dynamics and cellular tension. *Nat Rev Mol Cell Biol*, 11, 633-43.
- PARSONS, J. T., MARTIN, K. H., SLACK, J. K., TAYLOR, J. M. & WEED, S. A. 2000. Focal adhesion kinase: a regulator of focal adhesion dynamics and cell movement. *Oncogene*, 19, 5606-13.
- PARTRIDGE, T. A., MORGAN, J. E., COULTON, G. R., HOFFMAN, E. P. & KUNKEL, L. M. 1989. Conversion of mdx myofibres from dystrophin-negative to -positive by injection of normal myoblasts. *Nature*, 337, 176-9.
- PEARSON, G., ROBINSON, F., BEERS GIBSON, T., XU, B. E., KARANDIKAR, M., BERMAN, K. & COBB, M. H. 2001. Mitogen-activated protein (MAP) kinase pathways: regulation and physiological functions. *Endocr Rev*, 22, 153-83.

- PEAULT, B., RUDNICKI, M., TORRENTE, Y., COSSU, G., TREMBLAY, J. P., PARTRIDGE, T., GUSSONI, E., KUNKEL, L. M. & HUARD, J. 2007. Stem and progenitor cells in skeletal muscle development, maintenance, and therapy. *Mol Ther*, 15, 867-77.
- PECHLIVANIS, M., SAMOL, A. & KERKHOFF, E. 2009. Identification of a short Spir interaction sequence at the C-terminal end of formin subgroup proteins. *J Biol Chem*, 284, 25324-33.
- PELHAM, R. J., JR. & WANG, Y. 1997. Cell locomotion and focal adhesions are regulated by substrate flexibility. *Proc Natl Acad Sci U S A*, 94, 13661-5.
- PELLEGRIN, S. & MELLOR, H. 2007. Actin stress fibres. *J Cell Sci*, 120, 3491-9.
- PELLINEN, T. & IVASKA, J. 2006. Integrin traffic. *J Cell Sci*, 119, 3723-31.
- PELOSI, L., GIACINTI, C., NARDIS, C., BORSELLINO, G., RIZZUTO, E., NICOLETTI, C., WANNENES, F., BATTISTINI, L., ROSENTHAL, N., MOLINARO, M. & MUSARO, A. 2007. Local expression of IGF-1 accelerates muscle regeneration by rapidly modulating inflammatory cytokines and chemokines. *FASEB J*, 21, 1393-402.
- PENNICA, D., SHAW, K. J., SWANSON, T. A., MOORE, M. W., SHELTON, D. L., ZIONCHECK, K. A., ROSENTHAL, A., TAGA, T., PAONI, N. F. & WOOD, W. I. 1995. Cardiotrophin-1. Biological activities and binding to the leukemia inhibitory factor receptor/gp130 signaling complex. *J Biol Chem*, 270, 10915-22.
- PERCY, M. E., CHANG, L. S., MURPHY, E. G., OSS, I., VERELLEN-DUMOULIN, C. & THOMPSON, M. W. 1979. Serum creatine kinase and pyruvate kinase in Duchenne muscular dystrophy carrier detection. *Muscle Nerve*, 2, 329-39.
- PETERSON, J. M. & PIZZA, F. X. 2009. Cytokines derived from cultured skeletal muscle cells after mechanical strain promote neutrophil chemotaxis in vitro. *J Appl Physiol*, 106, 130-7.
- PETROF, B. J. 2002. Molecular pathophysiology of myofiber injury in deficiencies of the dystrophin-glycoprotein complex. *Am J Phys Med Rehabil*, 81, S162-74.
- PHILLIPS, G. D., HOFFMAN, J. R. & KNIGHTON, D. R. 1990. Migration of myogenic cells in the rat extensor digitorum longus muscle studied with a split autograft model. *Cell Tissue Res*, 262, 81-8.
- PLANCHON, S. M., WAITE, K. A. & ENG, C. 2008. The nuclear affairs of PTEN. *J Cell Sci*, 121, 249-53.
- POLLITT, A. Y. & INSALL, R. H. 2009. WASP and SCAR/WAVE proteins: the drivers of actin assembly. *J Cell Sci*, 122, 2575-8.
- PORTER, J. D., GUO, W., MERRIAM, A. P., KHANNA, S., CHENG, G., ZHOU, X., ANDRADE, F. H., RICHMONDS, C. & KAMINSKI, H. J. 2003. Persistent over-expression of specific CC class chemokines correlates with macrophage and T-cell recruitment in mdx skeletal muscle. *Neuromuscul Disord*, 13, 223-35.
- PRYKHOZHIIJ, S. V. & NEUMANN, C. J. 2008. Distinct roles of Shh and Fgf signaling in regulating cell proliferation during zebrafish pectoral fin development. *BMC Dev Biol*, 8, 91.
- QUACH, N. L., BIRESSI, S., REICHARDT, L. F., KELLER, C. & RANDO, T. A. 2009. Focal adhesion kinase signaling regulates the expression of caveolin 3 and beta1 integrin, genes essential for normal myoblast fusion. *Mol Biol Cell*, 20, 3422-35.

- QUATTROCELLI, M., CASSANO, M., CRIPPA, S., PERINI, I. & SAMPAOLESI, M. 2010. Cell therapy strategies and improvements for muscular dystrophy. *Cell Death Differ*, 17, 1222-9.
- QUINLAN, J. G., LYDEN, S. P., CAMBIER, D. M., JOHNSON, S. R., MICHAELS, S. E. & DENMAN, D. L. 1995. Radiation inhibition of mdx mouse muscle regeneration: dose and age factors. *Muscle Nerve*, 18, 201-6.
- QUINLAN, M. E., HEUSER, J. E., KERKHOFF, E. & MULLINS, R. D. 2005. Drosophila Spire is an actin nucleation factor. *Nature*, 433, 382-8.
- QUINLAN, M. E., HILGERT, S., BEDROSSIAN, A., MULLINS, R. D. & KERKHOFF, E. 2007. Regulatory interactions between two actin nucleators, Spire and Cappuccino. *J Cell Biol*, 179, 117-28.
- RAFTOPOULOU, M., ETIENNE-MANNEVILLE, S., SELF, A., NICHOLLS, S. & HALL, A. 2004. Regulation of cell migration by the C2 domain of the tumor suppressor PTEN. *Science*, 303, 1179-81.
- RAFTOPOULOU, M. & HALL, A. 2004. Cell migration: Rho GTPases lead the way. *Dev Biol*, 265, 23-32.
- RANZATO, E., BALBO, V., BOCCAFOSCHI, F., MAZZUCCO, L. & BURLANDO, B. 2009. Scratch wound closure of C2C12 mouse myoblasts is enhanced by human platelet lysate. *Cell Biol Int*, 33, 911-7.
- REGEN, C. M. & HORWITZ, A. F. 1992. Dynamics of beta 1 integrin-mediated adhesive contacts in motile fibroblasts. *J Cell Biol*, 119, 1347-59.
- REIF, K., NOBES, C. D., THOMAS, G., HALL, A. & CANTRELL, D. A. 1996. Phosphatidylinositol 3-kinase signals activate a selective subset of Rac/Rho-dependent effector pathways. *Curr Biol*, 6, 1445-55.
- RELAIX, F., MONTARRAS, D., ZAFFRAN, S., GAYRAUD-MOREL, B., ROCANCOURT, D., TAJBAKSH, S., MANSOURI, A., CUMANO, A. & BUCKINGHAM, M. 2006. Pax3 and Pax7 have distinct and overlapping functions in adult muscle progenitor cells. *J Cell Biol*, 172, 91-102.
- RICHARDSON, B. E., BECKETT, K., NOWAK, S. J. & BAYLIES, M. K. 2007. SCAR/WAVE and Arp2/3 are crucial for cytoskeletal remodeling at the site of myoblast fusion. *Development*, 134, 4357-67.
- RIDLEY, A. J. 2001. Rho GTPases and cell migration. *J Cell Sci*, 114, 2713-22.
- RIVELINE, D., ZAMIR, E., BALABAN, N. Q., SCHWARZ, U. S., ISHIZAKI, T., NARUMIYA, S., KAM, Z., GEIGER, B. & BERSHADSKY, A. D. 2001. Focal contacts as mechanosensors: externally applied local mechanical force induces growth of focal contacts by an mDia1-dependent and ROCK-independent mechanism. *J Cell Biol*, 153, 1175-86.
- ROBERTS, A. B., SPORN, M. B., ASSOIAN, R. K., SMITH, J. M., ROCHE, N. S., WAKEFIELD, L. M., HEINE, U. I., LIOTTA, L. A., FALANGA, V., KEHRL, J. H. & ET AL. 1986. Transforming growth factor type beta: rapid induction of fibrosis and angiogenesis in vivo and stimulation of collagen formation in vitro. *Proc Natl Acad Sci U S A*, 83, 4167-71.

- ROBERTSON, T. A., MALEY, M. A., GROUNDS, M. D. & PAPADIMITRIOU, J. M. 1993. The role of macrophages in skeletal muscle regeneration with particular reference to chemotaxis. *Exp Cell Res*, 207, 321-31.
- ROCHLIN, K., YU, S., ROY, S. & BAYLIES, M. K. 2010. Myoblast fusion: when it takes more to make one. *Dev Biol*, 341, 66-83.
- ROHATGI, R., HO, H. Y. & KIRSCHNER, M. W. 2000. Mechanism of N-WASP activation by CDC42 and phosphatidylinositol 4, 5-bisphosphate. *J Cell Biol*, 150, 1299-310.
- ROHATGI, R., MA, L., MIKI, H., LOPEZ, M., KIRCHHAUSEN, T., TAKENAWA, T. & KIRSCHNER, M. W. 1999. The interaction between N-WASP and the Arp2/3 complex links Cdc42-dependent signals to actin assembly. *Cell*, 97, 221-31.
- ROHATGI, R., NOLLAU, P., HO, H. Y., KIRSCHNER, M. W. & MAYER, B. J. 2001. Nck and phosphatidylinositol 4,5-bisphosphate synergistically activate actin polymerization through the N-WASP-Arp2/3 pathway. *J Biol Chem*, 276, 26448-52.
- ROSENBLATT, J. D. & PARRY, D. J. 1992. Gamma irradiation prevents compensatory hypertrophy of overloaded mouse extensor digitorum longus muscle. *J Appl Physiol*, 73, 2538-43.
- ROSENTHAL, S. M., BROWN, E. J., BRUNETTI, A. & GOLDFINE, I. D. 1991. Fibroblast growth factor inhibits insulin-like growth factor-II (IGF-II) gene expression and increases IGF-I receptor abundance in BC3H-1 muscle cells. *Mol Endocrinol*, 5, 678-84.
- ROSENTHAL, S. M. & CHENG, Z. Q. 1995. Opposing early and late effects of insulin-like growth factor I on differentiation and the cell cycle regulatory retinoblastoma protein in skeletal myoblasts. *Proc Natl Acad Sci U S A*, 92, 10307-11.
- ROYAL, I., LAMARCHE-VANE, N., LAMORTE, L., KAIBUCHI, K. & PARK, M. 2000. Activation of cdc42, rac, PAK, and rho-kinase in response to hepatocyte growth factor differentially regulates epithelial cell colony spreading and dissociation. *Mol Biol Cell*, 11, 1709-25.
- RUDNICKI, M. A., SCHNEGELSBERG, P. N., STEAD, R. H., BRAUN, T., ARNOLD, H. H. & JAENISCH, R. 1993. MyoD or Myf-5 is required for the formation of skeletal muscle. *Cell*, 75, 1351-9.
- SACCO, A., DOYONNAS, R., KRAFT, P., VITOROVIC, S. & BLAU, H. M. 2008. Self-renewal and expansion of single transplanted muscle stem cells. *Nature*, 456, 502-6.
- SACHIDANANDAN, C., SAMBASIVAN, R. & DHAWAN, J. 2002. Tristetraprolin and LPS-inducible CXC chemokine are rapidly induced in presumptive satellite cells in response to skeletal muscle injury. *J Cell Sci*, 115, 2701-12.
- SAIKA, S., OKADA, Y., MIYAMOTO, T., YAMANAKA, O., OHNISHI, Y., OOSHIMA, A., LIU, C. Y., WENG, D. & KAO, W. W. 2004. Role of p38 MAP kinase in regulation of cell migration and proliferation in healing corneal epithelium. *Invest Ophthalmol Vis Sci*, 45, 100-9.
- SAINI, A., AL-SHANTI, N., FAULKNER, S. H. & STEWART, C. E. 2008. Pro- and anti-apoptotic roles for IGF-I in TNF-alpha-induced apoptosis: a MAP kinase mediated mechanism. *Growth Factors*, 26, 239-53.

- SAINI, A., AL-SHANTI, N. & STEWART, C. E. 2006. Waste management - cytokines, growth factors and cachexia. *Cytokine Growth Factor Rev*, 17, 475-86.
- SALERNO, M. S., DYER, K., BRACEGIRDLE, J., PLATT, L., THOMAS, M., SIRIETT, V., KAMBADUR, R. & SHARMA, M. 2009. Akirin1 (Mighty), a novel promyogenic factor regulates muscle regeneration and cell chemotaxis. *Exp Cell Res*, 315, 2012-21.
- SANDER, E. E., VAN DELFT, S., TEN KLOOSTER, J. P., REID, T., VAN DER KAMMEN, R. A., MICHIELS, F. & COLLARD, J. G. 1998. Matrix-dependent Tiam1/Rac signaling in epithelial cells promotes either cell-cell adhesion or cell migration and is regulated by phosphatidylinositol 3-kinase. *J Cell Biol*, 143, 1385-98.
- SATOH, S. & TOMINAGA, T. 2001. mDia-interacting protein acts downstream of Rho-mDia and modifies Src activation and stress fiber formation. *J Biol Chem*, 276, 39290-4.
- SCHAFER, G., WEBER, S., HOLZ, A., BOGDAN, S., SCHUMACHER, S., MULLER, A., RENKAWITZ-POHL, R. & ONEL, S. F. 2007. The Wiskott-Aldrich syndrome protein (WASP) is essential for myoblast fusion in *Drosophila*. *Dev Biol*, 304, 664-74.
- SCHAFER, K. & BRAUN, T. 1999. Early specification of limb muscle precursor cells by the homeobox gene *Lbx1h*. *Nat Genet*, 23, 213-6.
- SCHALLER, M. D. & PARSONS, J. T. 1994. Focal adhesion kinase and associated proteins. *Curr Opin Cell Biol*, 6, 705-10.
- SCHIAFFINO, S. & MAMMUCARI, C. 2011. Regulation of skeletal muscle growth by the IGF1-Akt/PKB pathway: insights from genetic models. *Skelet Muscle*, 1, 4.
- SCHIENDA, J., ENGLEKA, K. A., JUN, S., HANSEN, M. S., EPSTEIN, J. A., TABIN, C. J., KUNKEL, L. M. & KARDON, G. 2006. Somitic origin of limb muscle satellite and side population cells. *Proc Natl Acad Sci U S A*, 103, 945-50.
- SCHLAEPFER, D. D. & MITRA, S. K. 2004. Multiple connections link FAK to cell motility and invasion. *Curr Opin Genet Dev*, 14, 92-101.
- SCHLAEPFER, D. D., MITRA, S. K. & ILIC, D. 2004. Control of motile and invasive cell phenotypes by focal adhesion kinase. *Biochim Biophys Acta*, 1692, 77-102.
- SCHMALBRUCH, H. & LEWIS, D. M. 2000. Dynamics of nuclei of muscle fibers and connective tissue cells in normal and denervated rat muscles. *Muscle Nerve*, 23, 617-26.
- SCHMID, A. C., BYRNE, R. D., VILAR, R. & WOSCHOLSKI, R. 2004. Bisperoxovanadium compounds are potent PTEN inhibitors. *FEBS Lett*, 566, 35-8.
- SCHMIDT, A. & HALL, A. 2002. Guanine nucleotide exchange factors for Rho GTPases: turning on the switch. *Genes Dev*, 16, 1587-609.
- SCHMIDT, C., BLADT, F., GOEDECKE, S., BRINKMANN, V., ZSCHIESCHE, W., SHARPE, M., GHERARDI, E. & BIRCHMEIER, C. 1995. Scatter factor/hepatocyte growth factor is essential for liver development. *Nature*, 373, 699-702.
- SCHUH, M. 2011. An actin-dependent mechanism for long-range vesicle transport. *Nat Cell Biol*, 13, 1431-6.
- SCHULTZ, E. 1996. Satellite cell proliferative compartments in growing skeletal muscles. *Dev Biol*, 175, 84-94.

- SCHULTZ, E., GIBSON, M. C. & CHAMPION, T. 1978. Satellite cells are mitotically quiescent in mature mouse muscle: an EM and radioautographic study. *J Exp Zool*, 206, 451-6.
- SCHULTZ, E., JARYSZAK, D. L., GIBSON, M. C. & ALBRIGHT, D. J. 1986. Absence of exogenous satellite cell contribution to regeneration of frozen skeletal muscle. *J Muscle Res Cell Motil*, 7, 361-7.
- SCHULTZ, E., JARYSZAK, D. L. & VALLIERE, C. R. 1985. Response of satellite cells to focal skeletal muscle injury. *Muscle Nerve*, 8, 217-22.
- SCHULTZ, E. & LIPTON, B. H. 1982. Skeletal muscle satellite cells: changes in proliferation potential as a function of age. *Mech Ageing Dev*, 20, 377-83.
- SCHULTZ, E. & MCCORMICK, K. M. 1994. Skeletal muscle satellite cells. *Rev Physiol Biochem Pharmacol*, 123, 213-57.
- SCHUMACHER, N., BORAWSKI, J. M., LEBERFINGER, C. B., GESSLER, M. & KERKHOFF, E. 2004. Overlapping expression pattern of the actin organizers Spir-1 and formin-2 in the developing mouse nervous system and the adult brain. *Gene Expr Patterns*, 4, 249-55.
- SCHWARTZ, M. A. & HORWITZ, A. R. 2006. Integrating adhesion, protrusion, and contraction during cell migration. *Cell*, 125, 1223-5.
- SCICCHITANO, B. M., RIZZUTO, E. & MUSARO, A. 2009. Counteracting muscle wasting in aging and neuromuscular diseases: the critical role of IGF-1. *Aging (Albany NY)*, 1, 451-7.
- SEALE, P., SABOURIN, L. A., GIRGIS-GABARDO, A., MANSOURI, A., GRUSS, P. & RUDNICKI, M. A. 2000. Pax7 is required for the specification of myogenic satellite cells. *Cell*, 102, 777-86.
- SEGER, R. & KREBS, E. G. 1995. The MAPK signaling cascade. *FASEB J*, 9, 726-35.
- SEMSARIAN, C., SUTRAVE, P., RICHMOND, D. R. & GRAHAM, R. M. 1999. Insulin-like growth factor (IGF-I) induces myotube hypertrophy associated with an increase in anaerobic glycolysis in a clonal skeletal-muscle cell model. *Biochem J*, 339 (Pt 2), 443-51.
- SEPP, K. J. & AULD, V. J. 2003. RhoA and Rac1 GTPases mediate the dynamic rearrangement of actin in peripheral glia. *Development*, 130, 1825-35.
- SERVANT, G., WEINER, O. D., HERZMARK, P., BALLA, T., SEDAT, J. W. & BOURNE, H. R. 2000. Polarization of chemoattractant receptor signaling during neutrophil chemotaxis. *Science*, 287, 1037-40.
- SHARMA, G. D., HE, J. & BAZAN, H. E. 2003. p38 and ERK1/2 coordinate cellular migration and proliferation in epithelial wound healing: evidence of cross-talk activation between MAP kinase cascades. *J Biol Chem*, 278, 21989-97.
- SHARPLES, A. P., AL-SHANTI, N., LEWIS, M. P. & STEWART, C. E. 2011. Reduction of myoblast differentiation following multiple population doublings in mouse C(2) C(12) cells: A model to investigate ageing? *J Cell Biochem*.
- SHEEHAN, S. M. & ALLEN, R. E. 1999. Skeletal muscle satellite cell proliferation in response to members of the fibroblast growth factor family and hepatocyte growth factor. *J Cell Physiol*, 181, 499-506.

- SHI, X. & GARRY, D. J. 2006. Muscle stem cells in development, regeneration, and disease. *Genes Dev*, 20, 1692-708.
- SIEG, D. J., HAUCK, C. R. & SCHLAEPFER, D. D. 1999. Required role of focal adhesion kinase (FAK) for integrin-stimulated cell migration. *J Cell Sci*, 112 (Pt 16), 2677-91.
- SIESSER, P. M. & HANKS, S. K. 2006. The signaling and biological implications of FAK overexpression in cancer. *Clin Cancer Res*, 12, 3233-7.
- SIRIETT, V., SALERNO, M. S., BERRY, C., NICHOLAS, G., BOWER, R., KAMBADUR, R. & SHARMA, M. 2007. Antagonism of myostatin enhances muscle regeneration during sarcopenia. *Mol Ther*, 15, 1463-70.
- SKUK, D., GOULET, M. & TREMBLAY, J. P. 2011. Transplanted myoblasts can migrate several millimeters to fuse with damaged myofibers in nonhuman primate skeletal muscle. *J Neuropathol Exp Neurol*, 70, 770-8.
- SKUK, D., ROY, B., GOULET, M., CHAPDELAIN, P., BOUCHARD, J. P., ROY, R., DUGRE, F. J., LACHANCE, J. G., DESCHENES, L., HELENE, S., SYLVAIN, M. & TREMBLAY, J. P. 2004. Dystrophin expression in myofibers of Duchenne muscular dystrophy patients following intramuscular injections of normal myogenic cells. *Mol Ther*, 9, 475-82.
- SLACK-DAVIS, J. K., MARTIN, K. H., TILGHMAN, R. W., IWANICKI, M., UNG, E. J., AUTRY, C., LUZZIO, M. J., COOPER, B., KATH, J. C., ROBERTS, W. G. & PARSONS, J. T. 2007. Cellular characterization of a novel focal adhesion kinase inhibitor. *J Biol Chem*, 282, 14845-52.
- SMITH, C. K., 2ND, JANNEY, M. J. & ALLEN, R. E. 1994. Temporal expression of myogenic regulatory genes during activation, proliferation, and differentiation of rat skeletal muscle satellite cells. *J Cell Physiol*, 159, 379-85.
- SMYTHE, G. M. & GROUNDS, M. D. 2001. Absence of MyoD increases donor myoblast migration into host muscle. *Exp Cell Res*, 267, 267-74.
- SMYTHE, G. M., HODGETTS, S. I. & GROUNDS, M. D. 2000. Immunobiology and the future of myoblast transfer therapy. *Mol Ther*, 1, 304-13.
- SMYTHE, G. M., HODGETTS, S. I. & GROUNDS, M. D. 2001. Problems and solutions in myoblast transfer therapy. *J Cell Mol Med*, 5, 33-47.
- SNOW, M. H. 1977. The effects of aging on satellite cells in skeletal muscles of mice and rats. *Cell Tissue Res*, 185, 399-408.
- SNOW, M. H. 1983. A quantitative ultrastructural analysis of satellite cells in denervated fast and slow muscles of the mouse. *Anat Rec*, 207, 593-604.
- SPANGENBURG, E. E. & BOOTH, F. W. 2002. Multiple signaling pathways mediate LIF-induced skeletal muscle satellite cell proliferation. *Am J Physiol Cell Physiol*, 283, C204-11.
- SPITALI, P., RIMESSI, P., FABRIS, M., PERRONE, D., FALZARANO, S., BOVOLONTA, M., TRABANELLI, C., MARI, L., BASSI, E., TUFFERY, S., GUALANDI, F., MARALDI, N. M., SABATELLI-GIRAUD, P., MEDICI, A., MERLINI, L. & FERLINI, A. 2009. Exon

- skipping-mediated dystrophin reading frame restoration for small mutations. *Hum Mutat*, 30, 1527-34.
- ST PIERRE, B. A. & TIDBALL, J. G. 1994. Differential response of macrophage subpopulations to soleus muscle reloading after rat hindlimb suspension. *J Appl Physiol*, 77, 290-7.
- STANYON, C. A. & BERNARD, O. 1999. LIM-kinase1. *Int J Biochem Cell Biol*, 31, 389-94.
- STEPHENS, L., ELLSON, C. & HAWKINS, P. 2002. Roles of PI3Ks in leukocyte chemotaxis and phagocytosis. *Curr Opin Cell Biol*, 14, 203-13.
- STEVENSON, E. J., KONCAREVIC, A., GIRESI, P. G., JACKMAN, R. W. & KANDARIAN, S. C. 2005. Transcriptional profile of a myotube starvation model of atrophy. *J Appl Physiol*, 98, 1396-406.
- STEWART, C. E. & ROTWEIN, P. 1996. Insulin-like growth factor-II is an autocrine survival factor for differentiating myoblasts. *J Biol Chem*, 271, 11330-8.
- STILES, B., GILMAN, V., KHANZENSON, N., LESCHE, R., LI, A., QIAO, R., LIU, X. & WU, H. 2002. Essential role of AKT-1/protein kinase B alpha in PTEN-controlled tumorigenesis. *Mol Cell Biol*, 22, 3842-51.
- STRAFACE, G., APRAHAMIAN, T., FLEX, A., GAETANI, E., BISCETTI, F., SMITH, R. C., PECORINI, G., POLA, E., ANGELINI, F., STIGLIANO, E., CASTELLOT, J. J., JR., LOSORDO, D. W. & POLA, R. 2009. Sonic hedgehog regulates angiogenesis and myogenesis during post-natal skeletal muscle regeneration. *J Cell Mol Med*, 13, 2424-35.
- SUGITA, H. & TAKEDA, S. 2010. Progress in muscular dystrophy research with special emphasis on gene therapy. *Proc Jpn Acad Ser B Phys Biol Sci*, 86, 748-56.
- SUMI, T., MATSUMOTO, K. & NAKAMURA, T. 2001. Specific activation of LIM kinase 2 via phosphorylation of threonine 505 by ROCK, a Rho-dependent protein kinase. *J Biol Chem*, 276, 670-6.
- SUMMAN, M., MCKINSTRY, M., WARREN, G. L., HULDERMAN, T., MISHRA, D., BRUMBAUGH, K., LUSTER, M. I. & SIMEONOVA, P. P. 2003. Inflammatory mediators and skeletal muscle injury: a DNA microarray analysis. *J Interferon Cytokine Res*, 23, 237-45.
- SUMMAN, M., WARREN, G. L., MERCER, R. R., CHAPMAN, R., HULDERMAN, T., VAN ROOIJEN, N. & SIMEONOVA, P. P. 2006. Macrophages and skeletal muscle regeneration: a clodronate-containing liposome depletion study. *Am J Physiol Regul Integr Comp Physiol*, 290, R1488-95.
- SUN, H., LESCHE, R., LI, D. M., LILIENTAL, J., ZHANG, H., GAO, J., GAVRILOVA, N., MUELLER, B., LIU, X. & WU, H. 1999. PTEN modulates cell cycle progression and cell survival by regulating phosphatidylinositol 3,4,5,-trisphosphate and Akt/protein kinase B signaling pathway. *Proc Natl Acad Sci U S A*, 96, 6199-204.
- SUZUKI, A., KAISHO, T., OHISHI, M., TSUKIO-YAMAGUCHI, M., TSUBATA, T., KONI, P. A., SASAKI, T., MAK, T. W. & NAKANO, T. 2003. Critical roles of Pten in B cell homeostasis and immunoglobulin class switch recombination. *J Exp Med*, 197, 657-67.

- SUZUKI, J., YAMAZAKI, Y., LI, G., KAZIRO, Y. & KOIDE, H. 2000. Involvement of Ras and Ral in chemotactic migration of skeletal myoblasts. *Mol Cell Biol*, 20, 4658-65.
- SUZUKI, S., YAMANOUCI, K., SOETA, C., KATAKAI, Y., HARADA, R., NAITO, K. & TOJO, H. 2002. Skeletal muscle injury induces hepatocyte growth factor expression in spleen. *Biochem Biophys Res Commun*, 292, 709-14.
- SZCZEPANOWSKA, J. 2009. Involvement of Rac/Cdc42/PAK pathway in cytoskeletal rearrangements. *Acta Biochim Pol*, 56, 225-34.
- TAJBAKHSH, S., BORELLO, U., VIVARELLI, E., KELLY, R., PAPKOFF, J., DUPREZ, D., BUCKINGHAM, M. & COSSU, G. 1998. Differential activation of Myf5 and MyoD by different Wnts in explants of mouse paraxial mesoderm and the later activation of myogenesis in the absence of Myf5. *Development*, 125, 4155-62.
- TAJBAKHSH, S. & BUCKINGHAM, M. E. 1994. Mouse limb muscle is determined in the absence of the earliest myogenic factor myf-5. *Proc Natl Acad Sci U S A*, 91, 747-51.
- TAJBAKHSH, S., ROCANCOURT, D. & BUCKINGHAM, M. 1996. Muscle progenitor cells failing to respond to positional cues adopt non-myogenic fates in myf-5 null mice. *Nature*, 384, 266-70.
- TAJBAKHSH, S., ROCANCOURT, D., COSSU, G. & BUCKINGHAM, M. 1997. Redefining the genetic hierarchies controlling skeletal myogenesis: Pax-3 and Myf-5 act upstream of MyoD. *Cell*, 89, 127-38.
- TAKENAWA, T. & MIKI, H. 2001. WASP and WAVE family proteins: key molecules for rapid rearrangement of cortical actin filaments and cell movement. *J Cell Sci*, 114, 1801-9.
- TAMURA, M., GU, J., MATSUMOTO, K., AOTA, S., PARSONS, R. & YAMADA, K. M. 1998. Inhibition of cell migration, spreading, and focal adhesions by tumor suppressor PTEN. *Science*, 280, 1614-7.
- TATSUMI, R., ANDERSON, J. E., NEVORET, C. J., HALEVY, O. & ALLEN, R. E. 1998. HGF/SF is present in normal adult skeletal muscle and is capable of activating satellite cells. *Dev Biol*, 194, 114-28.
- TATSUMI, R., SHEEHAN, S. M., IWASAKI, H., HATTORI, A. & ALLEN, R. E. 2001. Mechanical stretch induces activation of skeletal muscle satellite cells in vitro. *Exp Cell Res*, 267, 107-14.
- TEDESCO, F. S., DELLAVALLE, A., DIAZ-MANERA, J., MESSINA, G. & COSSU, G. 2010. Repairing skeletal muscle: regenerative potential of skeletal muscle stem cells. *J Clin Invest*, 120, 11-9.
- TEIXEIRA, C. F., ZAMUNER, S. R., ZULIANI, J. P., FERNANDES, C. M., CRUZ-HOFLING, M. A., FERNANDES, I., CHAVES, F. & GUTIERREZ, J. M. 2003. Neutrophils do not contribute to local tissue damage, but play a key role in skeletal muscle regeneration, in mice injected with Bothrops asper snake venom. *Muscle Nerve*, 28, 449-59.
- TERANISHI, S., KIMURA, K. & NISHIDA, T. 2009. Role of formation of an ERK-FAK-paxillin complex in migration of human corneal epithelial cells during wound closure in vitro. *Invest Ophthalmol Vis Sci*, 50, 5646-52.
- TIDBALL, J. G. 1995. Inflammatory cell response to acute muscle injury. *Med Sci Sports Exerc*, 27, 1022-32.

- TIDBALL, J. G. 2005. Inflammatory processes in muscle injury and repair. *Am J Physiol Regul Integr Comp Physiol*, 288, R345-53.
- TOLLEFSEN, S. E., SADOW, J. L. & ROTWEIN, P. 1989. Coordinate expression of insulin-like growth factor II and its receptor during muscle differentiation. *Proc Natl Acad Sci U S A*, 86, 1543-7.
- TORRENTE, Y., EL FAHIME, E., CARON, N. J., DEL BO, R., BELICCHI, M., PISATI, F., TREMBLAY, J. P. & BRESOLIN, N. 2003. Tumor necrosis factor-alpha (TNF-alpha) stimulates chemotactic response in mouse myogenic cells. *Cell Transplant*, 12, 91-100.
- TOTSUKAWA, G., YAMAKITA, Y., YAMASHIRO, S., HARTSHORNE, D. J., SASAKI, Y. & MATSUMURA, F. 2000. Distinct roles of ROCK (Rho-kinase) and MLCK in spatial regulation of MLC phosphorylation for assembly of stress fibers and focal adhesions in 3T3 fibroblasts. *J Cell Biol*, 150, 797-806.
- TOUMI, H., F'GUYER, S. & BEST, T. M. 2006. The role of neutrophils in injury and repair following muscle stretch. *J Anat*, 208, 459-70.
- TREMBLAY, J. P., MALOUIN, F., ROY, R., HUARD, J., BOUCHARD, J. P., SATOH, A. & RICHARDS, C. L. 1993. Results of a triple blind clinical study of myoblast transplantations without immunosuppressive treatment in young boys with Duchenne muscular dystrophy. *Cell Transplant*, 2, 99-112.
- TURNER, C. E. 1994. Paxillin: a cytoskeletal target for tyrosine kinases. *Bioessays*, 16, 47-52.
- TURNER, N. J. & BADYLAK, S. F. 2011. Regeneration of skeletal muscle. *Cell Tissue Res*.
- ULLRICH, O., REINSCH, S., URBE, S., ZERIAL, M. & PARTON, R. G. 1996. Rab11 regulates recycling through the pericentriolar recycling endosome. *J Cell Biol*, 135, 913-24.
- VAN DEUTEKOM, J. C., BREMMER-BOUT, M., JANSON, A. A., GINJAAR, I. B., BAAS, F., DEN DUNNEN, J. T. & VAN OMMEN, G. J. 2001. Antisense-induced exon skipping restores dystrophin expression in DMD patient derived muscle cells. *Hum Mol Genet*, 10, 1547-54.
- VANDENBURGH, H. H., KARLISCH, P., SHANSKY, J. & FELDSTEIN, R. 1991. Insulin and IGF-I induce pronounced hypertrophy of skeletal myofibers in tissue culture. *Am J Physiol*, 260, C475-84.
- VANHAESEBROECK, B., JONES, G. E., ALLEN, W. E., ZICHA, D., HOOSHMAND-RAD, R., SAWYER, C., WELLS, C., WATERFIELD, M. D. & RIDLEY, A. J. 1999. Distinct PI(3)Ks mediate mitogenic signalling and cell migration in macrophages. *Nat Cell Biol*, 1, 69-71.
- VASYUTINA, E., LENHARD, D. C. & BIRCHMEIER, C. 2007. Notch function in myogenesis. *Cell Cycle*, 6, 1451-4.
- VASYUTINA, E., STEBLER, J., BRAND-SABERI, B., SCHULZ, S., RAZ, E. & BIRCHMEIER, C. 2005. CXCR4 and Gab1 cooperate to control the development of migrating muscle progenitor cells. *Genes Dev*, 19, 2187-98.
- VELASCO, B., CACICEDO, L., ESCALADA, J., LOPEZ-FERNANDEZ, J. & SANCHEZ-FRANCO, F. 1998. Growth hormone gene expression and secretion in aging rats is age dependent and not age-associated weight increase related. *Endocrinology*, 139, 1314-20.

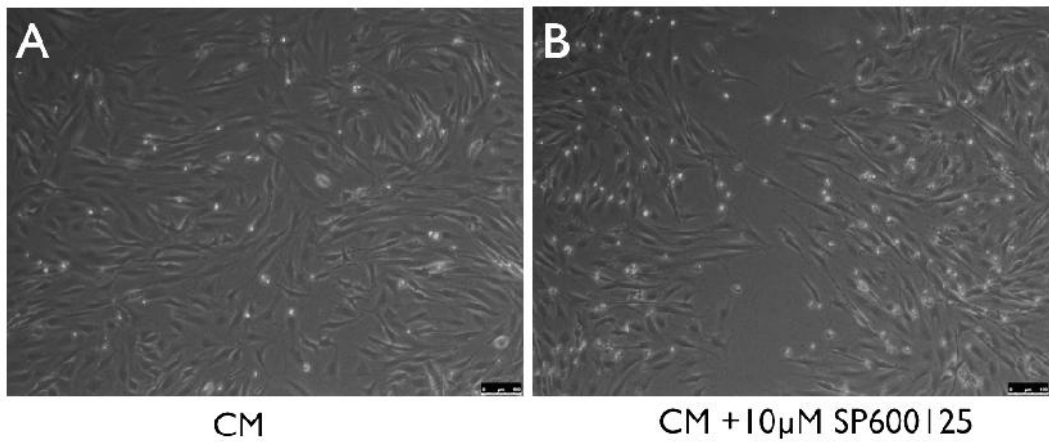
- VERGANI, L., DI GIULIO, A. M., LOSA, M., ROSSONI, G., MULLER, E. E. & GORIO, A. 1998. Systemic administration of insulin-like growth factor decreases motor neuron cell death and promotes muscle reinnervation. *J Neurosci Res*, 54, 840-7.
- VISSER, M., PAHOR, M., TAAFFE, D. R., GOODPASTER, B. H., SIMONSICK, E. M., NEWMAN, A. B., NEVITT, M. & HARRIS, T. B. 2002. Relationship of interleukin-6 and tumor necrosis factor-alpha with muscle mass and muscle strength in elderly men and women: the Health ABC Study. *J Gerontol A Biol Sci Med Sci*, 57, M326-32.
- VOLONTE, D., LIU, Y. & GALBIATI, F. 2005. The modulation of caveolin-1 expression controls satellite cell activation during muscle repair. *FASEB J*, 19, 237-9.
- VUKMIRICA, J., MONZO, P., LE MARCHAND-BRUSTEL, Y. & CORMONT, M. 2006. The Rab4A effector protein Rabip4 is involved in migration of NIH 3T3 fibroblasts. *J Biol Chem*, 281, 36360-8.
- WANG, W., PAN, H., MURRAY, K., JEFFERSON, B. S. & LI, Y. 2009. Matrix metalloproteinase-1 promotes muscle cell migration and differentiation. *Am J Pathol*, 174, 541-9.
- WANG, Y. & SASSOON, D. 1995. Ectoderm-mesenchyme and mesenchyme-mesenchyme interactions regulate Msx-1 expression and cellular differentiation in the murine limb bud. *Dev Biol*, 168, 374-82.
- WARREN, G. L., O'FARRELL, L., SUMMAN, M., HULDERMAN, T., MISHRA, D., LUSTER, M. I., KUZIEL, W. A. & SIMEONOVA, P. P. 2004. Role of CC chemokines in skeletal muscle functional restoration after injury. *Am J Physiol Cell Physiol*, 286, C1031-6.
- WATT, D. J., KARASINSKI, J., MOSS, J. & ENGLAND, M. A. 1994. Migration of muscle cells. *Nature*, 368, 406-7.
- WEAVER, A. M., YOUNG, M. E., LEE, W. L. & COOPER, J. A. 2003. Integration of signals to the Arp2/3 complex. *Curr Opin Cell Biol*, 15, 23-30.
- WEBB, D. J., DONAIS, K., WHITMORE, L. A., THOMAS, S. M., TURNER, C. E., PARSONS, J. T. & HORWITZ, A. F. 2004. FAK-Src signalling through paxillin, ERK and MLCK regulates adhesion disassembly. *Nat Cell Biol*, 6, 154-61.
- WEBB, D. J., NGUYEN, D. H. & GONIAS, S. L. 2000. Extracellular signal-regulated kinase functions in the urokinase receptor-dependent pathway by which neutralization of low density lipoprotein receptor-related protein promotes fibrosarcoma cell migration and matrigel invasion. *J Cell Sci*, 113 (Pt 1), 123-34.
- WEBB, S. E., LEE, K. K., TANG, M. K. & EDE, D. A. 1997. Fibroblast growth factors 2 and 4 stimulate migration of mouse embryonic limb myogenic cells. *Dev Dyn*, 209, 206-16.
- WEBSTER, C. & BLAU, H. M. 1990. Accelerated age-related decline in replicative life-span of Duchenne muscular dystrophy myoblasts: implications for cell and gene therapy. *Somat Cell Mol Genet*, 16, 557-65.
- WEI, L., LIU, Y., KANETO, H. & FANBURG, B. L. 2010. JNK regulates serotonin-mediated proliferation and migration of pulmonary artery smooth muscle cells. *Am J Physiol Lung Cell Mol Physiol*, 298, L863-9.

- WELF, E. S. & HAUGH, J. M. 2011. Signaling pathways that control cell migration: models and analysis. *Wiley Interdiscip Rev Syst Biol Med*, 3, 231-40.
- WHITE, E. S., ATRASZ, R. G., HU, B., PHAN, S. H., STAMBOLIC, V., MAK, T. W., HOGABOAM, C. M., FLAHERTY, K. R., MARTINEZ, F. J., KONTOS, C. D. & TOEWS, G. B. 2006. Negative regulation of myofibroblast differentiation by PTEN (Phosphatase and Tensin Homolog Deleted on chromosome 10). *Am J Respir Crit Care Med*, 173, 112-21.
- WHITE, J. D., BOWER, J. J., KUREK, J. B. & AUSTIN, L. 2001. Leukemia inhibitory factor enhances regeneration in skeletal muscles after myoblast transplantation. *Muscle Nerve*, 24, 695-7.
- WHITMAN, M. 1998. Smads and early developmental signaling by the TGFbeta superfamily. *Genes Dev*, 12, 2445-62.
- WORTHYLAKE, R. A. & BURRIDGE, K. 2003. RhoA and ROCK promote migration by limiting membrane protrusions. *J Biol Chem*, 278, 13578-84.
- WOZNIAK, A. C. & ANDERSON, J. E. 2007. Nitric oxide-dependence of satellite stem cell activation and quiescence on normal skeletal muscle fibers. *Dev Dyn*, 236, 240-50.
- XIA, H., NHO, R. S., KAHM, J., KLEIDON, J. & HENKE, C. A. 2004. Focal adhesion kinase is upstream of phosphatidylinositol 3-kinase/Akt in regulating fibroblast survival in response to contraction of type I collagen matrices via a beta 1 integrin viability signaling pathway. *J Biol Chem*, 279, 33024-34.
- YABLONKA-REUVENI, Z. & RIVERA, A. J. 1994. Temporal expression of regulatory and structural muscle proteins during myogenesis of satellite cells on isolated adult rat fibers. *Dev Biol*, 164, 588-603.
- YABLONKA-REUVENI, Z., SEGER, R. & RIVERA, A. J. 1999. Fibroblast growth factor promotes recruitment of skeletal muscle satellite cells in young and old rats. *J Histochem Cytochem*, 47, 23-42.
- YAHIAOUI, L., GVOZDIC, D., DANIALOU, G., MACK, M. & PETROF, B. J. 2008. CC family chemokines directly regulate myoblast responses to skeletal muscle injury. *J Physiol*, 586, 3991-4004.
- YAMADA, K. M. & ARAKI, M. 2001. Tumor suppressor PTEN: modulator of cell signaling, growth, migration and apoptosis. *J Cell Sci*, 114, 2375-82.
- YAMANA, N., ARAKAWA, Y., NISHINO, T., KUROKAWA, K., TANJI, M., ITOH, R. E., MONYPENNY, J., ISHIZAKI, T., BITO, H., NOZAKI, K., HASHIMOTO, N., MATSUDA, M. & NARUMIYA, S. 2006. The Rho-mDia1 pathway regulates cell polarity and focal adhesion turnover in migrating cells through mobilizing Apc and c-Src. *Mol Cell Biol*, 26, 6844-58.
- YANG, L., LI, J. & XIAO, X. 2011. Directed evolution of adeno-associated virus (AAV) as vector for muscle gene therapy. *Methods Mol Biol*, 709, 127-39.
- YANG, X. M., VOGAN, K., GROS, P. & PARK, M. 1996. Expression of the met receptor tyrosine kinase in muscle progenitor cells in somites and limbs is absent in Splotch mice. *Development*, 122, 2163-71.
- YAO, S. N. & KURACHI, K. 1993. Implanted myoblasts not only fuse with myofibers but also survive as muscle precursor cells. *J Cell Sci*, 105 (Pt 4), 957-63.

- YE, M., HU, D., TU, L., ZHOU, X., LU, F., WEN, B., WU, W., LIN, Y., ZHOU, Z. & QU, J. 2008. Involvement of PI3K/Akt signaling pathway in hepatocyte growth factor-induced migration of uveal melanoma cells. *Invest Ophthalmol Vis Sci*, 49, 497-504.
- YOUNG, H. E., STEELE, T. A., BRAY, R. A., HUDSON, J., FLOYD, J. A., HAWKINS, K., THOMAS, K., AUSTIN, T., EDWARDS, C., CUZZOURT, J., DUENZL, M., LUCAS, P. A. & BLACK, A. C., JR. 2001. Human reserve pluripotent mesenchymal stem cells are present in the connective tissues of skeletal muscle and dermis derived from fetal, adult, and geriatric donors. *Anat Rec*, 264, 51-62.
- ZACKS, S. I. & SHEFF, M. F. 1982. Age-related impeded regeneration of mouse minced anterior tibial muscle. *Muscle Nerve*, 5, 152-61.
- ZAMMIT, P. S. 2008. All muscle satellite cells are equal, but are some more equal than others? *J Cell Sci*, 121, 2975-82.
- ZAMMIT, P. S., CARVAJAL, J. J., GOLDING, J. P., MORGAN, J. E., SUMMERBELL, D., ZOLNERCIKS, J., PARTRIDGE, T. A., RIGBY, P. W. & BEAUCHAMP, J. R. 2004a. Myf5 expression in satellite cells and spindles in adult muscle is controlled by separate genetic elements. *Dev Biol*, 273, 454-65.
- ZAMMIT, P. S., GOLDING, J. P., NAGATA, Y., HUDON, V., PARTRIDGE, T. A. & BEAUCHAMP, J. R. 2004b. Muscle satellite cells adopt divergent fates: a mechanism for self-renewal? *J Cell Biol*, 166, 347-57.
- ZAMMIT, P. S., PARTRIDGE, T. A. & YABLONKA-REUVENI, Z. 2006. The skeletal muscle satellite cell: the stem cell that came in from the cold. *J Histochem Cytochem*, 54, 1177-91.
- ZHANG, L., YU, Q., HE, J. & ZHA, X. 2004. Study of the PTEN gene expression and FAK phosphorylation in human hepatocarcinoma tissues and cell lines. *Mol Cell Biochem*, 262, 25-33.
- ZHANG, Q. G., WU, D. N., HAN, D. & ZHANG, G. Y. 2007. Critical role of PTEN in the coupling between PI3K/Akt and JNK1/2 signaling in ischemic brain injury. *FEBS Lett*, 581, 495-505.
- ZHAO, M. 2007. PTEN: a promising pharmacological target to enhance epithelial wound healing. *Br J Pharmacol*, 152, 1141-4.
- ZHAO, P. & HOFFMAN, E. P. 2004. Embryonic myogenesis pathways in muscle regeneration. *Dev Dyn*, 229, 380-92.
- ZHENG, Y. 2001. Dbl family guanine nucleotide exchange factors. *Trends Biochem Sci*, 26, 724-32.
- ZHOU, L. & LU, H. 2010. Targeting fibrosis in Duchenne muscular dystrophy. *J Neuropathol Exp Neurol*, 69, 771-6.

APPENDICES

APPENDIX 1. WOUND HEALING ASSAY WITH JNK INHIBITOR SP600125.



Wound healing assay with CM+vehicle (DMSO) (A) or with CM+10 μ M SP600125 (JNK inhibitor) (B). Preliminary wound healing assay experiments demonstrated inhibited wound healing of C2C12 myoblasts at 30h with CM+10 μ M SP600125 (JNK inhibitor) vs CM. Data is representative of at least 2 experiments performed in triplicate.

APPENDIX 2. ABSTRACT OF CONFERENCE PROCEEDINGS

Abstract presented on MYOAGE workshop “Muscle Mass regulation” (Acaya, Italy. September, 2011)

Inhibition of C2C12 myoblast differentiation by serial passaging or treatment with the phosphotyrosine phosphatase inhibitor BpV(Hopic), differentially affects the expression of Spire1, Spire2 and Formin1, Formin2 genes

Introduction: Skeletal muscle growth and repair are complex processes, depending on the proliferation, migration, differentiation and fusion of muscle precursor cells. The differentiation and fusion of myoblasts into multinucleated myotubes is a complex process requiring further investigation, particularly the role of actin cytoskeleton regulation. It was hypothesized that the expression of 4 genes (Spire1, Spire2, Formin1 and Formin2), involved in actin nucleation, would be altered during the differentiation of C2C12 cells. Spire and Formin proteins are known to interact with each other to form a proposed cooperative mechanism for actin nucleation. The expression of Spire and Formin genes during skeletal muscle differentiation has not been previously investigated. It was previously demonstrated that serial passaging of C2C12 cells results in reduced myotube formation (photomicroscopy), reduced creatine kinase activity (enzyme assay) and reduced expression of myogenic regulatory factors MyoD and Myogenin (RT-PCR). Our objective was to study how the mRNA expression level (RT-PCR) of Spire1, Spire2, Formin1 and Formin2 genes was affected during C2C12 differentiation after replicative passaging or treatment with the phosphotyrosine phosphatase inhibitor Bpv(Hopic), which is also able to inhibit the differentiation process in these cells. Following growth to confluence, cells were transferred to differentiation medium in the absence or presence of passaging or absence or presence of a single dose of the Bpv(Hopic) (10 μ M).

Results: Reduced MyoD and Myogenin gene expression levels were confirmed in serially passaged (50 passages – p50) C2C12 cells vs non-passaged cells (p0) and also in both p0 and p50 cells after treatment with 10 μ M BpV (Hopic).

A fold decrease (mean \pm SEM) in the expression of Spire1 gene was observed after treatment with BpV(Hopic) in p0 cells (2.52 \pm 0.34 at 24hr, $P < 0.001$; 1.21

+/- 0.064 at 48hr, P<0.05) and p50 cells (1.89 +/- 0.02 at 24hr, P<0.001; 1.31 +/- 0.04 at 48hr, P<0.005). A decrease was also observed in p50 DM cells vs p0 DM cells (1.43 +/- 0.12 at 24hr, P<0.05; 1.3 +/-0.02 at 48hr, P=0.05; 1.21 +/-0.05 at 72hr, P<0.05). Spire 2 expression was decreased by BpV(Hopic) in p0 cells (1.69 +/-0.13 at 48hr, P<0.01; 2.18 +/-0.09 at 72hr, P<0.005) and p50 cells (1.68 +/-0.2 at 48hr, P<0.05; 2.92 +/- 0.25 at 72hr, P<0.05). Spire2 expression was not affected by passage. By contrast, Formin1 gene expression was increased after treatment with Bpv(Hopic) in p0 cells (1.84 +/-0.17 at 48hr, P<0.005; 1.71 +/- 0.045 at 72 hrs, P<0.001) and to a smaller extent in p50 cells (1.15 +/-0.03 at 48hr, P<0.05). Formin2 expression was very low in p0 cells, but significantly increased in p50 cells (4.35 +/-0.88 at 24hr, P<0.05; 6 +/-1 at 48hr, P<0.05; 7 +/- 3.32 at 72hr, P<0.05). Its expression was not affected by BpV(Hopic) treatment.

Conclusion: It was confirmed that both serial passaging and BpV (Hopic) treatment reduce the expression of myogenic regulatory factors in C2C12 myoblasts and that when differentiation and fusion is inhibited by these conditions, the expression levels of genes involved in actin nucleation are differentially affected. It was proposed that balanced expression of Spire and Formin genes is necessary for the formation of multinucleated myotubes, with Spire 1 and 2 being suppressed with reduced fusion and Formin 1 and 2 increased with reduced fusion, suggesting targets for future preventive wasting therapies. Future gene knock-down studies and studies looking at the protein level of Spires and Formins would be essential to verify their involvement and precise function in skeletal muscle.